Republic of Iraq

Ministry of Higher Education and Scientific Research

Babylon University

College of Materials Engineering

Department of Metallurgical Engineering

Improvement of Mechanical Properties and Corrosion Behavior of Biomedical CoCrMo Alloy

A Thesis

Submitted to the Council of the College of Materials Engineering/ University of Babylon in Partial Fulfillment of the Requirements for the Degree of Master of Science in Materials Engineering/ Metallurgical

Nuha Hasan Jabr Mohammed

(B.Sc. In Metallurgical Engineering, 2016)

(Higher Diploma in Metallurgical Engineering, 2019)

Supervised by

Prof. Dr. Nawal Mohammed Dawood

2021A.D 1442 A.H

وزارة التعليم العالي والبحث الـــعلمي
جـامـــعـــــــــة بـابـــــــــل
كليـــــــة هنـــــــــــدسة المواد
قسـم هنـــــــــــدسـة المـعـادن

تحسين الخواص الميكانيكية وسلوك التأكل لسبيكة CoCrMo الحياتية

رسالة

مقدمة إلى كلية هندسة المواد/ جامعة بابل وهي جزء من متطلبات نيل درجة الماجستير في هندسة المواد/ المعادن

من قبل

نهى حسن جبر محمد

بإشراف

أ.د. نوال محمد داود

2021م 1442هـ

بسم الله الرحمن الرحيم

صدق الله العظيم

سورة سبأ الآية ﴿٦﴾

Examining committee Certification

We certify that have read this thesis entitled **"Improvement of Mechanical Properties and Corrosion Behavior of Biomedical CoCrMo Alloy"** and as an examining committee, we have examined the student**(Nuha Hasan Jabr)** in contents and that is related to it, and that in our opinion it meets the standard of a thesis for the degree of Master of science in Materials Engineering.

Signature:

Prof. Dr. Haydar H . J. Jamal Al Deen

(Committee Chair)

Date: / / 2022

Signature:

Prof. Dr. Ekbal MS. Salih

(Committee Member)

Date : / / 2022

Signature:

Asst. Prof.Dr.Iman Adnan Annon

(Committee Member)

Date : / / 2022

Signature:

Prof. Dr. Nawal Mohammed Dawood

(Supervisor)

Date : / / 2022

Signature:

Prof. Dr.Saad Hameed Al Shafaie

Head of Metallurgy Engineering Department

Date : / / 2022

Signature:

Prof. Dr.Imad Ali Disher

Dean of the College of Materials Engineering

Date : / / 2022

Supervisor Certification

We certify that this thesis entitled "**Improvement of Mechanical Properties and Corrosion Behavior of Biomedical CoCrMo Alloy"** was prepared by (**Nuha Hasan Jabr**) under our supervision at department Metallurgical Engineering / University Babylon in a partial fulfillment of the requirements for the degree of Master of Science in Materials Engineering / Metallurgical Engineering .

Signature:

Name:

Prof. Dr. Nawal Mohammed Dawood

(Supervisor)

Date: / / 2022

Dedication

(وَإِذ تَأَذَّنَ رَبُّكُم لَئِن شَكَرتُم لَأَزيدَنَّكُم)

I thank God for His bounty as He made it possible for me to accomplish this work by his grace, I praise you first and foremost.

A big thank to the spirit of my father who always accompanies me in every step of my life.

To my mother who struggles to help me reach this stage, without a reproach or a complaint.

To my brothers and sisters who always support me, you are my life candles

A special thank to Dr. Nahidh for helping and believing in me.

To my friends .. Ban , Qabas, Noor, Nada who gave been supporting me all way long and helped me make this hard stage.

Nuha Hasan 2021

Acknowledgments

Great thanks to allah Almighty my Creator and inspirational for being merciful to me and gave me health, strength and protection.

I cannot express enough thanks and gratitude to my supervisor, ***Prof. Dr. Nawal Mohammed Dawood*** *who support, helped, encouraged, and gave me all the acknowledgement I need to finish my research. It was a great privilege and honor to work and study under Their guidance.*

Special thanks go to ***Prof. Dr.Mohammed Almaamori*** *for his helping.*

My thank to everyone work in metallic and non-metallic laboratories in Materials Engineering college/ University of Babylon.

Nuha Hasan 2021

Table of Contents

Chapter Three :Experimental Work

Chapter Four: Results and Discussion

List of Abbreviations and Symbols

Abbreviation	Description
ASTM	American society for testing and materials
BCC	Body Center Cubic
CCM	Cobalt-Chrome-Molybdenum
EDS	Energy dispersive spectroscopy analysis
FCC	Face Center Cubic
HB	Brinlle Hardness
HCP	Hexagonal close packet
LOM	Light optical microscope
mpy	Mils per year
mV	Milli Volt
OCP	Open Circuit Potential
PM	Powder Metallurgy
SEM	Scanning Electron Microscope
XRD	X- Ray Diffraction
µAm	Micro Ampere
γ	Gamma phase
Ɛ	Abslon phase

Abstract

Cobalt-chromium-molybdenum alloy(F75) is considered one of the important alloys that are widely used in orthopedic applications and dental implants. The aim of this study is to investigate the effect of adding some elements (boron and tungsten and adding boron carbide ceramic material) on the physical, mechanical and electrochemical properties of this alloy.

Powder metallurgy method used to prepare alloys ,each of the tungsten and boron was added in a different proportion(0.5,1,1.5)wt% while boron carbide was added in different proportions (1,3 and 5)wt%. The mixing process took place for 5hr , then compacted at a constant pressure of 700 Mpa. The dimensions of the samples after the pressing process were d=13mm and t = 5 mm . The sintering process accomplished at temperature 850^{o}C for 6 hr of all samples are sufficient to satisfy completely and to transform all element into alloy structure.

The results indicate that the addition of boron leads to a clear decrease in the porosity, while the addition of tungsten has a low benefit in the porosity ratios for the prepared alloy. As for the addition of boron carbide to the F75 alloy led to a noticeable increase in the porosity values of the alloy.

Density results after sintering show an increase in the density of both boron containing and tungsten sspecimens and a significant decrease in the density of boron-carbide-containing specimens.

The results of XRD showed that all specimens (with and without additives) which compacted at 700 MPa and sintered at 850 ^{o}C for 6hr consists of three phases at room temperature (CoCrMo, CoCr and Co_2Mo_3). But in the case of adding boron carbide to the alloy, it showed breathing phases with clear beck of boron carbide in the diagram.

The hardness of the prepared alloy was significantly increased with the addition of a little boron and boron carbide In all proportions, the addition of tungsten had a

slight effect on hardness value. Specimens with 1.5wt% boron has the higher hardness of all adding elements.

The wear resistance increased with addition of B,W and B_4C to CoCrMo alloys , The specimen of (5wt%) B_4C has lower weigh loss during wear test under different loads.

Corrosion resistance increased significantly after adding boron and tungsten in a different proportion(0.5,1,1.5)wt% , where the corrosion rate of base alloy decreasing from (13.49 $\mu A/cm^2$) and(18.989 $\mu A/cm^2$) in Ringer's solution and artificial saliva respectively to (0.0013372 $\mu A/cm^2$) and (4.808 $\mu A/cm^2$) after addition 1.5 wt% B .While the corrosion rate of base alloy decreasing from (13.49 $\mu A/cm^2$) and(18.989 $\mu A/cm^2$) in Ringer's solution and artificial saliva respectively to (4.310 $\mu A/cm^2$) and (3.3209 $\mu A/cm^2$) after addition 1.5 wt% W .Also for the addition of boron carbide, increased the corrosion resistance of the cobalt chromium-molybdenum alloy, with different addition (1,3,5)wt%.

Improvement percentage of boron addition reached to (99.99wt%) with (1.5wt% B)in Ringers solution .while the best improvement percentage of tungsten addition is (82.51wt%) when tungsten contain is 1.5wt% in artificial saliva, and improvement percentage of boron carbide reached to (99.61%)with (5wt% B_4C) in artificial saliva .

The ion release test confirmed that all of the Co,Cr and Mo ions dissolved in the ringer and salvia solution decreased significantly after adding a percentage of 1,5 wt% B and of 1.5 wt% W

Note that both the dissolved boron and tungsten ions were not detected due to the small amount of dissolved ions in the corrosive solutions. And also adding boron carbide in each of the corrosive solution.

Chapter One

1.1. Introduction

A biomaterial is a synthetic material used to replace part of a living system or to function in intimate contact with living tissue**[1].**The implant which used as Biomaterial could be metals, polymers, ceramics, and composites**[2].**

Biomaterials have been used extensively to improve the quality of human life, replacing dysfunctional or arthritic hips, atherosclerotic arteries, decaying teeth, and even repairing injured tissues such as cartilage and skin. The aging population will require even greater replacement and repair of soft and hard tissues such as bones, cartilage, blood vessels, or even entire organs **[3].** Traditional materials such as metals, ceramics, polymers, semiconductors, and glasses are still used for material science and engineering; all of these materials have been used in a variety of biomedical applications such as cardiovascular stents and orthopedic implants**[4]**

Traditionally the study of biomaterials focuses on issues such as biocompatibility, host-tissue reaction to implants, cytotoxicity, and basic structure-property relationships .These issues are important. They provide a strong scientific basis for a clear understanding of many successful medical devices such as the mechanical heart valve**[5].**

The success of a biomaterial in the body depends on factors such as the material properties, design, and biocompatibility of the material used, as well as other factors not under control of the engineer, including the technique used by the surgeon, the health and condition of the patient, and the activities of the patient **[1].**

Metallic biomaterials continue to be used extensively for the fabrication of surgical implants primarily . The high strength and resistance to fracture that this class of material can provide, assuming proper processing, gives reliable long-term implant performance in major load-bearing situations. Coupled with a relative ease of fabrication of both simple and complex shapes using well-established and widely available fabrication techniques (e.g., casting, forging, machining), this has promoted metal use in the fields of orthopedics and dentistry primarily, the two areas in which highly loaded devices are most common although similar reasons have led to their use for forming cardiovascular devices**[6].**

Cobalt-based alloys is one of the only alloys with its good corrosion resistance and good mechanical strength in severe environments, which is due to alloying additions and the formation of the chromium oxide Cr_2O_3 passive layer. They are now frequently used for the metal-on-metal hip resurfacing joints due to their better corrosion resistance and wear performance **[7].**

1.2. Metallic Biomaterials

Metallic biomaterials (ie, alloys that comprise medical devices) have been in use for over 80 years, particularly in dental applications, and since the 1960s in a wide range of orthopedic, cardiovascular, spinal, and other applications**[8]** .Indeed, metallic biomaterials have been and will continue to be an essential part of medical devices for the foreseeable future, because of their unmatched strength, toughness, modulus, and fracture and fatigue resistances. The principal alloys used in medical devices consist of 316L stainless steel, cobalt-chromium-molybdenum (CoCrMo) alloys and titanium alloys**[9,10]**. Table (1.1) summarized(shows) metals used for different implants division.

Table(1-1). Implants division and type of metals used[11]

Division	Example of implants	Type of metal
Cardiovascular	Stent Artificial valve	316L SS; CoCrMo; Ti Ti6Al4V
Orthopaedic	Bone fixation (plate, screw, pin) Artificial joints	316L SS; Ti; Ti6Al4V CoCrMo; Ti6Al4V; Ti6Al7Nb
Dentistry	Orthodontic wire Filling	316L SS; CoCrMo; TiNi; TiMo AgSn(Cu) amalgam, Au
Craniofacial	Plate and screw	316L SS; CoCrMo; Ti; Ti6Al4V
Otorhinology	Artificial eardrum	316L SS

Metallic implants attracted high attention compared to other biomaterials as a result of their high impact strength, high ductility, high wear resistance, and toughness. These features make metals appropriate contender for orthopedic load-bearing application and fixation devices such as bone plates and screws, joint replacement, as well as dental implants. Since the late 18th century, metals have been used as biomaterials when Fe, Au, Ag, and Pt were used as pins and wires to fix bone fractures**[12].**

The main property required of a metal as biomaterial is that it does not illicit an adverse reaction when placed into services, that means to be a biocompatible material. As well, good mechanical properties, osseointegration, high corrosion resistance and excellent wear resistance are required. That is, the material used as implants are expected to be highly nontoxic and should not cause any inflammatory or allergic reactions in the human body **[13]**. Figure(1.1) clarify different clinic applications for metal implants

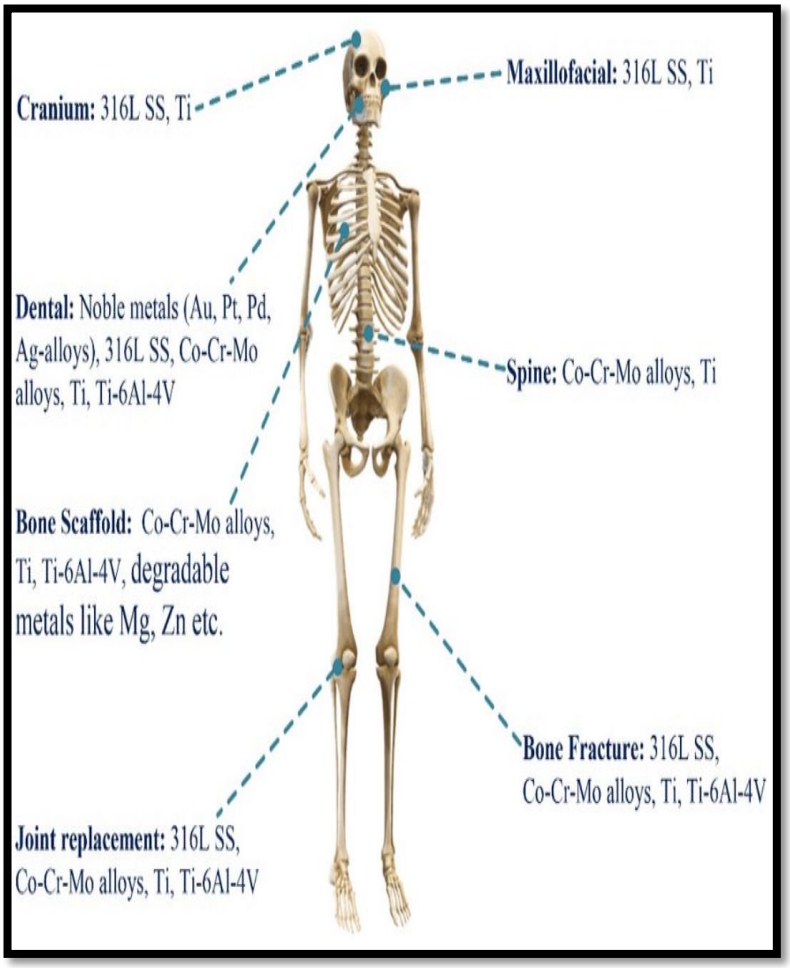

Figure(1.1): Different clinic applications for metal implants. Metal implants are mainly used in stents and hard tissue repair, which includes maxillofacial, spine and orthopedic fixation implants. WSS: wall shear stress; B: new bones**[14].**

1.2.1. Stainless Steel

316L is one of the oldest and most common alloys used for human implants, recent developments have led to newer stainless steels with improved mechanical strength and enhanced corrosion resistance. The chromium promotes the passivation ability while the molybdenum enhances the corrosion resistance of the stainless steel. However, the resistance of 316L stainless steel is not sufficiently high against of pitting and stress cracking corrosions **[15].**

Stainless steel is utilized for a broad choice of applications because of its lower cost, easy accessibility, excellent manufacture properties, accepted biocompatibility, and great strength. The 316L and 316 grades are the most frequently used steel alloys. Type 316L is recommended by ASTM for the fabrication of implants for the clear reason that its lower carbon content reduces the possibility of chromium carbide appearance which normally affects in the corrosion of intergranular**[16].**

1.2.2. Ti alloys

Titanium alloys are fast emerging as the first choice for majority of applications due to the combination of their outstanding characteristics such as high strength, low density, high immunity to corrosion, complete inertness to body environment, enhanced compatibility, low Young´s modulus and high capacity to join with bone or other tissues. Their lower Young´s modulus, superior biocompatibility and better corrosion resistance in comparison with conventional stainless steels and cobalt-based alloys, make them an ideal choice for bioapplications .Because of the mentioned desirable properties, titanium and titanium alloys are widely used as hard tissue replacements in artificial bones, joints and dental implants**[17].**

1.2.3 Dental alloys

Since the early 1900s, a wide range of metals and their alloys are used in surgically implanted medical devices, prostheses and dental materials, in order to provide improved physical and chemical properties, such as strength, durability and corrosion resistance**.** The classes of metals used in medical devices and dental materials include stainless steels, cobalt–chromium alloys, and titanium(as alloys and unalloyed) **.**In addition, dental casting alloys are based on precious metals (gold, platinum, palladium, and silver), nickel, and copper and may in some cases contain smaller amounts of many other

elements, added to improve castability, handling, ceramic bond, or other physical properties**[18].**

Dental alloys are commonly custom precision-cast for restoration of missing tooth structure, but wrought forms (shaped by the manufacturer or the clinician) are also common, and dental amalgam is an alloy that forms in situ in a tooth cavity preparation after mixing of a Ag–Sn alloy with mercury. Dental alloys are used in a variety of applications, ranging from restorations (either permanent or temporary) to files, instruments, and burs for tooth modification or to guide tooth movement. Because of these many uses, the environments in which the alloys must function are diverse, as are the physical requirements of the alloys**[19].** Alloys used in dental applications classify as shown in Table (1.2)

Commonly used dental alloys may be classified as shown in Table (1.2)[18]

Precious alloys	*Nonprecious alloys*
Conventional crown and bridge alloys	Nickel-based
High gold	Type A-Base Ni–Cr, major secondary element: Be
Low gold	Type B-Base Ni–Cr, major secondary element: Fe
Ag-based	Type C-Base Ni–Cr, major secondary element: Mo
Alloys for the porcelain-fused-to metal	Type D-Base Ni–Cr, major secondary element: Mn
technique	Type *E*-Base Ni–Cr–Fe
High gold	CoCr-based, modified CoCr + Pt, Ru, Nb, Au, In, Fe-CoCr
Low gold (NIOM Type B)	Cu-based (bronze)
Pd-based: Pd Ag, Pd Sn, Pd Cu, Pd Cr,	Titanium: Ti grade 1-4 , Ti-6Al-4V, Ti-6Al-7Nb, Ti- Mo, Ti-40Zr, Ti-Pd-Co, Ti-50Ni, Ti-42.5Ni-7.5Pd, Ti-5Al-13Ta,
Pd Co	Ti-5Ag, Ti-20Ag

1.2.4. CoCrMo alloy

The cobalt–chromium–molybdenum (Co–Cr–Mo) alloy is one of the most widely used metal-bearing materials in artificial joint systems. The Co–Cr–Mo alloy has good mechanical properties, castability, corrosion resistance, and wear resistance, whereas stainless-steel and titanium alloys have a disadvantage with regard to corrosion resistance and wear resistance, respectively**[20].**

The two basic types of cobalt-chromium alloys are cobalt chromium molybdenum (CoCrMo) alloy and cobalt nickel chromium molybdenum (CoNiCrMo) alloy**[21].**Table (1.3) shows the composition of CoCr alloys.

Table(1.3):Comparison of Various Co-Cr Alloy [22]

Element	CoCrMo(F75)		CoCrWNi(F90)		CoNiCrMo(F562)		CoNiCrMoWFe(F563)	
	Min.	Max	Min.	Max.	Min.	Max.	Min.	Max.
Cr	27.0	30.0	19.0	21.0	19.0	21.0	18.00	22.00
Mo	5.0	7.0	–	–	9.0	10.5	3.00	4.00
Ni	–	2.5	9.0	11.0	33.0	37.0	15.00	25.00
Fe	–	0.75	–	3.0	–	1.0	4.00	6.00
C	–	0.35	0.05	0.15	–	0.025	–	0.05
Si	–	1.00	–	1.00	–	0.15	–	0.50
Mn	–	1.00	–	2.00	–	0.15	–	1.00
W	–	–	14.0	16.0	–	–	3.00	4.00
P	–	–	–	–	–	0.015	–	–
S	–	–	–	–	–	0.010	–	0.010
Ti	–	–	–	–	–	1.0	0.50	3.50
Co			Balance					

The cast alloy containing28 wt%Cr and 6 wt%Mo (balance Co) has been used for many years to produce medical implants such as hips, knees, ankles and bone plates**[23].**

The wrought Co–Cr–Mo alloys exhibit superior mechanical and chemical properties compared with the cast alloys due to a finer grain size and more homogenous microstructure**.** Although fabrication of surgical implants by conventional methods are common, powder metallurgy (P/M)route offers additional advantages. Pressing and sintering, hot isostatic pressing and powder injection molding are being used**.** The properties of P/M implants are comparable with those of the wrought alloys. Furthermore, through P/M route one can increase certain properties by micro alloying **.**It also offers the possibility of fabricating near-net shape parts with a porous surface, providing suitable location sites for bone growth**[24].**

1.3. Application of CoCrMo alloy

1.3.1 . Dental Implant

Since 1949 it has been estimated that over 80% of partial dentures were made of CoCrMo alloy, and after 1969, more than 87%. In present almost all the metal plates of partial dentures are made of Co-Cr-Mo alloys **[25].**

Metal alloys based on chromium and cobalt are widely used in the dentistry field, as dental works and medical instruments. CoCrMo casting alloys have been used for many years to achieve partial dentures, replacing almost all gold alloys **[26].**

Metals and alloys used in dental applications should have, at least the following properties:

- chemical properties of the dental work should provide good resistance to corrosion and respectively no physical changes on contact with oral fluids **[27];**

- mechanical and physical characteristics, such as conductivity, melting point, strength and thermal expansion coefficient should be favorable, showing changes from one application to another, with certain minimum value;

- the chemical nature of the alloys should not cause toxic or allergic reactions to the patient;

- alloys, metals and materials must be easily accessible, in case of emergency and relatively inexpensive **[28].**

The cast CoCrMo alloys are used on a large scale on manufacturing of various surgical devices, which are implanted in the body **[29].**

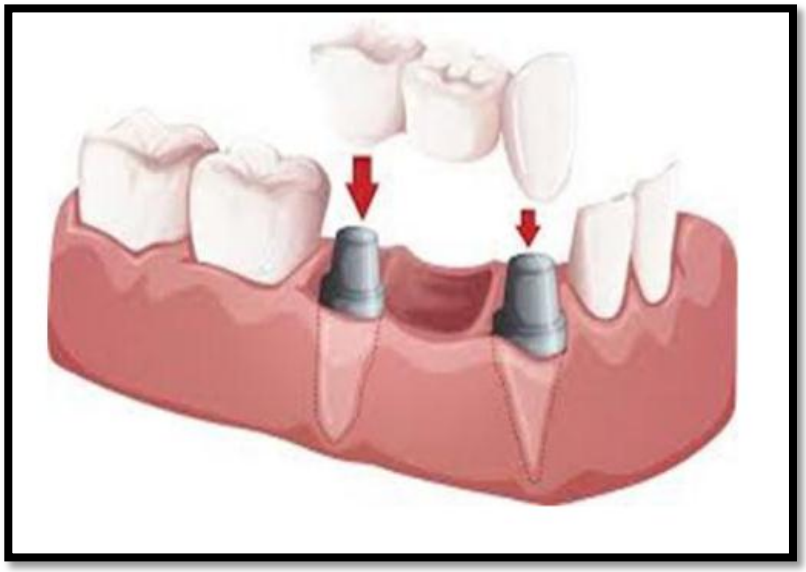

Figure(1.2): Dental Implant **[30]**

1.3.2. Orthopaedic implants

CoCrMo is a biomedical grade alloy which is widely used in the manufacturing of orthopaedic implants such as hip and knee replacement joints

because of it has high hardness, high corrosion resistance, and excellent biocompatibility**[31].**

1.3.2.1.Knee Implant

Co-Cr-Mo alloys have been used for many decades in making artificial joints due to their excellent wear and corrosion resistance even in chloride environment due to the spontaneous formation of passive oxide layer within the human body environment **[32].**Unfortunately, human joints are prone to degenerative and inflammatory diseases that result in pain and joint stiffness which requires surgery to replace it. Figure (1.3) shows an example of a knee replacement and how the alloy sits in the joints to replace the damaged parts **[33].**

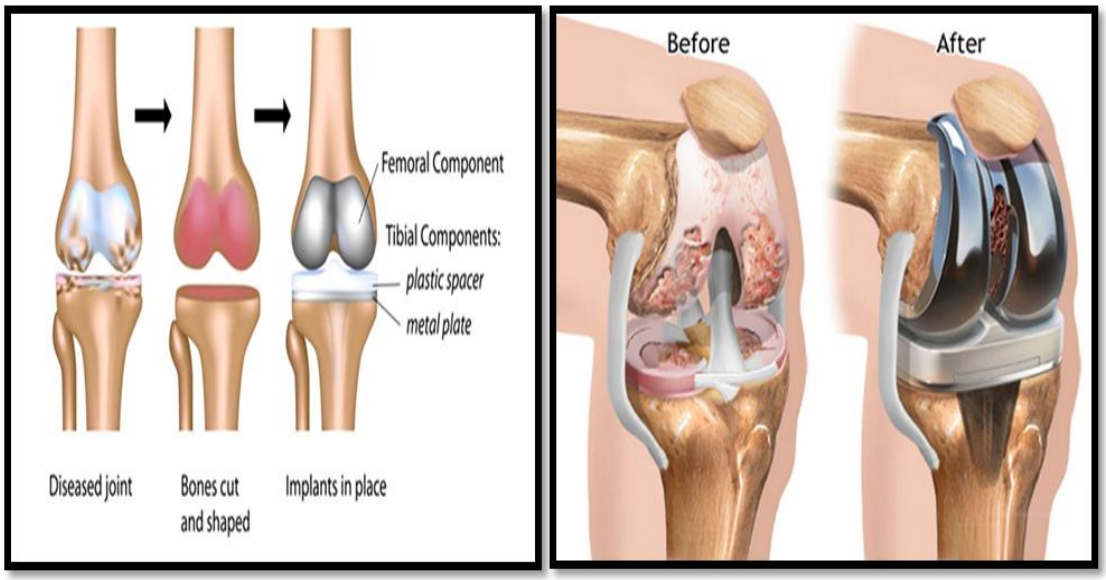

Figure(1.3): knee implant **[34]**

1.3.2.2. Hip replacement

Hip replacement is the other orthopedic application which uses cobalt chrome alloy it was first performed in 1960. This is also done when a specific part in the hip is damaged or infected which requires replacement an alloy is used through surgery to replace it. The alloy is used for its high

biocompatibility with the body tissues and blood, and also the high corrosion resistance. Fig (1.4) shows an example of the hip replacement **[35].**

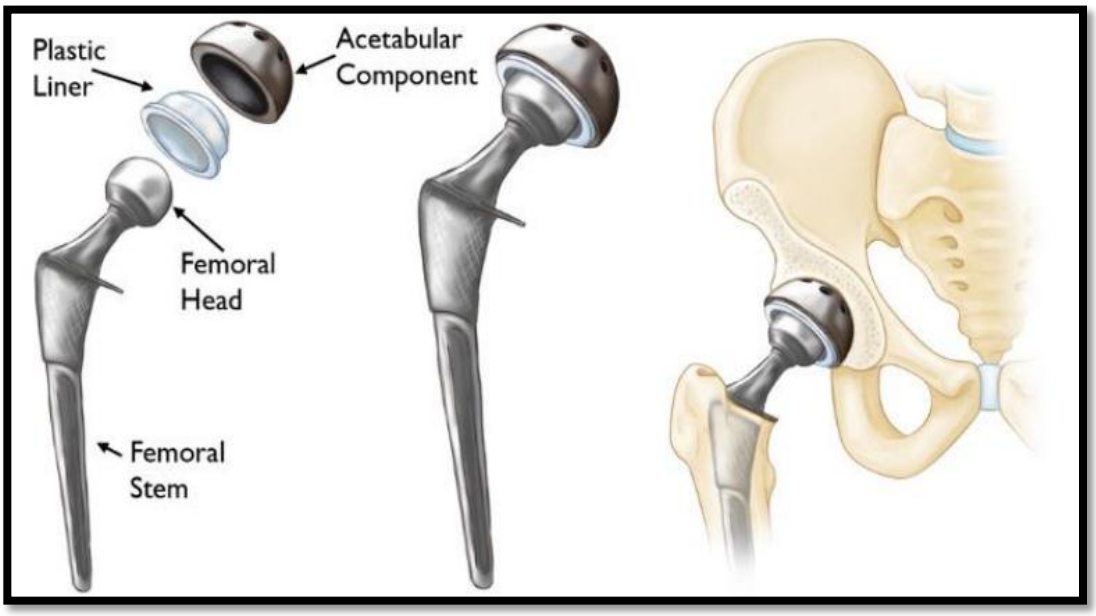

Figure(1.4): Hip Replacement**[35]**

1.3.Spinal implants

Spinal implants are often made of different types of elements such as titanium alloy, stainless steel ,and even CoCrMo. They come in different shapes and sizes to accommodate different ages. There are different types of spinal implants and they include rods which are used along with hooks and screws to immobilize involvement in spinal levels and to contour spine into correct alignment. Pedicle screws, they are specially designed screws which are controlling implanted into the pedicles of the spinal vertebrate. Finally, plates are often used in the cervical spine. Figure (1.3) shows an example of the spinal implant**[36].**

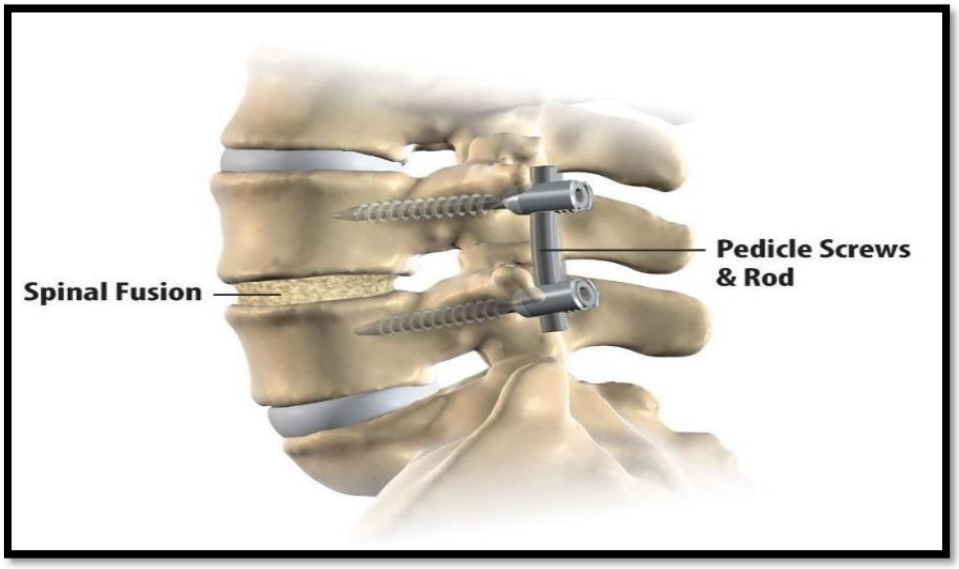

Figure (1.3): Spinal Implant **[36]**

1.4.Aim of this work

The aim of this work to prepare biomedical CoCrMo alloy(F75) via powder metallurgy technique further to investigate the influence of alloying elements addition of B ,W with different percentages (0.5, 1, 1.5) wt% and B_4C with (1, 3, 5) wt% on properties of the prepared alloys.

Many tests were done to evaluate the performance of preparing alloys ,these tests include:

Microstructure characterization (OM, XRD,SEM and EDS), Also Mechanical tests such as hardness, compression test and wear test were achieved. Electrochemical test such as open circuit , potentiondynamic polarization test and metals ions release were conductive in Ringer solution and artificial saliva.

Chapter Two

2.1. Introduction

This chapter provides a general description of CoCrMo alloy matter used in implants and bone construction. There will be a focus on chemical compositions, physical metallurgy, mechanical properties, biocompatiblity, microstructure, phase diagram of CoCrMo, corrosion resistance, wear properties, alloying element effect on CoCrMo alloys. and manufacturing via powder metallurgy technique (blending and mixing of the powder and sintering). This chapter includes also corrosion behavior of CoCrMo base alloy, the human body as a corrosive environment, type of corrosion in CoCrMo alloy. A suitable literature review is also presented at the end of this chapter.

2.2. Brief History of CoCr and CoCrMo Alloys

In modern history, metals have been used as implants since more than 100 years ago when Lane first introduced metal plate for bone fracture fixation in 1895**[37].** In the early development, metal implants faced corrosion and insufficient strength problems **[38].** Shortly after the introduction of the 18-8 stainless steel in 1920s, which has had far-superior corrosion resistance to anything in that time, it immediately attracted the interest of the clinicians. Thereafter, metal implants experienced vast development and clinical use. The metallic alloys found wider applications in medical implants than pure metals due to their enhanced mechanical properties and tribological properties besides good biocompatibility**[39].**

Cobalt-chromium (CoCr)alloys discovered for the first time by the researcher Elwood Haynes in 1907, and it was known as Stellite. Also, he found out that adding molybdenum (Mo) could improve the mechanical properties of CoCr alloys. In the1930s,Cobalt-chromium-molybdenum (CoCrMo) alloys were first introduced into dentistry and orthopedics under commercial name Vitallium **[40].** Cobalt-

chromium alloys have many applications in the medical field, e.g. coronary stents, intervertebral disc replacement, and knee and hip replacement **[41].**

Co-Cr-Mo alloys are playing important roles in many applications because of the good mechanical properties, good corrosion resistance and minimum ion released, and high biocompatibility as compared to stainless steels and titanium alloys. Therefore, in the case of artificial hip joints, they are used for the head of the hip prosthesis. Cobalt-based alloys are highly resistant to corrosion even in chloride environment due to spontaneous formation of passive oxide layer within the human body environment **[42].**

In the 1950s and early 1960s, metal-on-metal-type and metal-on- polymer-type artificial hip joints using Vitallium were developed. The former are represented by the McKee-Farrar joint, and the latter were pioneered by Charnley **[43].** Other Co-Cr alloys such as Co-Cr-W-Ni (L-605, HS25, ASTM F 90) **[44]**, Co-Ni-Cr-Mo (MP35N, ASTM F 562), and Co-Cr-Fe-Ni-Mo (Elgiloy, ASTM F 1058 grade 1) system alloys, which are still used in practical applications at the present time, had been developed in the early 1960s. Thus, the Co-Cr alloys have a long history consisting of more than 80 years of use as dental and medical materials. Currently, cast and wrought Co-Cr alloys are widely used for implants such as artificial joints, denture wires, and stents. Metal-on-metal-type total hip replacements made of Co-Cr-Mo alloys were revived in the late 1980s **[43]** because the loosening of the metal-on-UHMWPE (ultrahigh molecular weight polyethylene)-type artificial hip joints was found to be related to osteolysis caused by the formation of UHMWPE wear debris **[45].**

2.3. CoCrMo Phases and Phase Diagram

According to the phase diagram (figure 2.1), CCM alloy consists of two primary phase matrixes: 1) γ-fcc phase 2) ε-hcp phase. The γ-fcc is the high temperature phase and is formed at room temperature by quenching the CCM alloy.

The ε-hcp phase is the low temperature phase characterized by plate like striations (martensite) in the microstructure. The ε-hcp martensitic phase is known to enhance strength and wear resistance of the alloy but it also leads to low elongation or poor elongation. Various tensile test experiments on CCM alloys with ε-hcp phase as dominant phase have shown brittle fracture with poor elongation and UTS. It also results in high strain hardening exponent. On the contrary, γ-fcc metastable phase at room temperature has shown impressive elongation behaviour and UTS. Precipitation strengthening in the form of carbides and nitrides further improves the mechanical properties for room and high temperature applications**[46][47].** Hence, considerable amount of research has been done to obtain metastable γ-fcc phase matrix for CCM alloys in comparison to ε-hcp phase matrix.

According to Thermo-Calculation the following five phases are present in the (cobalt-chromium binary system above 800◦C Figure (2.1))

-Liquid phase

-Cobalt-rich face-centered cubic (FCC) phase

Cobalt-rich hexagonal close-packed (HCP) phase

-Sigma phase

-Chromium-rich body-centered cubic (BCC) phase

The melting point of pure cobalt and pure chromium is 1495◦C and 1906◦C respectively.

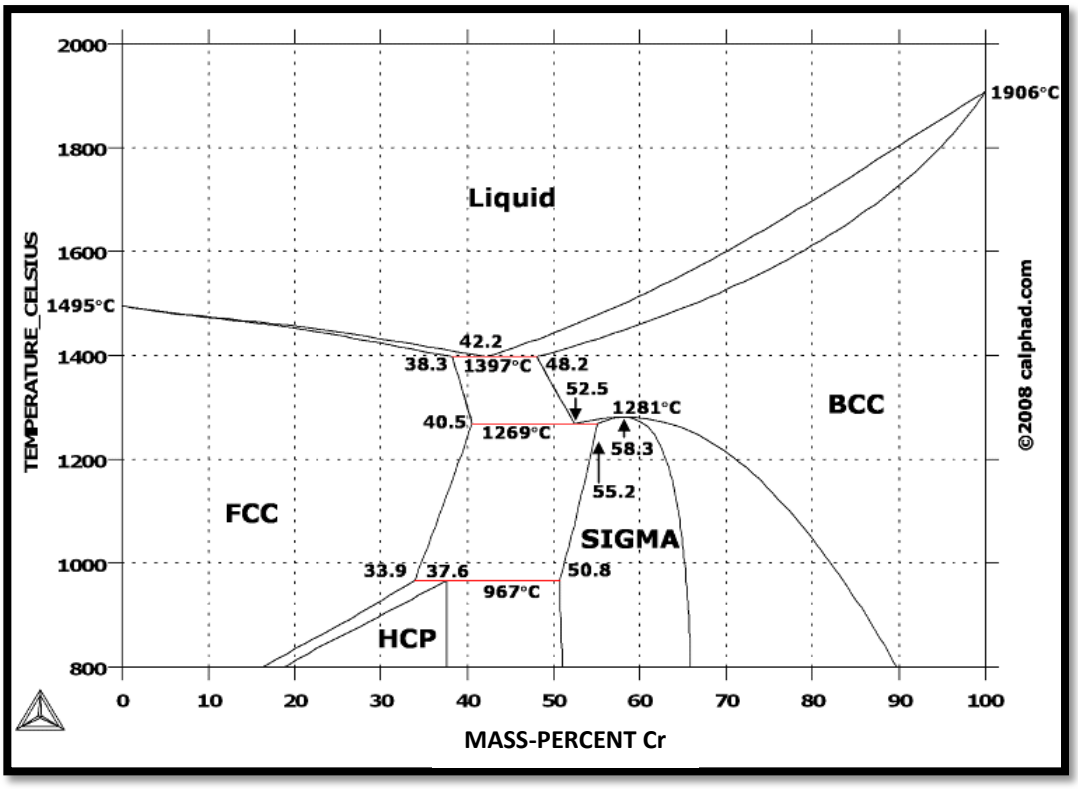

Figure (2.1) **Co-Cr phase diagram [48]**

2.4. Microstructure of CoCrMo

Processing techniques used to fabricate a final product influences the mechanical properties of metals. Thermal and mechanical strains can influence the microstructure of CoCrMo materials and ultimately the material properties. The microstructure can provide an insight into the processing history of the metallic sample of interest. One important relationship is between microstructure and mechanical properties. The microstructure of an alloy is a detailed view of grains and (orderly array of crystal lattices in space) and grain boundaries (higher energy sites with great atomic distortions). Smaller grains result in a higher yield strength for the material. Grain size and second phase precipitates can affect strength, ductility, and wear resistance. Metallurgical methods can be used to adjust these properties **[49].**

Another mechanism to improve mechanical properties of homogenous alloys (single phase solid solutions) is through solid solution hardening. Heterogeneous

alloys (multiphase alloys) mechanical strength is determined by the size and distribution of the different phases. The fabrication of implants casting of Co-Cr based alloys is not a preferred technique, as solidification during casting results in large dendritic grains **[50].**

The CoCrMo as-cast F75 alloy has been in alloy used in orthopedic implants since the 1950s. Hot-isostatic pressing (HIP) and homogenization heat treatments have been routinely used to improve the mechanical properties by reducing the porosity in castings. Hot isostatic pressing can sinter fine powders that are then forged to a final shape **[51].**

Typical microstructures after forging is 8 microns – significantly smaller than the as cast alloy **[52].** Figures (2.2) and (2.3)shows typical as-cast (F75) and wrought (F1537) Co-28Cr-6Mo microstructures, respectively. As-cast microstructures tend to display a lamellar or dendritic microstructure, whereas wrought alloys to show an equiaxial structure.

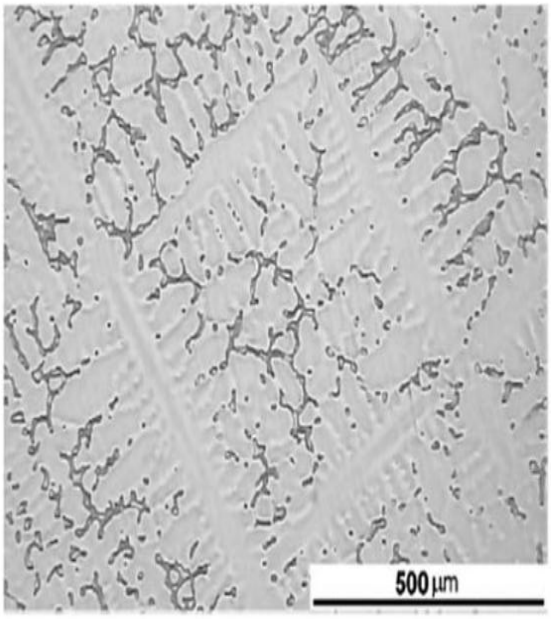

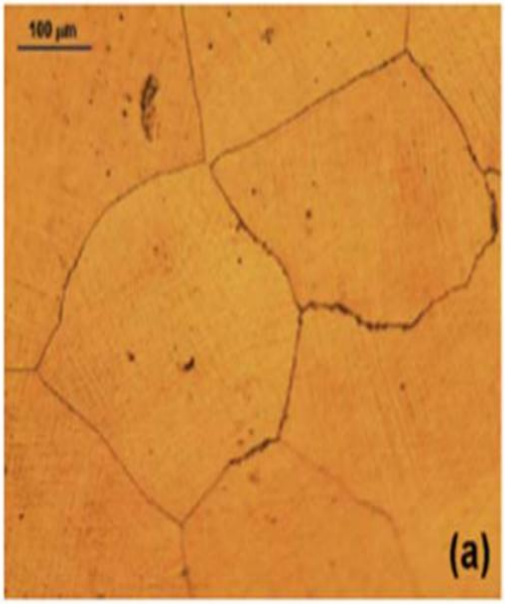

Figure (2.2): Typical As-Cast Microstructure (left) **[53];**

Figure (2.3): Typical Wrought Microstructure (right) **[54]**

2.5. Effect of Alloying Elements

In industrial applications, cobalt based alloys are used broadly because of its high wear and corrosion resistance. These applications include unlubricated systems or high temperatures. Cobalt based alloys mainly contain multi-elements mostly (Cr), (Mn), (Ni), (Mo), (Si), (Fe), (C) and (W).

Chromium plays an important role in Co-based alloys. It has a dual function. It is vital in precipitation to strengthen as it's the main carbide former, where the carbide is chromium-rich. As well, its play important role in the matrix as a solute where it enhances strength, corrosion resistance, and oxidation. Tungsten and molybdenum serve to provide additional strength and enhance general corrosion resistance of the alloys. They participate as carbides or intermetallic compounds when present in large quantities during alloy solidification and promote the precipitation of carbide **[55].**

Nickel has the same effect of Mo and W where it serves as a strengthening solution element. In addition, it can be used to stabilize the FCC phase**[56].** Cobalt-based alloy depends on the carbon content to a maximum of 3 wt%.

Carbon content plays important role in wear resistance because of carbide formation, therefore carbide volume fraction in the alloys increase when (C) content increases .Carbon is used as low as possible in these alloys to avoid the formation of carbide.

Silicon should use in certain level for carbide-strengthened alloys .Mostly, it's important in processing due to its ability intake oxygen to form silicon oxide thus protecting the layer from oxidation**[57].**

2.6. Additions in present research

2.6. 1. Boron

Boron is a non metallic element and the only non-metal of the group 13 of the periodic table elements. Boron is electron-deficient, possessing a vacant p-orbital. It has several forms, the most common of which is amorphous boron, a dark powder, unreactive to oxygen, water, acids and alkalis. It reacts with metals to form borides. At standard temperatures boron is a poor electrical conductor but is a good conductor at high temperatures**[58].**

Table(2.1) Physical properties of Boron[58]

Density at 20°C	Melting Point	Atomic number	Atomic mass
2.3 $g.cm^{-3}$	2076 °C	5	10.81$g.mol^{-1}$

Cobalt based alloys may also acquire other elements for special objectives, for example, addition of boron (B) can reduce the Tm of the alloy, therefore it reduces the needed temperature for the furnace. Otherwise , the presence of boron can enhance the mobility of the alloy during the hard facing welding operation owing to the feature of low melting point **[59, 60].**

2.6.2. Tungsten

Tungsten (W): is a transitional element that belongs to group VI of the periodic table of elements, together with molybdenum and chromium. Tungsten is not oxidized in air at ordinary temperatures and is highly resistant to acids. Its chemical properties resemble those of molybdenum**[61].**

Industrial, medical, and military uses of tungsten have been expanding rapidly; therefore, the potential tungsten spread into the environment is rapidly increasing **[62].** Tungsten is a valuable metal because it has the highest melting point of all metals, as well as great strength at high temperatures and good conductivity for

electricity and heat. It is used to increase the hardness and tensile strength of steel; it plays a vital role in the production of a number of other alloys noted for their hardness, such as the chromium, cobalt, and tungsten alloys used for tipping and facing lathe tools**[63].**

Table(2.2) Physical properties of Tungsten [61]

Density	melting point	atomic number	atomic weight	oxidation states
19.3 g/cm^3	3410°C	74	183.9	+2, +3, +4, +5,+6

2.6.3. Boron carbide

Boron carbide (B_4C) is a high-performance ceramic particle that has low density, a large degree of chemical inertness, thermal stability at elevated temperatures, and outstanding thermo-electrical characteristics**[64].** The extra hardness of boron carbide provides it the surname "black diamond."B_4C ceramic particles are produced by carbothermal reduction process of boron oxide (B_2O_3) and carbon in an electric arc furnace**[65].**

Boron carbide applications are concentrated where hardness is the principal requirement, including grit blasting nozzles, bearings, light-weight ballistic armor, etc. For these applications it is normally processed by hot-pressing in order to optimize the properties, since it does not sinter readily except at very high temperature (>2100◦C). Its use as a matrix for composite materials is very limited as a consequence**[66].** B_4C particles have outstanding physical and mechanical properties such as a high melting point and hardness, good strength to abrasion, high impact strength, excellent chemical resistance, and high absorption capacity for neutrons**[67].**

2.7. The criteria of using CoCrMo alloy as a biomaterial

Biomaterial in the body depends on factors such as the material properties, design, and biocompatibility of the material used, as well as other factors not under control of the engineer, including the technique used by the surgeon, the health and condition of the patient, and the activities of the patient. In cobalt chrome alloy there are three main reasons for the choice of the biomaterials these include **[1]:**

2.7.1. Mechanical properties

The implant must have the balance required for the physical and mechanical properties needed to perform what is expected. The specific improvement of properties such as ductility, elasticity, yield stress, and time-dependent deformation, absolute strength, fatigue strength, hardness, and wear resistance depending on the type and functions of the implant segment **[68].**

Because of their excellent mechanical properties, high corrosion resistance, and high wear resistance, Co-Cr alloys have been recognized as effective metallic biomaterials and have been used as materials for dental and medical devices since a cast Co-Cr-Mo alloy, Vitallium, was developed in the 1930s. Further increases in the usage of Co-Cr alloys are still expected as well. Their wear resistance properties are particularly excellent as compared with those of other metallic biomaterials such as stainless steels and Ti alloys**[69].**

2.7.2. Chemical properties

It is well known that the main reason for cytotoxicity is related to metal ion release due to the relatively poor corrosion resistance of the materials in the aggressive medium found in the human body **[70].** Although oxides that are usually formed on the metal surface can act as an anti - corrosion burrier, it is not strong enough to act as a protective layer to prevent extensive corrosion. From the point of view of safety, there is no doubt that the enhancement of anti - corrosion and anti-

wear properties are required before the materials can be widely applied clinically **[71].**

In recent years the biocompatibility is realized by the formation of surface layers. The anticorrosive depends on the surface of the chrome oxide layer passive film. This is connected with the biological activity of the implanted metals and their corrosion. It's known that cobalt based alloys have not only high corrosion resistance but also low toxicity even if the concentration is 1000 higher than normal **[72].**

2.7.3. Biocompatibility

The materials applied as implants are expected to be highly nontoxic and should not cause any inflammatory or allergic reactions in the human body. The achievement of the biomaterials is essentially dependent on the response or the reaction of the human body with the implants, and this determines the biocompatibility of a material**[73].**

One of the recent definition of biocompatibility is "the ability of a biomaterial to perform its desired function with respect to a medical therapy, without eliciting any undesirable local or systemic effects in the recipient or beneficiary of that therapy, but generating the most appropriate beneficial cellular or tissue response in that specific situation, and optimising the clinically relevant performance of that therapy" **[74].** In metals, biocompatibility involves the acceptance of an artificial implant by the surrounding tissues and by the body as a whole. The metallic implants do not irritate the surrounding structures, do not incite an excessive inflammatory response, do not stimulate allergic and immunologic reactions, and do not cause cancer**[75].**

The two main factors that influence the biocompatibility of a material are the host response induced by the material and the degradation of the material in the body environment. Bioactive materials are highly preferred as they give rise to high

integration with the surrounding bone, however, tolerant implants are also accepted for implant manufacturing. When implants are exposed to human tissues and fluids, several reactions take place between the host and the implant material and these reactions dictate the acceptability of these materials by our system **[74].**

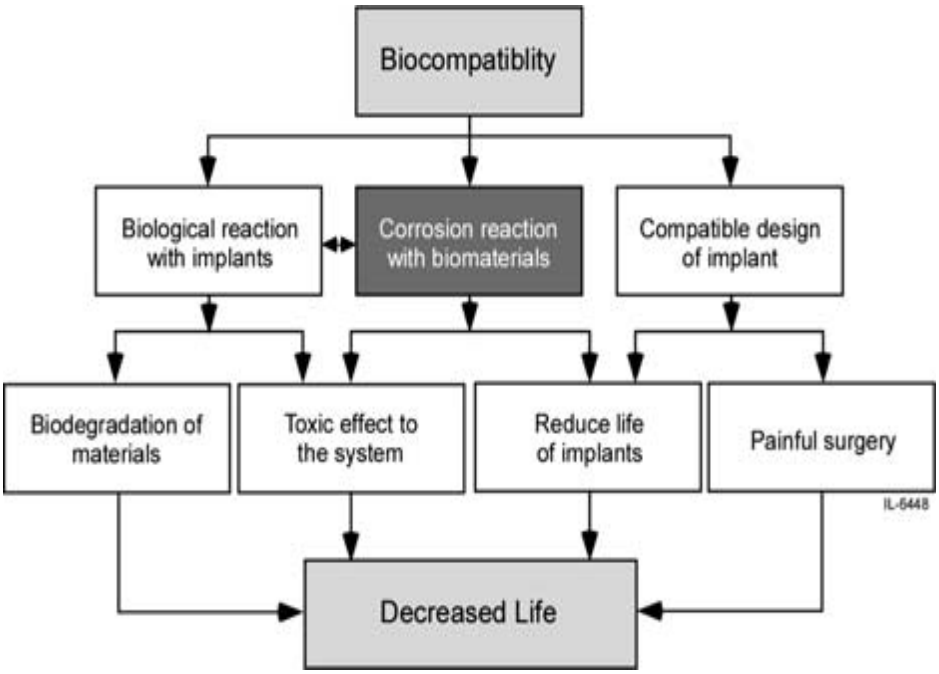

Fig. (2.4) Factors and their effects on biocompatibility **[76].**

2.8. Corrosion of CoCrMo alloy

The corrosion resistance of the implant alloy is a very important determinant of its biocompatibility. The nature of the environment and the surface treatments has a marked influence on corrosion**[77].**

In metallic biomaterials, corrosion is the undesirable chemical reaction of metal with its environment. Tissue fluid in the human body contains proteins, water, dissolved oxygen and other various ions including hydroxide and chloride. As a result, the human body posses an extremely aggressive environment for metals used in implantation. So, the resistance of corrosion of a metal implant is main requirement of its biocompatibility. Table (2.3) show Comparison of Stainless Steel , Cobalt-Chrome, Titanium and Nitionl **[78].**

Table (2.3) Comparison of Stainless Steel , Cobalt-Chrome, Titanium and Nitionl [78].

Attribute	Stainless Steel	Cobalt-Chrome	Titanium	Nitinol
Strength	medium (300/560 MPa)	high (600/1140 MPa)	high (880/950 MPa)	high (500/1400 MPa)
Stiffness	high (200 GPa)	High (200 GPa)	moderate (90 GPa)	very low (~25 GPa)
Fatigue	Good in load control	Good in load control	Good in load control	Good in strain control
Corrosion	Good – Cr_2O_3 (500 mV)	Good– Cr_2O_3 (500 mV)	Excellent – TiO_2 (800 mV)	Excellent – TiO_2 (800 mV)
Other	MRI artifacts	L-605 is radiopaque	Can be radiopaque	Shape Memory

Co-Cr-Mo alloys have high corrosion resistance in compared with stainless steel especially in the human body as a result of high contents chromium that forms a thin film of a passive oxide of chromium (Cr2O3)**[79].** This film serves as a barrier to corrosion reactions and forms spontaneously on the Co-Cr-Mo alloy surface, as well it separates the metal surface from the environments. Furthermore, molybdenum contents are applied to improve localised corrosion resistance. In the absence of passive films the driving force for the corrosion of implants increases. The integrity of these films is correlated strongly to the chemical and mechanical stability of implants in the human bodies**[80].**

2.8.1.Types of Corrosion in CoCrMo alloy

CoCrMo alloys forms a protective oxide (Cr2O3) layer. The protective nature of this film is determined by the film's composition, structure, thickness, and the amount of defects present. Additionally, environmental factors (pH, chloride ions, exposure duration, etc.) can alter the protectiveness of this film. Also the corrosion behavior of such alloys is influenced by manufacturing conditions (cold working and thermal treatments) **[81]**

The passive film of CoCrMo is the kinetic limiting barrier to corrosion in aqueous solution. It acts as a physical barrier to both cation and anion transport to the metal surface, and a barrier to electron dissolution. The human body is a highly corrosive environment for metals and this oxide film is the barrier between a well-functioning hip replacement and revision surgery. Body fluids (human plasma, synovial fluid of joints) are composed of 0.9% sodium chloride (NaCl) with additional inorganic salts and various protein molecules (synovial fluid has hyaluronic acid and lubricin, and the plasma has albumin, transferrin, globulin, fibrinogen) **[81].**

Corrosion may be general or localised. General corrosion involves the uniform dissolution of the metal surface. In contrast, localised corrosion can take place on a passive metal surface in the presence of aggressive ions. Here, localised attack occurs in specific sites where there are high local dissolution rates, which lead to high rates of penetration **[82].**

Chloride ions will enhance the localised corrosion process and occur at local sites caused by imperfections where there are pits or inclusions **[83].**

There are several forms of localised corrosion, but pitting, crevice corrosion, fretting, and tribocorrosion are the most relevant types of artificial hip joints.
Pitting corrosion is confined to a point or small hole within the metal. Pitting can initiate at sites where there are small surface defects such as a scratch or a dent, a small change in chemical composition of the alloy or damage to the oxide film. In the pit, there is a rapid depletion of oxygen, and the pit becomes a net anode, undergoing rapid dissolution. This anodic reaction produces electrons that are used in oxygen reduction reactions at the external surface. The generation of metal ions in the pit cavity leads to a net positive charge in the pit, resulting in an influx of chloride ions to maintain the charge balance. Hydrolysis of metal cations causes a

decrease in pH. These factors promote pit growth, as high Crevice corrosion is associated with the formation of stagnant solution in crevices or occluded areas such as those formed under washers, fastener heads, lap joints, and clamps. The mechanism of crevice corrosion is similar to that of pitting corrosion: depletion of oxygen, more acidic conditions and build-up of aggressive ionic species such as chloride enhance metal dissolution and produce accelerated attack within the crevice. However, the difference is that an external crevice former is required to initiate corrosion on the surface **[83].**

Fretting corrosion can also occur where micro-motion between two surfaces causes depassivation leading to localised corrosion. These small amplitude displacements occur when the total amplitude of movement is smaller than the contact width of the prosthetic joint. The micromotion between the faying surfaces, which can often happen over a crevice, causes depassivation followed by a period of active dissolution during the repassivation process, increasing the concentration of metal ions in the cavity leading to acidification through hydrolysis and ingress of chloride ions for charge balance. Minor movements of the hip joint frequently occur when people adjust or change position and so fretting corrosion can accelerate wear**[84].**

Table (2.4): Types of Corrosion in the Conventional Materials Used for Biomaterial Implants [85]

Type of Corrosion	Material	Implant Location	Shape of the Implant
Pitting	304 SS, Cobalt based alloy	Orthopedic/ Dental alloy	
Crevice	316 L stainless steel	Bone plates and screws	
Stress Corrosion Cracking	C0CrMo, 316 LSS	Only in in vitro	
Corrosion Fatigue	316 SS, CoCrNiFe	Bone cement	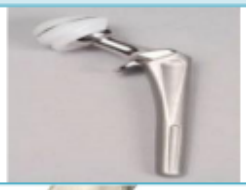
Fretting	Ti5Al2.5Fe, CoCrSS	Ball Joints	
Galvanic	304 SS/316SS, CoCr+Ti5Al2.5Fe., 316SS/Ti5Al2.5Fe or CoCrMo	Oral Implants Skrews and nuts	
Selective Leaching	Mercury from gold	Oral implants	

2.9.Wear of Metallic Biomaterials

Property of wear can be defined as damage to a solid surface, including progressive loss of material because relative motion between that surface and a contacting substance or substances as shown in Figure (2.5). Recently main concern, for further development of metallic implant materials is among others, stress transmission between hard tissue and metallic implant components which are in

contact since further bone degradation and bone adsorption should be avoided. Namely, a great difference between bone and metallic implant materials hardness and other mechanical and tribological characteristics may lead to further bone loss and degradation **[86].**

The process of wear can rupture the protective oxide film inherently present on the alloys surface, which can lead to accelerated attack in the presence of a corrosive environment **[87].**

High wear resistance avoids loosening of the implant and reactions in the tissue in which it is deposited, improving the patient quality of life. The friction that causes corrosion is a huge worry as it discharges non-compatible metallic ions .Mechanical loading can also accelerate wear processes as it results in corrosion fatigue**[88].**

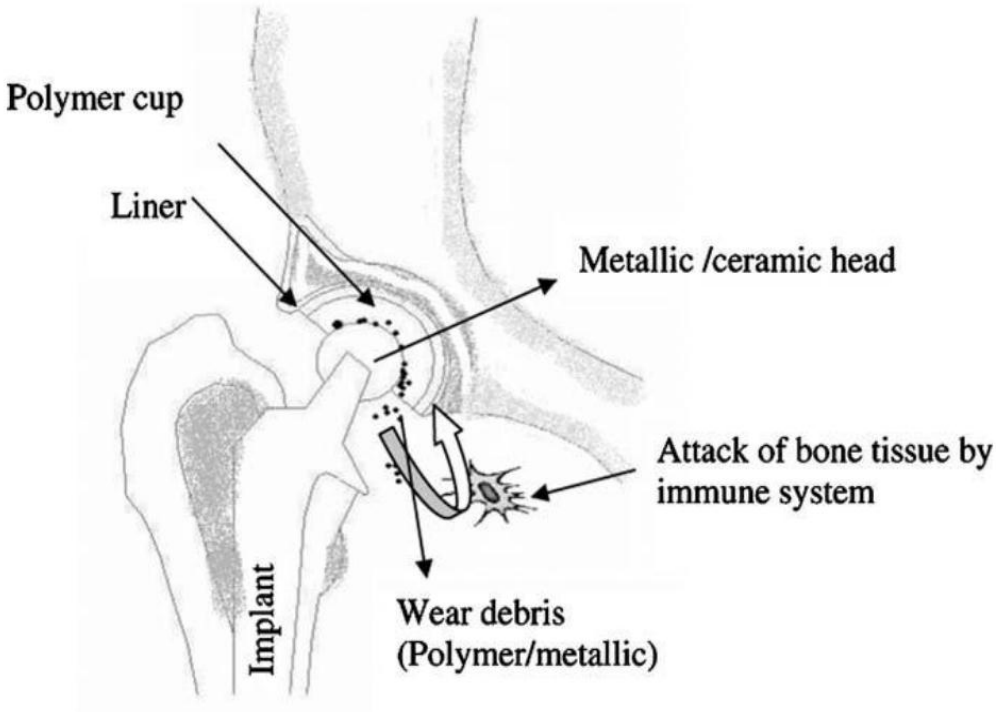

Figure (2.5): Wear of Total Joint Replacements **[89].**

2.9.1.Wear Testing Methods

Given the aforementioned limitations, especially in terms of the tribological properties, it is important to characterize the wear and friction of developed biomaterials using a suitable test methodology. The methods that are most commonly used in the study of the wear behavior of metallic biomaterials are the pin-on-disc, block-on-disc and ball-on-disc **[90].** Table (2.5) summarizes the advantages and disadvantages of various wear test configurations.

Table (2.5):Advantages and Disadvantages of Different Wear Test Configurations [91].

Test	Advantages	Disadvantages	Test format
Pin-on-Disk	After run-in,surface pressure remains constant. Easy to determine wear volume and wear rate	Difficult to stratify the pin. If the pin does not stand perfectly vertical on the plate, the edge contacts results. A very long run-in time is therefore necessary. The front edge of the pin can skim off lubricant. This makes a defined lubrication state impossible	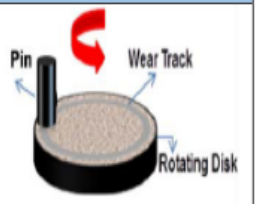
Ball-on-Disk	High surface pressures are possible. The ball skims off lubricant less than a pin does.The model is similar to a linear friction bearing and a radial friction bearing	Very small contact ratio: The contact surface of the ball is small compared to the sliding track on the disk. The contact area is enlarged by wear. Difficult to determine the wear volume of the ball.	
Block-on-disc	The model is capable of simulating a variety of harsh field conditions, e.g., high temperature, high speed, and high loading pressure.		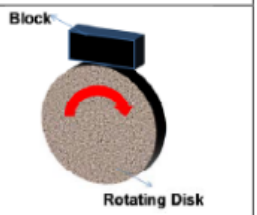

2.9.2.Wear Mechanisms

The wear mechanism depends on the load, sliding speed, hardness and roughness of the wear surface،lubrication, and so on; meanwhile, the debris feature and wear type are two external manifestations of the wear mechanism**[92].** Understanding of wear mechanisms is very important in order to design materials which are suitable for wear reduction **[93].** Wear mechanisms generally can be grouped into six generic types:

1- Adhesive Wear

The wear of adhesive is caused by the surface interaction and welding of the junctions at the sliding contact. This mechanism of wear is affected by the bonding type (metallic, ionic, covalent and van der Waals) in the contact junction. The weaker part of the materials in contact is removed and transferred to the counter surface if the bond in the junction is stronger than the bond in the bulk. Surface removal results in a rough appearance and a large volume of worn material, thereafter, severe wear **[93].**

2- Delamination Wear

The debris is plates, the length to the thickness is ten times caused by forming and fracture such as a cylinder in internal combustion machining may by occur in abrasive wear. It is seen that the ductility increases the strength of material against delamination **[91].**

3- Fatigue Wear

The debris of wear is generated by cyclic loading of the contact. Fatigue wear can be characterized by crack formation and flaking of surface material **[93].**

4- Erosion Wear

Caused by impact of solid or liquid or gaseous particles form losses in weight or removal of particles in which the fluid carry the particles .it is depended on the kinetic energy for particles and the emission of the energy on the surface.

5- Tribochemical Wear

Tribochemical wear results from the removal of reaction products/layers formed in situation from the contacting surface.

6- Abrasive Wear

The remove of material by hard particles slide between two surfaces in relative motion. The surface deforms plastically and grooves are produced in the surface **[94].** More than one type of mechanism can be involved in a wear situation. Also, these individual mechanisms can interact sequentially to form a more complex wear process. However, one mechanism generally is the controlling and primary mechanism. The relative importance or occurrence of individual mechanisms can change with changes in tribosystem parameters. Therefore, materials can exhibit transitions in wear behavior as a result of changes in other operational parameters, such as load, velocity, and friction**[95].**

2.10. Processing Techniques of CoCrMo alloy

The properties of CoCrMo alloys are affected obviously by the manufacturing operation. Fabrication technique can be classified as casting and powder metallurgy.

2.10.1.Casting

Processes of casting are among the oldest methods for industrialization metal goods. In more early casting processes (much of which are still used today)whereby a totally molten metal is poured into a mold cavity according to the desired shape;

the second step of the process is solidification, and this is when the metal assumes the shape of the mold but experiences some shrinkage**[96],** the mold or form used must be destroyed in order to remove the product after solidification. The need for a permanent mold, which could be used to product components in endless quantities, was the obvious alternative **[97]**.

Casting techniques are employed when:

1. the finished shape is so large or complicated that any other method would be impractical, 2. a particular alloy is so low in ductility that forming by either hot or cold working would be difficult, and 3. in Compared with other manufacturing processes, the final step in the refining of even ductile metals may involve a casting process **[96].**

The casting process involved the following steps:

1. Melting
2. Pouring it into a previously made mould
3. Allowing the molten metal to cool and solidify in the mould.
4. Remove the solidified component from the mould and cleaning it **[98].**

2.10.2 Powder Metallurgy

The powder metallurgy technique aims at converting metal powders, utilizing pressure and heat, by a thermal process (sintering) that eliminates the traditional melting and is done below the melting point of the most critical product. The use of the P/M in the biomedical area is recent and its great advantage is the production of prosthesis near to the final format (near net shapes), dense or with controlled porosity, and generally less expensive than the conventional processes **[99].**

The steps include: Preparation of powders, blending and mixing of powders, cold compaction, and sintering **[100][101].**

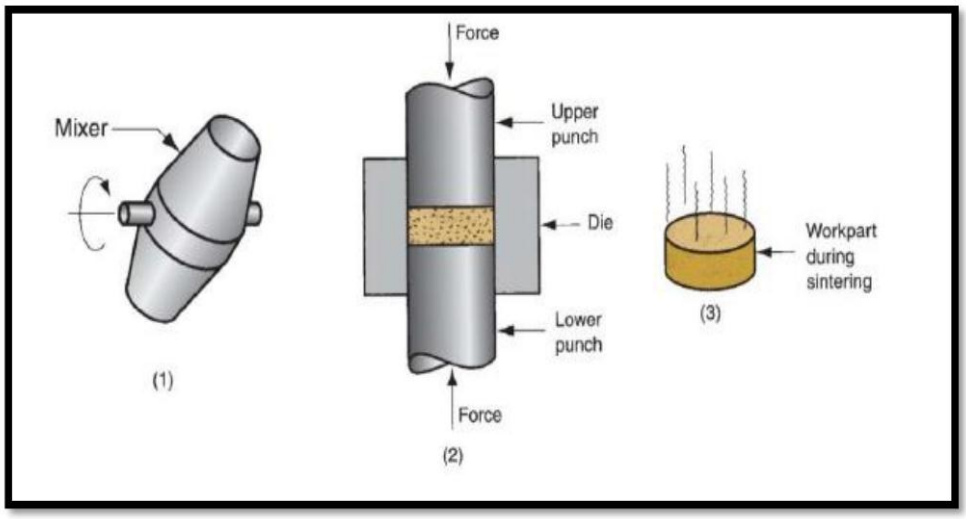

Figure (2.6): Basic Steps of Powder Metallurgy Technique: (1) Mixing of Powders; (2) Pressing of Powders; (3): Sintering **[101].**

The performance of metal powders during processing and the properties of the products are dependent upon the characteristics of the metal powders that are used, such as particle shape, particle size, particle size distribution, compressibility of powders, apparent density, and purity of powders **[102].**

Powder metallurgy is an important commercial technology and this because of the following considerations:

1.PM parts can be accumulated and produced to net shape or near net shape, which eliminate or decrease the requirement for subsequent machining **[103].**

2.PM process is low in wasting materials -about 97% of the starting powders are converted to product **[104, 105]**. This compares satisfactorily to processes of casting in which sprues, runner, and risers **[104].**

3.In PM parts, a production of porous metal parts such as filters, gears, and oil-impregnated bearings can be made with a particular level of porosity **[106].**

4.Some metals that are hard to manufacture by other methods they can be shaped by powder metallurgy such as Tungsten filaments for incandescent lamp bulbs [105].

5.PM distinguishes in a way of producing such as certain alloy combinations and cermets made by PM cannot be shaped in other ways **[104].**

6.PM is the most favorable casting processes in dimensional control, tolerances of + 0.13 mm is held regularly **[104].**

There are Limitations associated with PM processing **[107]:**

1.Owing to the fairly high compacting pressures required to press the powder, the wear on the dies is high.

2.Due to high rate of wear of dies, high costs for dies and presses the method is rendered uneconomical particularly for small runs.

3.Since the compacted parts must be ejected from the die without fracture, therefore, the shapes that may be made by this method are limited.

4.Equipments required are very costly.

5.A completely dense product is not possible without heating the product after pressing operation.

6.In the low melting powders such as zinc, tin, and cadmium, occasionally some thermal difficulties appear..

7.The physical properties obtained by this process are lower than those obtained by other processes.

2.10.2.1 Blending and Mixing of the Powders

Blending is an operation of intermingling of powders of the same composition or substance but possibly different in particle sizes. The metallic powders must be completely homogenized to ensure successful compaction and sintering outcomes. Different particle sizes are often blended to reduce porosity, while mixing is defined as the through intermingling of powders of several or more different materials **[92].**

The mixing process is used to produce a homogeneous distribution of powders in least possible time. The mixing time will range from a few minutes to 24 hours or even a few days depending on the results desired. Long mixing time leads to work hardening of particles, thus it must be avoided. Mixing may be either dry or wet. Wet mixing is used to produce a uniform mixture of powder particles. It may be obtained by the addition of alcohol, benzene or acetone as a liquid medium in adequate amount in order to bring the powder to the consistency of a thin paste. After completion of the mixing process, benzene or acetone is removed by during the mix in air or in a controlled oven up to 50 ºC **[108, 109].**

2.10.2.2 Compacting of the Powders

The compaction process is the shaping step which the very complex geometries can be achieved with sufficient strength to withstand ejection from the tools and subsequent handling up to the completion of sintering, without breakage or damage. The pressure used for producing green compact of the component depends upon the material and the characteristics of the powder used. The compacting process must be designed so as the pressure will be uniformly distributed on the affected area **[110].**

The part after compacting is called a green compact with a density called the green density, Figure (2.7) illustrates the effect of the compaction pressure [**92].**

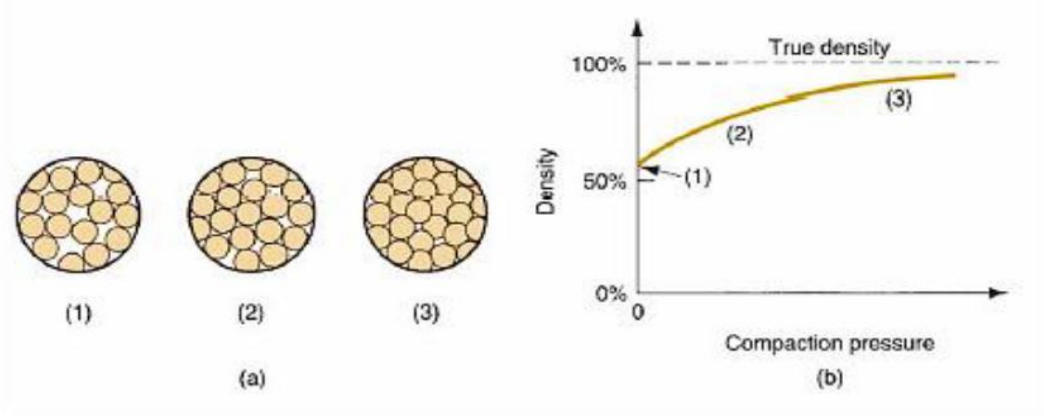

Figure (2.7): (A) Effect of Pressure on Particles Arrangement during Compaction; (B) Density of the Powders as a Function of Pressure **[92].**

2.10.2.3 Sintering

The Sintering process is a heat treatment operation performed on the green compact to bond its metallic particles in order to increase strength and hardness**.** The treatment is usually done at temperatures between 0.7and 0.9 of the melting point of the metal**.** Sintering processes can be divided into two types: solid-state sintering and liquid-phase sintering**.** The solid-state sintering which termed when the metal remains un-melted at the treatment temperatures. The liquid-state sintering termed when a minor constituent become molten at the treatment temperature, the amount of liquid phase must be limited so that the part retain in shape**[111]** .Figure(2.8) shows on a microscopic scale, the changes that occur during sintering of metallic powders **[92].**

The driving force of solid state sintering is the difference in free energy or chemical potential between the free surface of the particles and contact points of linked particles **[112].**

The rate of particle bonding during sintering depends on temperature, materials, particle size. Small particles are more energetic, so they sinter faster. Parameters such as particle size and surface area, temperature, time, green density, pressure, and atmosphere are effective parameters during sintering **[113].**

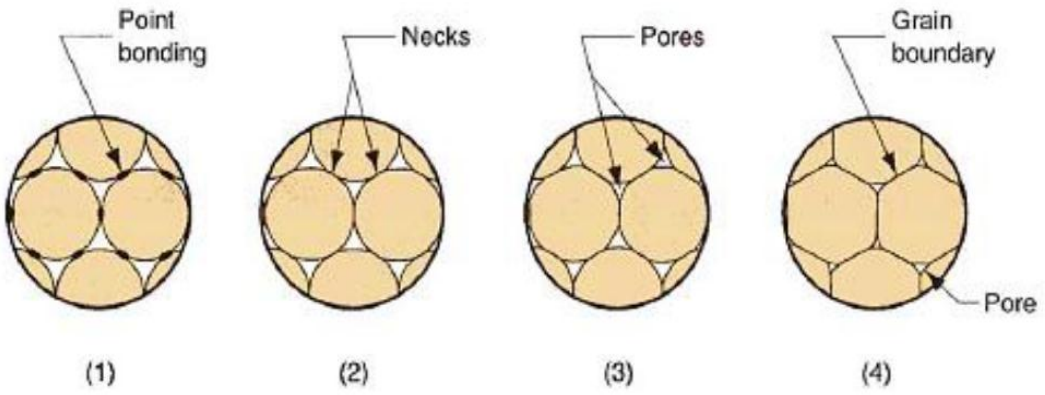

Figure (2.8): Change during Sintering of Metallic Powders: (1) Particles Bonding is started at Contact Region; (2) Contact Region Grow into Necks; (3) The Pores between Particles are Reduced in Size; and (4) Grain Boundaries Develop between Particles in Place of Necked Regions **[92].**

2.11 Effectof Sintering Temperature andTime on Porosity

The porosity of a part in powder metallurgy is highly dependent on the sintering temperature and its duration. At sintering, diffusion processes cause necks to form and grow at these contact points and densification of P/M compacts can be achieved during sintering **[114].**

Generally, higher sintering temperatures and longer sintering times promote greater densification of sintered parts. So the mean density of parts prepared by the powder metallurgy process is increasing with the increase in sintering temperature. It is mainly due to the decrease in total fractional porosity with the increase in temperature and time of sintering as shown in Figure (2.9) **[115, 116].**

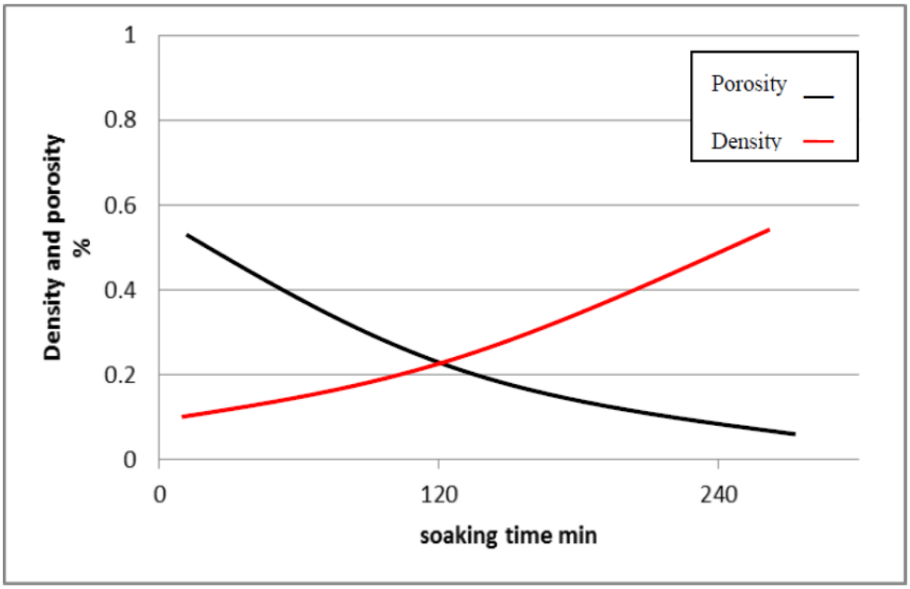

Figure (2.9):Effect of sintering time on the porosity and the density of sintered parts**[116].**

2.12 Literature Review

Numerous studies have been made on Cobalt chromium alloy as implant alloys in human body.

In 2005, Robert W.W., et al., [117] studied the electrochemical corrosion of cast Co-28Cr-6Mo implant alloy in different biological solutions (serum, urine and joint fluid) by using cyclic voltammeter, potentiodynamic scan and impedance spectroscopy method. It was observed that Co–Cr–Mo implant has corrosion current densities between 1.65–2.59 μA/cm2in three biological solutions. Impedance and Tafel analyses plot results found same indications. It's concluded that the resistance of Co–Cr–Mo implant alloy to corrosion in joint fluid and serum at 37ºCis better than that of urine.

In 2007, Lee, S.H., et al.,[118] studied the effect of Fe addition on the microstructures and mechanical properties ,A series of Co-Cr-Mo alloys with Fe contents ranging from 5 to 20 mass% were prepared in order to study the effect of Fe addition on the microstructures and mechanical properties (tensile strength, yield strength, elongation, and Rockwell C scale hardness) of Ni- and C-free Co-CrMo alloys. Fe was added with the composition of Co-29Cr-6Mo-xFe (where x ¼ 0, 5, 10, and 20). Alloys were heat-treated at 1230C for 3 h and 1250C for 5 h. These heat treatment conditions were decided as considering pre-heat treatment followed by hot-forging process. An optical microscope and an XRD were used to determine the microstructure and identify the crystal structure. The volume ratio of phase to " phase increases not only with heat treatment temperature and time but also with Fe content. The tensile strength, yield strength, and elongation are significantly improved by Fe addition. However, the tendency toward phase formation becomes higher as the Fe content increases, causing a deterioration of mechanical properties. From the viewpoint of mechanical properties, the amount of Fe addition should be less than 10 mass% in pre-heated condition of Co-29Cr-6Mo alloys.

In 2008, Dourandish, M., et al.[119] investigated the sintering of biocompatible CoCrMo alloy manufactures stepwisely for porosity-graded composite structures. These composite structures provide strength at the core and a porous layer for the

tissue growth. To evaluate the process a two grades of gas atomized CoCrMo powder with an average particle size of 19 and 63 μm were used. The microstructural of the sintered specimens was evaluated. The findings showed an intermediate sintering temperature of 1280C° for 120 min and argon can be used in developed of the porosity graded composite layers can be produced e.g. a relative dense core (5% porosity) with a porous layer (33% porosity).

In 2008 Lee, S.H., et al. [120] focused on the significant improvement in mechanical properties of biomedical Co Cr Mo alloys with combination of N addition and Cr enrichment. An examination of a Ni free Co, Cr and Mo alloy under as cast condition was done by means of tensile tests and microstructure observations. The findings of the observation shows that the solubility of N in CoCrMo alloys increases with increasing Cr content from 29 to 34 mass %. This result suggests that there is a significant improvement in mechanical properties such as yield stress, tensile stress and fracture elongation. Also the increasing amount of Cr content has also contributed to the improved mechanical properties

In 2009, Songur, M., et al. [121] investigated the electrochemical corrosion properties of metal alloys used in orthopaedic implants. The study investigated 316 stainless steel, CoCrMo and Ti6A14V alloys in simulated body conditions at 37C° by using Tafel Plots, mixed potential and electrochemical impedance spectroscopy. The results show that the Ti6A14V has the highest corrosion resistance followed by CoCrMo alloy. The best pairs of alloys for galvanic corrosion with the minimum galvanic potential and current values were Ti6A14V_CoCrMo, as the mixed potential theory and Tafel method suggests. The study accomplished that the most suitable material for implant applications in the human body is Ti6A14V.

In 2011, Rodrigues, W. C., et al. [122] focused on powder metallurgical processing of Co, 28%Cr, 6%Mo for dental implants: physical, mechanical and

electrochemical properties. This study examined the powder metallurgical production of a CoCrMo alloy for dental implants in conventional parameters. The study investigated the achievement of the applications of these parameters an alloy with enough green density, low porosity after sintering, considerable hardness and impulsively passive behavior in the ringer solution. The results show that the physical, mechanical and electrochemical properties of the alloy are affected by a small variation of the sintering temperature with comparison of samples with different sintering temperatures.

In 2012, Milošev, I. [123] studied the metallic materials used in biomedical applications have become increasingly important as the number of various implanted devices, e.g., orthopedic, cardiovascular, dental, and ophthalmological implants, constantly increases. In addition to titanium-based alloys and stainless steel, cobalt–chromium–molybdenum alloy (CoCrMo) is one of the most important materials used in orthopedic applications, i.e., total hip replacements. The increasing number of implanted hip replacements is the result of the prolongation of the average life expectancy and an active lifestyle in older age. Among the diseases of the joint that in most cases require surgical treatment, osteoarthritis is the most important. After implantation of a hip prosthesis, pain is reduced and the functionality of the joint is recovered. The average lifetime of the implanted prosthesis is about 15 years. Compared to implants used in the 1970s, the lifetime of contemporary hip prostheses progressively increases because of progress in surgical techniques, treatment, material manufacturing, and quality control. The ultimate goal is to produce hip prostheses that would endure the average postsurgical lifetime of more than 20 years and enable the patient to live an active lifestyle without pain. To achieve this goal, understanding alloy behavior in vitro and in vivo is crucial.

In 2012, Balagna, C., et al.[124] aim to study the evaluation of the temperature effects on the structure, microstructure, mechanical and tribological properties of the

considered substrates (CoCrMo alloys), after the removal of the coating by polishing. The substrates are characterized through X-ray diffraction (XRD), scanning electron microscopy with energy dispersion spectrometry (SEM-EDS) and profilometry. The mechanical behavior is evaluated by the macro- andmicro-hardness and bending tests, whereas the tribological properties are analyzed through a ball on disctest. A comparison between the as-received alloys and thermal treated substrates is reported. The biocompatibility feature is not reported in this work. The substrate crystalline structure changed during the heat treatment, inducing the formation of the hexagonal cobalt phase and the decrement of the cubic one. This crystallographic modification does not seem to influence the tribological behavior of the substrates. On the contrary, it affects the strength and ductility of the substrates.

In 2013, Valero-Vidal, C., et al.[125] studied the electrochemical behaviour of thermal treated CoCrMo alloys with different carbon content in their bulk alloy composition has been analysed. Both the amount of carbides in the CoCrMo alloys and the chemical composition of the simulated body fluid affect the electrochemical properties of these biomedical alloys, thus passive dissolution rate was influenced by the mentioned parameters. Lower percentage of carbon in the chemical composition of the bulk alloy and thermal treatments favour the homogenization of the surface (less amount of carbides), thus increasing the availability of Cr to form the oxide film and improving the corrosion resistance of the alloy.

In 2014, Zangeneh, S., et al.[126] studied the precipitation of nanoscale carbides in Co–28Cr–5Mo–0.3C implant alloy during tungsten inert gas(TIG) welding has been systematically investigated. Based on the high resolution transmission electron microscopy (HRTEM) results, the nanoscale precipitates are Cr-rich M23C6-type carbides, with 10–100 nm in size, and precipitation mostly occurred at hcp/fcc interfaces. In addition, X-ray diffraction analysis(XRD) showed that higher amount of a thermal ε-martensitic (E2-fold those found in the solution-treated sample) can

be achieved after the welding process. Apparently, the higher content of a thermal martensite after welding is responsible for the precipitation of M23C6 carbides in nanoscale and significant enhancement of hardness (850 HVN) is the concomitant result of that.

In 2014, Chen, Y., et al.[127] aims to elucidate the synergy effects of this phase and carbide on the wear behavior of low-carbon (LC) and high-carbon (HC) cobalt–chromium–molybdenum (CoCrMo) alloys, by using pin-on-disc tests under Hanks0lubricated conditions. Fractured or torn-offs-phase precipitates were observed to be the main reason for abrasion for both LC and HC alloys. Carbides were torn off at the initial high contact pressure to form pitting ;s-phase precipitates around the pitting were uprooted and led to micro cracks, which is considered as surface fatigue of HC alloy. In contrast, strain-induced martensite observed on the worn surface was contributed to the increase of hardness and abrasion resistance of LC alloy.

In 2014, Abbass , M., K., et al. [128] studied the corrosion resistance properties of CoCrMo alloy which was immersed in artificial saliva at 37±1 ºC. The surface of the specimen was analyzed before and after the immersion using an optical microscope. In order to test the corrosion resistance, an electrochemical measurement by polarization was performed. The findings of the study showed that the galvanic corrosion demonstrated that the CoCrMo alloy had localized corrosion in artificial saliva at 37± 1ºC.

In 2014, Yamanaka, K., et al.[129] studied the solidification microstructures of Co–28Cr–9W–1Si (wt%) alloys with different carbon contents(0.005–0.33 wt%) were characterized using scanning electron microscopy, electron backscatter diffraction, and electron probe microanalysis. The as-cast alloys exhibited cellular dendritic microstructures, and the amount of grain boundary carbide precipitates

increased with increasing carbon concentration. It was revealed that the interdendritic segregation of Cr, W, Si, and C, resulted in interdendritic precipitation. Consequently, adding carbon was found to decrease the grain sizes of as-cast alloys. Our results will contribute to the development of disk materials made of biomedical Ni-free Co–Cr–W-based alloys with refined grain sizes.

In 2015 , Alfirano,[130] studied the effects of addition of alloying elements listed in ASTM F75, Precipitates in biomedical Co-Cr-Mo cast alloys are closely related to their wear and mechanical properties. It is important to elucidate the effects of addition of alloying elements listed in ASTM F75 on precipitation and dissolution in order to control microstructural changes in fabricating biomedical Co-Cr-Mo alloy implants. In this study, Si and Mn were selected as the alloying elements. The chemical compositions of two cast alloys were Co-28Cr-6Mo-0.25C with containing 1mass% Si dan Mn. The alloys were solution treated at temperatures at 1448 to 1548 K for holding time of 1.8-43.2 ks, followed by water quenching. The precipitates in the as-cast alloy with Si addition were M23C6 carbide, η-phase (M6C-M12C type carbide) and π-phase (M2T3X type carbide with a β-Mn structure), while M23C6 carbide and η-phase were detected in the as-cast alloy with Mn addition. The alloy with Si addition required longer solution treatment time for complete precipitate dissolution as compared with the alloy with Mn addition. The phase and morphology of precipitates observed during solution treatment depended on the heat treatment temperature and holding time and alloy composition.

In 2015, Khilfa, A. H., et al., [131] investigated the effect of Germanium and Yttrium as alloying element on the corrosion, wear, and .compressive strength behavior of CoCrMo (F75) alloy prepared by powder metallurgy technique. The prepared base alloy with the chemical composition of (62.4%Co, 28%Cr, 6%Mo, 0.5%Ni, 1%Si, 1%Mn, 0.75%Fe, 0.35%C). Each of the alloying elements (Ge and Y) was added with the percentage of (0.5, 1and 1.5) wt. % then the additives were

mixed together with 0.5%, 1% for each element at the expense of Cobalt. The powders mixed for 5hr then was compacted with a fixed compacting pressure of (800) MPa to obtain. The sintering process accomplished at temperature 950 C° for 5h under vacum conditions (10^{-4} torr). The Wear rate of CoCrMo with and without additives increases as the time and load is increased. The wear resistance increases with the addition of Ge element and it's increased as Ge additives increase. While it decreases with the addition of Y element and the wear rate of the samples increases as Ge &Y, Y content increases. The corrosion resistance of CoCrMo alloy improved after the addition of each Ge or Y in artificial saliva and Hank's solution; It was shown that higher improvement with the addition of the Ge and Y mixture where the percentage of improvement was (**886**.6%) for (1%Ge+1%Y) alloy in artificial saliva. While the improvement percentage in Hank's solution was (654.5% and 5087.5%) for each 0.5% Ge+0.5%Y) and (1%Ge+1%Y) alloys respectively. The corrosion resistance increase as Ge or Y additives increase.

In 2016, Hassani, F. Z., et al.[132] studied the influences of heat treatments on the microstructural features and, consequently, on the mechanical and wear characteristics of Co–Cr–Mo–C alloys commonly used as hip and knee implant materials, are investigated. Specimens of Co–Cr–Mo–C alloy in the as-cast condition were solution treated at 1230°C for 3 h, and then either were quenched in water or furnace cooled. The achieved microstructures of the heat-treated samples, characterized by fine globular and lamellar-type carbides due to the different thermal-treatment conditions, was proved to affect the material microstructural, mechanical and wear behavior. The wear behavior was evaluated by means of pin-on-disk wear tests, which showed that the wear properties are strongly affected by the carbides shape, distribution, and size. It was proved that both large carbides precipitated in as-cast alloys, and also lamellar-type car-bides induced by slow cooling after solubilization caused lower wear resistance than the globular fine carbides that were dispersed in the solution-treated and water-quenched specimens.

In 2018, Abtan. E. A., [133] investigated the effect of Indium and Tellurium as alloying element on the corrosion, wear behavior of CoCrMo (F75) alloy prepared by powder metallurgy technique. The prepared base alloy with the chemical composition of (60.4%Co, 28%Cr, 6%Mo, 2.5%Ni, 1%Si, 1%Mn, 0.75%Fe, 0.35%C). Each of the alloying elements (In and Te) was added with the percentage of (0.5, 1,1.5, and 2) wt. % then the additives were mixed together wit 0.5%, 1% for each element at the expense of Cobalt. The results showed that the addition of (In) to CoCrMo alloy increases the wear resistance of these alloys and the wear rate decrease as In content increase. While the addition of Te decreases the wear resistance. The corrosion resistance of CoCrMo alloy improved after the addition of each In or Te in artificial saliva and Hank's solution.

In 2019, Marco A.L., et al . [134] in this study, the effect of boron addition on the corrosion behavior of CoCrMo alloys was studied using linear polarization resistance, potentiodynamic polarization curves, electrochemical impedance spectroscopy, and cyclic voltammetry. The samples were analyzed under as-cast and heat treatment conditions after 21 days of immersion in phosphate-buffered saline (PBS) solution at 37◦C. The corrosion resistance was improved by both boron and heat treatments. The best performance was observed for a heat-treated alloy having a very small amount of boron, which had an increased resistance to corrosive attack. Such behavior was attributed to the homogenized microstructure achieved by boron and heat treatment that helped to form a stable passive layer of chromium oxide which endured the 21 days of immersion.

In 2020 , Omar M. A., et al.[135] this paper evaluates and demonstrates the methods for additively manufactured stent and the use of material ASTM F75 Cobalt-based superalloy (CoCrMo) by evaluating the chemical content, hot iso-static pressing process, mechanical properties, and electrochemical polishing. The commercialise stent available had cause issues in the like of unmatch fitting in the blood vessel, with highly dependent on surgeon guessing during angioplasty; thus,

the risk of restenosis or thrombosis can occur. By SLM technique, it creates complex products with high geometric accuracy while allowing the design freedom to produce patient-specific stent. The chemical composition has been assessed by Energy-Dispersive X-ray spectroscopy (EDX) and showed the presence of element Cobalt, Chromium, Molybdenum, and Carbon content. The compressive, flexural, and hardness testing has been conducted to determine the behaviour for an as-built sample and HIPing where the stiffness is drastically improved by 10%.

In 2020, Dong, X., et al.[136] investigated the influence of microstructure on corrosion behavior of Selective laser melting(SLM) and Cast Co-Cr-Mo-W alloy by using electrochemical techniques. The passive property and non-corrod-ibility of SLM Co-Cr-Mo-W alloy were mainly ascribed to the microstructure (content and structure distribution of precipitates). The higher content of precipitates can cause severe microsegregation phenomenon and form an inhomogeneous structure, which is the main reason for the inferior corrosion resistance. In addition, the segregated large precipitates work as effective micro-cathode, resulting pitting corrosion and increased corrosion rate.

Chapter Three

3.1.General View

In this chapter, materials and equipment used in this study are presented. Experimental procedure used to prepare samples from the elemental powders by powders mixing , compaction and finally sintering based onto standard steps of powder metallurgy technique, have been also presented in detail. Several tests such as hardness , corrosion resistance , wear resistance and phase identification by X-ray diffraction and microstructure are also explained .

3.2. Materials Used

The materials used to prepare CoCrMo (F75) alloys in this research are detailed in table (3.1) with average particle size, purity and the original ingredients from HWNANO-company in china.

Table (3.1) Powders used in alloys

Powder	Purity %	Average particle size (μm)
Cobalt	99.95	16.66
Chrome	99	38.96
Molybdenum	99.9	11.17
Manganese	99.9	6.438
Nickel	99.9	11.11
Silicon	99	22.24
Iron	99.7	6.229
Carbon	99.8	8.105
Boron	99.9	4.963
Tungsten	99	22.72
Boron Carbide	99	19.46

3.3Particles Size Analyzer

Particle size distribution of elemental powder (Co, Cr, Mo, Mn ,Ni, Si ,C, Fe, B,W and B_4C) was carried out in College of Materials Eng. /Ceramics and Building Materials Labs./University of Babylon" by Laser particle size analyzer of type: Better size 2000,China,as shown in Figure (3.1)

Figure (3.1): Laser Particle Size Analyzer

3.4. Design and Steps of the Experimental Procedures

The experimental program used in the present study is shown in Figure (3.2)

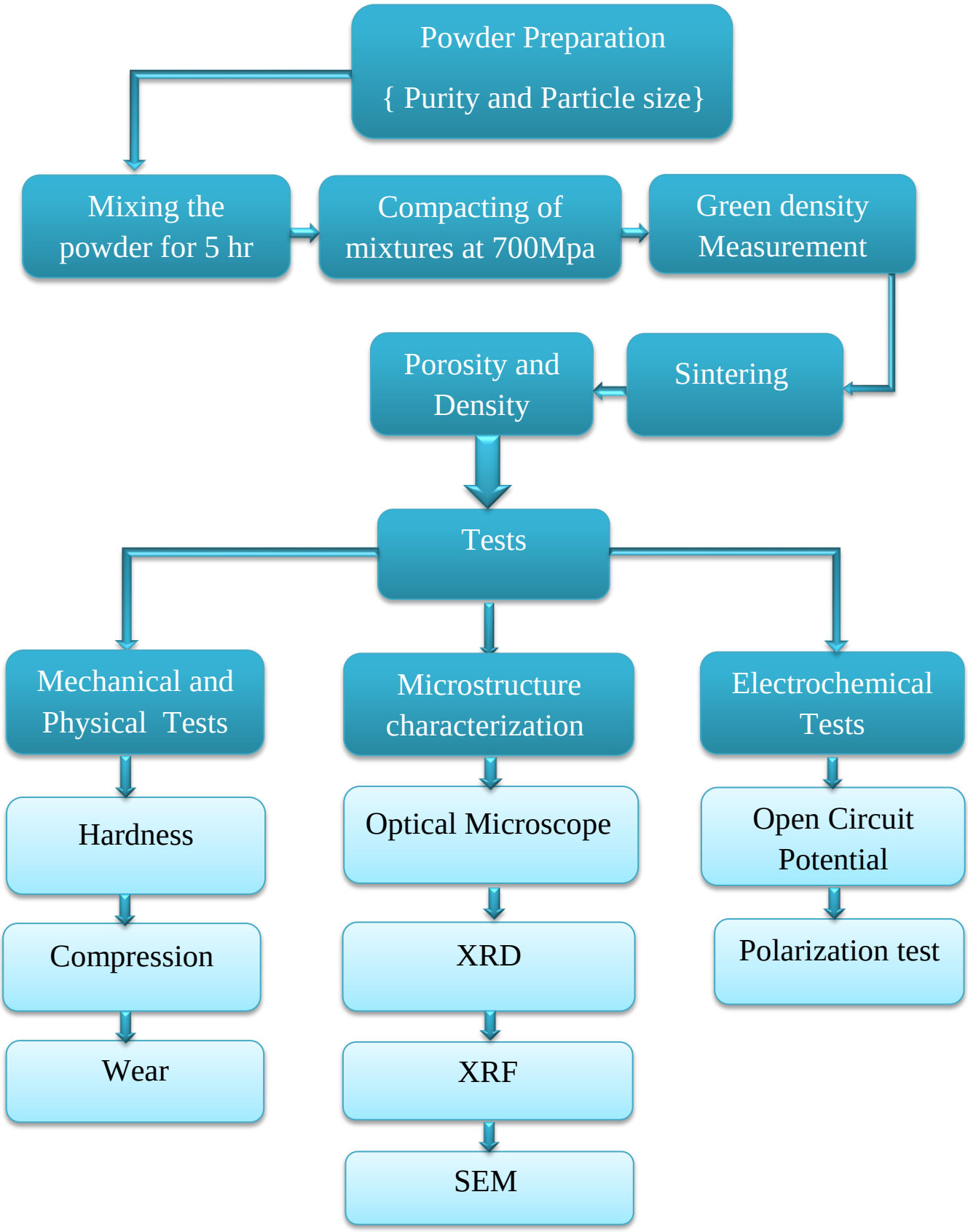

Figure (3.2): Program of the Present Study

3.5. Sample Preparation

Powder metallurgy technique was used to prepare the samples. The procedure involves four steps :

3.5.1. Preparation of mixing powders

Mixing mixtures from elemental powder given in table (3.1) with different weight percent have been prepared in this stage. The base mixture of F75 contain of (60.4% **Co** , 28% **Cr** , 6% **Mo**, 2.5% **Ni** , 1% **Mn** ,1% **Si** , 0.75% **Fe** , 0.35% **C**) have been prepared. Furthermore; additives from B ,W and B_4C each alone added to the base mixture to explain the effects of alloying element on the corrosion resistances , wear resistances and hardness , properties have been presented for sintered and aged specimens. Chemical Compositions of prepared alloys from elemental powders used in this study have been shown in table (3.2).

Table(3.2) The code and composition of the alloys which are used in this work

Alloys	Sample Coding	Alloy Compositions %										
		Co	Cr	Mo	Mn	Ni	Si	C	Fe	B	W	B_4C
A	Alloy A	Bal.	28	6	1	2.5	1	0.35	0.75	---	---	---
B	Alloy B1	Bal.	28	6	1	2.5	1	0.35	0.75	0.5	---	---
	Alloy B2	Bal.	28	6	1	2.5	1	0.35	0.75	1	---	---
	Alloy B3	Bal.	28	6	1	2.5	1	0.35	0.75	1.5	---	---
C	Alloy C1	Bal.	28	6	1	2.5	1	0.35	0.75	---	0.5	---
	Alloy C2	Bal.	28	6	1	2.5	1	0.35	0.75	---	1	---
	Alloy C3	Bal.	28	6	1	2.5	1	0.35	0.75	---	1.5	---
D	Alloy D1	Bal.	28	6	1	2.5	1	0.35	0.75	---	---	1
	Alloy D2	Bal.	28	6	1	2.5	1	0.35	0.75	---	---	3
	Alloy D3	Bal.	28	6	1	2.5	1	0.35	0.75	---	---	5

3.5.2. Mixing Procedure

The mixing of an elemental powders has been done by using a ball mill shown in the figure (3.2 a). Stainless steel balls with different diameters as shown in figure (3.2 b) has been used to mix and refine metal powders for about 5 hours. The increment in the number of contact areas between the elemental powder particles enhance the mixing process. wet mixing is done by using 0.5 cc of Ethyl alcohol to every 25 g of powder mixture. The wet mixing is used to minimize the temperature generated by friction between the balls with walls and powder.

a b

Figure (3.2) a: The Electrical Rolling Mixer , b: Stainless Steel Balls

3.5.3. Compaction of Blended Powder

In this stage Electric uniaxial hydraulic press as shown in figure (3.3) is used to compact the mixed powder to green samples with dimensions (D=13mm and t≈ 4-5 mm) that used for the tests .The die used was single action die made from stainless steel shown in figure (3.4) Graphite has been used as lubricant in order to minimize the friction between the punch and the die wall as well as the friction between the green compact and the die wall and to avoid the cracks initiated from the ejecting of green compact . Various compression stresses from (500 , 600, 700 ,

750 , 800) Mpa with loading rate (2 ton/ min) and period of applied pressure time is (4 min) has been used in order to determine the optimum compression stress that give higher density and low green porosity.

Fig (3.3) Electric hydraulic press one channel, CT430-CT440.

Figure(3.4) : Compaction die made from stainless steel.

3.5.4. Sintering of Green Compacts

The green compacted samples have been sintered in a tube furnace. the sintering process was performed in an argon atmosphere to inhibit the specimens oxidation.

The sintering process include the following steps:

1. Heating green compact from room temperature to 500 °C with heating rate 20 C/min

2. Soaking for (2) hours at 500 °C.

3. Heating from temperature 500 °C to 850 °C

4. Soaking for (6) hours at 850 °C.

5. Slow cooling in the furnace with continues argon circumstances to the room temperature. This procedure is agree with **[133]**.

Figure (3.5):Tube furnace with a continued stream of argon.

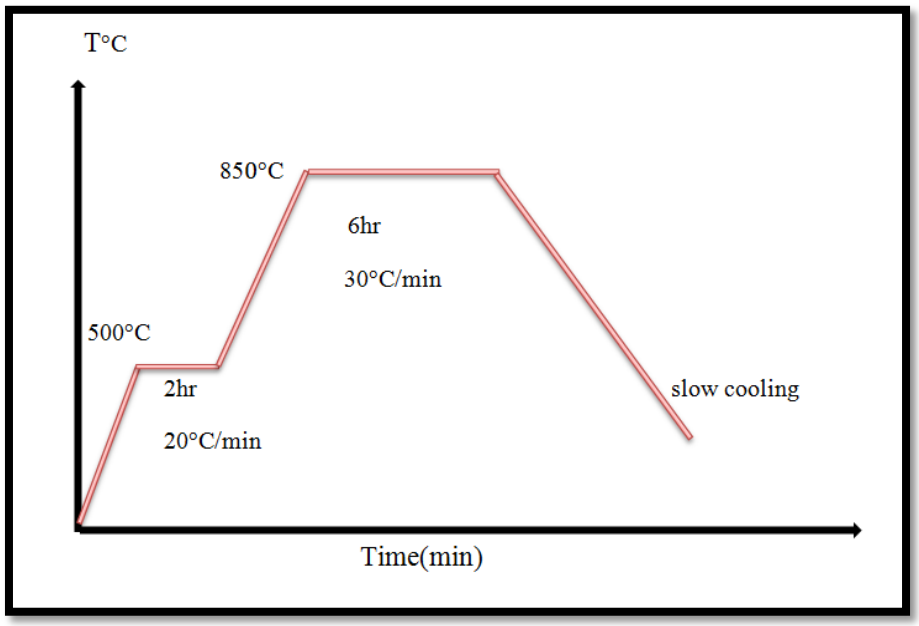

Fig (3.6): Heating cycle in sintering

3.6.Preparation of Samples for the Testing

The specimens after sintering process were grinded by using (180, 220, 320, 600, 800, 1000,1200,1500,2000 and 2500) grit SiC papers, then polished with a diamond past of 15 μm and metallographic polishing pads to get a bright mirror finish for the final step.

3.7. Physical and Mechanical Tests

Most tests were done at the Materials Eng. Labs. / University of Babylon.

3.7.1. Porosity and Density of Sintered Samples

The porosity of sintered samples are calculated according to ASTM B-328 **[137]**:

1- The specimen is dried up to 100 C° for 5h under vacuum for (10^{-4}) tor then cooled to room temperature by using vacuum drying furnace. The weight of dry spacemen is measured as mass A.

2-At room temperature, using a suitable evacuating pump which was manufactured for this purpose. The pressure was reduced over the immersed specimen in oil for 30 minutes.

3-The fully immersed specimen was weighted in the air as mass B.

4-Weighing the sample in water as mass F

5-Finally, the porosity is calculated as:

$$P=[B-A(B-F)D°*100]\ Dw \quad \text{... (3.1)}$$

$$\rho F=[AB-F]\ Dw \quad \text{... (3.2)}$$

Where:

Dw = density of water (0.9956 g/cm3)

D^o = density of oil (0.8 g/cm3)

3.7.2.Optical Microscope Analysis

The sintered specimens were etched at the room temperature .Table (3.3) illustrated the chemical composition of the etching solution **[138].** After etching process the samples were washed with water and dried.

Table (3.3) Chemical composition of etching solution [138]

NO.	Constituent	mL
1	HNO3	15
2	Acetic acid	15
3	HCL	60
4	Water	15

Then specimens cleaned with water and dried with hot air. The microstructure evaluated by using an optical microscopic of type: (BEL PHOTONICS) shown in Figure (3.7) with different magnification involved identification and measurement of the phases, shape and grain size are some characteristics of grain boundaries. Each of these has distinct characteristics.

Fig (3.7): Light optical microscope with (100x, 400x).

3.7.3. Scanning Electron Microscopy (SEM)

Scanning electron microscope observation is used to reveal the microstructure of etched samples . Different magnification has been used. As shown in figure (3.8) SEM examination has been done in Babylon university / collage of pharmacy.

3.7.4. Energy Dispersive X-ray Spectroscopy (EDX)

Energy dispersive analysis have been done for all samples in order to estimate the chemical composition of the corroded film and to see the distribution of alloying elements in the samples ,two areas has been taken for each sample. The test has been done in Babylon University/collage of pharmacy.

Figure (3.8) : Scanning Electron Microscope.

3.7.5. X-Ray Fluorescent Analysis (XRF)

(XRF) analyzer ,model(XEPOS) type (76004814), is used to explain the chemical composition for powders and alloys. The test has been done in Ministry of science and Technology.

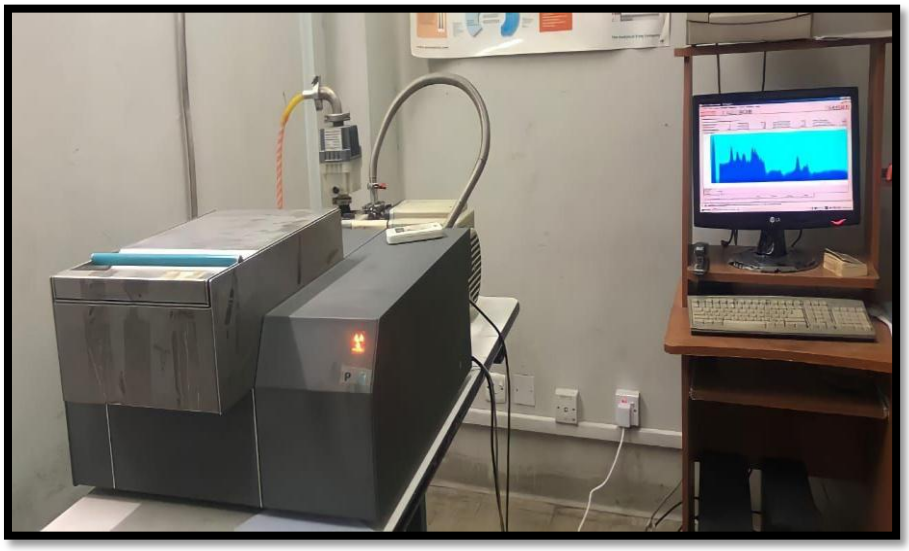

Fig (3.9) X-Ray Fluorescent (XRF).

3.7.6. X- Ray Diffraction Analysis (XRD)

The X-ray diffraction techniques have been taken for the alloys upon using XRD instrument. X-ray diffraction test was conducted for the green compacted

samples and for the same samples after sintering process. The XRD generator with Cu target at 40 KV and 30 mA, scanning speed 5° per minute was used. The scanning rate was ($0^0 - 100^0$).

Fig (3.10) X- Ray diffraction analysis type (XRD-6000)

3.7.7.Macrohardness Measurement

The macrohardness Brinlle test includes use of load (62.5kg/mm²) on the specimen to measure its hardness by a carbide ball diameter of (2.5 mm) for (10 sec) as shown in Figure (3.11) located in the metals laboratory in the Laboratories of the Department of Metallurgical Engineering -University of Babylon. The average value used was taken for three readings for each specimen to analysis the behavior of the alloys.

Fig (3.11) Wilson hardness machine type (UH-250).

3.7.8.Compression Test

The Compression test was performed according to ASTM (D695 - 85) at room temperature. By using computer control electronic universal testing machine, Model (wdw 200, No.W1124).The dimensions of samples are (10mm diameter and 14-18mm in height) the specimens were placed vertically between the jaws for measuring the compression strength is shown in figure (3.12). The test was run at a constant loading speed of 0.5 mm/ min. The compressive strength is calculated by using the following equations**[131]:**

$$\textit{Compressive strength (MPa)} = \frac{Max force(N)}{cross\ sectional\ .area(mm^2)} \qquad \ldots (3.3)$$

Figure (3.12): Compressive test

3.7.9. Dry Sliding Wear Test

The wear testing was down at the University of Babylon/Materials Eng. College-Metallurgical Eng. Labs, using wear tester device type (MT-4003, version 10). A pin on a disc device was used. Figure(3. 13)shows a schematic of pin-on-disk wear test system. The test was performed at room temperature, utilizing loads (10 and 15) N.A rotating speed of 400 rpm, a constant radius of 6.5mm with different sliding distances. Before starting the test, the specimen was weighed using a sensitive balance model M254 A with (±0.0001) accuracy. The specimen was weighed after 5, 10, 15, 20 and25 min, the rate of wear calculated according to the following equation(3.3)**[139]:**

$$R.W=\Delta w/2\pi rnt \qquad \text{....(3.3)}$$

Where:-

R.W:-wear rate (g/mm)

ΔW:-weight lost (gm) which is the difference in weight of the samples before and after the test.

t:-Sliding time (min.).

r:-The radius of the sample to the center of the disc (6.5mm).

n:-Disk rotational speed (400 rpm).

Fig (3.13) pin –on – disk wear instrument

3.8. Electrochemical Tests

Because of the importance of the CoCrMo alloys and their use as an implants within the human body, corrosion tests should be done on specimens to determine the behavior of corrosion of specimens in the human body. This test was done in Corrosion Laboratory in the Laboratories of the Department of Metallurgical Engineering -University of Babylon . In this test were used two different body solutions artificial Saliva and Ringer's solutions have chemical compositions as illustrated in Table (3.4) and (3.5) respectively **[140][141].** The pH of artificial saliva and Ringer's solution at 37°C were 5.8 and 7.4 respectively.

Table (3.4) Chemical composition of artificial saliva solution [140]

NO.	Constituent	(g/L)
1	NaCl	0.4
2	KCl	0.4
3	$CaCl_2.2H_2O$	0.906
4	$NaH_2PO_4.2H_2O$	0.69
5	$Na_2S.9H_2O$	0.005
6	Urea	1

Table (3.5) Chemical composition of Ringer solution [141]

NO.	Constituent	(g/mL)
1	Sodium chloride	0.860
2	Potassium chloride	0.030
3	Calcium chloride $2H_2O$	0.033

3.8.1.Open Circuit Potential (OCP)

The experimental arrangement for the measurement of open circuit potential is shown in figure (3.14) a schematic drawing describes the experimental situation. A 500 ml capacity glass electrolytic cell is used. The tests were carried out with the samples immersed in a Ringer's solution and artificial saliva. The potential of the working electrode is measured with respect to a Saturated Calomel electrode (SCE).

A voltmeter is connected between the working electrode and the saturated reference electrode. For each specimen three hours open circuit potential measurement was performed.

The first record was taken immediately after immersion then the voltage was monitored for the intired period of test at an interval of (5min).

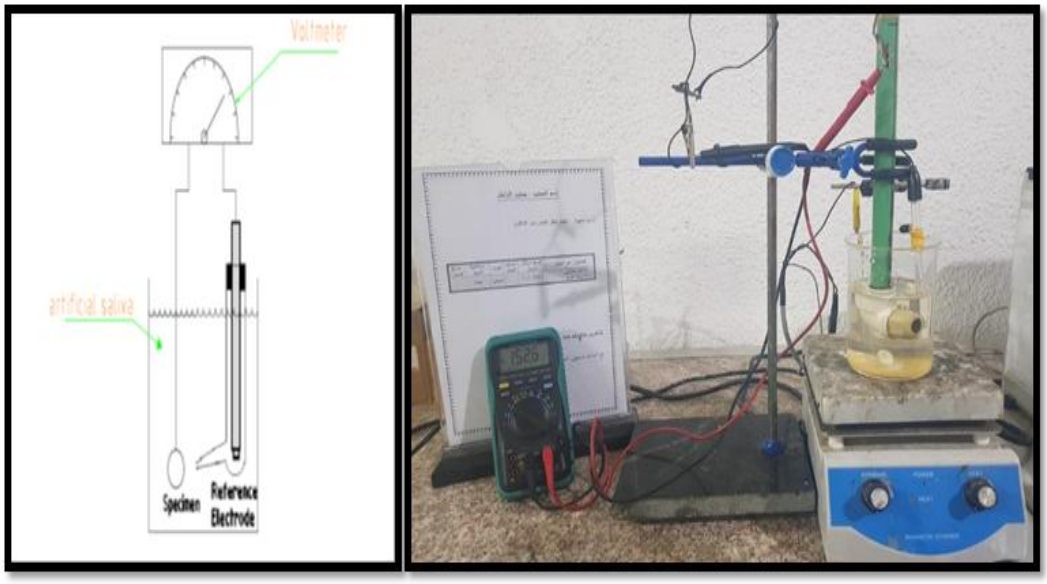

Fig (3.14): Schematic drawing and experimental arrangement for the open circuit potential measurement

3.8.2.Potentiodynamic Polarization

Electrochemical experiments were performed in three electrode cell containing and electrolytes similar to nature saliva and Ringer's solution. The counter electrode was Pt electrode and the reference electrode was SCE and working electrode (specimen) according to the American society for testing and materials (ASTM).

Figure (3.15) shows schematic diagram of potential dynamic polarization. The potentiodynamic polarization curves were plotted and both corrosion current density (I corr.) and corrosion potential were estimated by Tafel plots by using anodic and cathodic branches. The electrochemical system used is shown in Figure(3.13).

The test was conducted by stepping the potential using a scanning rate 0.4 mV/s from initial potential of 350 mV below the open circuit potential and the scan continued up to 350 mV above the open circuit potential. Corrosion rate measurement is obtained by using the following equation**[142]:**

$$Corrosion\ rate = \frac{0.13\ Icorr(Ew)}{\rho} \quad \text{....(3.4)}$$

Where:

E.W= equivalent weight (g/eq.)

ρ= density (g/cm^3)

0.13 = metric and time conversion factor

icorr.= current density (μA/cm^2).

mpy = Corrosion rate (mils per year)

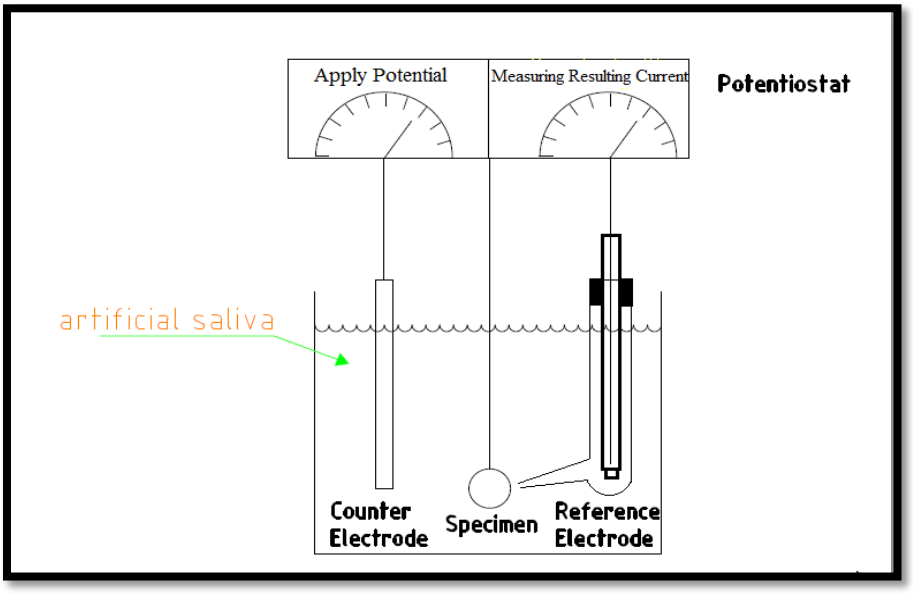

Fig (3.15) Schematic diagram of potentiodynamic polarization cell.

3.8.3.Metals Ions Release (Static Immersion Tests)

The test of static immersions is recognized in agreement with the currently specified JIS T-0304 standards for metallic biomaterial **[143]**.

Samples are immersed in plastic containers with 50 mL of each solution for three week in the incubator (Samples are immersed in small containers, where these containers are immersed in controlled water temperature) to keep the temperature at 37℃(±2).

Assessing the metals ion Co, Cr, Mo, B and W concentrations by Atomic Absorption flame as shown in Figure (3.14). The test has been done in university of Baghdad -Ibn Sina Factory.

Figure (3.16) Atomic absorption spectroscopy

Chapter Four

4.1 Introduction

Experimental results have been demonstrated in this chapter which involves the properties related to the samples that were prepared by powder metallurgy technique. The density of the sintering samples, microstructure analysis results from light optical microscope and SEM, phases analysis results from XRD technique, hardness results, compression results, dry sliding wear results and corrosion results have been cleared and discussed.

4.2 Particle Size Analysis

The particles size of (Co, Cr, Mo, Mn ,Ni, Si ,C, Fe, B,W and B_4C) powders have been analyzed. The results are shown in table (4.1)). It is clear that powders had an average particle size of about (4.963-38.96) µm. The particle size of the powder plays an important role in the behavior of the metal powders during compacting and sintering operations where dissimilar particle size ranges are favorite for good compacts and else, for good properties of sintered products.

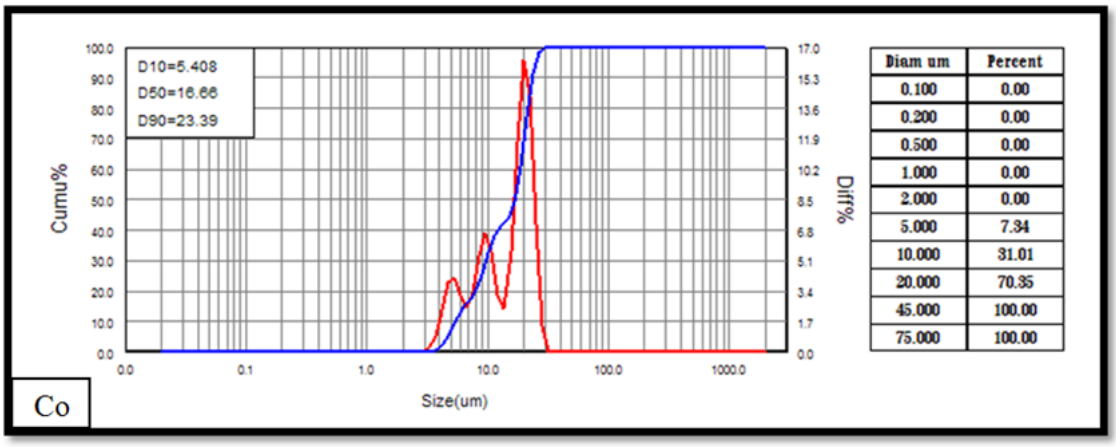

Diam um	Percent
0.100	0.00
0.200	0.00
0.500	0.00
1.000	0.00
2.000	0.00
5.000	7.34
10.000	31.01
20.000	70.35
45.000	100.00
75.000	100.00

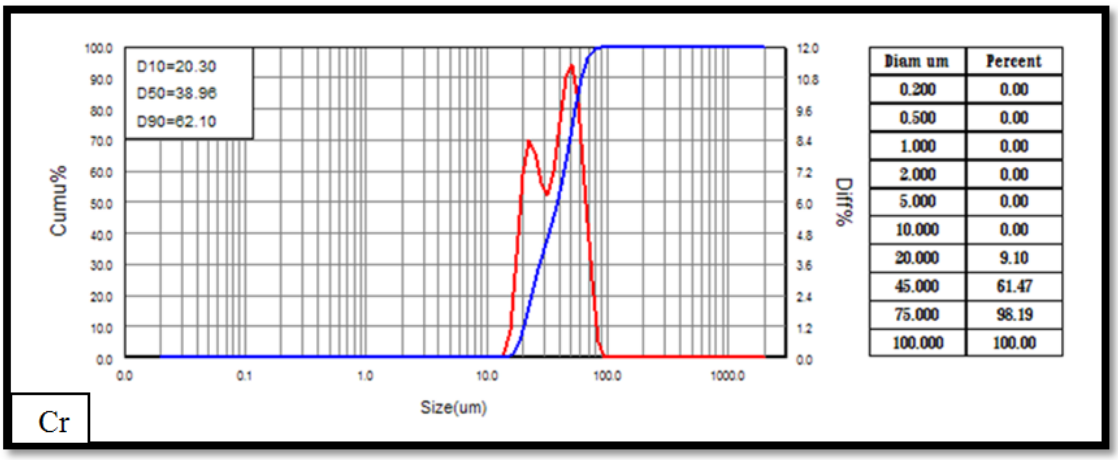

Diam um	Percent
0.200	0.00
0.500	0.00
1.000	0.00
2.000	0.00
5.000	0.00
10.000	0.00
20.000	9.10
45.000	61.47
75.000	98.19
100.000	100.00

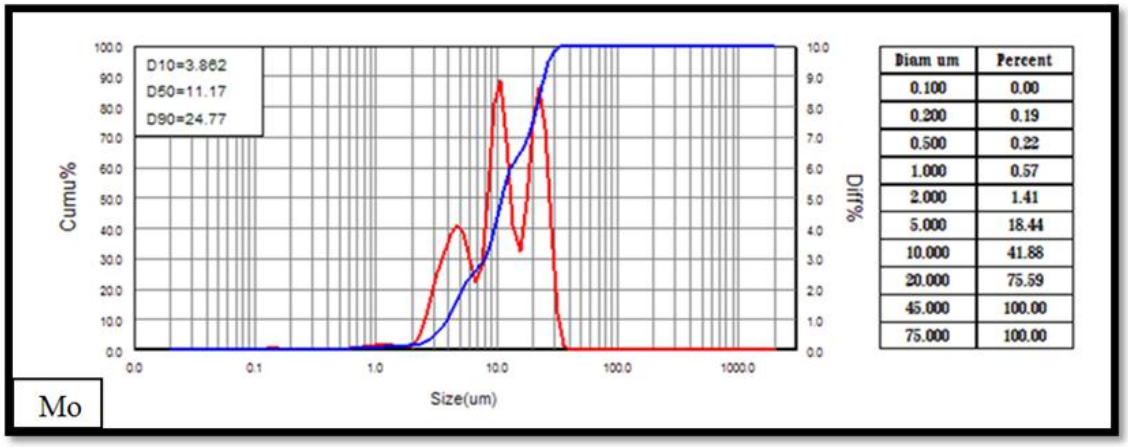

Diam um	Percent
0.100	0.00
0.200	0.19
0.500	0.22
1.000	0.57
2.000	1.41
5.000	18.44
10.000	41.88
20.000	75.59
45.000	100.00
75.000	100.00

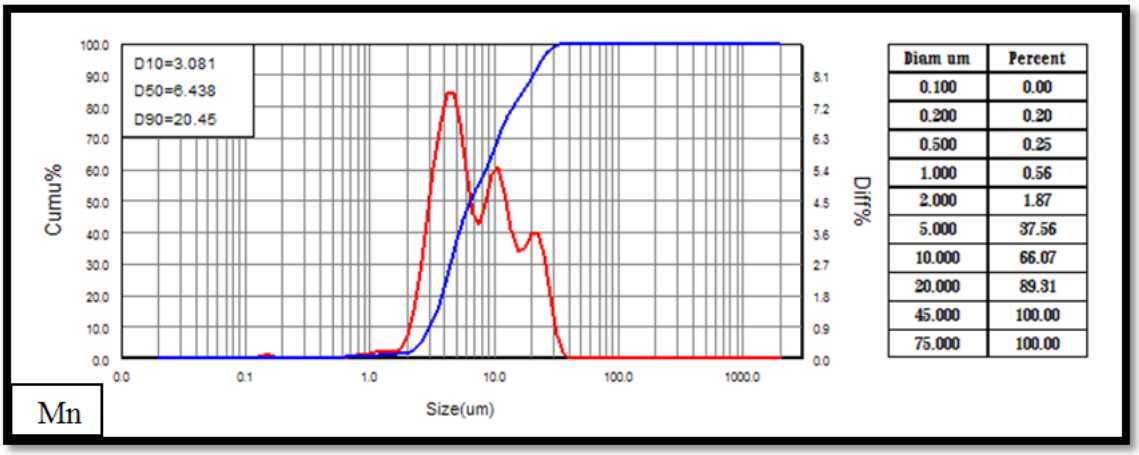

Diam um	Percent
0.100	0.00
0.200	0.20
0.500	0.25
1.000	0.56
2.000	1.87
5.000	37.56
10.000	66.07
20.000	89.31
45.000	100.00
75.000	100.00

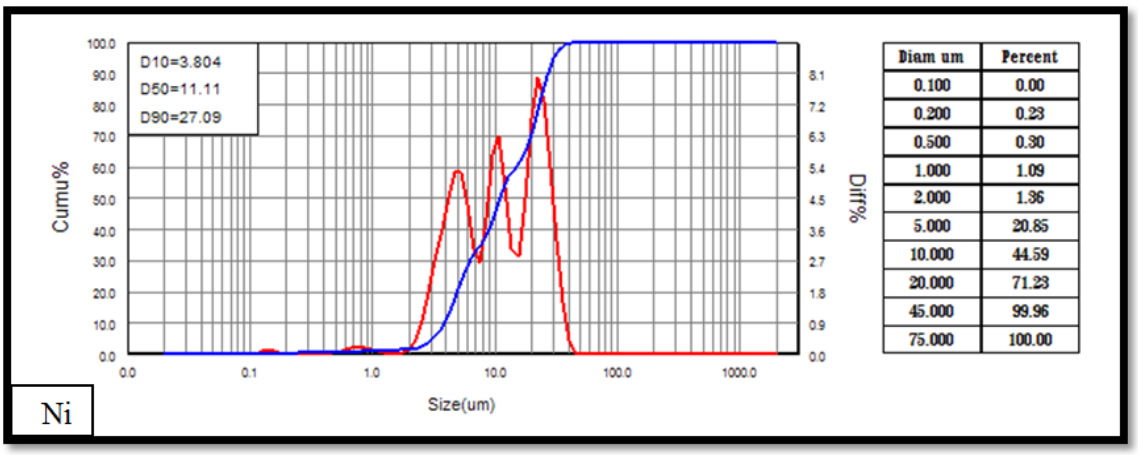

Diam um	Percent
0.100	0.00
0.200	0.23
0.500	0.30
1.000	1.09
2.000	1.36
5.000	20.85
10.000	44.59
20.000	71.23
45.000	99.96
75.000	100.00

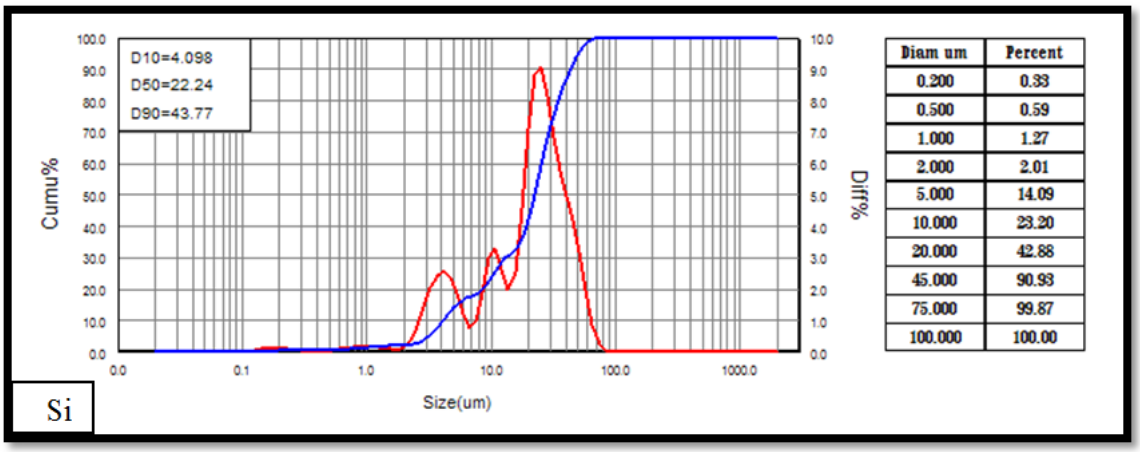

Diam um	Percent
0.200	0.33
0.500	0.59
1.000	1.27
2.000	2.01
5.000	14.09
10.000	23.20
20.000	42.88
45.000	90.93
75.000	99.87
100.000	100.00

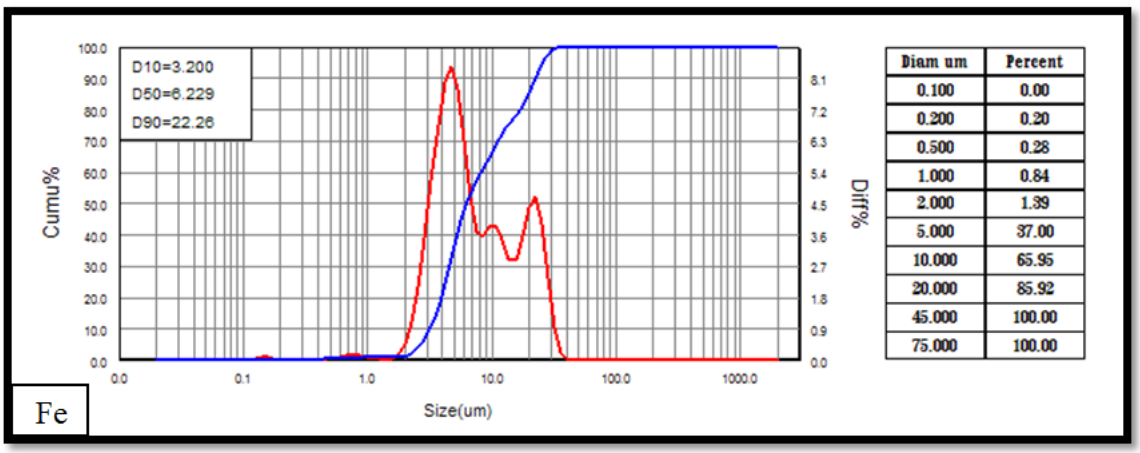

Diam um	Percent
0.100	0.00
0.200	0.20
0.500	0.28
1.000	0.84
2.000	1.39
5.000	37.00
10.000	65.95
20.000	85.92
45.000	100.00
75.000	100.00

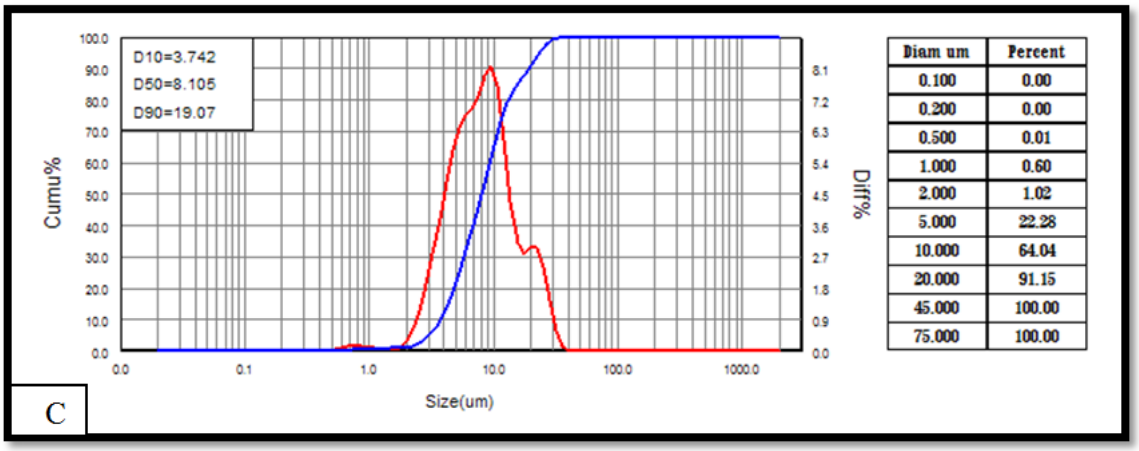

Diam um	Percent
0.100	0.00
0.200	0.00
0.500	0.01
1.000	0.60
2.000	1.02
5.000	22.28
10.000	64.04
20.000	91.15
45.000	100.00
75.000	100.00

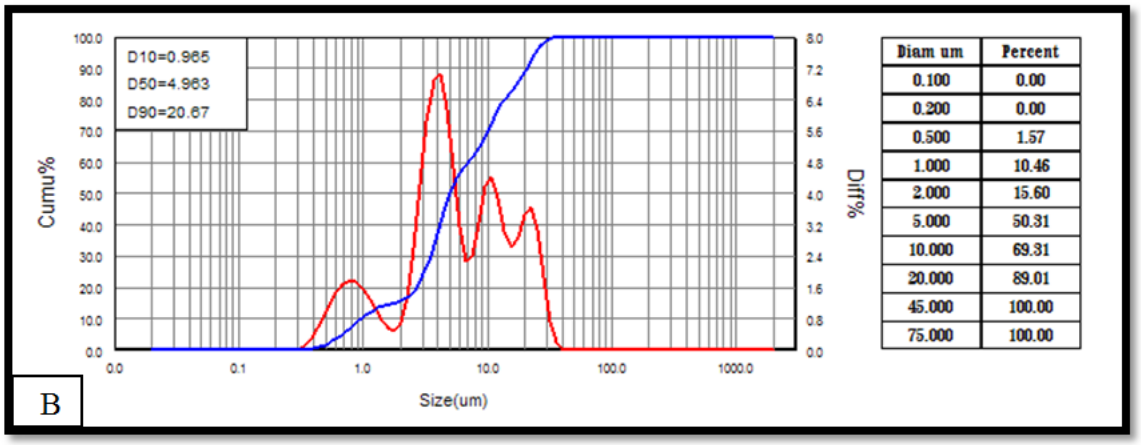

Diam um	Percent
0.100	0.00
0.200	0.00
0.500	1.57
1.000	10.46
2.000	15.60
5.000	50.31
10.000	69.31
20.000	89.01
45.000	100.00
75.000	100.00

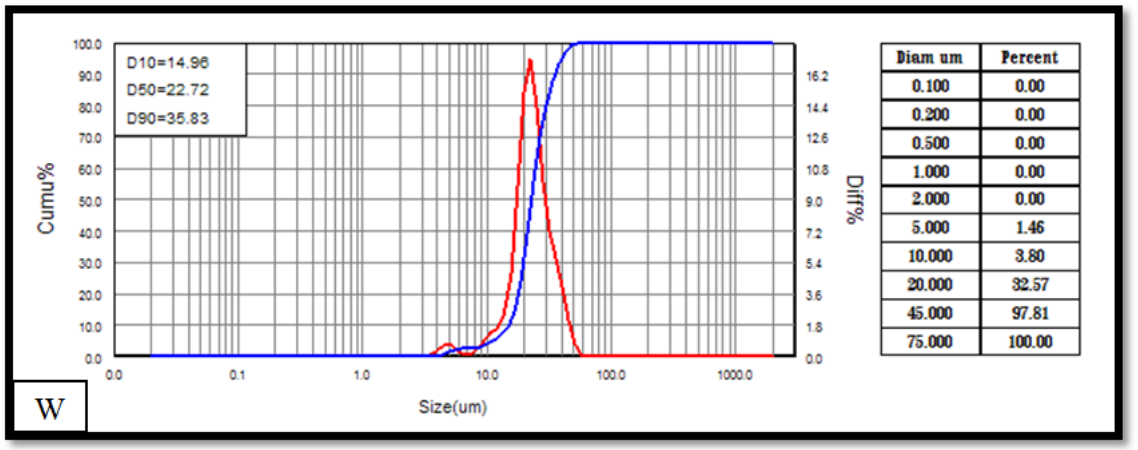

Diam um	Percent
0.100	0.00
0.200	0.00
0.500	0.00
1.000	0.00
2.000	0.00
5.000	1.46
10.000	3.80
20.000	32.57
45.000	97.81
75.000	100.00

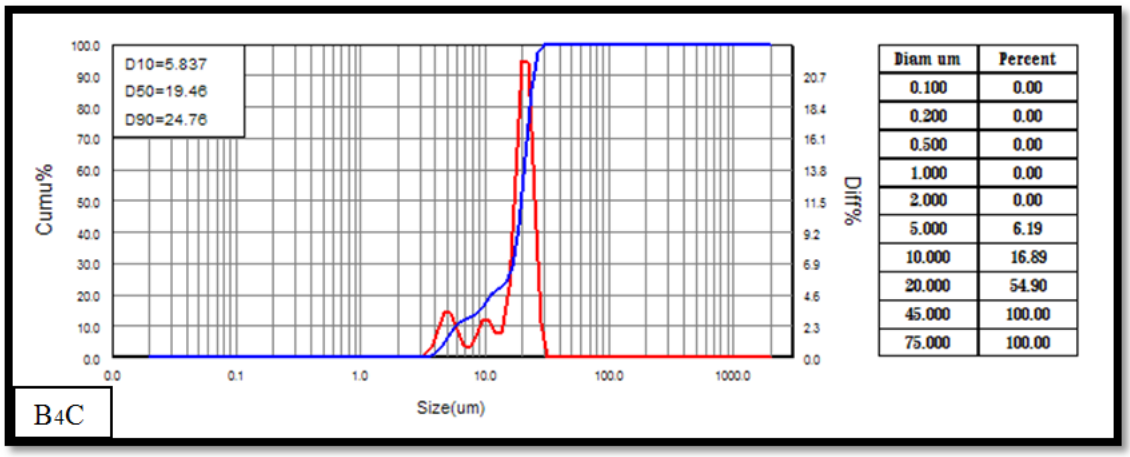

Figure (4.1): Particles size analysis for powders

Table (4.1): Particle size of powders used in alloys

Powder	Co	Cr	Mo	Mn	Ni	Si	Fe	C	B	W	B_4C
Average particle size(µm)	16.66	38.96	11.17	6.438	11.11	22.24	6.229	8.105	4.963	22.72	19.46

4.3 Effect of Compacting Pressure on Green Density

Figure (4.2) shows that if the compacting pressure increases, the green density increases too until it reaches a certain limit at which any further increase in the pressure has no or little effect on its value. So the preferred pressure was determined as 700 MPa for all the samples prepared in the present study.

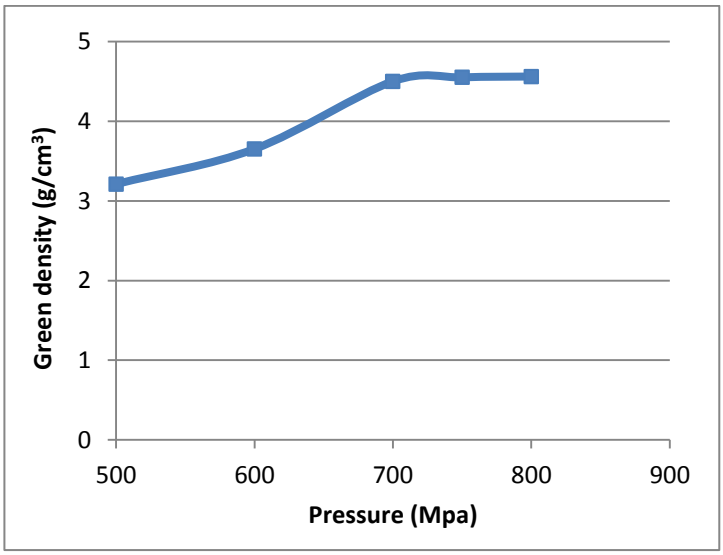

Figure (4.2): Green density vs. pressure before sintering.

4.4 Porosity of Sintered Specimens

The porosity measured for all used alloys after the sintering process and the effect of B , W and B_4C on the porosity values has been cleared in Figures (4.3), (4.4) and (4.5) respectively.

Figure (4.3) showed the effect of **B** content on the porosity of sintered specimens and there is decreasing in porosity values of specimens after sintering. The sintering decrease the porosity because it increase the density of parts prepared by powder metallurgy process**[115],**The porosity decreases with the increasing of B addition may be attributed to the role of B in enhancing interdiffusion between particles also B is refining the grain size **[144].**

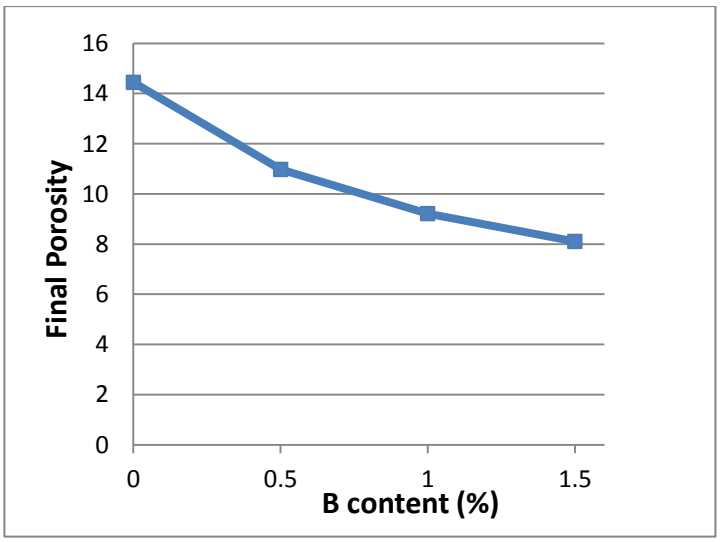

Figure (4.3) :Effect of **B** content on Final porosity for alloys A, B1, B2 and B3 after sintering.

Figure (4.4) showed the effect of **W** content on the porosity of sintered specimens and there is decreasing in porosity values of samples after sintering it can be seen that the porosity of sintered specimens decreased as the W content increases due to the better inter diffusion caused by these additives.

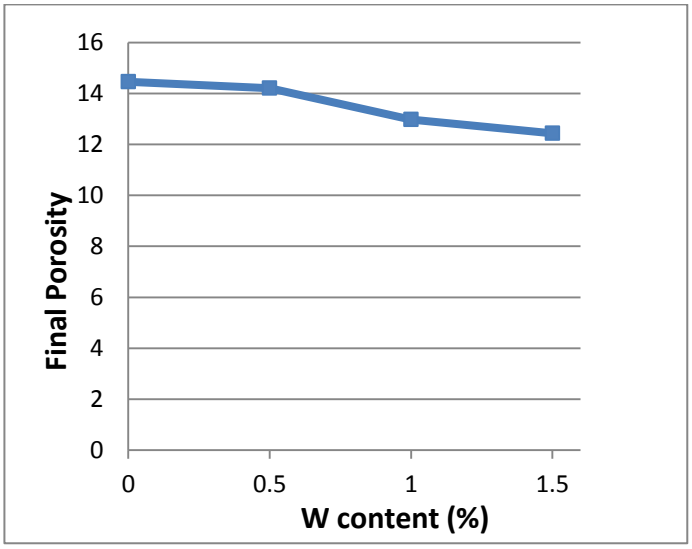

Figure (4.4): Effect of **W** content on final porosity for alloys A, C1, C2, and C3 after sintering.

Figure (4.5) shows the effect of adding B_4C ceramic material on the porosity of CoCrMo alloy after the sintering process. It seems clear from the figure that the increase in the proportion of B_4C led to an increase in the porosity and this could be due to the presence of the ceramic material which is composite material it's like the layers that prevents the convergence of particles during sintering and this may leads to reduced diffusion of particles after sintering and thus increased porosity.

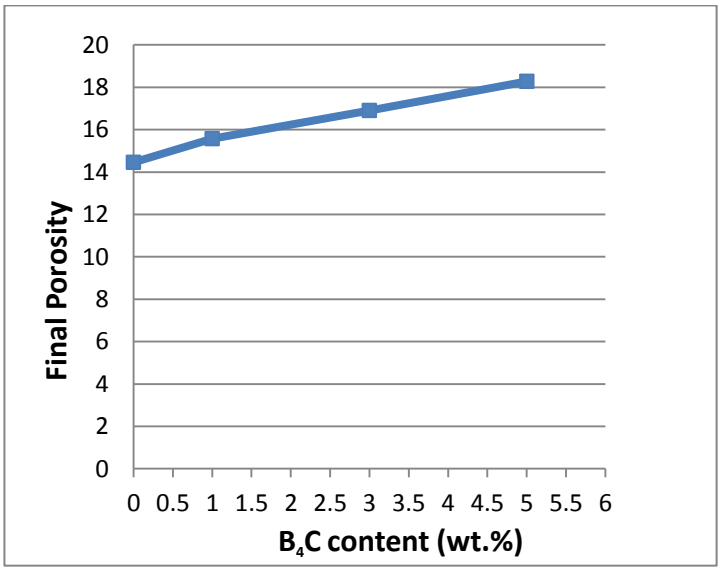

Figure (4.5): Effect of **B_4C** content on final porosity for alloys A, D1,D2 and D3 after sintering.

Table(4.2):show the porosity after sintering of all alloys

Sample code	Porosity after sintering	Improving %
A	14.45	
B1	10.98	75.985
B2	9.22	63.806
B3	8.11	56.124
C1	14.21	98.339
C2	12.97	89.757
C3	12.43	86.020
D1	15.57	107.750
D2	16.90	116.955
D3	18.28	126.505

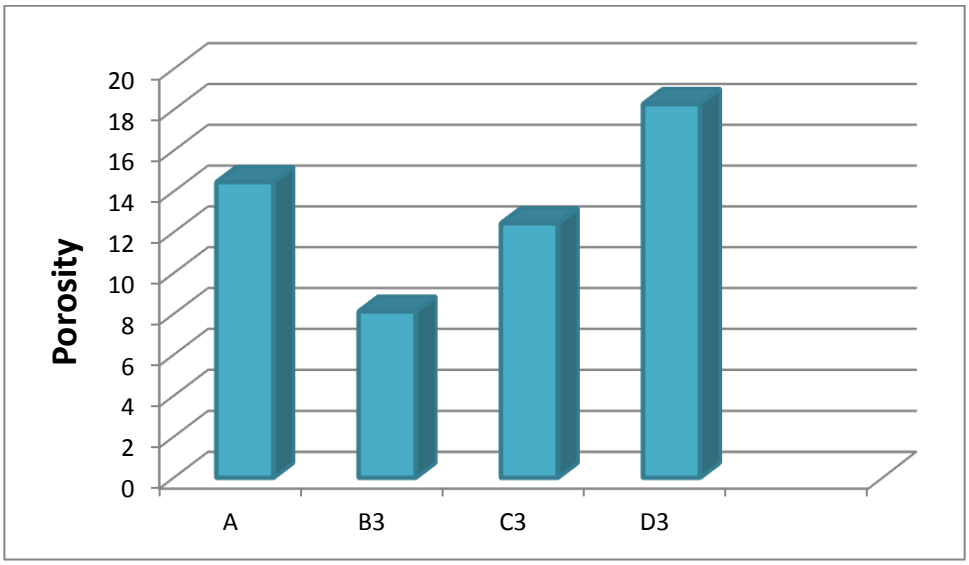

Figure(4.6) :Comparison of Porosity of all alloys

In figure (4.6) it shows that the lowest value of porosity of CoCrMo alloy is by adding1.5wt% B (B3) because the grain size of boron is smaller compared with base alloy that its fill a large number of pores.

4.5 Density of Sintered Specimens

The final density after the sintering process and the effect of **B** and **W** and **B_4C** on the density values has been cleared in Figures (4.7), (4.8) and (4.9) respectively. The density is inversely proportional with porosity .

Figure (4.7) showed the effect of B content on the density of sintered specimens and there is increase in density values of specimens after sintering. The increase in densities with the increasing of B addition may be attributed to the amounts of porosity existing in the compacted samples . The compacts enter the sintering process with low pores (high green density) so that all the activation thermal energy during sintering is spent in increasing the compacted density through the diffusion process that occurs to form the alloys so that the density increase**[145]**.

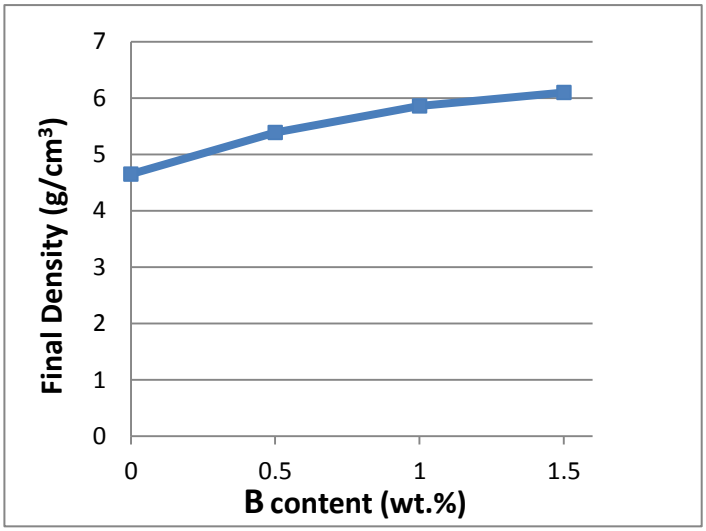

Figure (4.7): Effect of **B** content on final density of A,B1,B2 and B3 alloys after sintering

Figure (4.8) showed the effect of W content on the density of sintered specimens and there is an increase in density values of specimens after sintering

In the previous paragraph, the addition of tungsten to the alloy showed a slight decrease in the porosity values after sintering, despite this, the density values after sintering showed an increase in the density values .It is known that the density of W metal is relatively large, up to 19 compared to the density of cobalt (8) This can

lead to a noticeable increase in the density after the sintering process, although there is a slight decrease in the porosity.

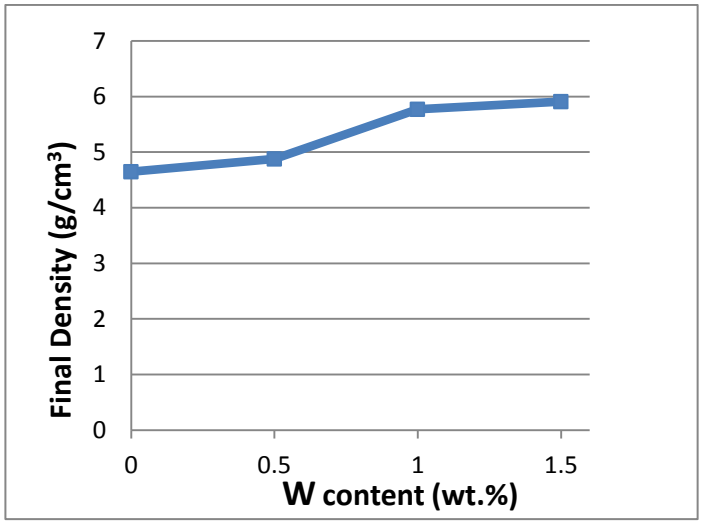

Figure (4.8): Effect of **W** content on final density of A,C1,C2 and C3 alloys after sintering

Figure (4.9) shows the effect of adding B_4C ceramic material on the density of CoCrMo alloy after the sintering process. From the figure, there is a noticeable decrease in the density values after adding B_4C, and this behavior may be due to the role of B_4C in increasing porosity after sintering also the low density of B_4C (2.52 g/cm^3)encourage to decreasing density of alloys.

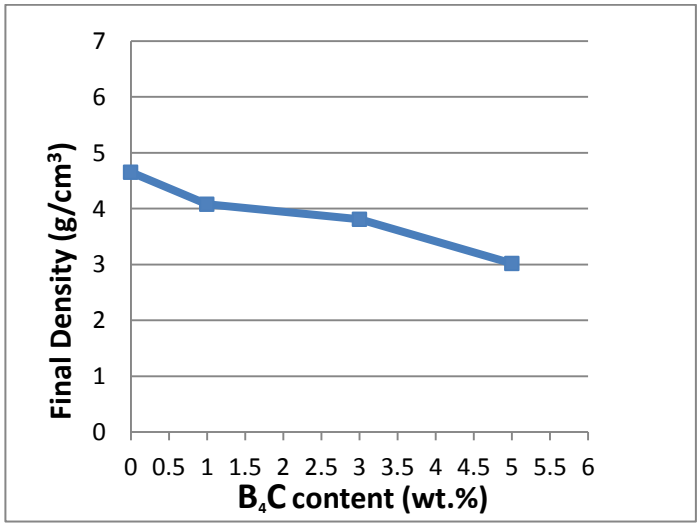

Figure (4.9): Effect of **B_4C** content on final density of A,D1,D2 and D3 alloys after sintering.

Table(4.3):show the density after sintering of all alloys

Sample code	Density after sintering	Improving %
A	4.65	
B1	5.39	115.913
B2	5.86	126.021
B3	6.10	131.182
C1	4.88	104.946
C2	5.77	124.086
C3	5.91	127.096
D1	4.08	87.741
D2	3.81	81.935
D3	3.02	64.946

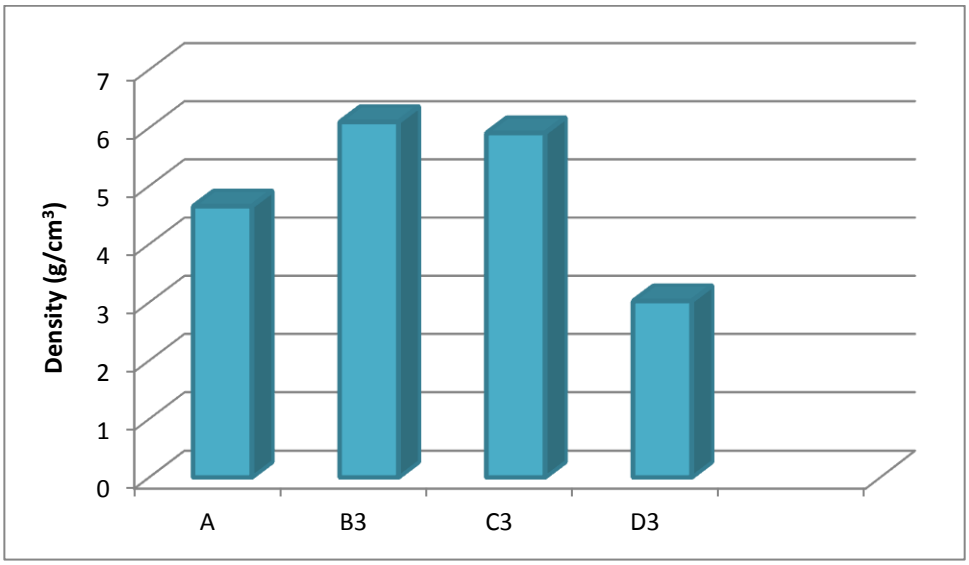

Figure(4.10) :Comparison of density of all alloys

4.6. Chemical Compositions analysis

The chemical compositions for the prepared alloys ,were analyzed by using (x-ray florescent test).

The composition analysis confirm that the main alloying elements are present within the specified limits. As shown in table (A1) to table(A4) ,in appendix(A) for alloy A(base), B3(1.5%B), C3(1.5%W) and D3(5%B_4C) respectively.

4.7 X-Ray Diffraction analysis

X-Ray diffraction test was done for elemental powders before and after sintering process for A, B3, C3 and D3 alloys. XRD test are used to determine the phases present in sintering samples.

4.7.1 X-Ray Diffraction (XRD) for Pure Powders

Figures (4.11), (4.12), (4.13), (4.14), (4.15) and (4.16) illustrate the X-ray diffraction for the used (Co, Cr, Mo, B, W and B_4C) powders respectively. The shown patterns matched to the standard patterns for mentioned.

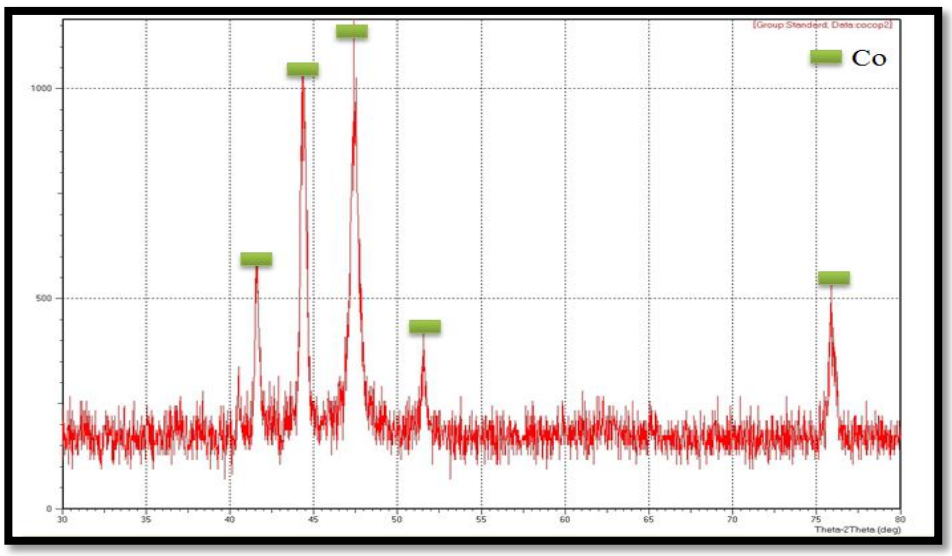

Figure (4.11): XRD patterns for **Co** powder

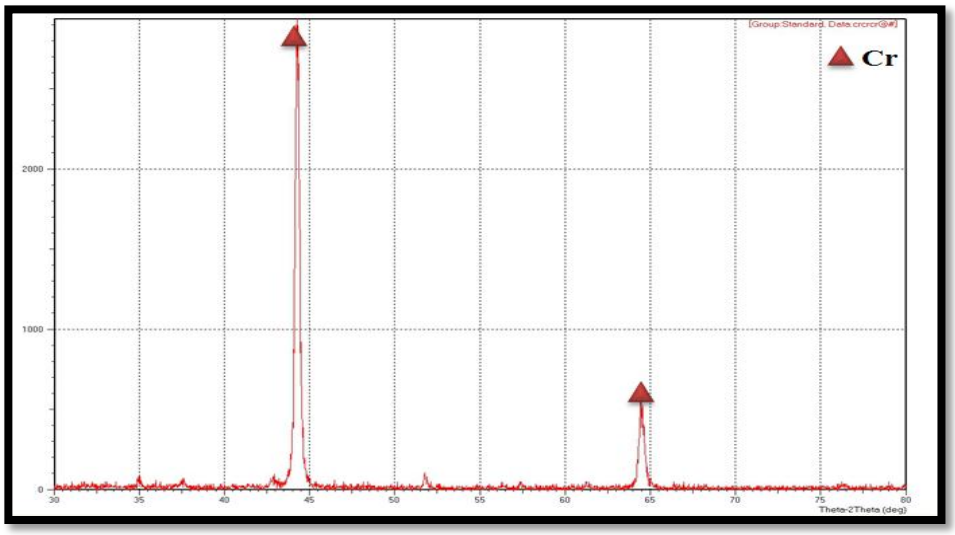

Figure (4.12): XRD patterns for **Cr** powder

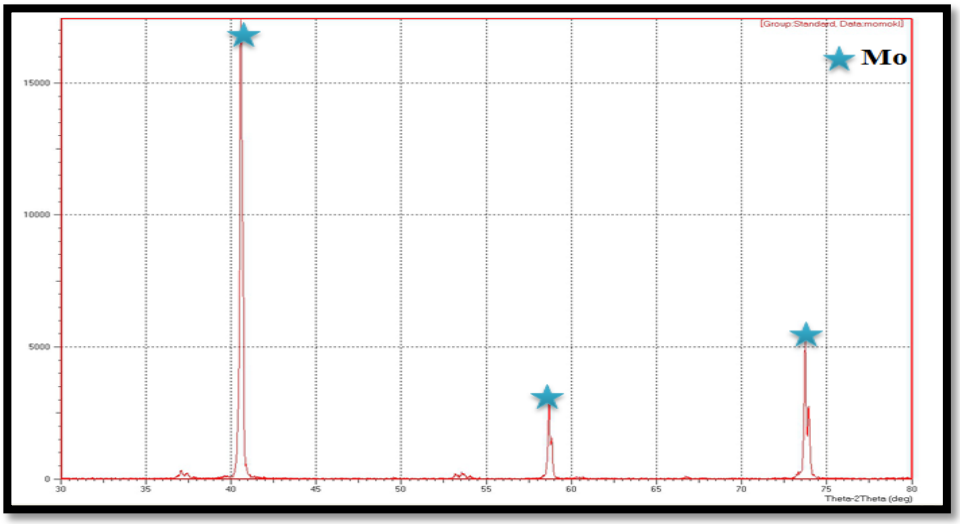

Figure (4.13): XRD patterns for **Mo** powder

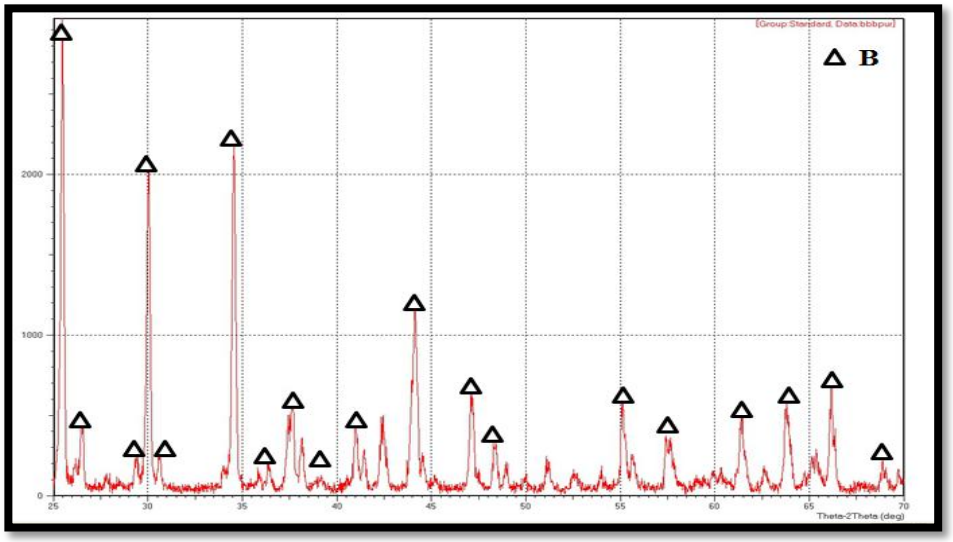

Figure (4.14): XRD patterns for **B** powder

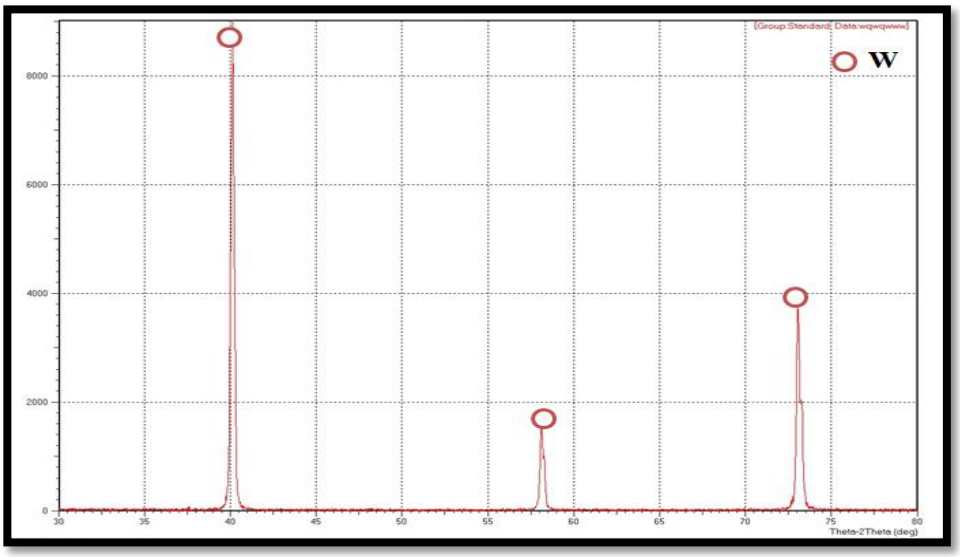

Figure (4.15): XRD patterns for **W** powder

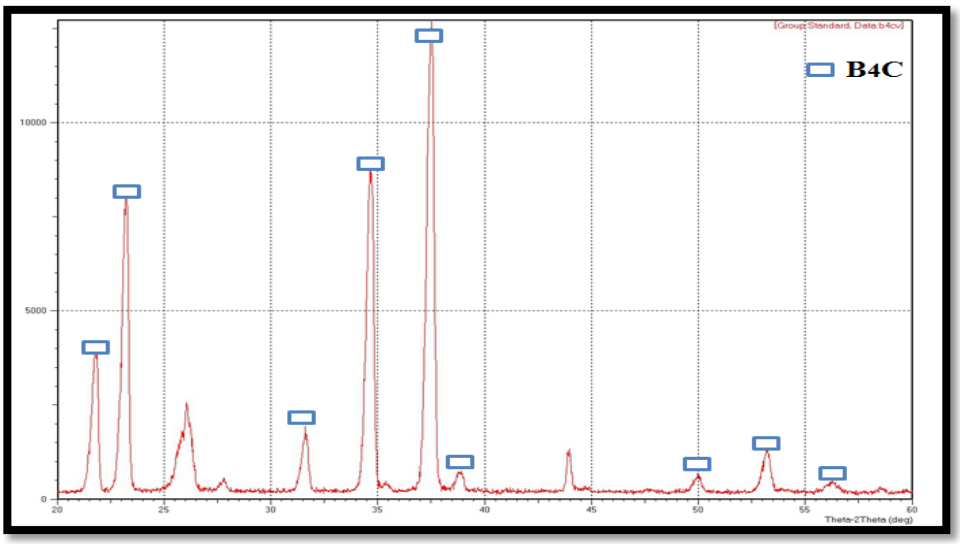

Figure (4.16): XRD patterns for **B4C** powder

4.7.2. XRD Patterns for Sintered Alloys

Figure (4.17), (4.18) and (4.19) illustrates XRD pattern for A, B3and C3 alloy after sintering process, all amount of Co, Cr and Mo transformed to (CoCrMo, CoCr and Co_2Mo_3) phases. This means that 850°C for 6h was enough to complete sintering process due to the enhancement of the interdiffusion between Co, Cr and Mo which in turn leads to an increase in the amount of CoCrMo phase. B and W was added to a maximum percentage 1.5% ,this is a small amount to be detected by the XRD technique.

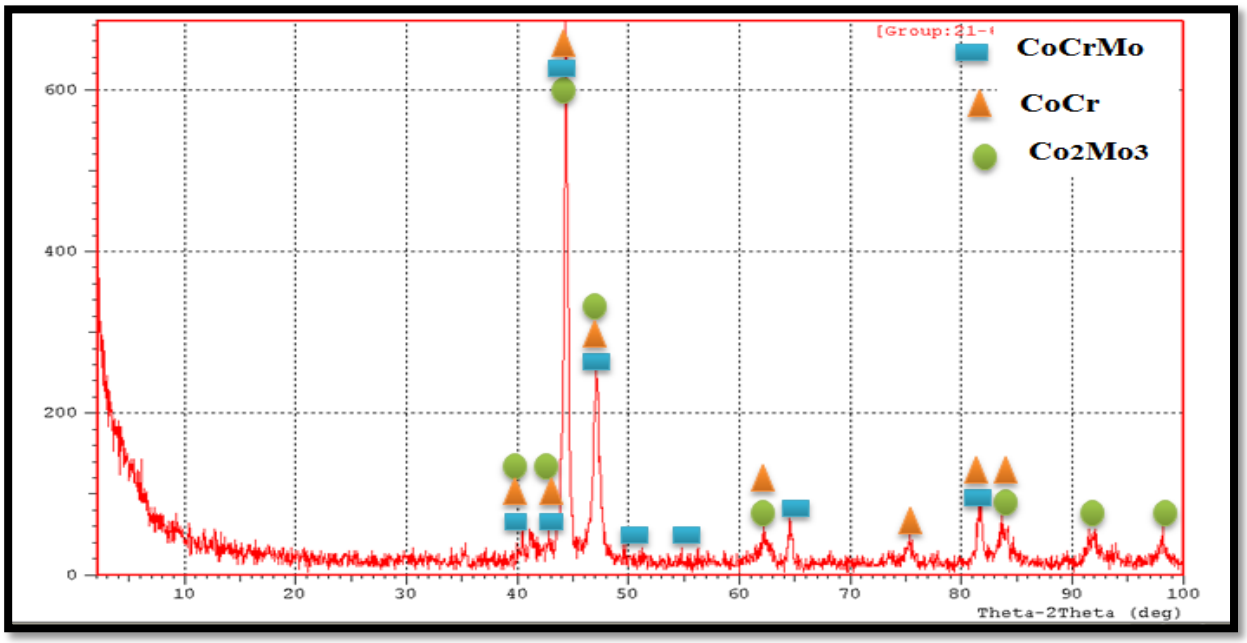

Figure (4.17): XRD pattern for **A** alloy after sintering.

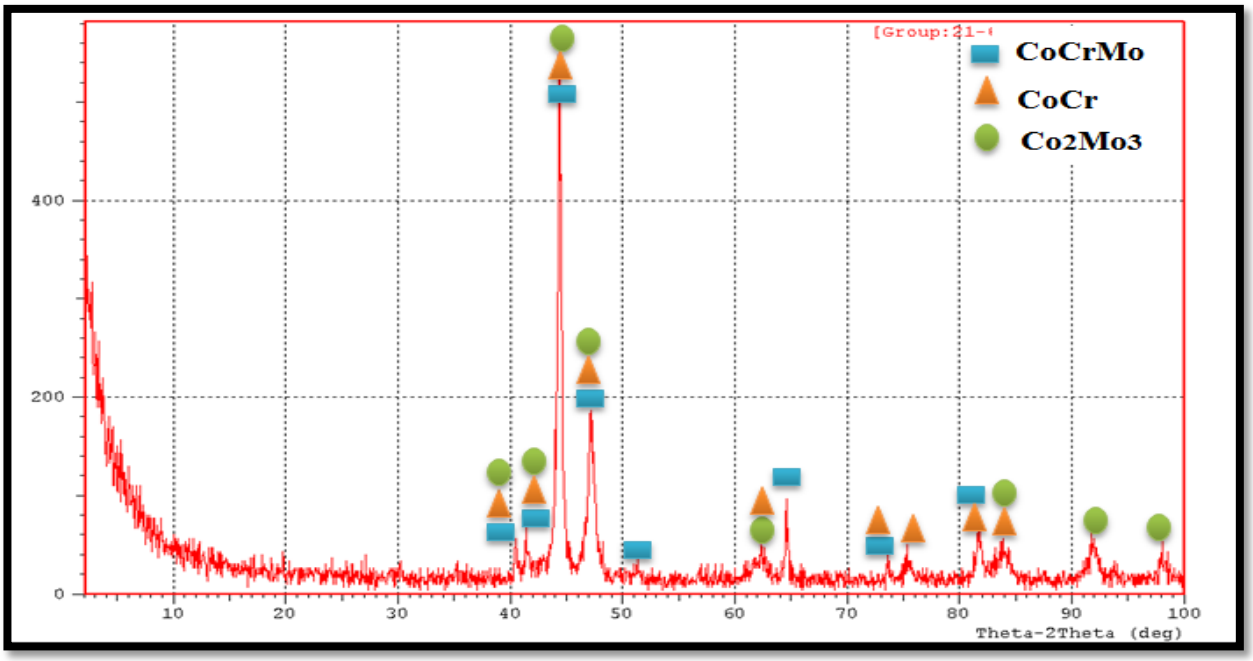

Figure (4.18): XRD pattern for **B3** alloy after sintering.

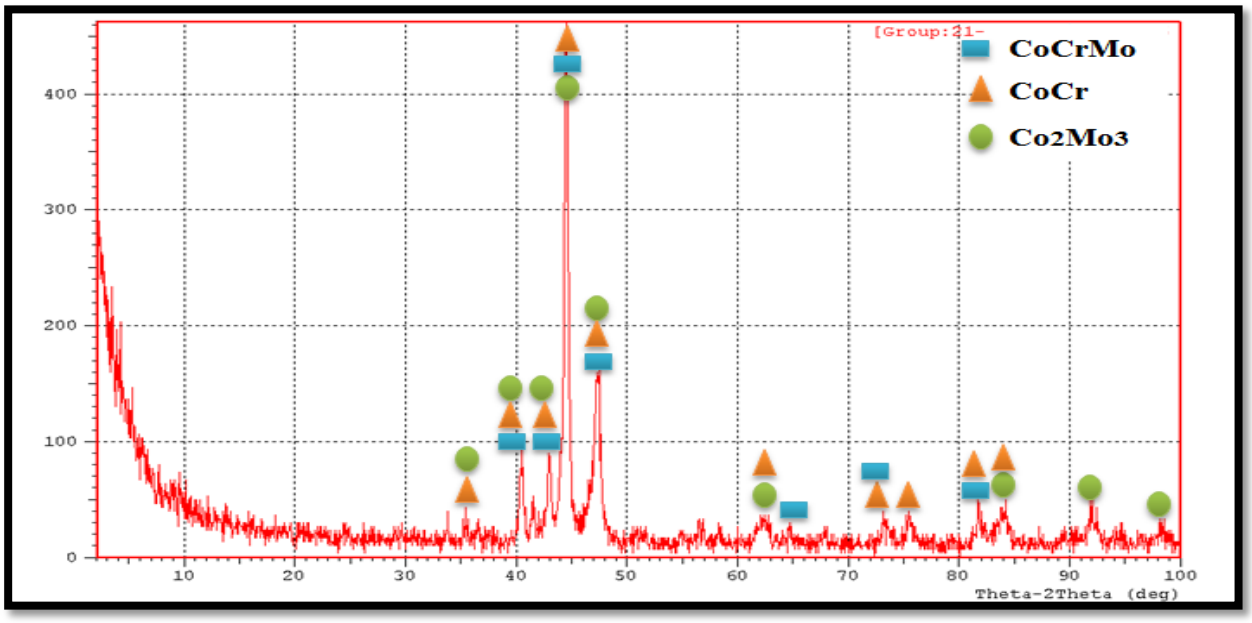

Figure (4.19): XRD pattern for **C3** alloy after sintering.

Figure (4. 20) illustrates XRD pattern for D3 alloy after sintering process, all amount of Co and Cr transformed to (CoCrMo, CoCr and Co_2Mo_3) phases this mean that 850°C and 6h was enough to complete sintering process due to the enhancement of the interdiffusion between Co, Cr and Mo which in turn leads to an increase in the amount of CoCrMo phase. B_4C was added to a maximum percentage 5% the amounts can be detected by the XRD method as shown in several large prominent peaks of B_4C.

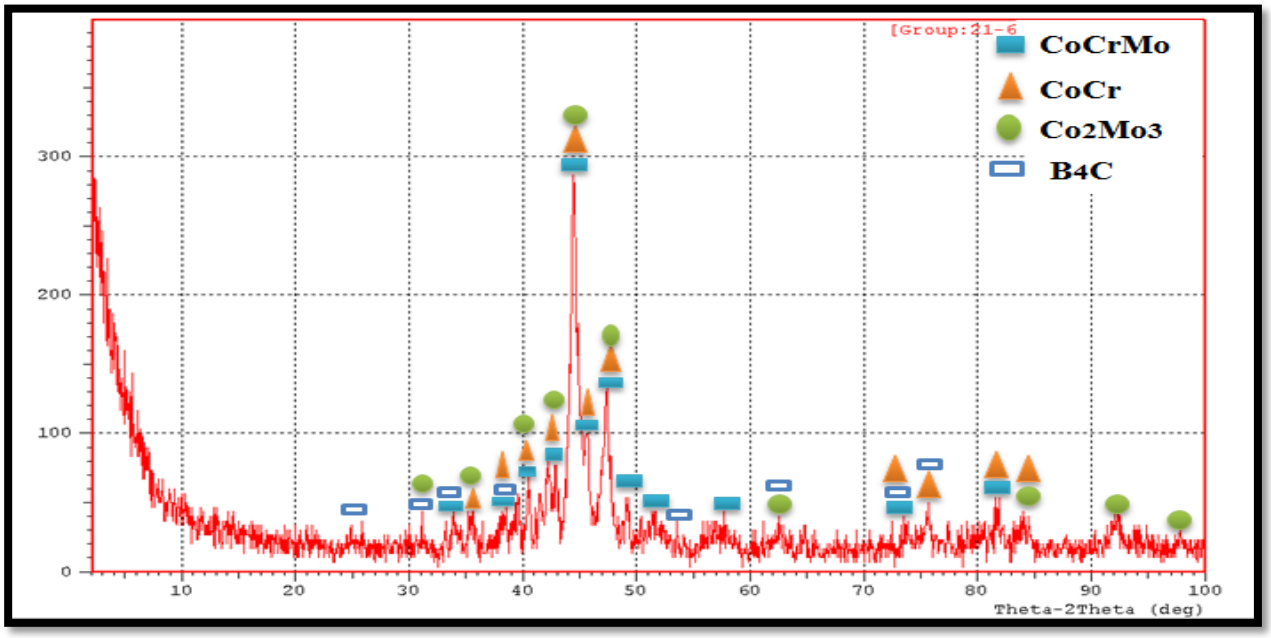

Figure (4.20): XRD pattern for **D3** alloy after sintering.

4.8 Microstructure Test

To reveal the microstructure of prepared specimens, two techniques have been done as follows

4.8.1 Light Optical Microscope

The specimens have been etched to reveal the grain boundaries in the microstructure. Pores of different size are irregular but have been rounded. The most common types of features in the microstructure in metallic materials are the boundaries between crystalline grains and /or the boundaries between different solid phases in multiphase alloys.

The metallography can give a simplified idea about the relationships between the microstructure of material and the microscopic properties because the size and the shape of grains have a direct effect on the behavior of material**[146].**

The samples have been etched to reveal the grain boundaries in the microstructure. Figures (4.21) ,(4.22),(4.23),(4.24),(4.25),(4.26),(4.27),(4.28) (4.29) and (4.30) shows the microstructure images that have been taken by using optical microscope for etched alloys(A, B1, B2, B3, C1, C2, C3, D1, D2 and D3) after sintering process with magnification of (200x & 400x).The microstructure showed grain boundaries, pores in different size and insures the formation of the phases(CoCrMo), (CoCr) and (Co_2Mo_3).There are many pores in different size can be seen on the surface and it is expected because the specimens are prepared by powder metallurgy technique**[145]**.

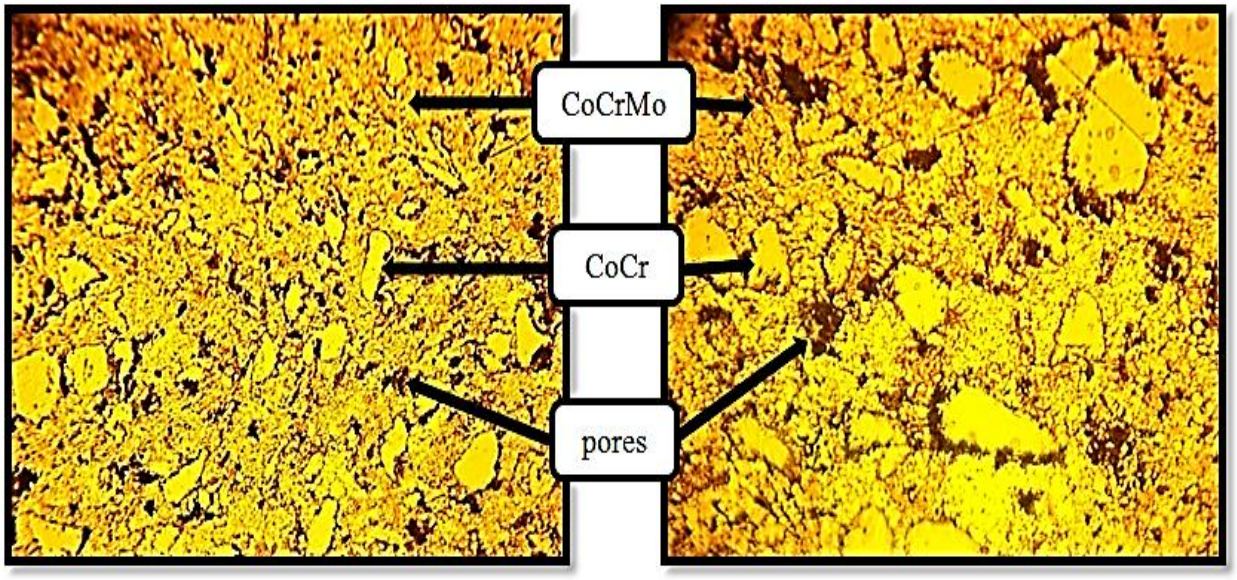

a b

Figure (4.21): Microstructure for **A** alloys after sintering and etching (a:200x &b:400x)

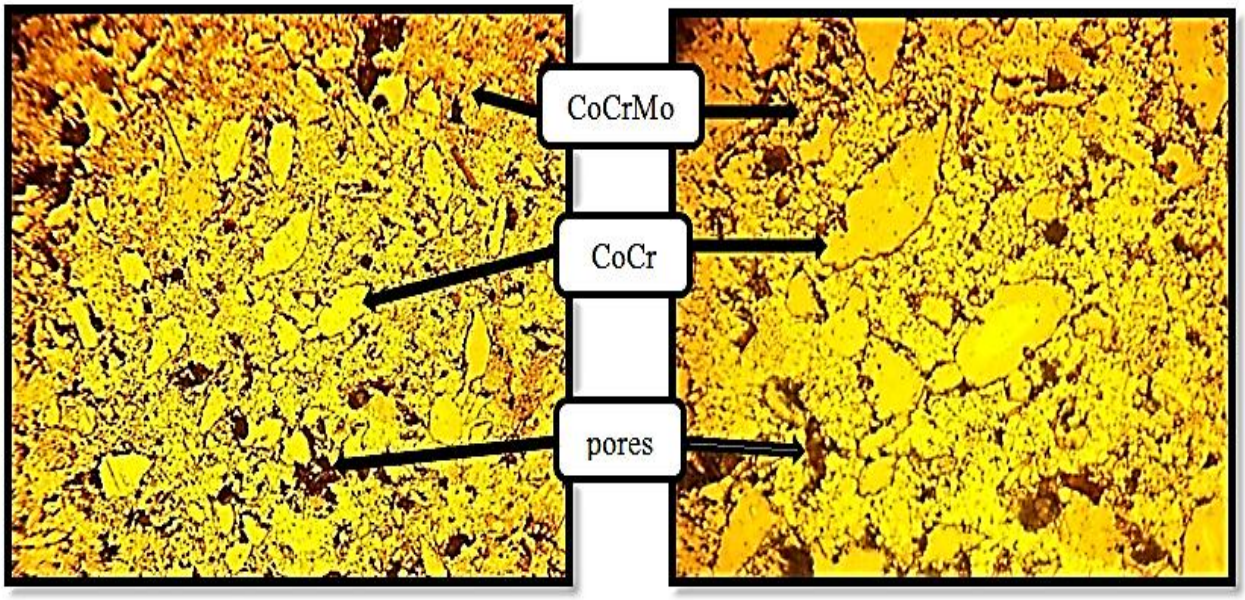

a b

Figure (4.22): Microstructure for **B1** alloys after sintering and etching (a:200x &b:400x)

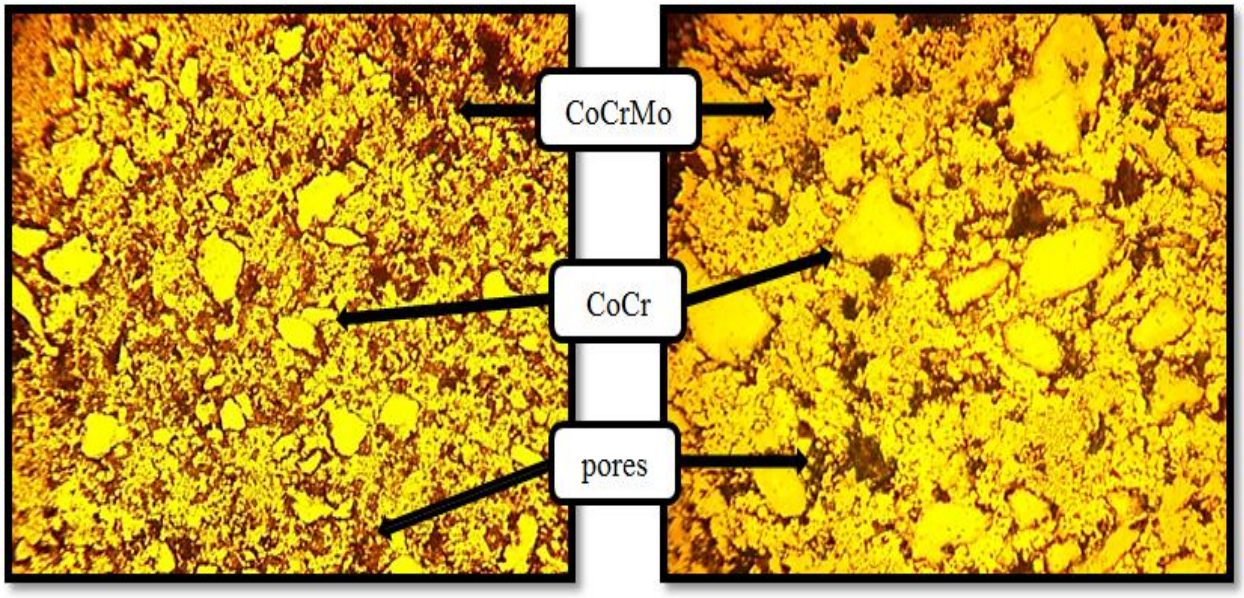

a b

Figure (4.23): Microstructure for **B2** alloys after sintering and etching (a:200x &b:400x)

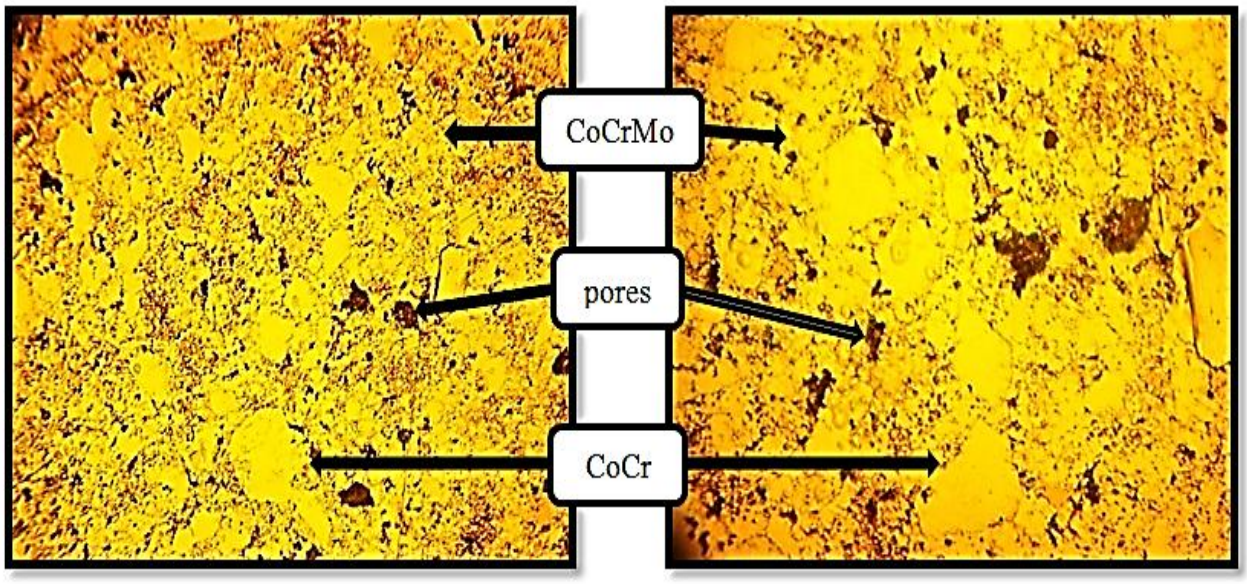

a b

Figure (4.24): Microstructure for **B3** alloys after sintering and etching (a:200x &b:400x)

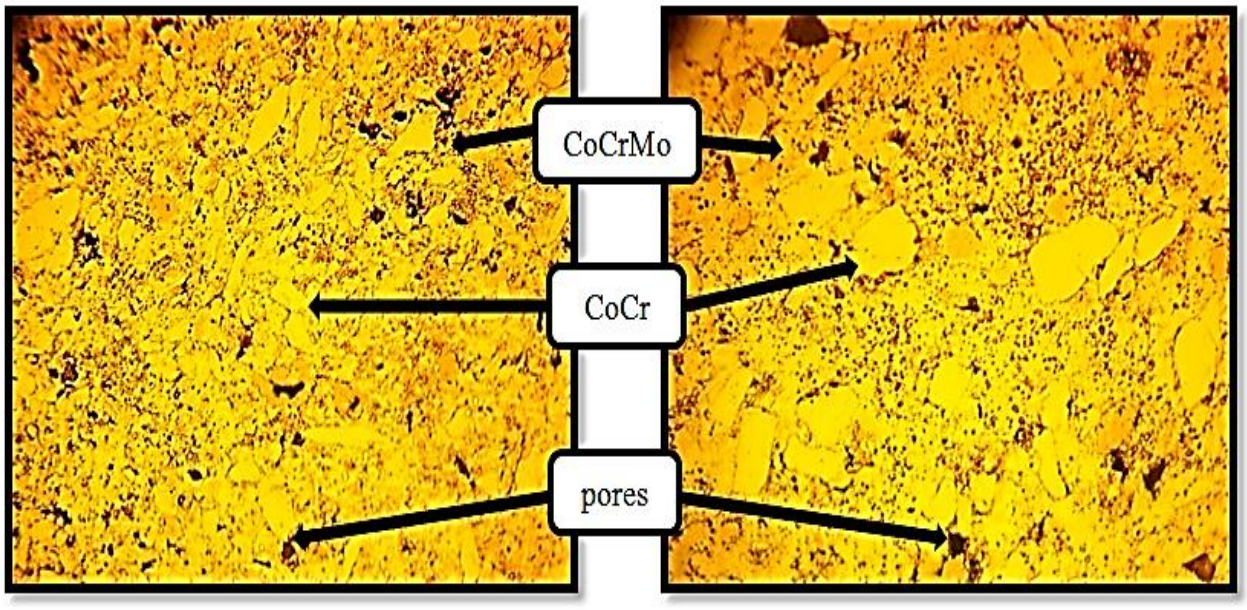

a b

Figure (4.25): Microstructure for **C1** alloys after sintering and etching (a:200x &b:400x)

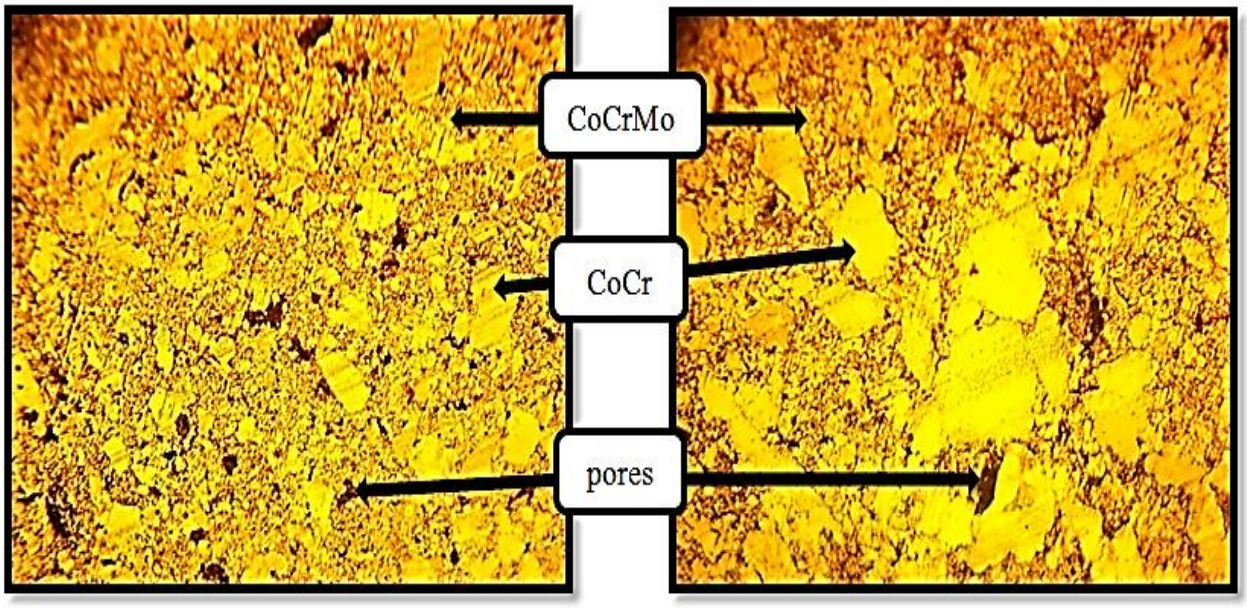

a b

Figure (4.26): Microstructure for **C2** alloys after sintering and etching (a:200x &b:400x)

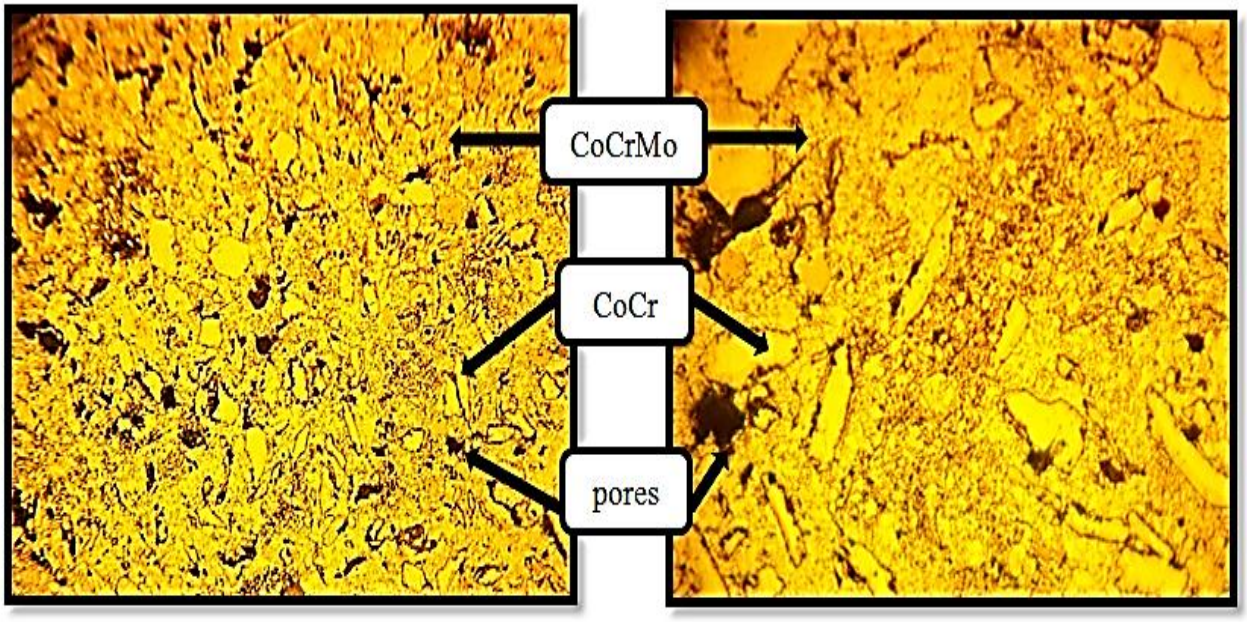

a b

Figure (4.27): Microstructure for **C3** alloys after sintering and etching (a:200x &b:400x)

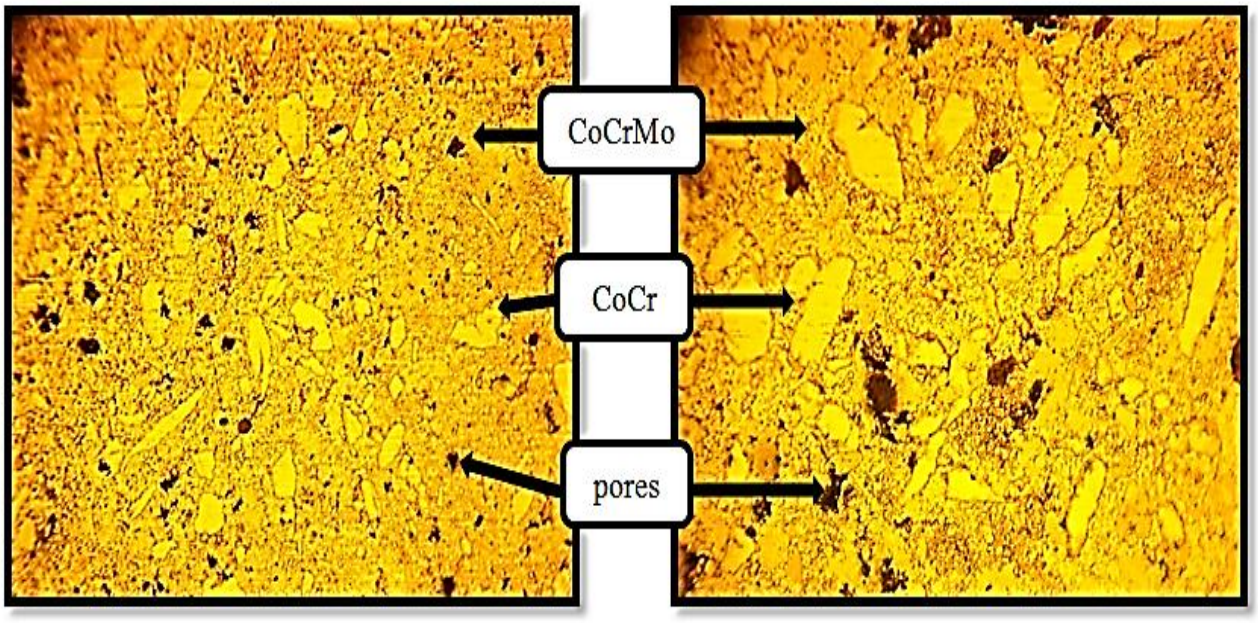

a b

Figure (4.28): Microstructure for **D1** alloys after sintering and etching (a:200x &b:400x)

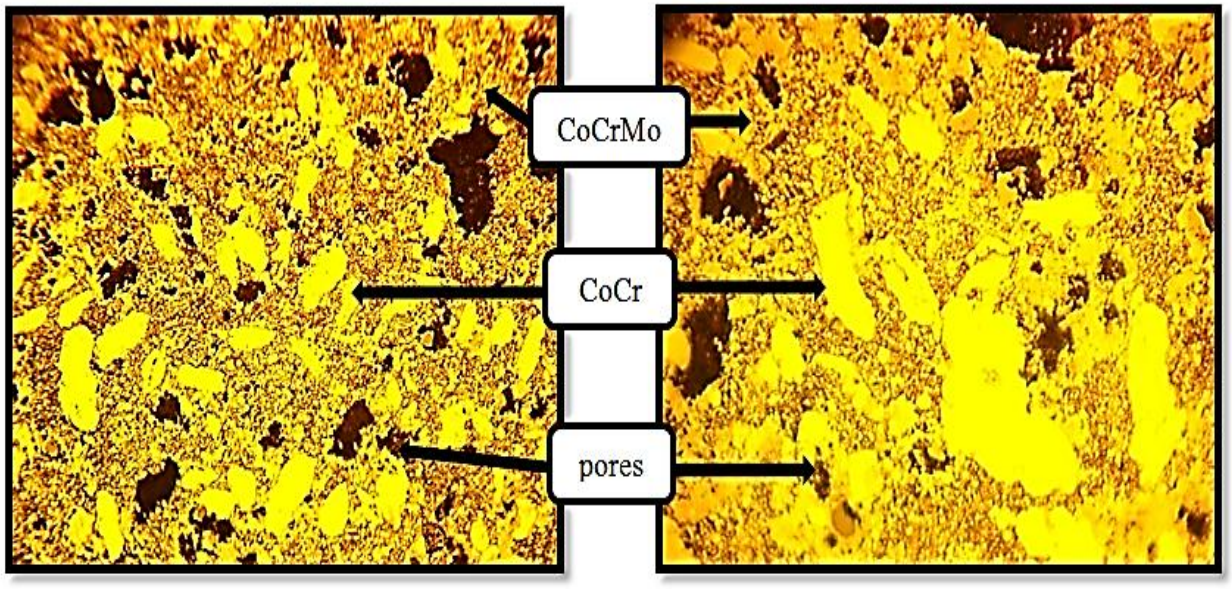

a b

Figure (4.29): Microstructure for **D2** alloys after sintering and etching (a:200x &b:400x)

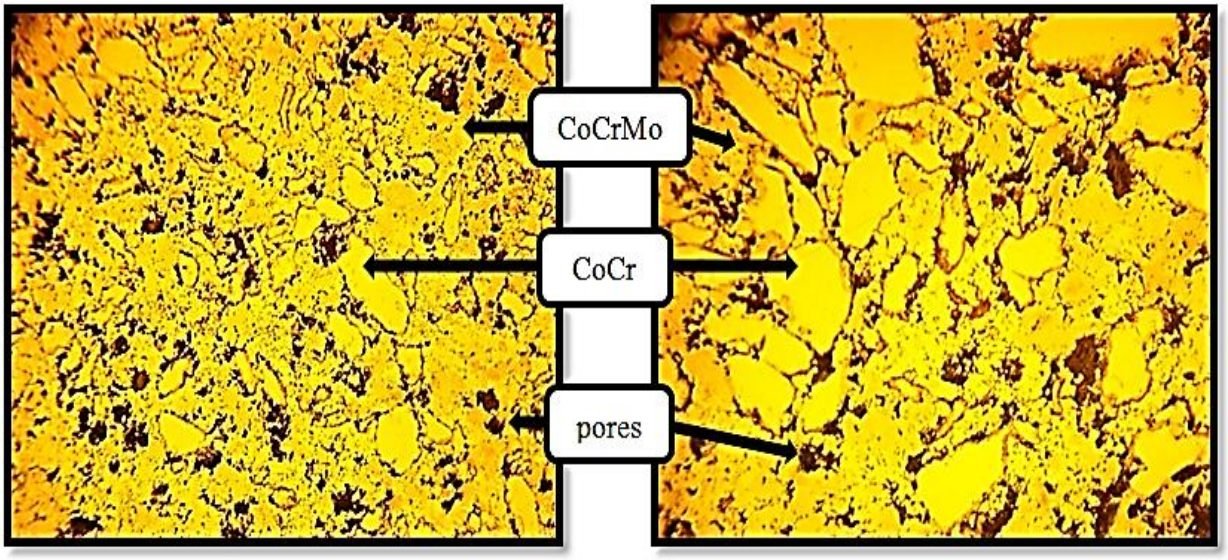

a b

Figure (4.30): Microstructure for **D3** alloys after sintering and etching (a:200x &b:400x)

4.8.2. Scanning Electron Microscope (SEM)

Figures (4.31), (4.32), (4.33) , (4.34) , (4.35) , (4.36) , (4.37) , (4.38) , (4.39) and (4.40) show the SEM of **A, B1, B2 , B3,C1,C2,C3,D1,D2** and **D3** alloys respectively with different magnification.

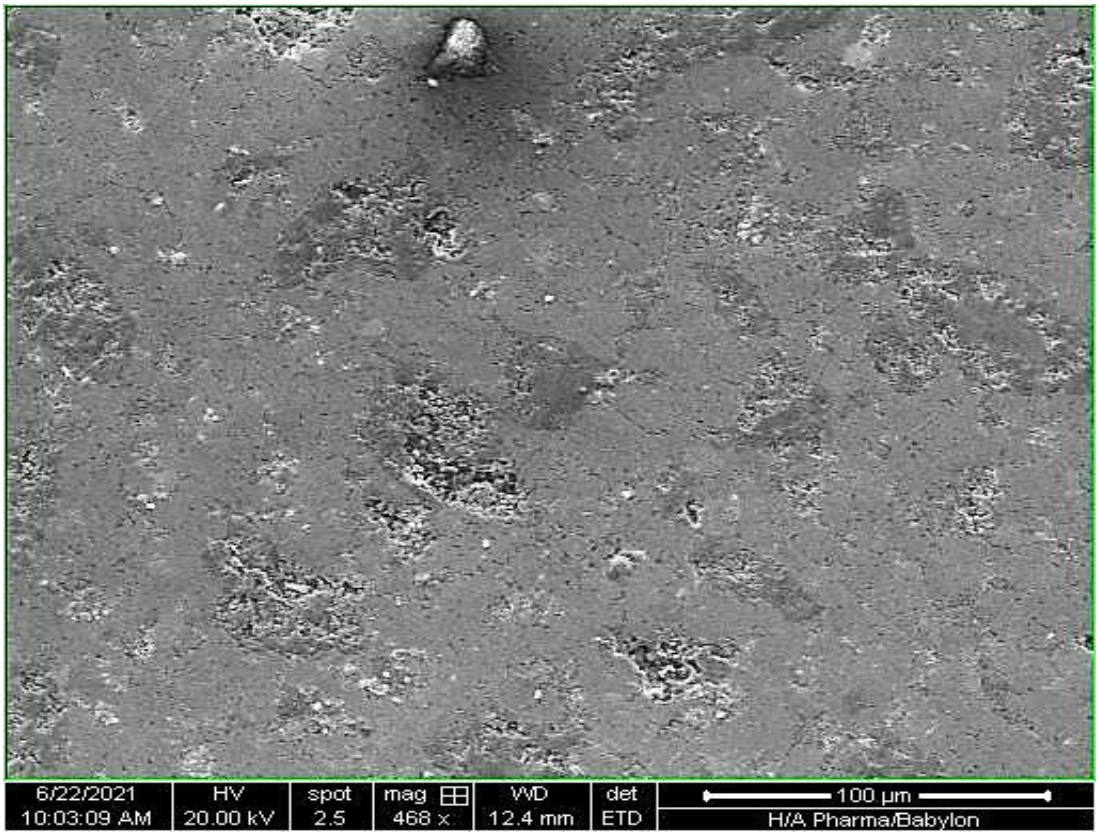

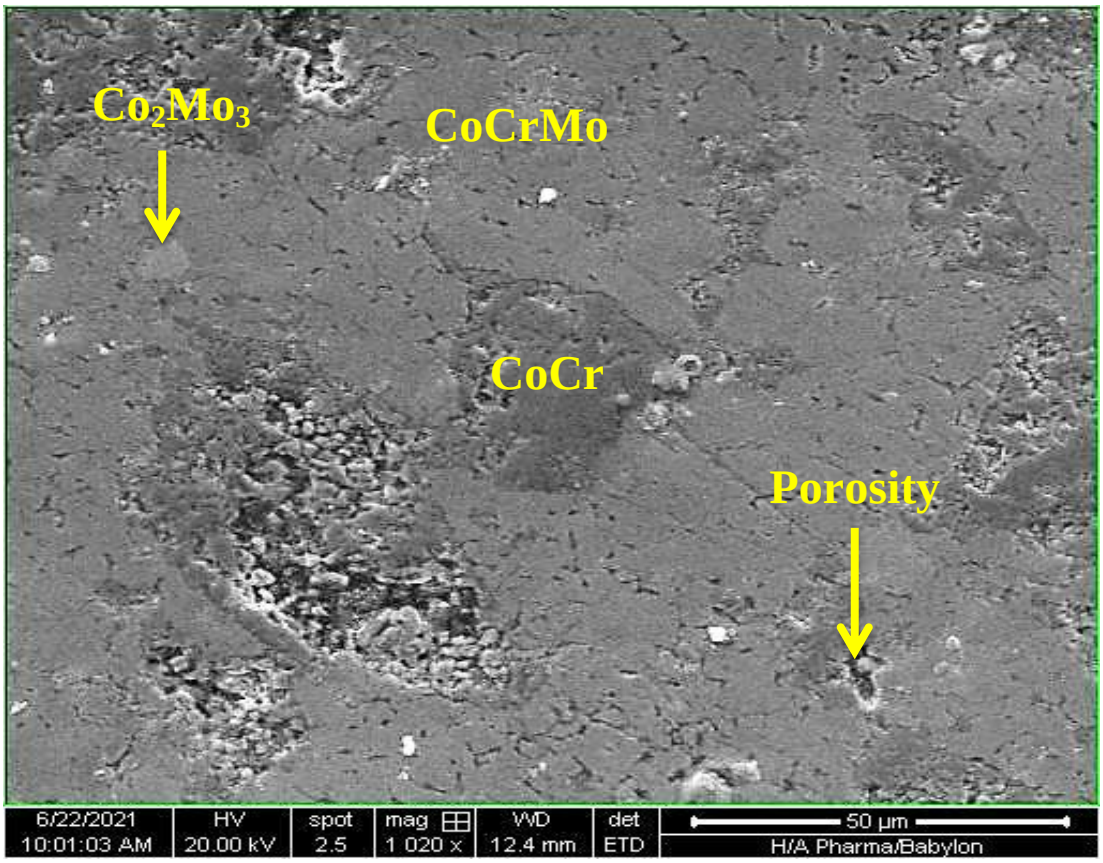

Figure(4.31): SEM images for **A** alloy with different magnification

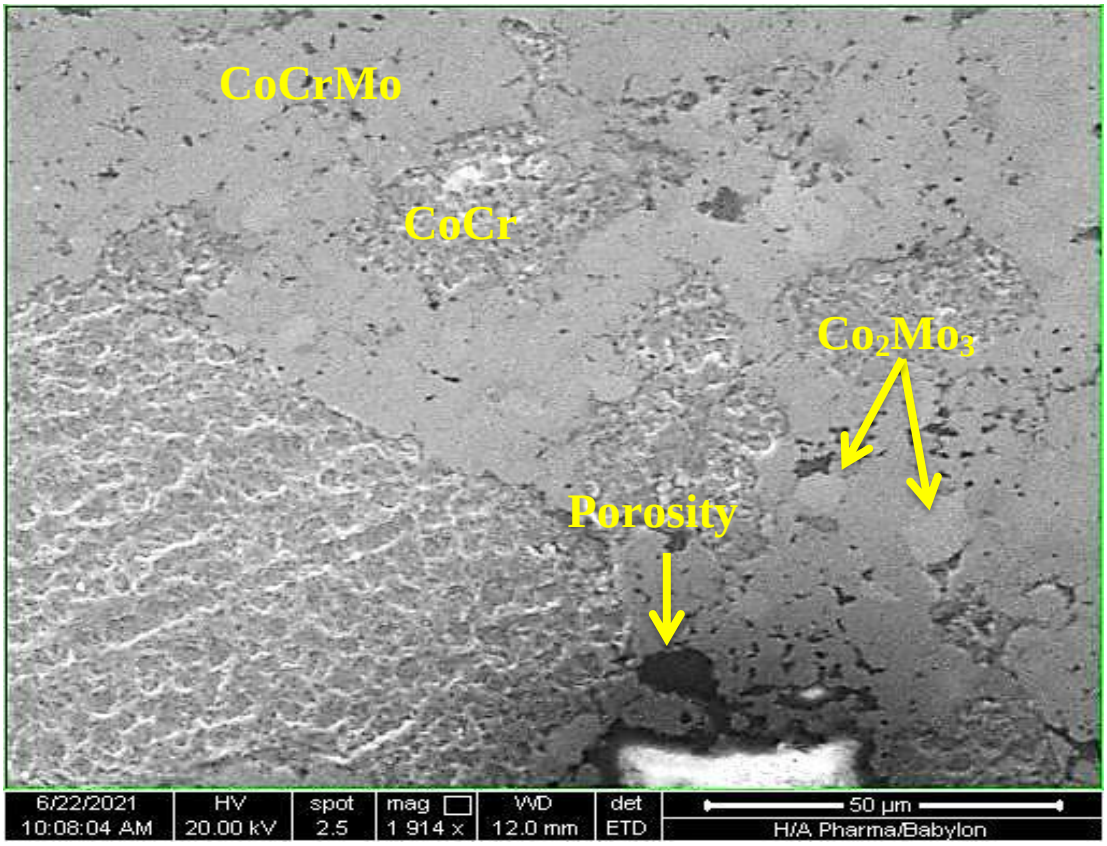

Figure(4.32): SEM images for **B1** alloy with different magnification

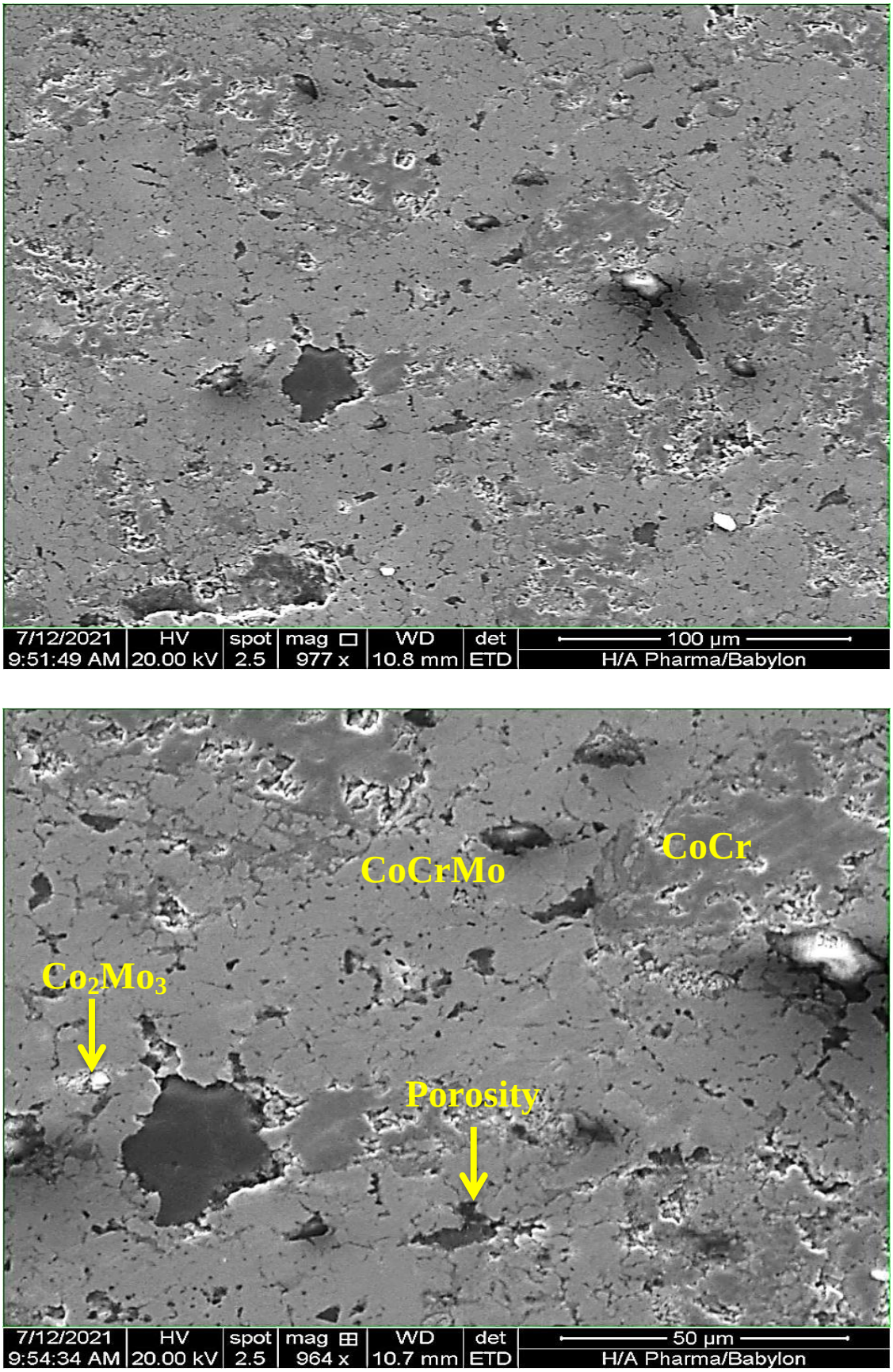

Figure(4.33): SEM images for **B2** alloy with different magnification

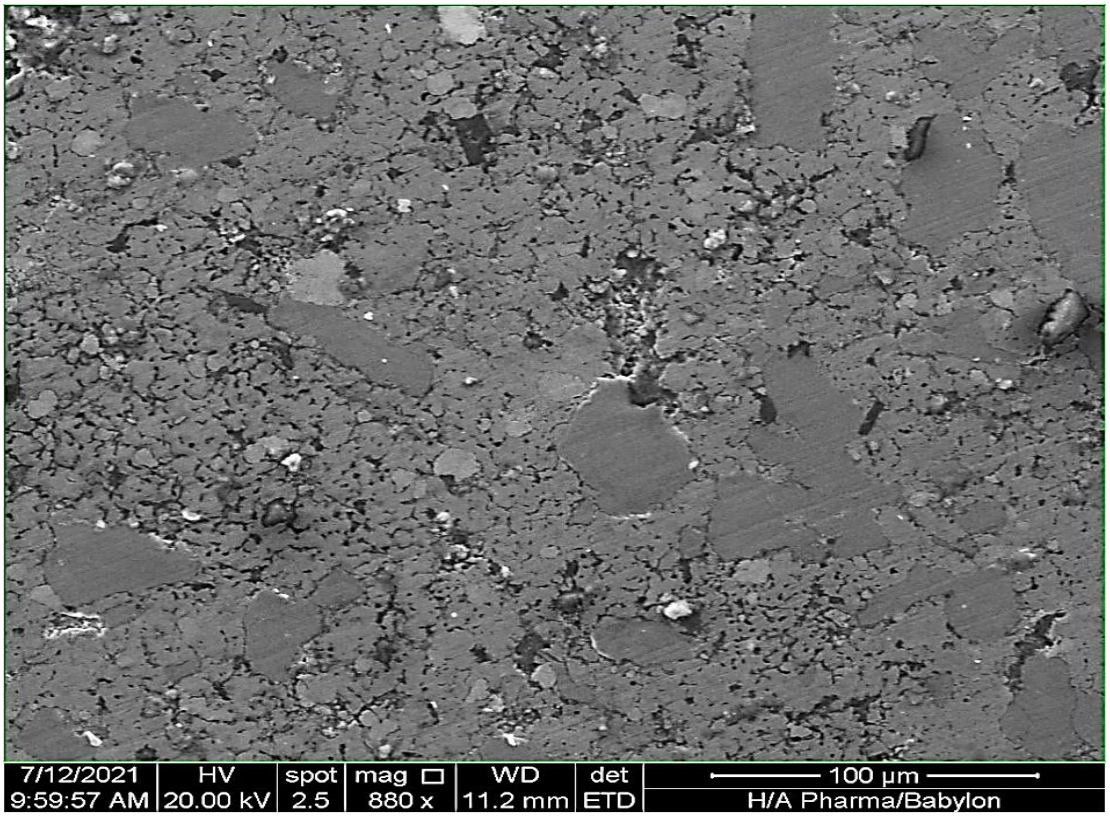

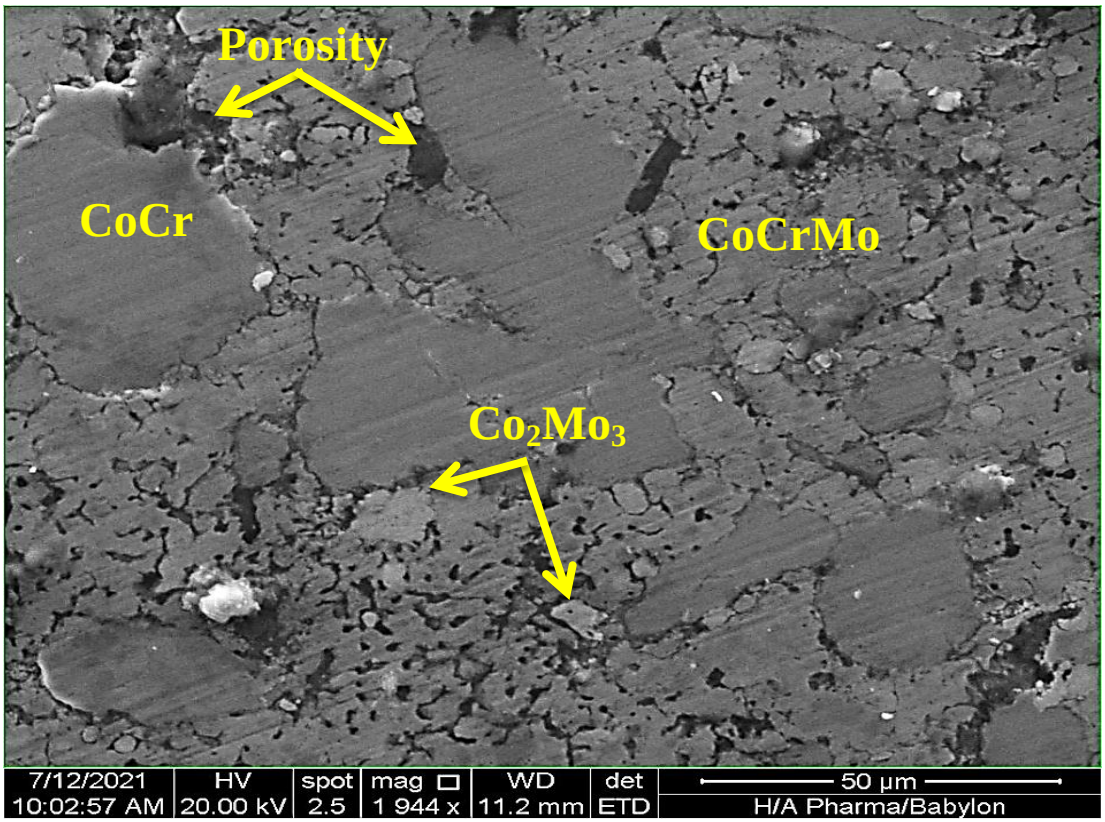

Figure(4.34): SEM images for **B3** alloy with different magnification

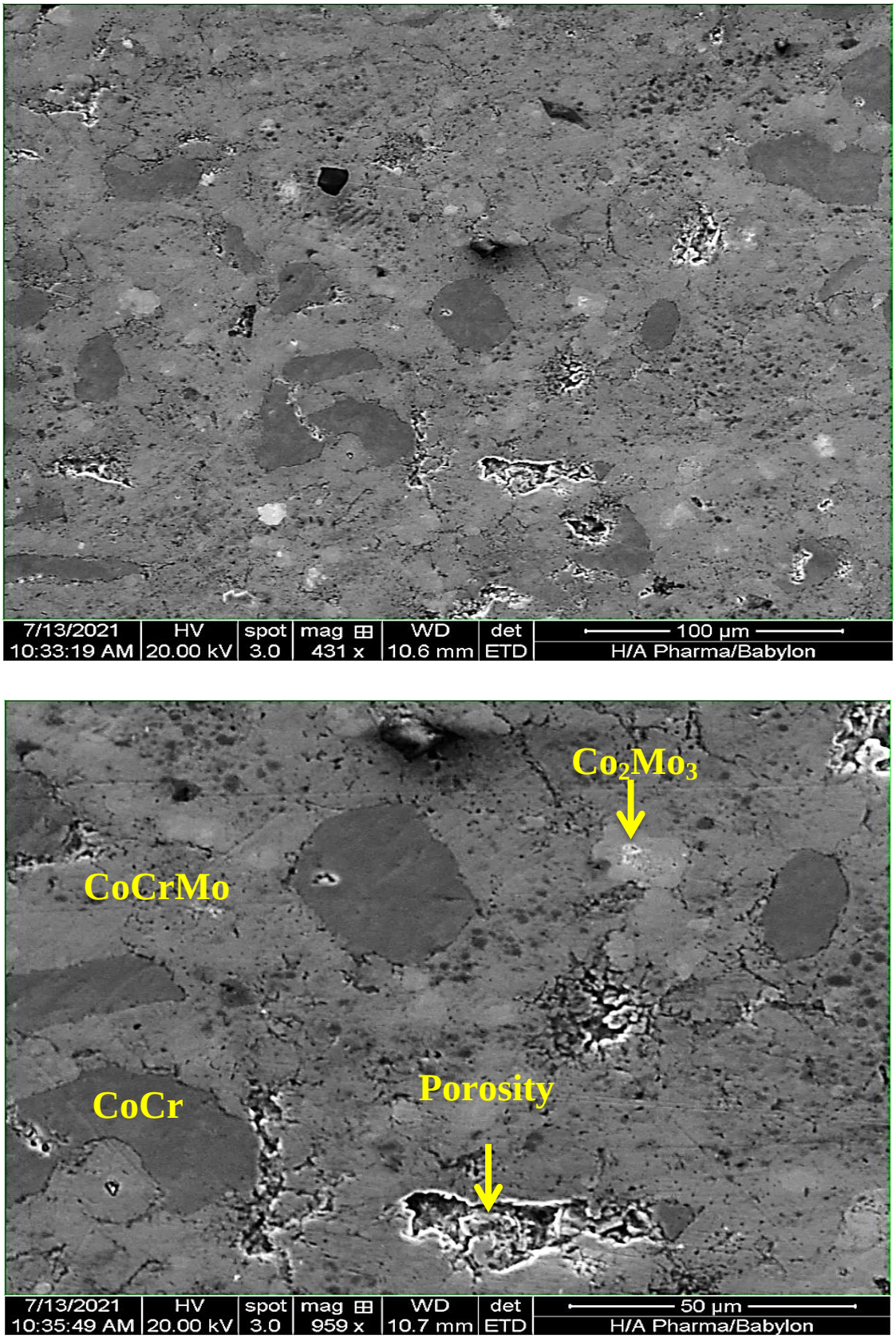

Figure(4.35): SEM images for **C1** alloy with different magnification

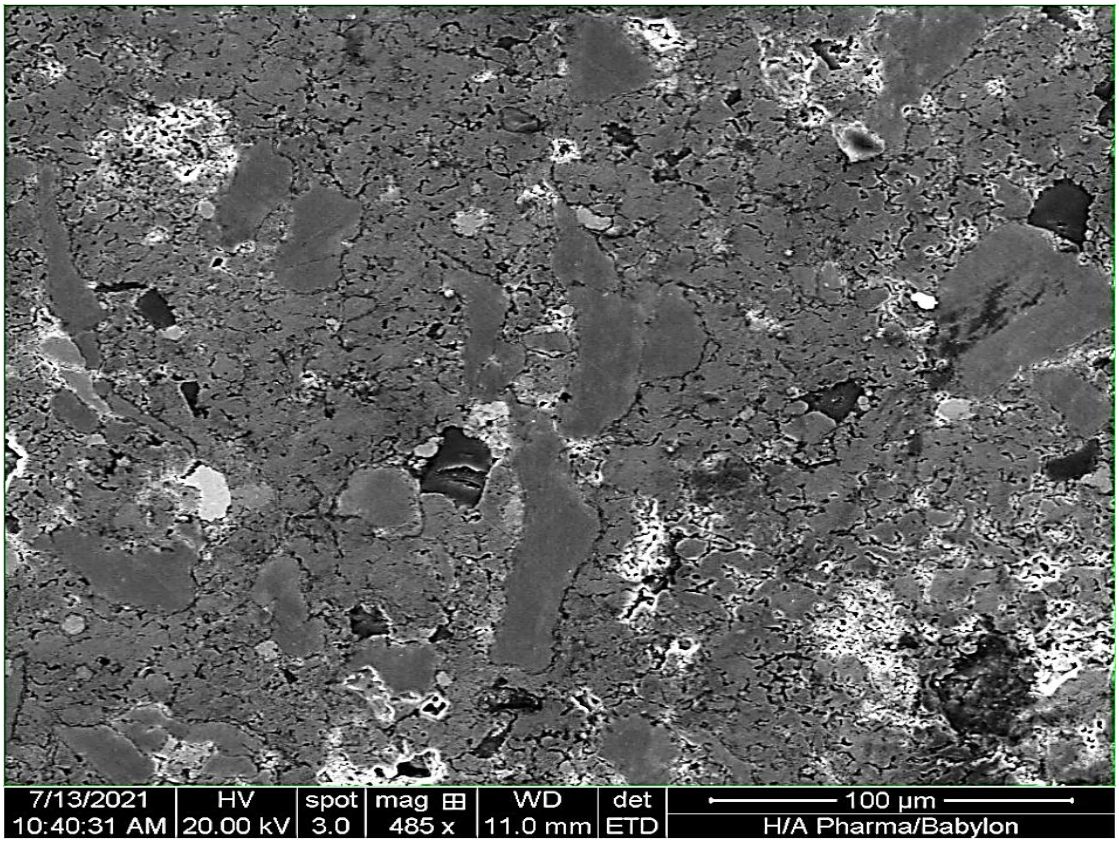

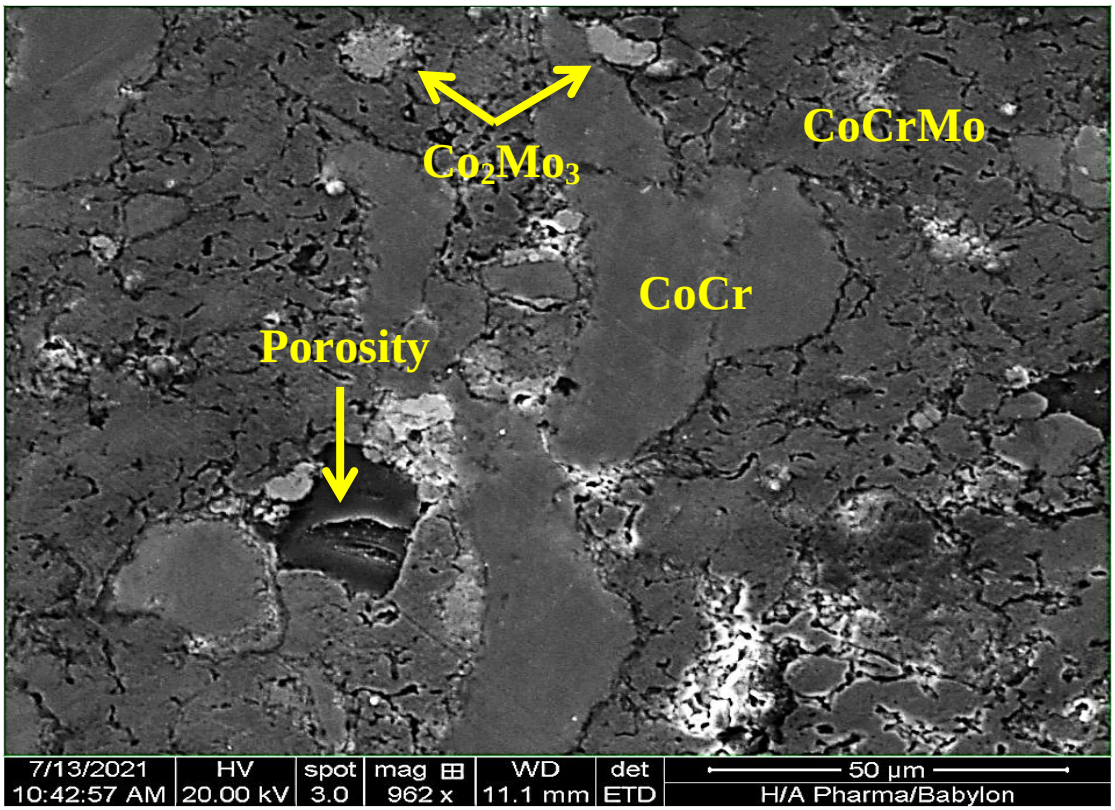

Figure(4.36): SEM images for **C2** alloy with different magnification

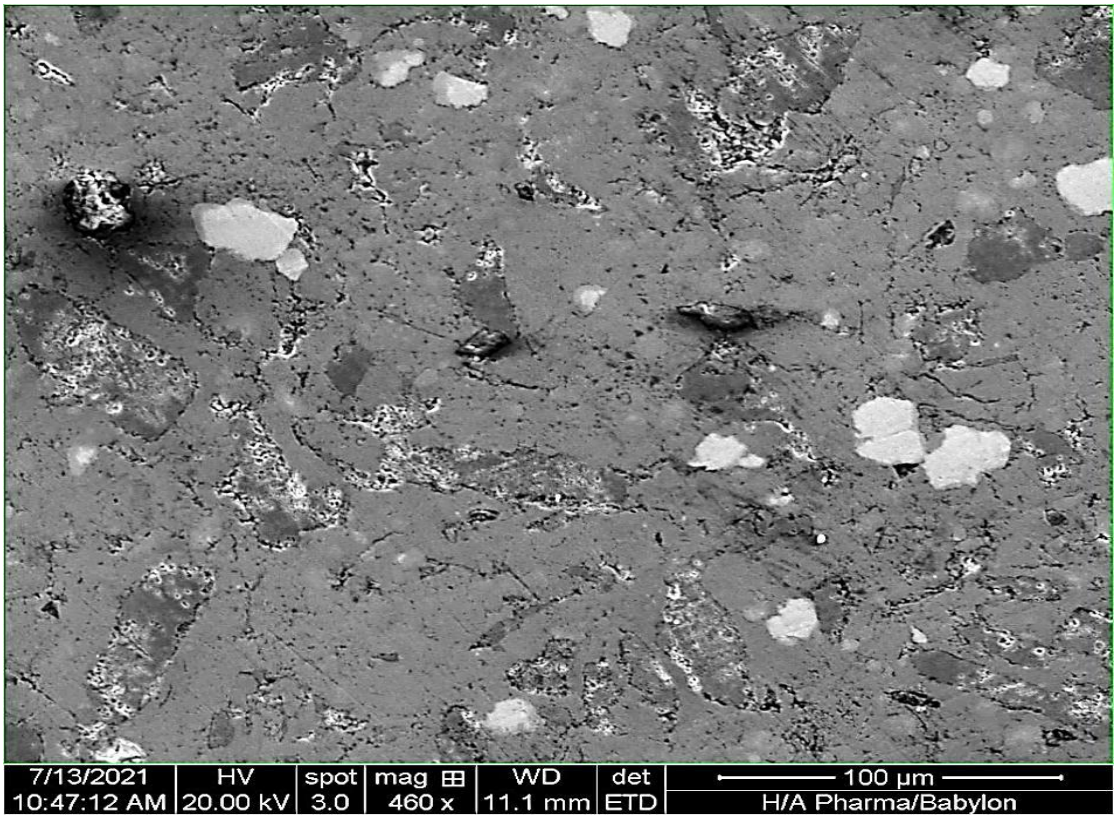

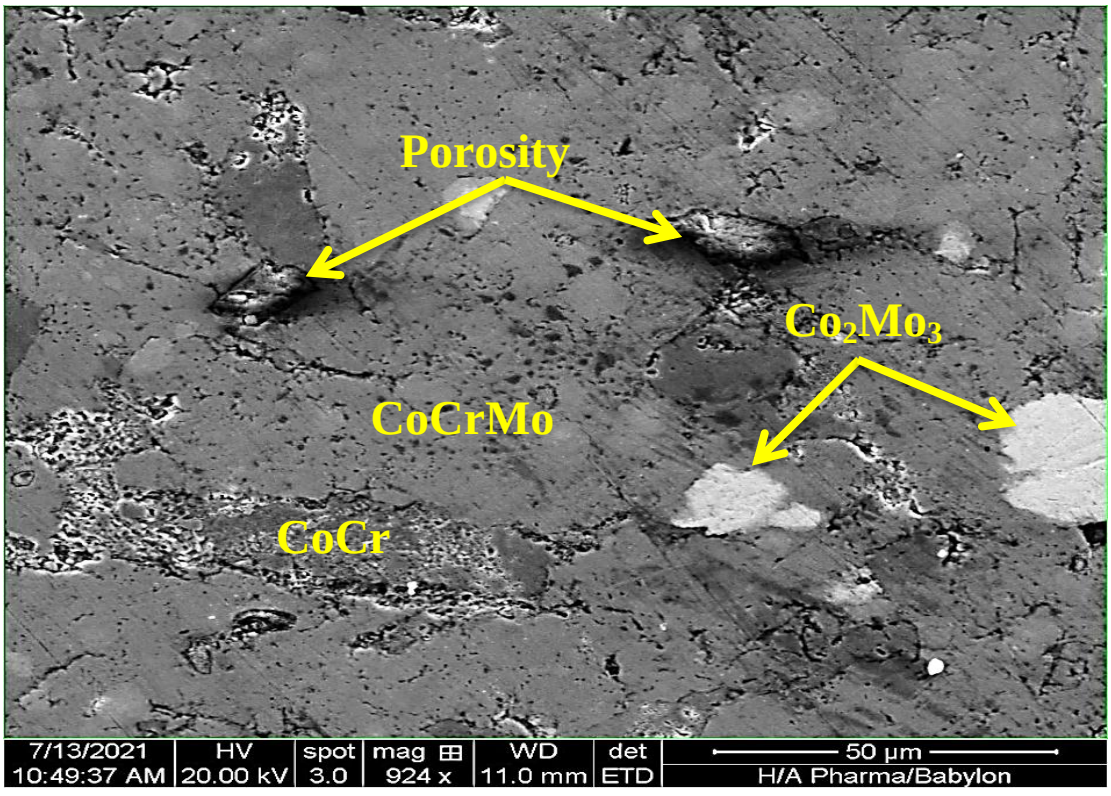

Figure(4.37): SEM images for **C3** alloy with different magnification

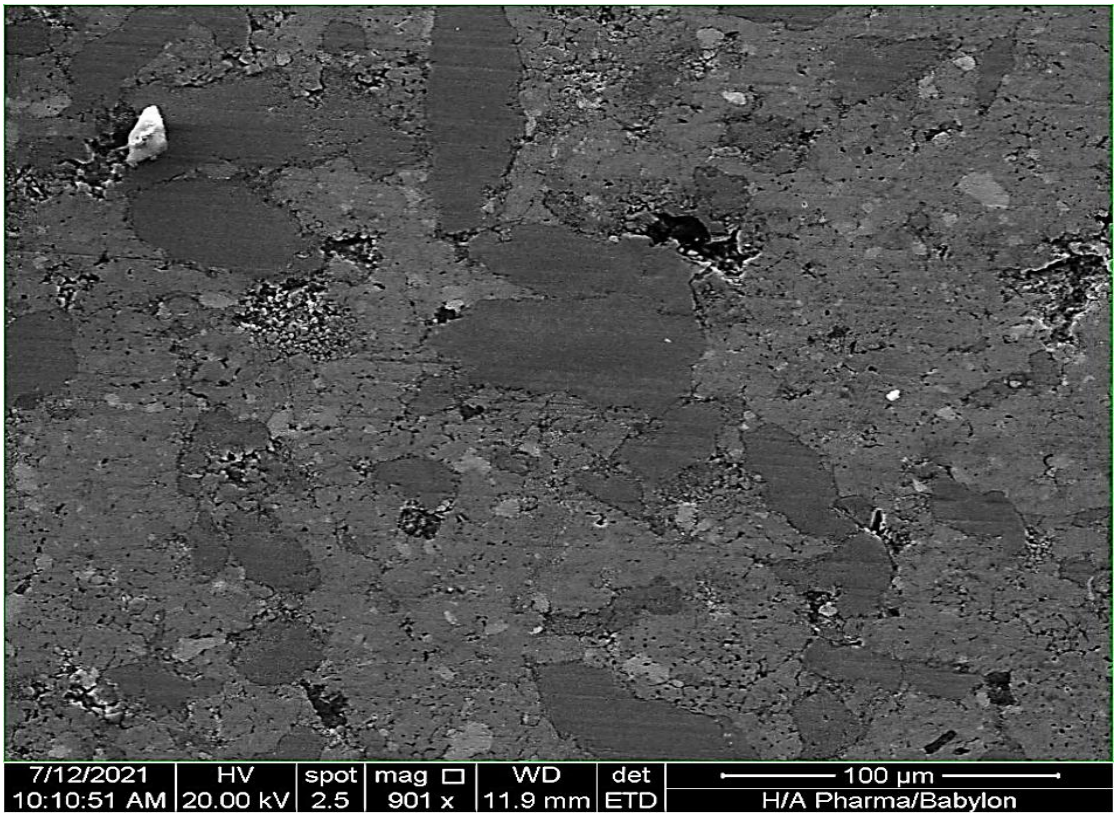

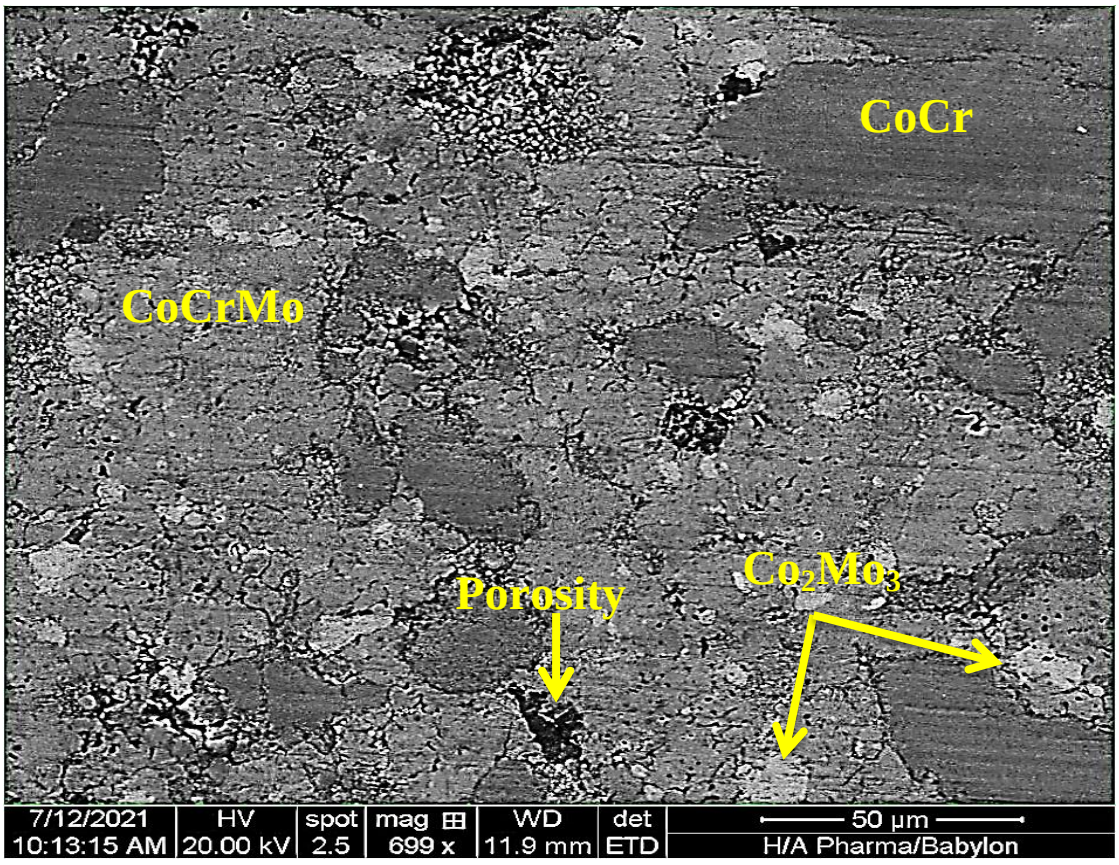

Figure(4.38): SEM images for **D1** alloy with different magnification

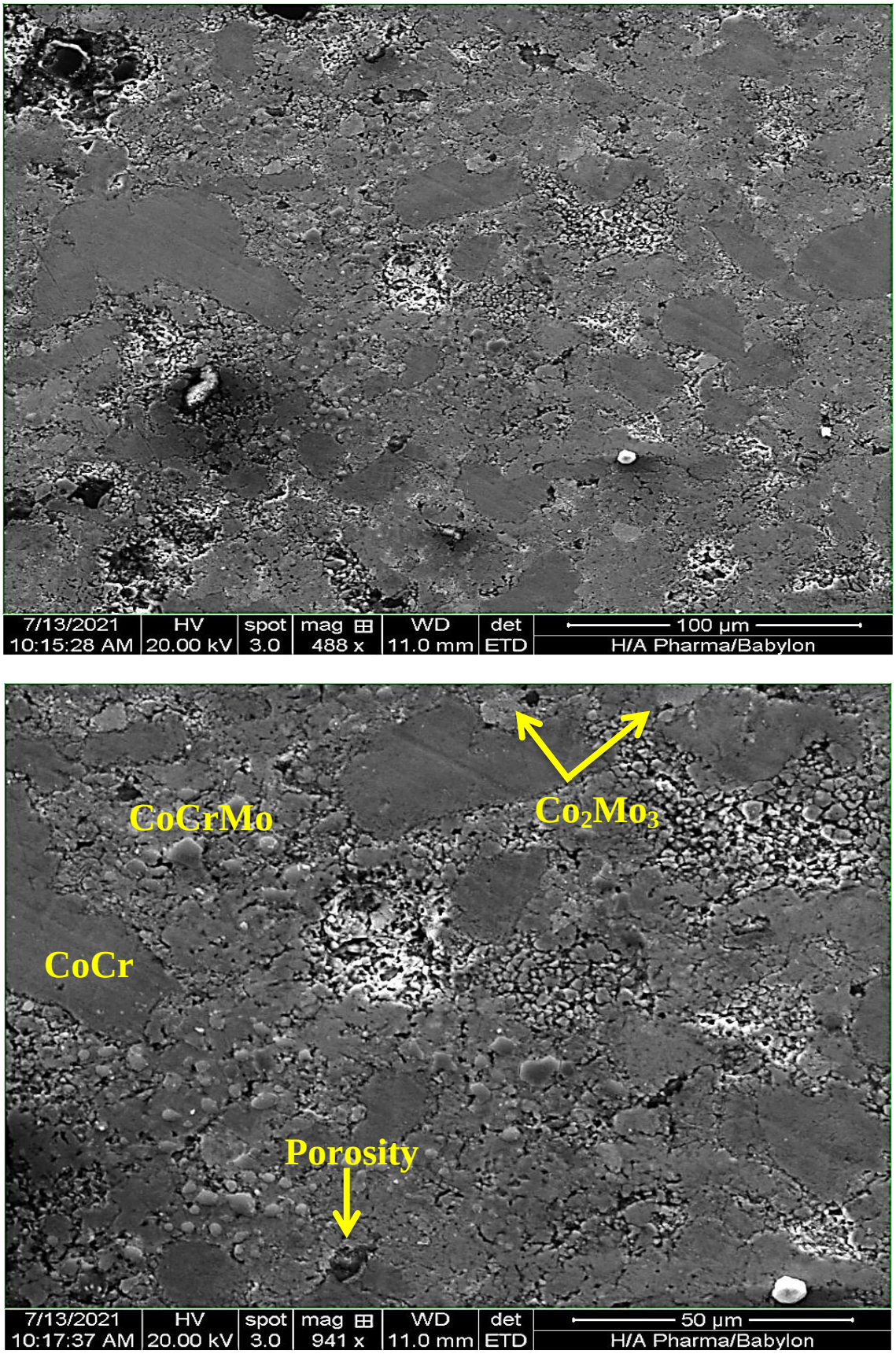

Figure(4.39): SEM images for **D2** alloy with different magnification

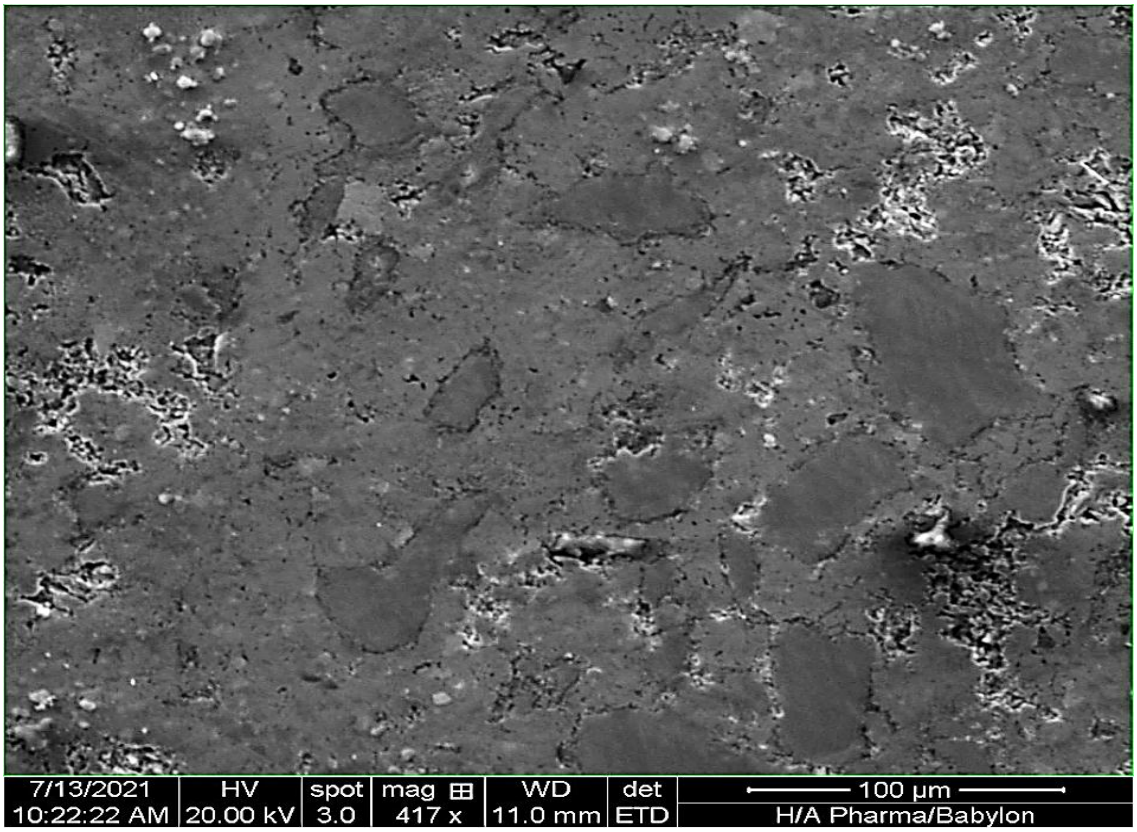

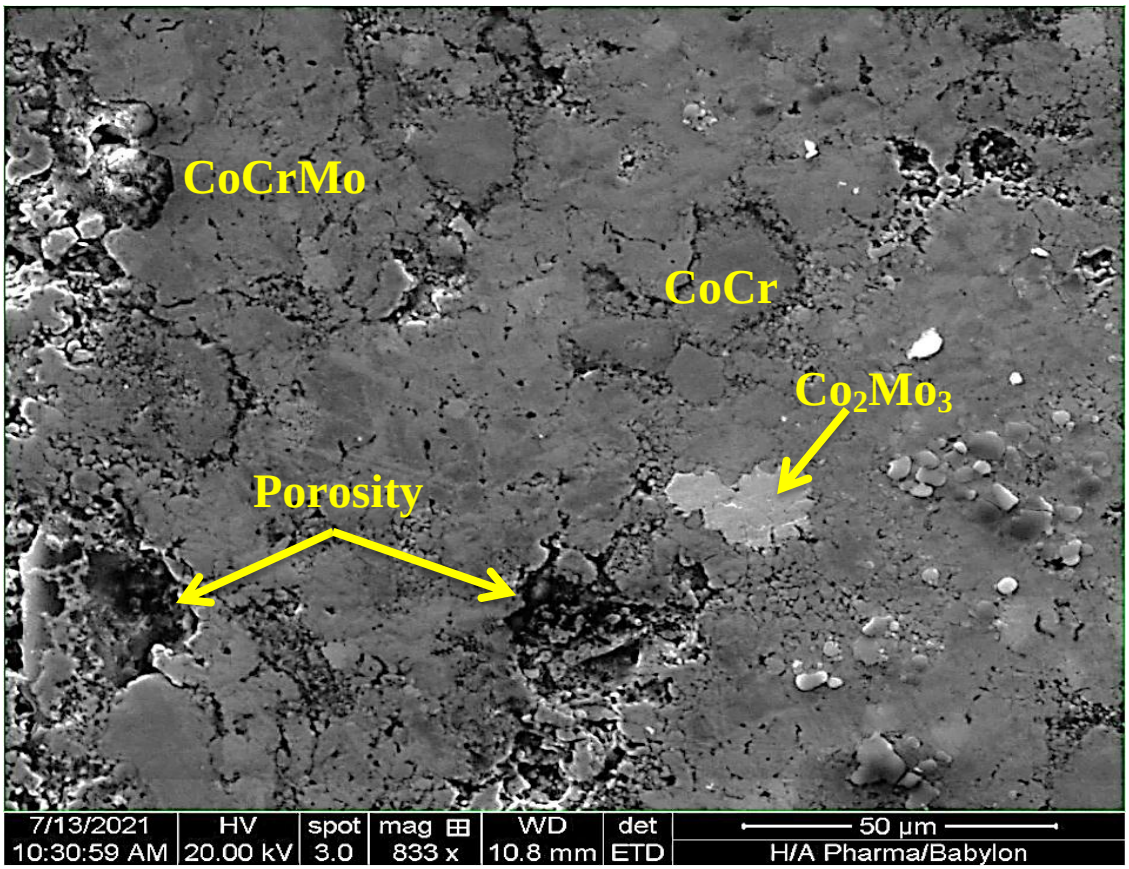

Figure(4.40): SEM images for **D3** alloy with different magnification

As shown from figure (4.31) to (4.40) that SEM are very sensitive to chemical composition as a result, the microstructure of sintered specimens showed a multiphase structure in which the two phases (CoCr and Co_2Mo_3) are embedded in uniformly matrix (CoCrMo –F.C.C), thus confirming the XRD results.

SEM images of etched alloys showed grain boundaries and pores in different sizes.

4.8.3. Energy Dispersive X-ray Spectroscopy (EDX)

Energy dispersive spectroscopy (EDS) utilized a high-energy focused electron beam to emit an X-ray spectrum of a solid specimen. EDS is able to identify the chemical composition that results from the contrast topography differences on an SEM image. Precision obtained from specimens is limited by statistical error. EDS was scanned on several different polished specimens. From figure (4.41) shows two EDS point analysis taken per specimen. Figure (4.41)shows the EDS spectrum of elements found in base CoCrMo alloys. The chemical analysis consist of cobalt, chromium, and molybdenum where quantified because the basic components of the alloy consist of these elements with the presence of other elements present in very small percentages these results are similar to **[147]** . On the other hand, the EDS analysis for the prepared specimens with (0.5 wt.% , 1 wt.% and 1.5 wt. %) addition of boron , Tungsten are shown in figures (4.42) to (4.47) respectively while EDS analysis for the prepared specimens with (1 wt.% , 3wt.% and 5 wt. %) addition of boron carbide are shown in figure (4.48), figure(4.49) and figure (4.50) respectively. It seems clear from the chemical analysis that boron and tungsten and the boron carbide ceramic material are present in the composition the chemist of prepared alloys. In addition to the main elements in the alloy (cobalt, chromium and molybdenum) with the presence of other elements present in very small percentages. As can be seen, the results of EDS analysis were relatively close from the percentage of addition , because the values gained from EDS analysis do not cover the total area , only the spot where the electron stroke**[148].**

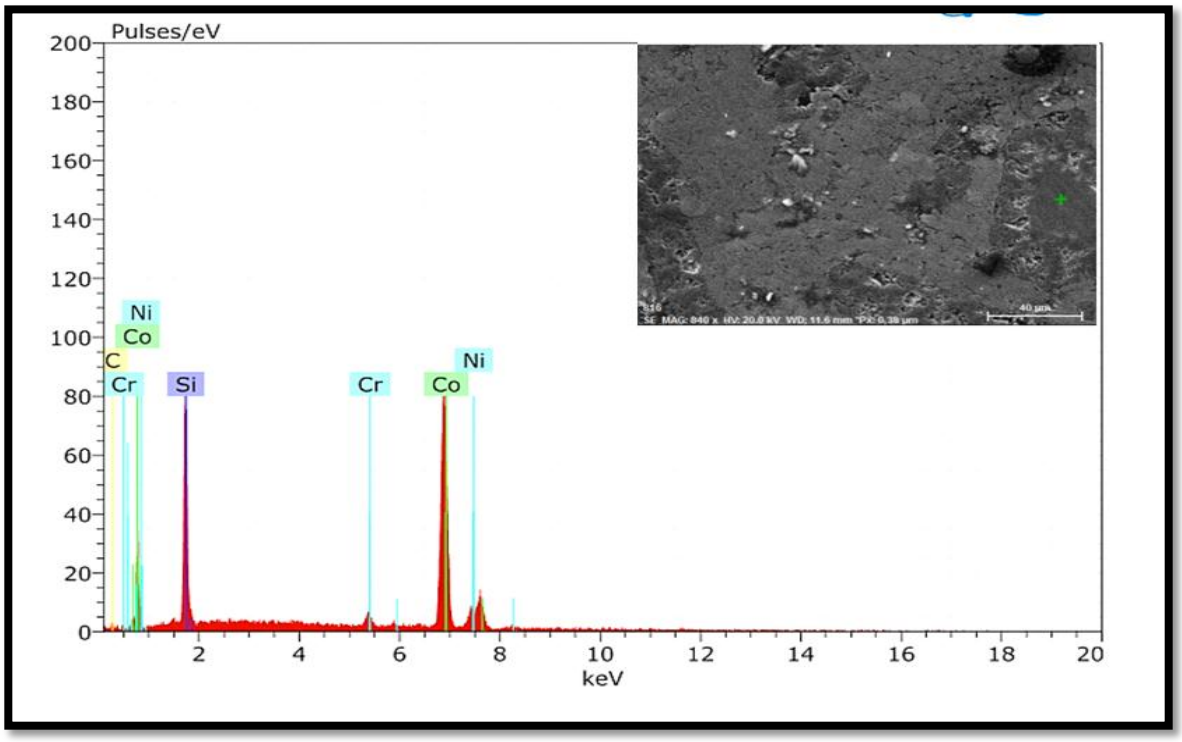

a

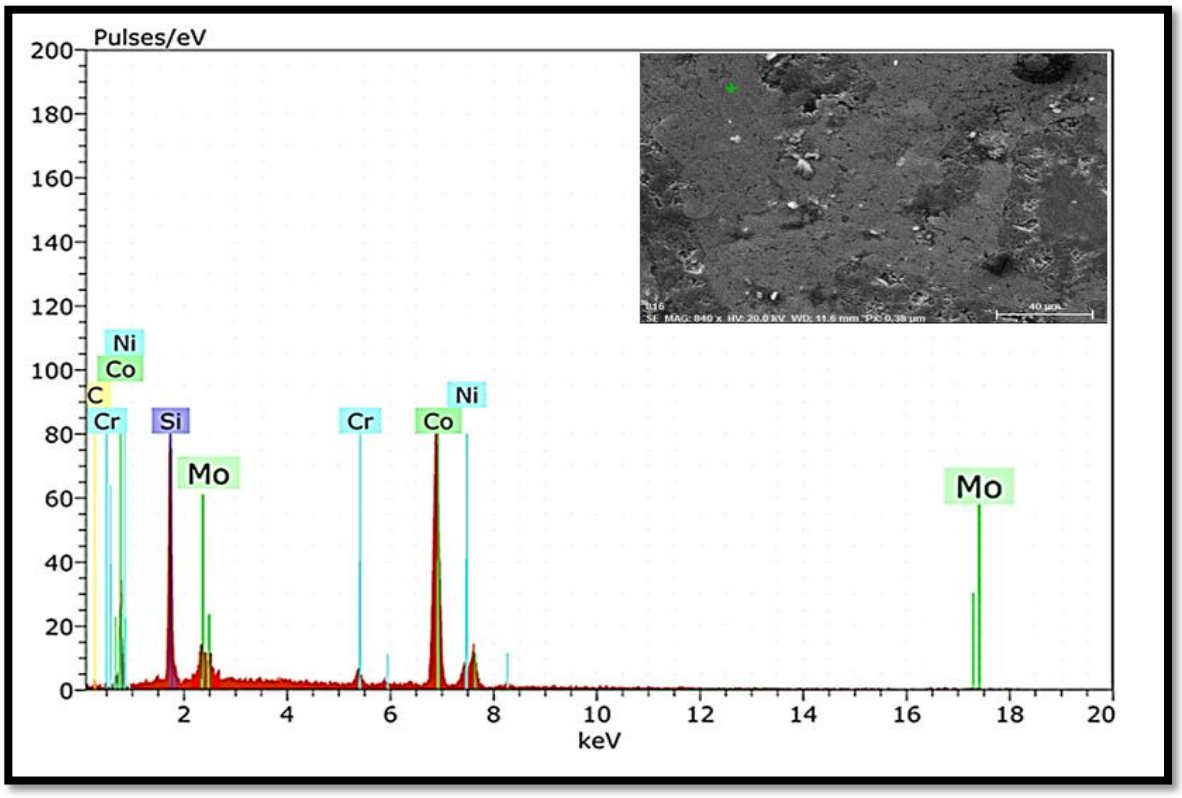

b

Figure(4.41) :EDS for **A** alloy

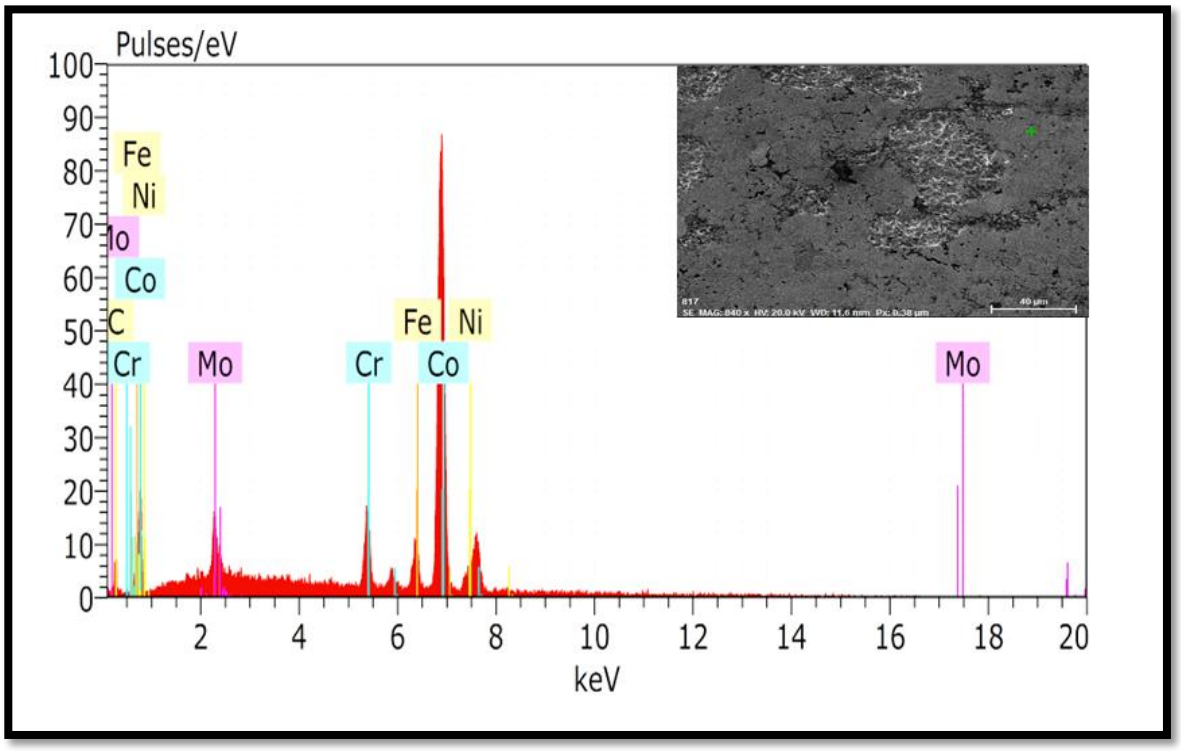

a

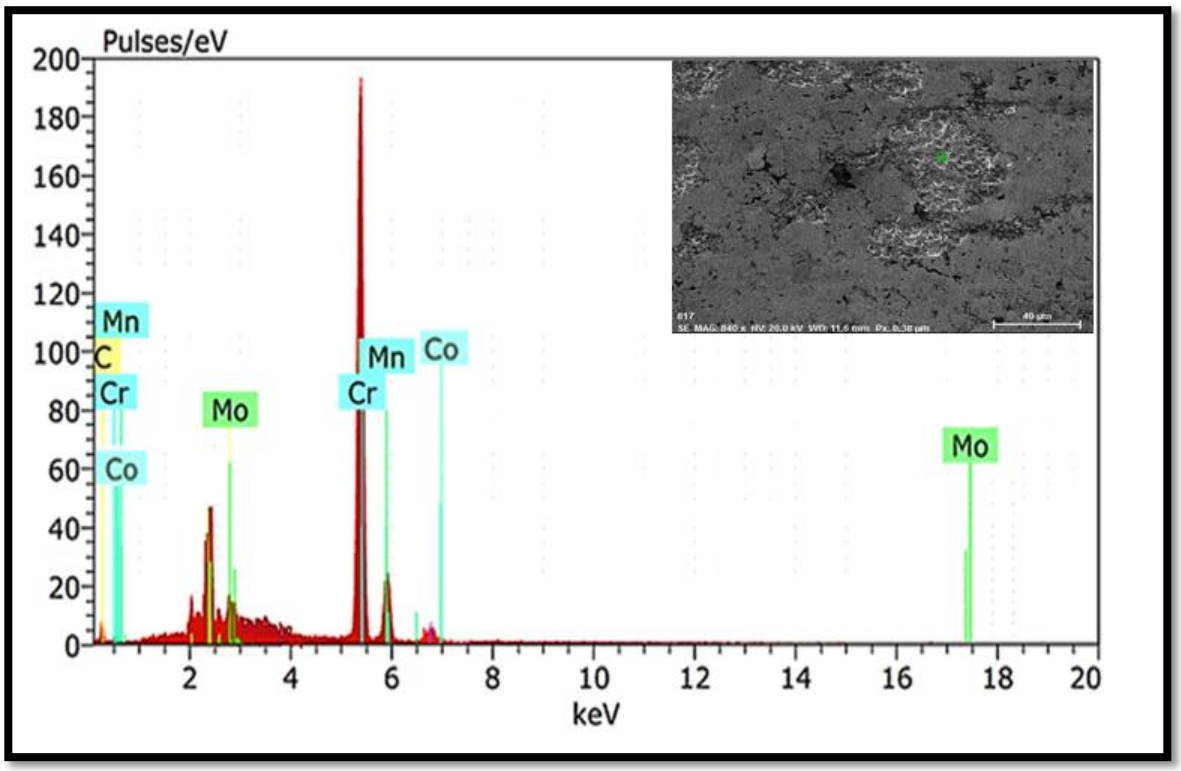

b

Fig(4.42):EDS for **B1** alloy

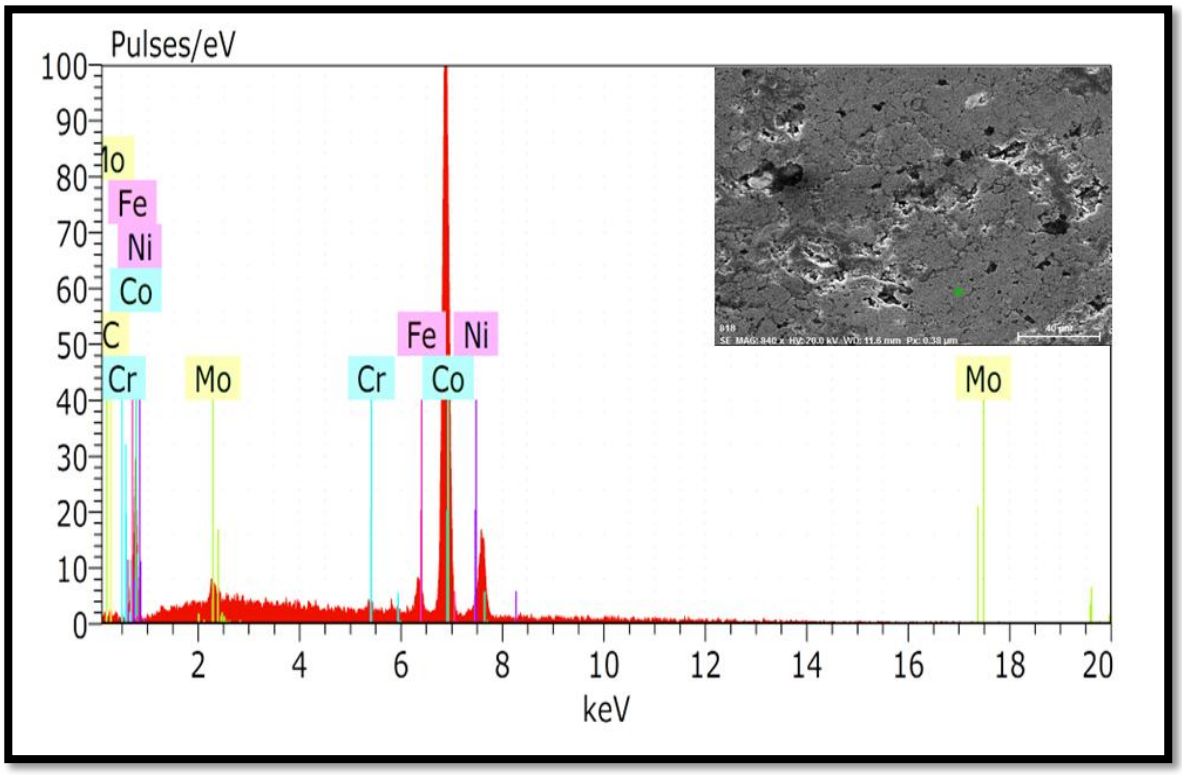

a

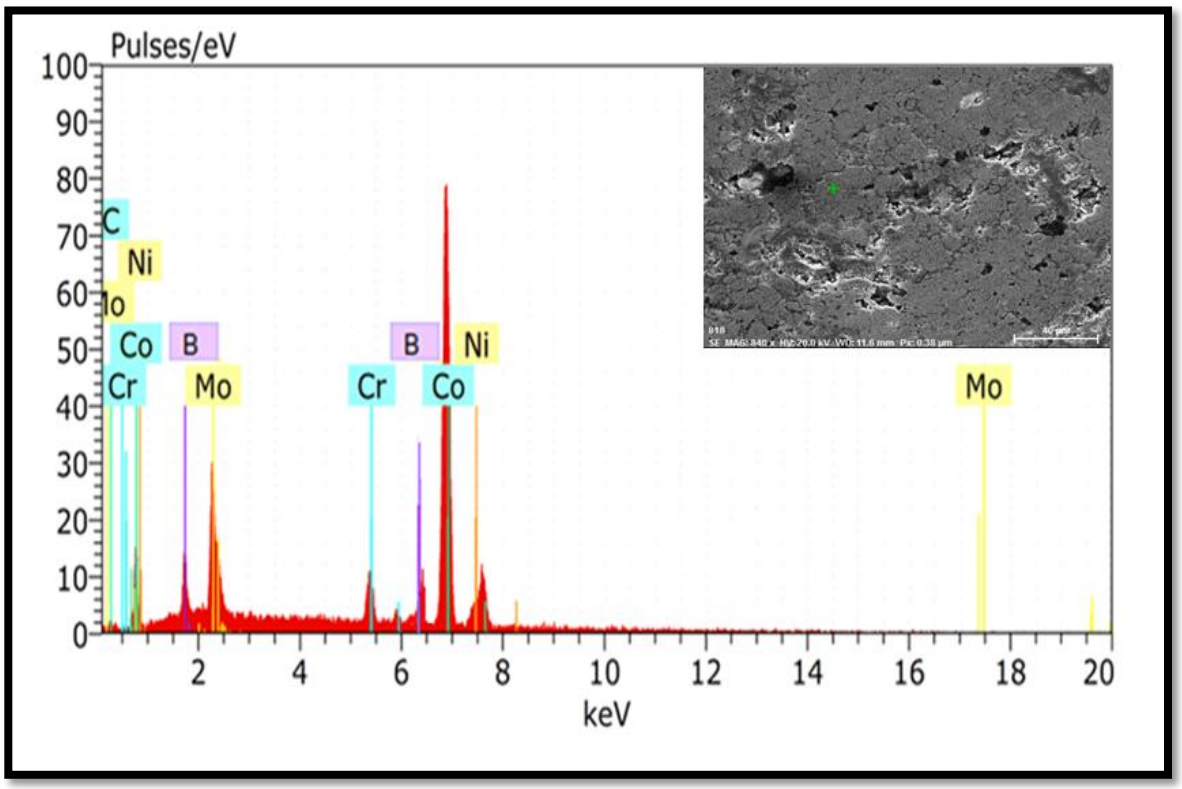

b

Figure(4.43) :EDS for **B2** alloy

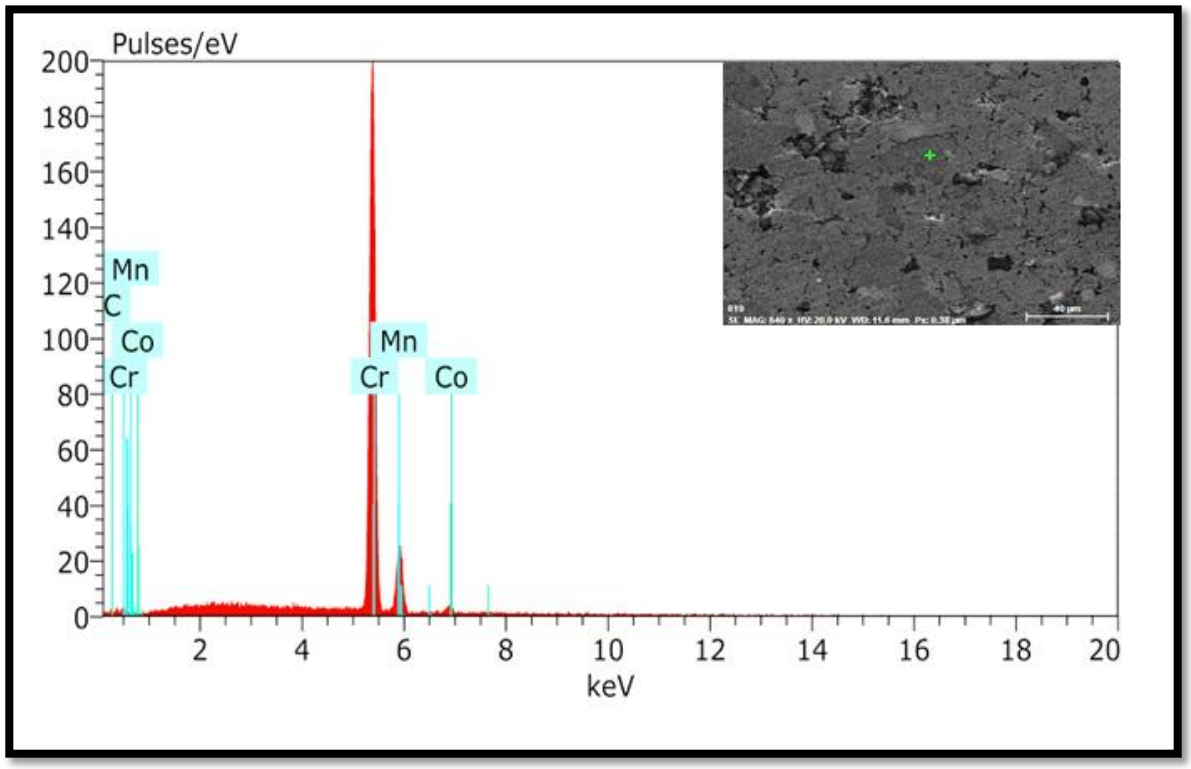

a

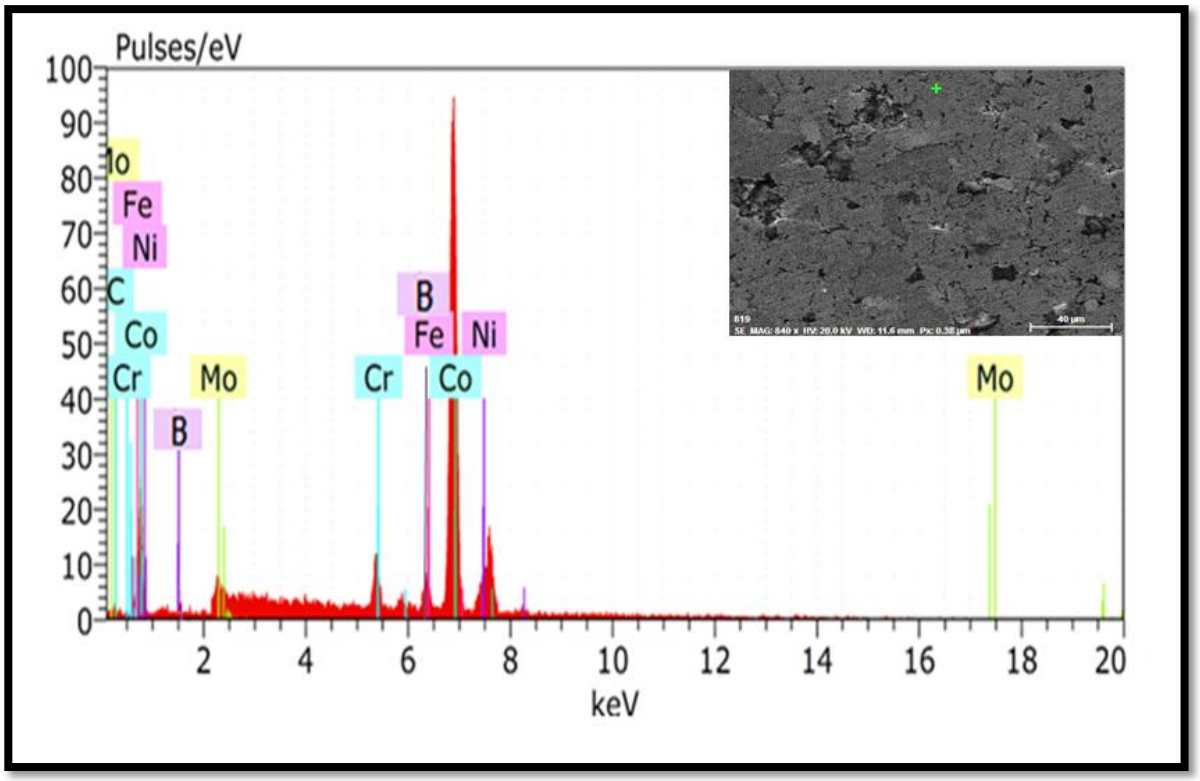

b

Figure(4.44) :EDS for **B3** alloy

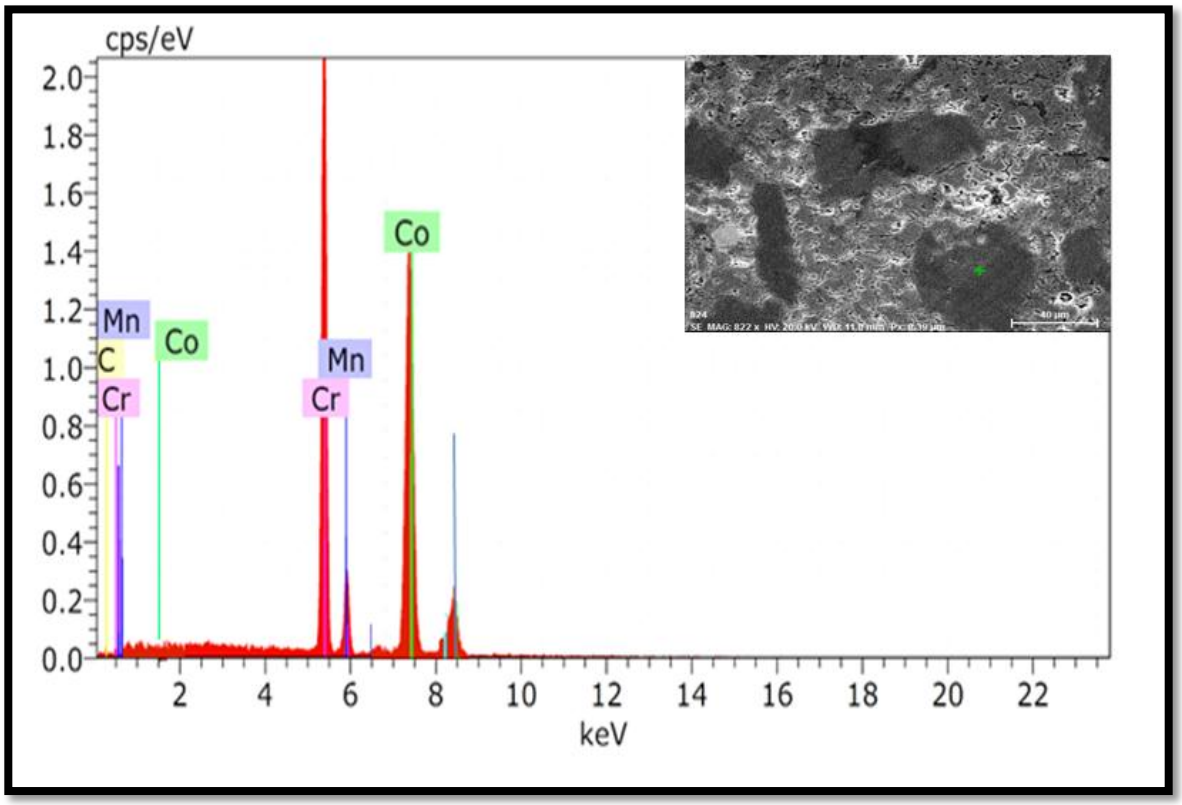

a

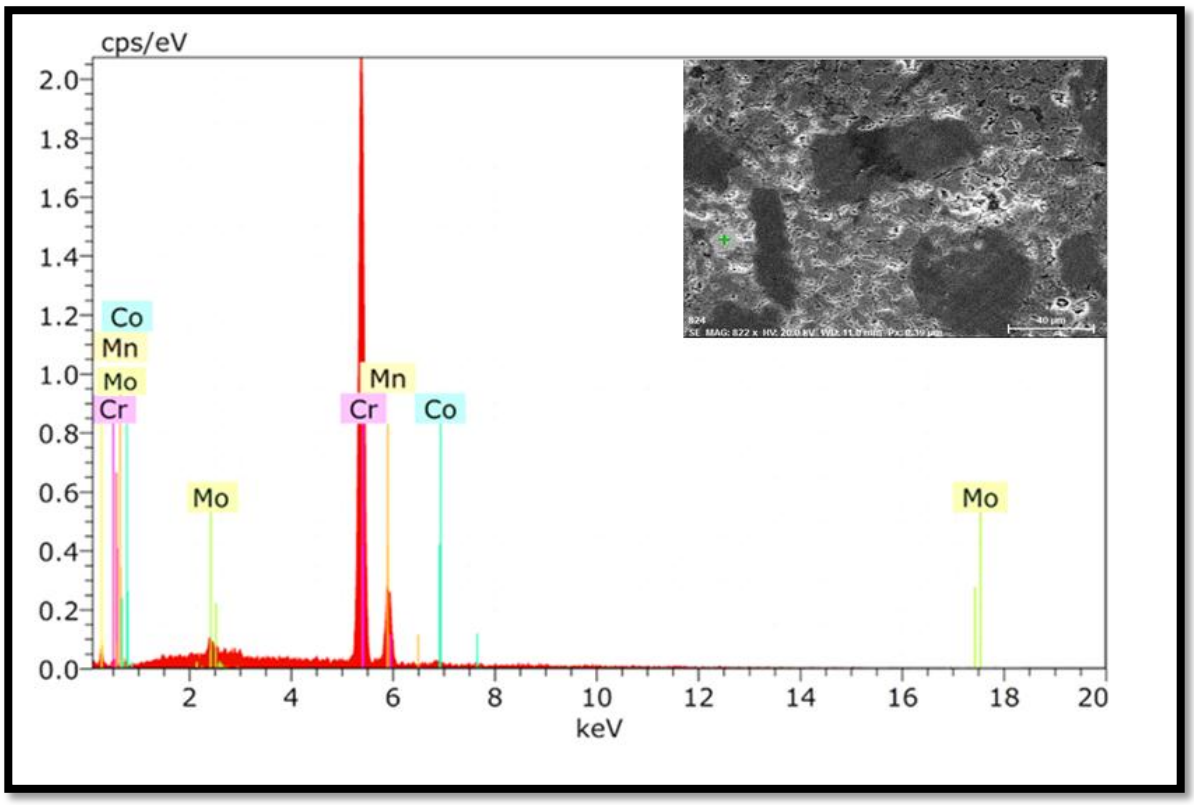

b

Figure(4.45) :EDS for **C1** alloy

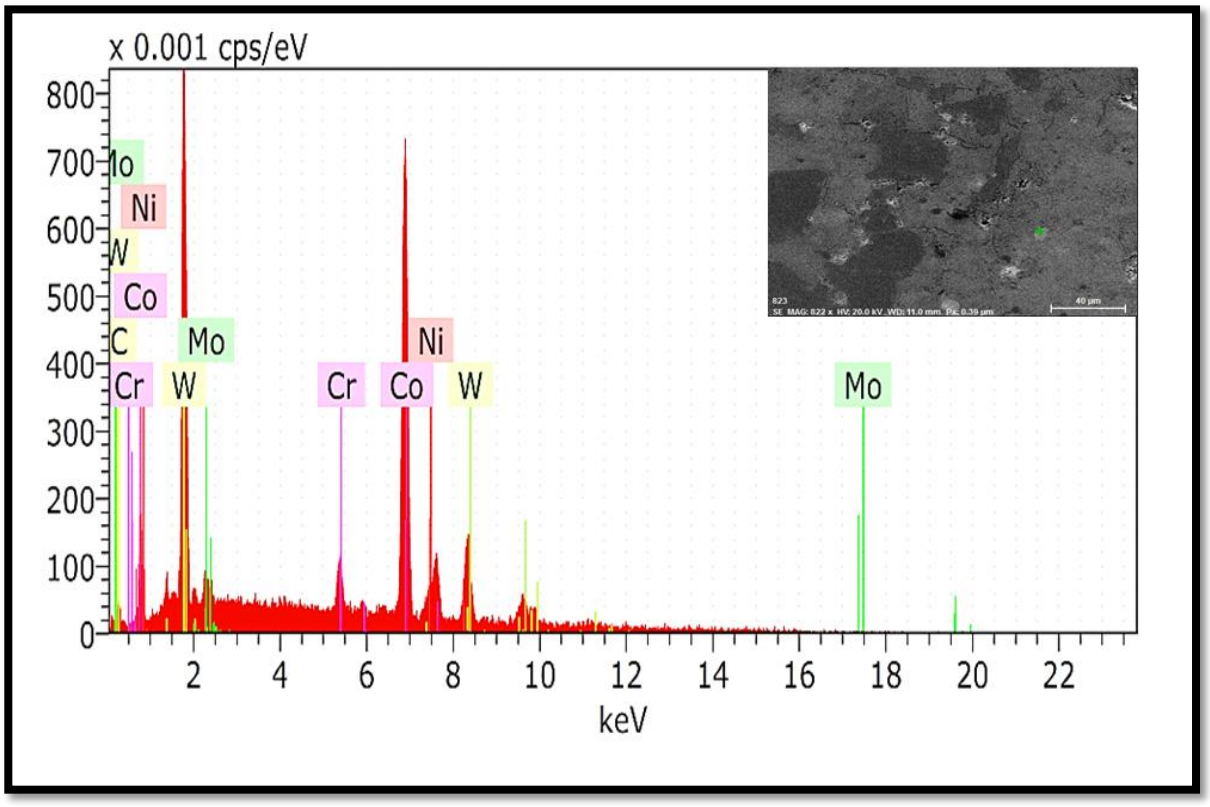

a

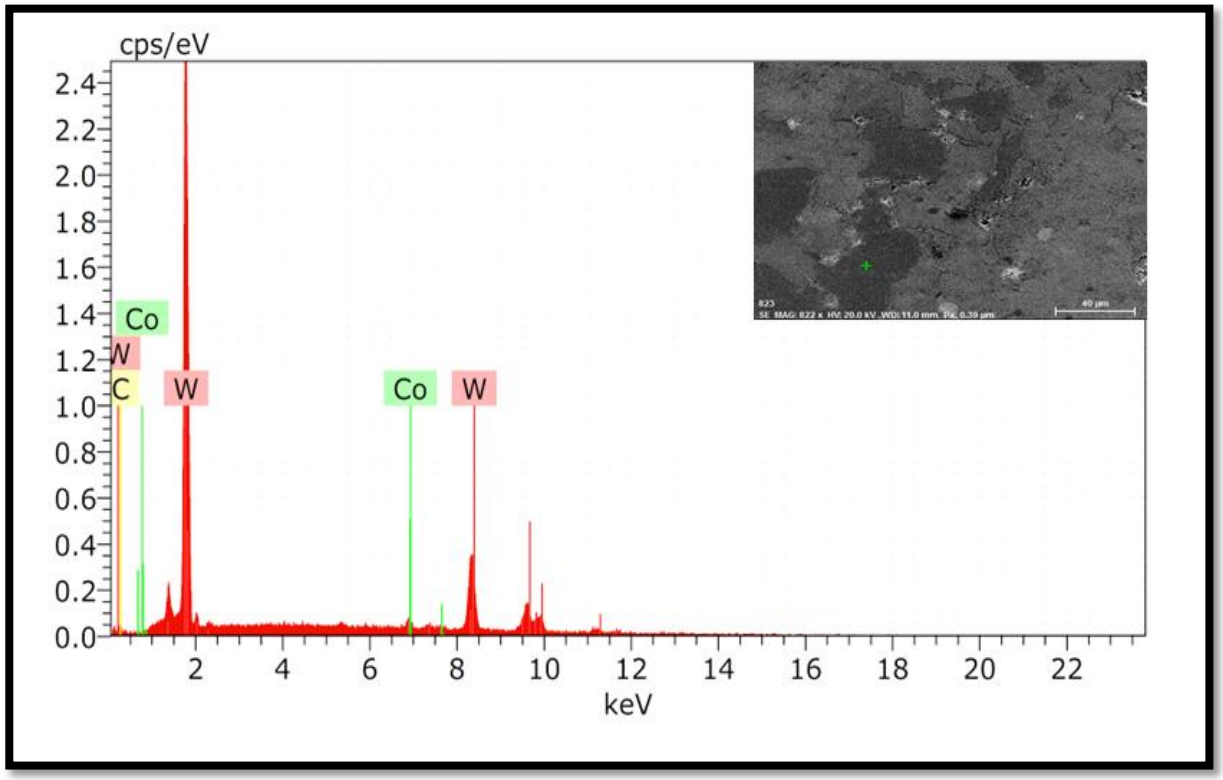

b

Figure(4.46) :EDS for **C2** alloy

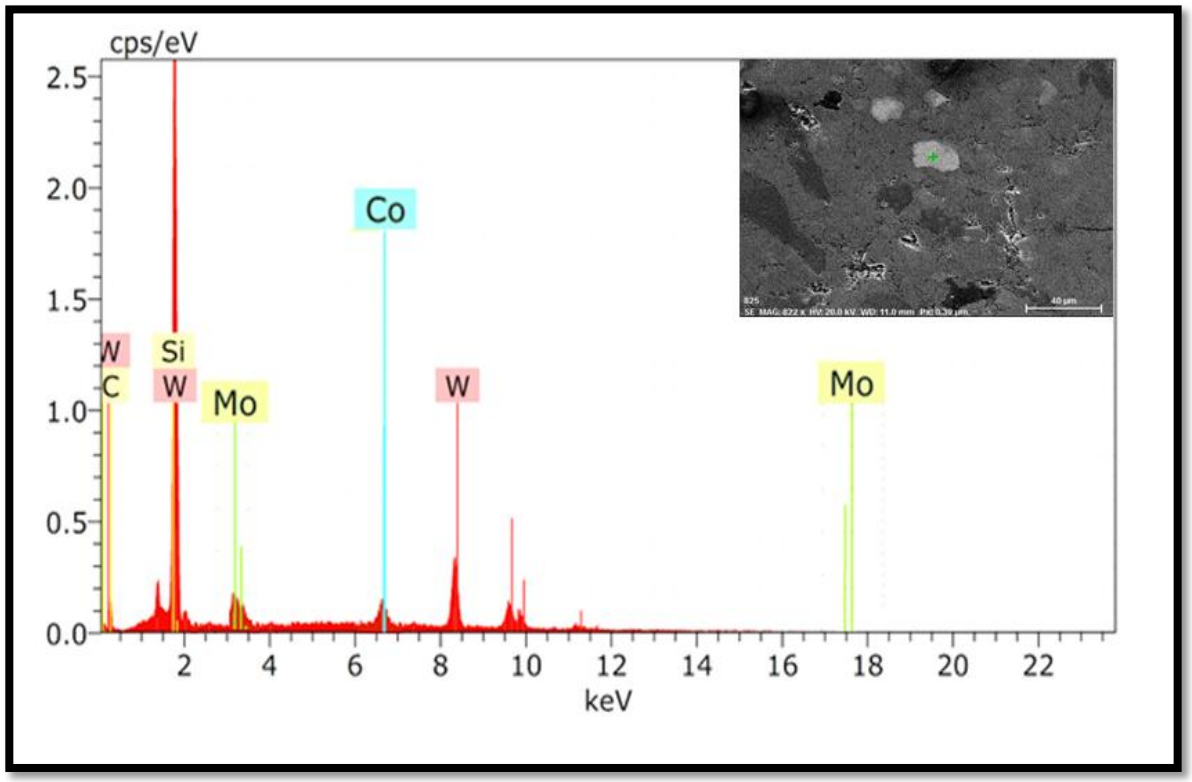

a

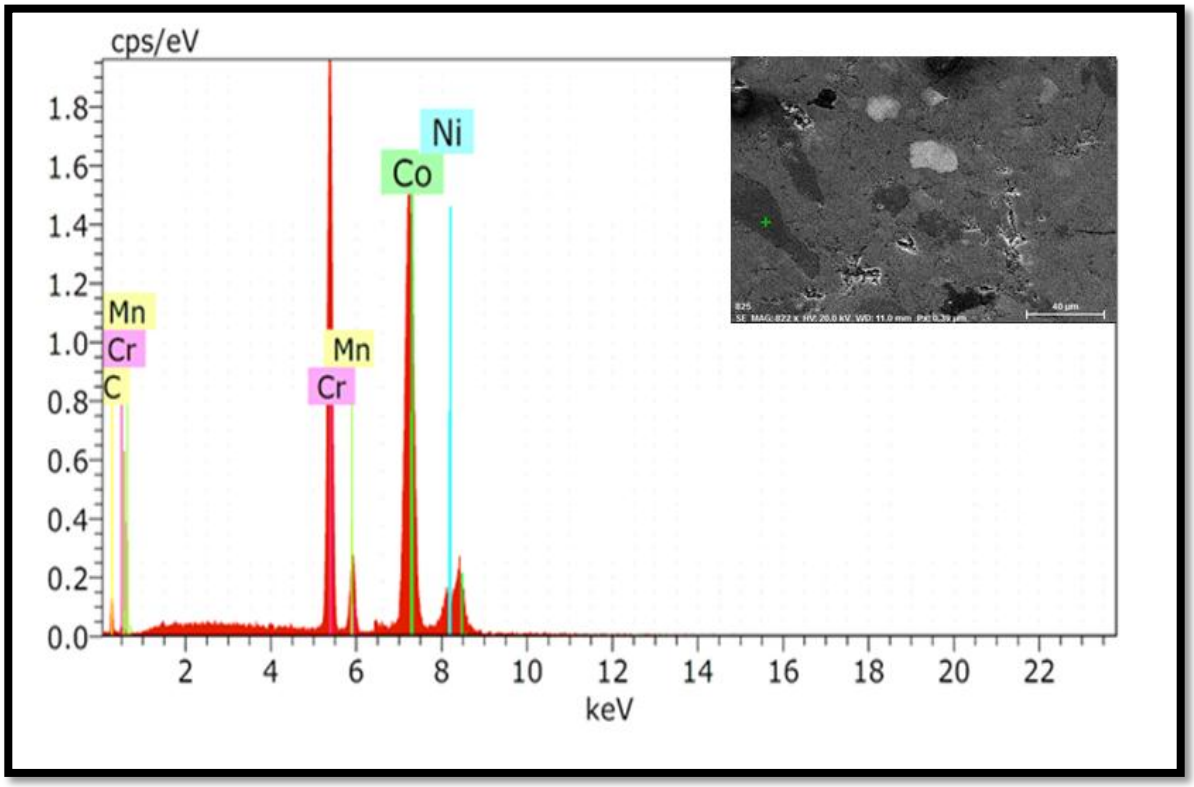

b

Figure(4.47) :EDS for **C3** alloy

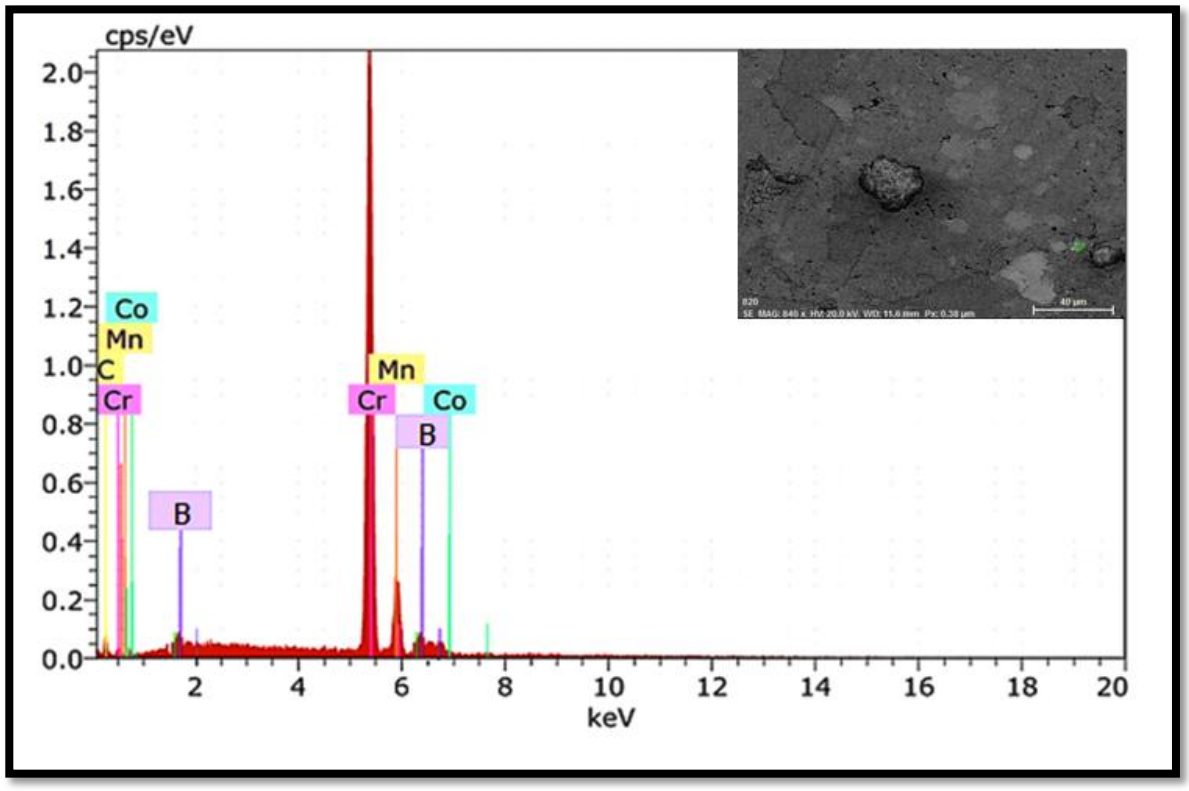

a

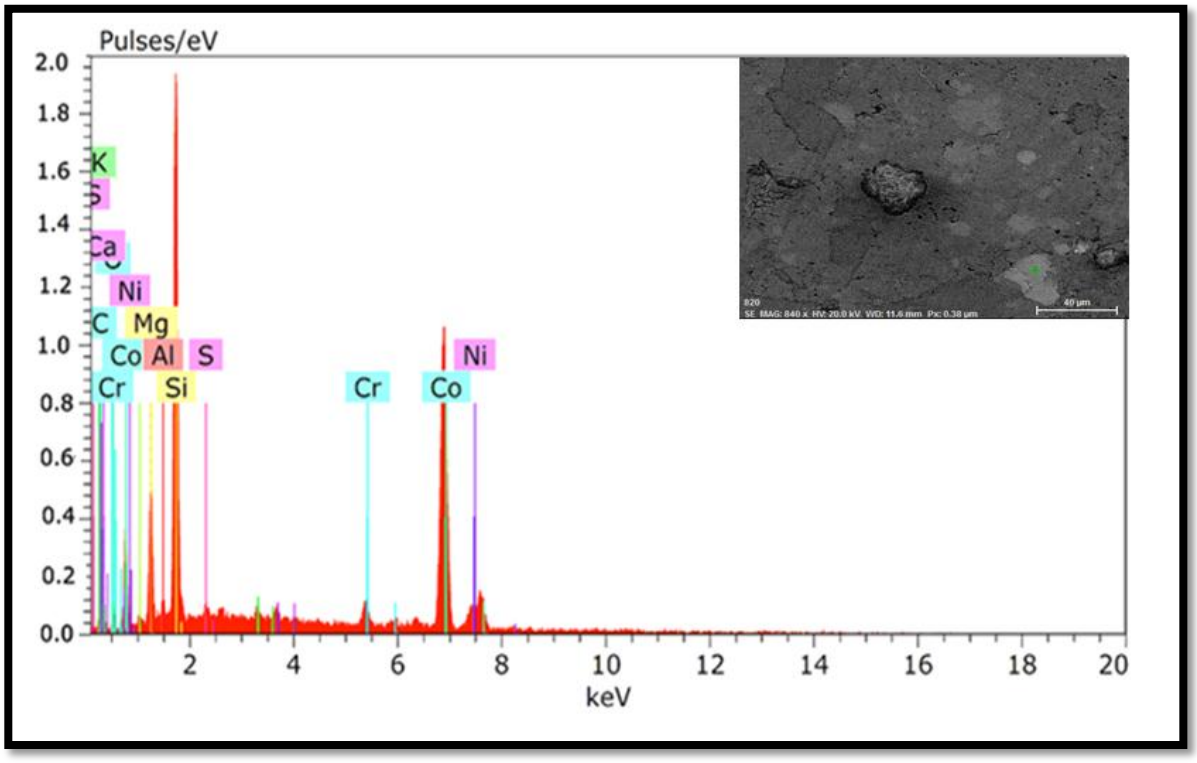

b

Figure(4.48) :EDS for **D1** alloy

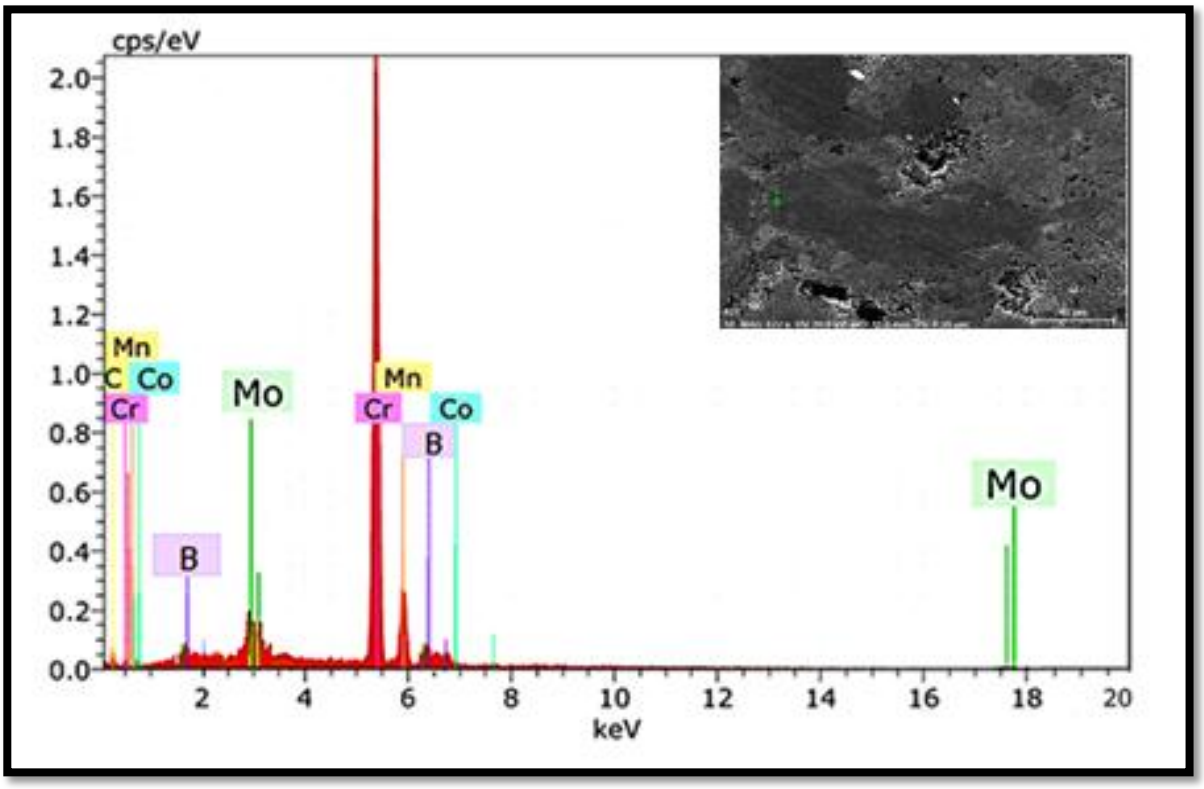

a

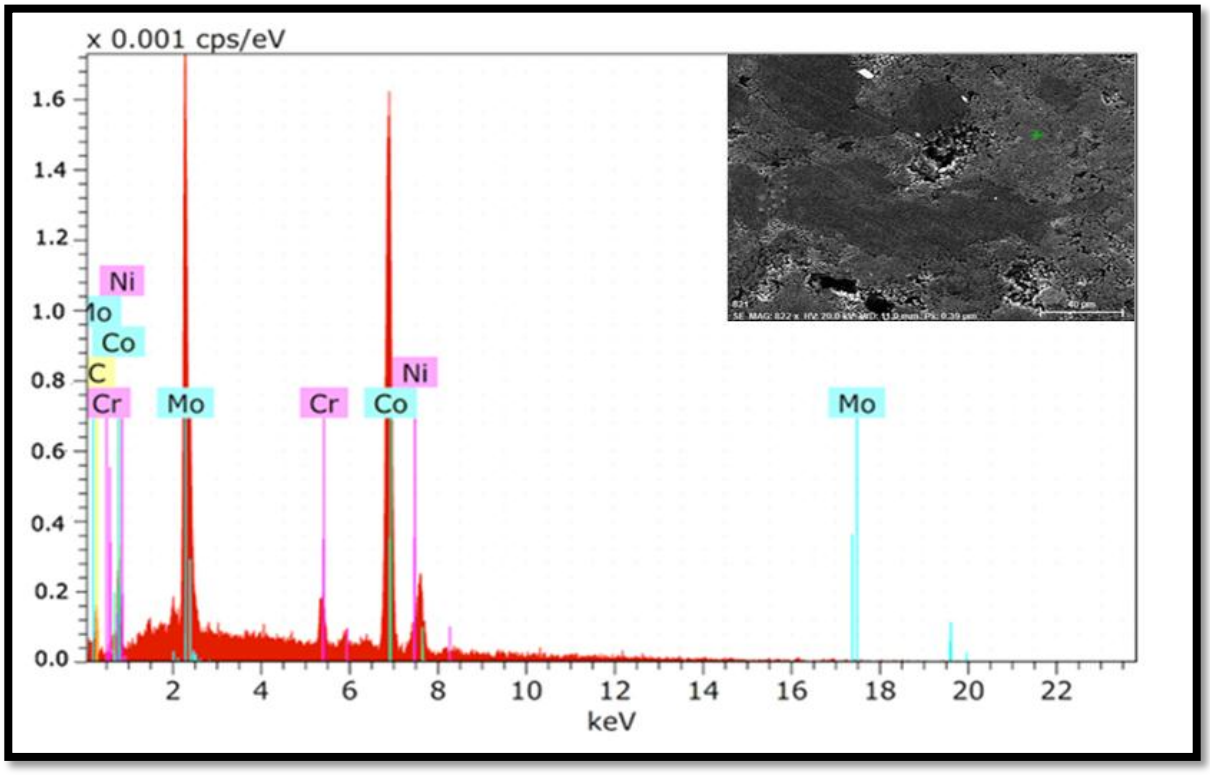

b

Figure(4.49) :EDS for **D2** alloy

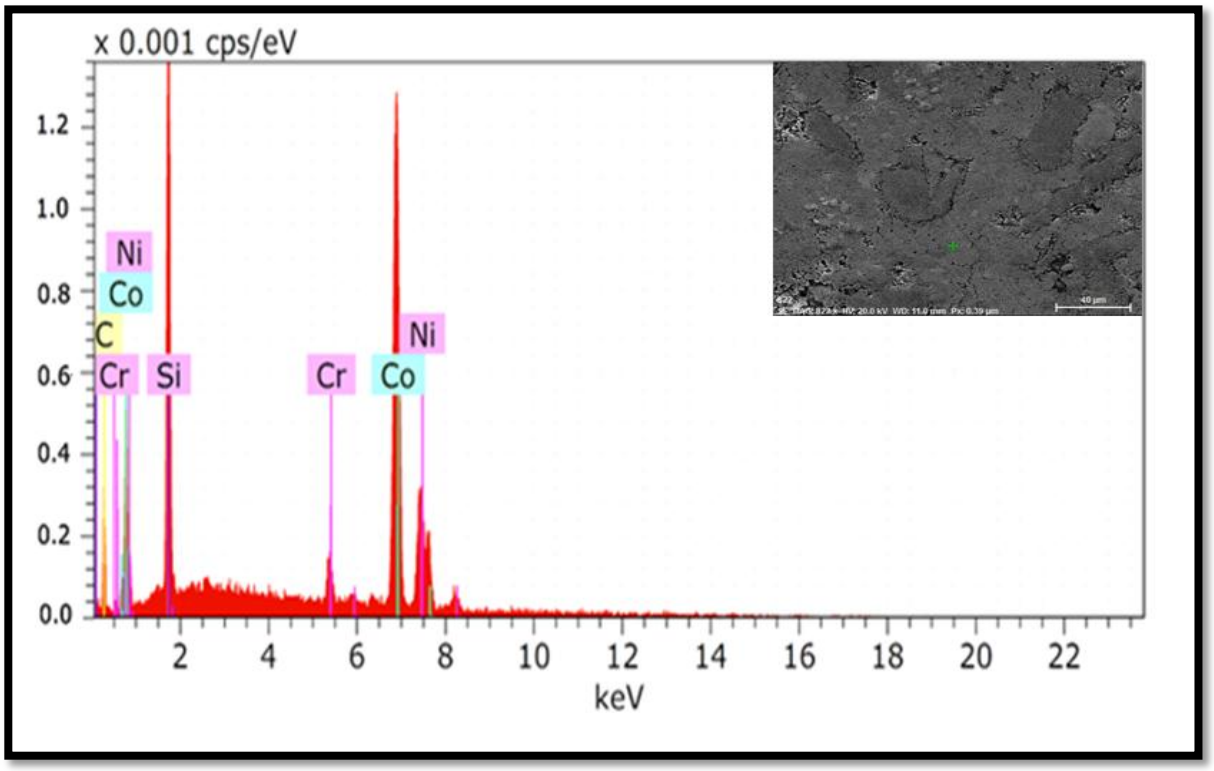

a

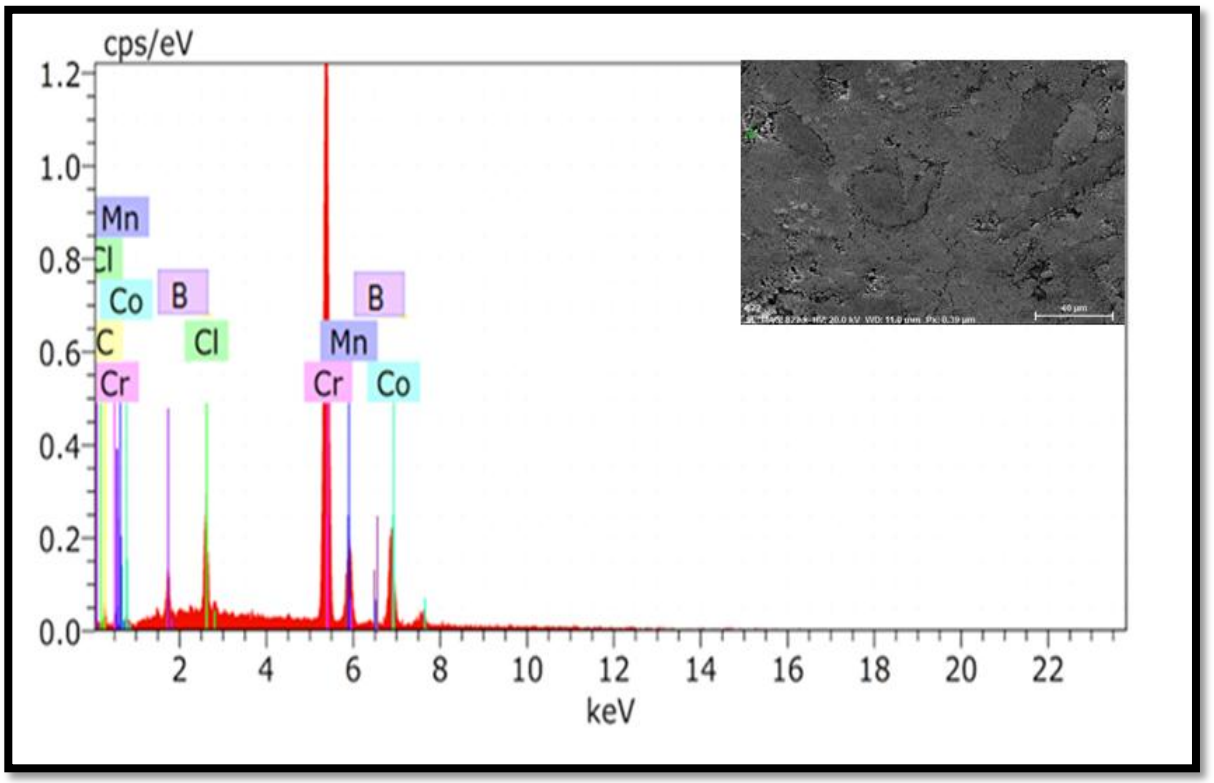

b

Figure(4.50) :EDS for **D3** alloy

4.9 Mechanical properties

4.9.1 Hardness Test

Brinlle hardness test is used to measure the hardness of the samples of all alloys and the results illustrated by figures(4.51),(4.52) and (4.53).

In figure (4.51) the hardness values for CoCrMo alloys with **B** additives are higher than A alloy.

The effect of **B** addition on the rising the hardness values of the samples is attributed to the role of B in reducing porosity (Figure (4.3)) .In general the hardness of CoCrMo alloys with B additives increases as the B content increases**[149].**

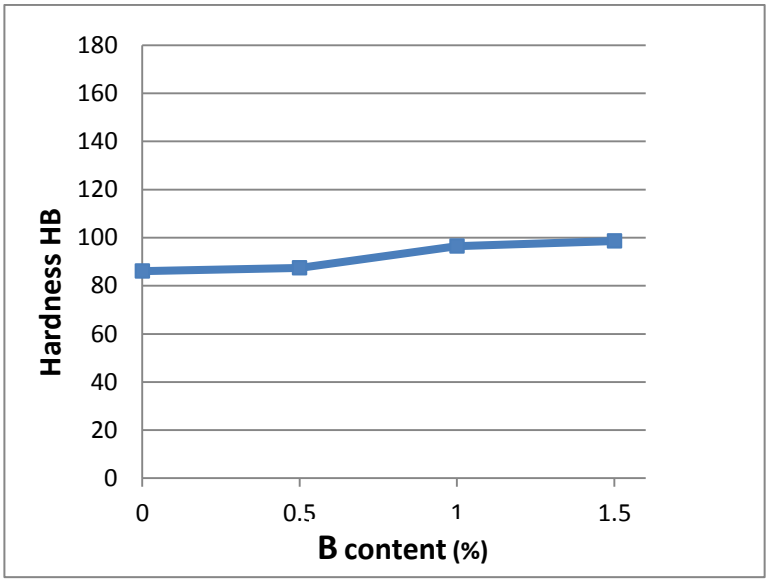

Figure (4.51): Effect of **B** content on the hardness for A, B1, B2 and B3 alloys.

From figure (4.52) it can be observed that the effect of W addition on the CoCrMo alloys is rising the hardness values of the samples because W is reducing porosity (Figure(4.4)) .In general the hardness of CoCrMo alloys with W additives increases as the W content increases**[150].**

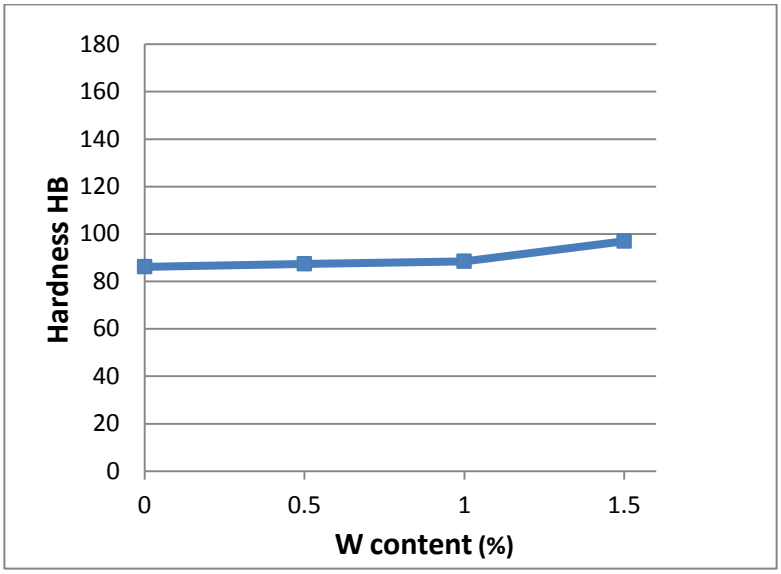

Figure (4.52): Effect of **W** content on the hardness for A, C1, C2 and C3 alloys.

From figure (4.53) it can be observed that CoCrMo with B_4C additive presented significantly higher hardness values in comparison with CoCrMo alloys, and the amount of hardness increases as the B_4C content increases.

This increase of hardness of CoCrMo with B_4C additive is related to CoCrMo alloy can be associated to the change of microstructure induced by B_4C addition. In fact, the higher level of hardness in CoCrMo with B_4C additive is expected since it is known that the B_4C is ceramic compound addition increase hardness of CoCrMo alloy.

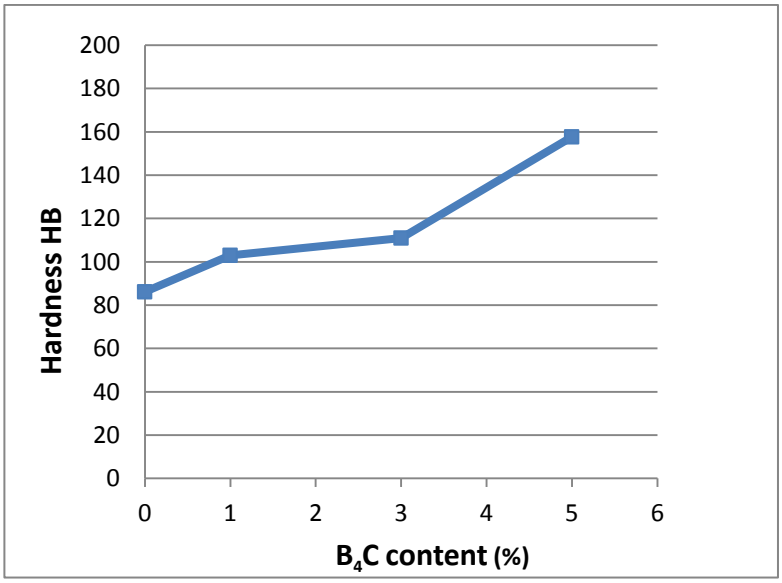

Figure (4.53): Effect of **B_4C** content on the hardness for A, D1, D2 and D3 alloys.

Table(4.4):shows the hardness of all alloys

Sample code	Hardness HB	Improving %
A	86.16	
B1	86.73	100.661
B2	96.5	112
B3	98.66	114.507
C1	87.3	101.323
C2	88.5	102.715
C3	97	112.581
D1	103	119.545
D2	111	128.830
D3	157.66	183.985

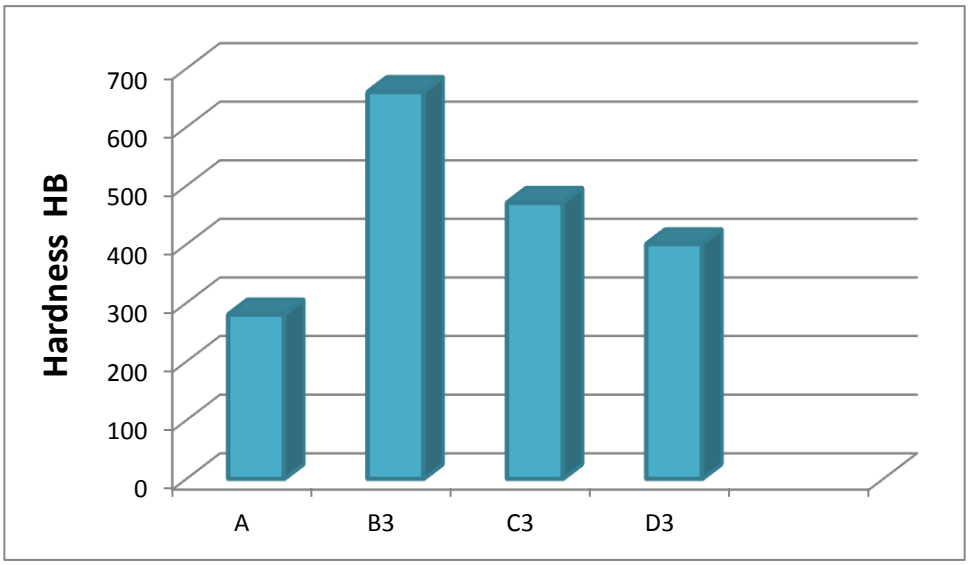

Figure(4.54): Comparison of hardness of all alloys

4.9.2. Compression Test

The result of compression test are cleared for all samples and illustrated in figures (4.55), (4.56) and (4.57).

Figure (4.55) shows the compression strength value for CoCrMo alloys with B additives are higher than CoCrMo alloy, this is because the alloys with B content have a high hardness value as compared with A alloy as shown in table(4.5). The reason behind this is the different percentages between the phases of the composed alloy, in addition the porosity of CoCr alloy with B additive decreases as the B additive increases. These parameters lead to increasing hardness as shown in figure (4.51), therefore the compression strength increase.

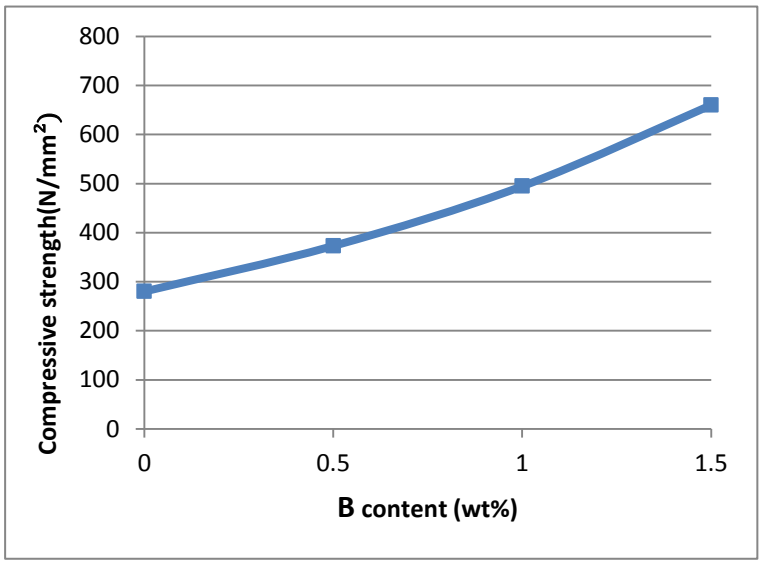

Figure (4.55): Compression strength for A, B1, B2 and B3

From figure (4.56) it can be noted that the compression strength for CoCrMo alloys with W additives are less than CoCrMo alloy, this is because alloys with W additive have a low hardness as compared with A and B alloys as shown in figure (4.52)

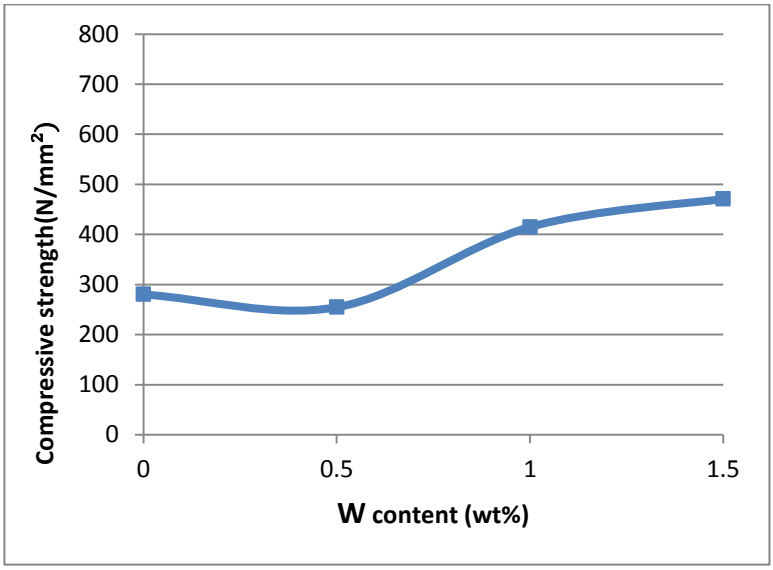

Figure (4.56) : Compression strength for A, C1, C2 and C3

From figure (4.57)) it can be noted that the addition of B_4C to the CoCrMo alloy led to an increase in the compressive strength. This increase is directly proportional with a quantity of B_4C added to the alloy which means that the highest compressive strength returns to the cobalt chromium alloy containing 5 wt% B_4C.The additions of 5 wt% B_4C leads to the highest compressibility of CoCrMo alloy due to the fine -tuning mechanism and also because of the good bonding strength B_4C with Co atoms , which makes the interactions region between CoCrMo and B_4C is difficult to appear by the display solution**[125].**

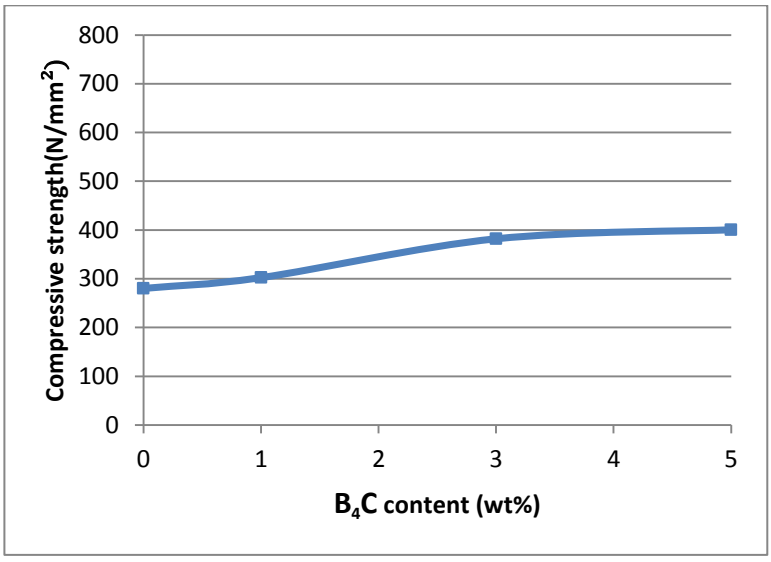

Figure (4.57): Compression strength for A, D1, D2 and D3

Table(4.5):shows the Compression strength of all alloys

Sample code	Compression strength(N/mm^2)	Improving %
A	280.11	
B1	372.9	133.126
B2	494.2	176.430
B3	659.9	235.586
C1	254.6	90.892
C2	414.8	148.084
C3	470.8	168.076
D1	302.2	107.886
D2	381.9	136.339
D3	400.3	142.908

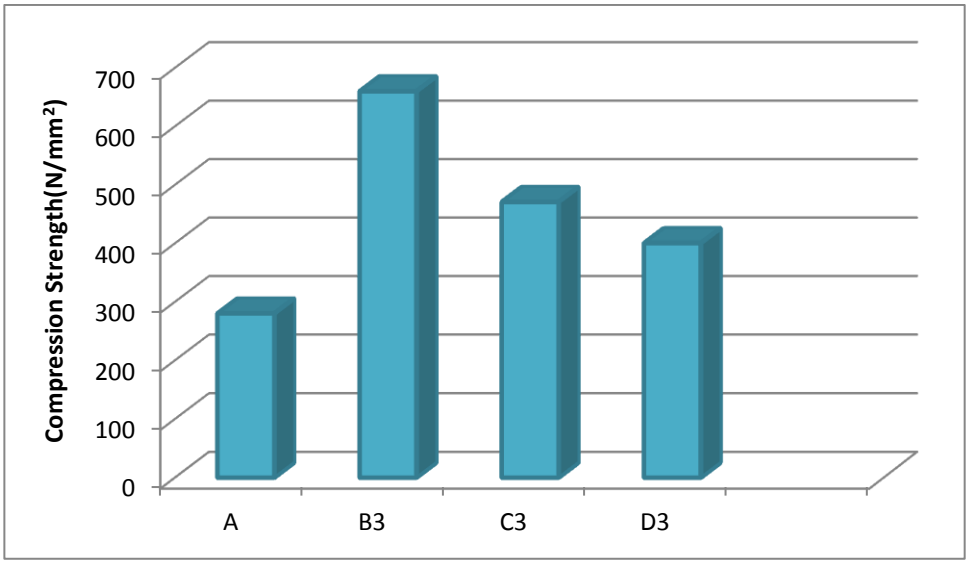

Figure(4.58): Comparison of compression strength of all alloys

4.8.3. Wear Test

Samples with (13) mm diameter subjected to wear test under various loads (10 and 15) N and for different times (5, 10, 15, 20 and 25) min at room temperature. The results have been presented and showed in the following figures:

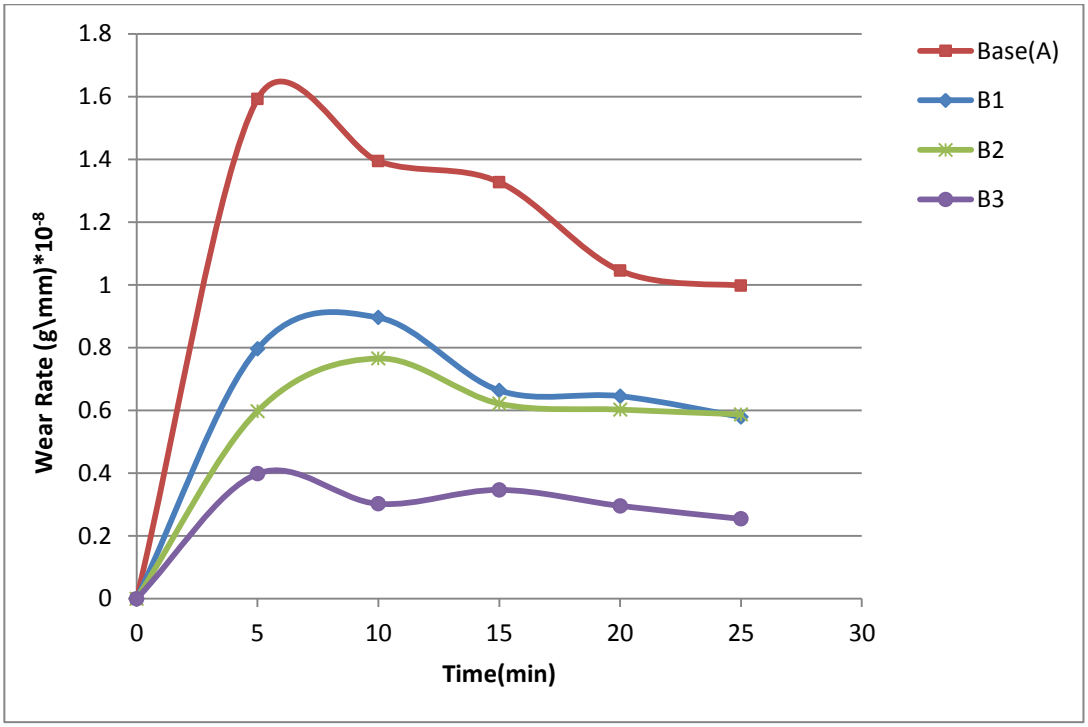

Figure (4.59): Wear rate vs time for A, B1, B2 and B3 alloy under 10N load

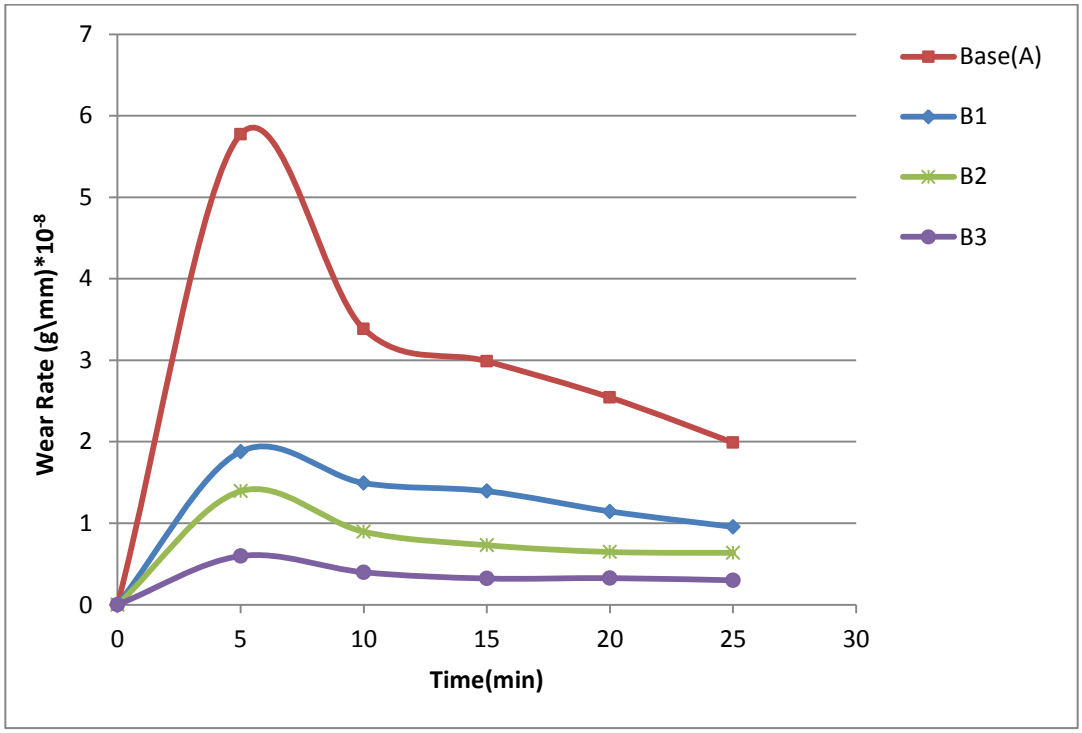

Figure (4.60): Wear rate vs time for A,B1,B2 and B3 alloy under 15N load

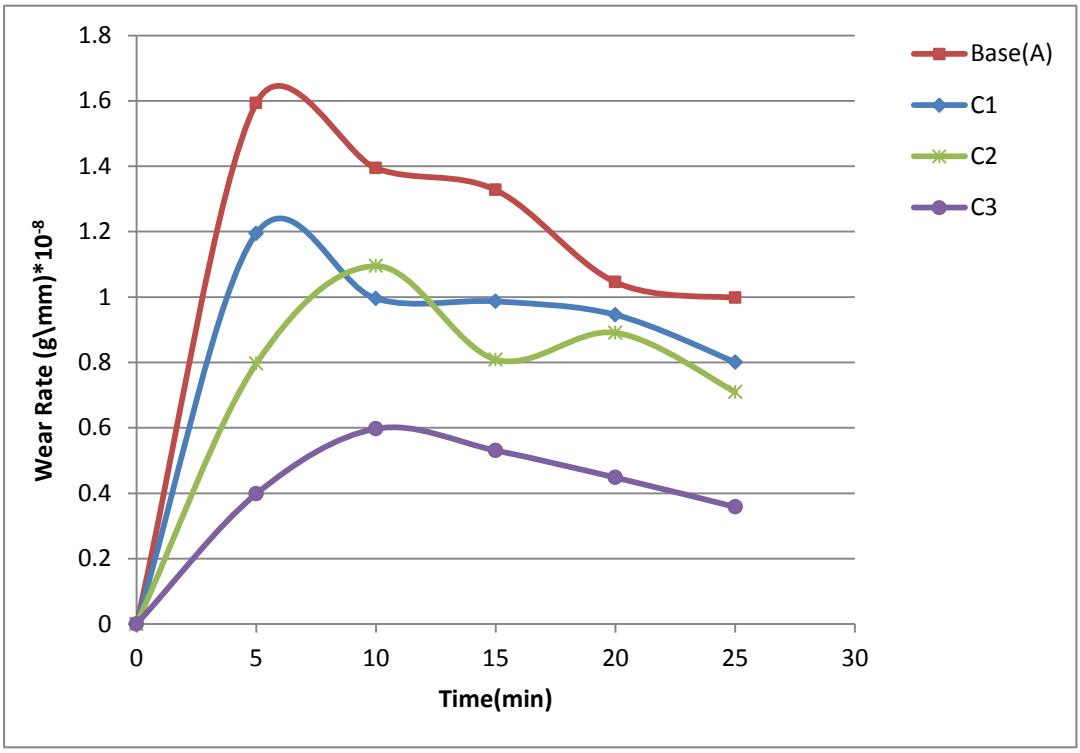

Figure (4.61): Wear rate vs time for A,C1,C2 and C3 alloy under 10N load

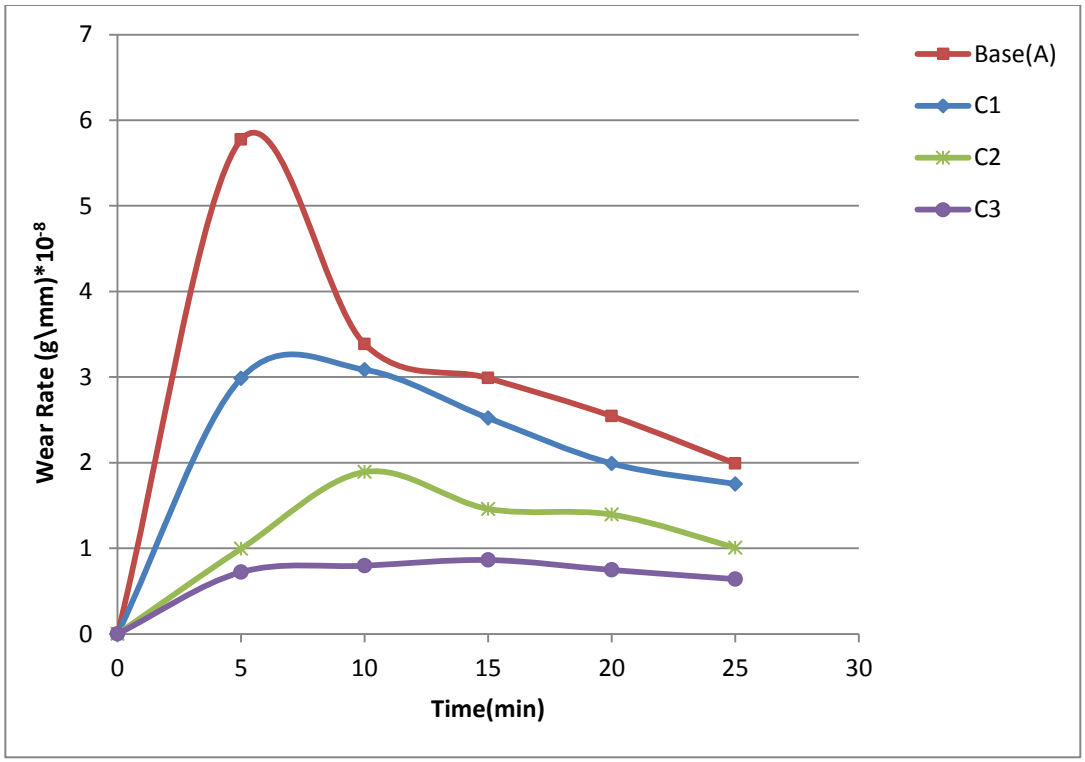

Figure (4.62): Wear rate vs time for A, C1, C2 and C3 alloy under 15N load

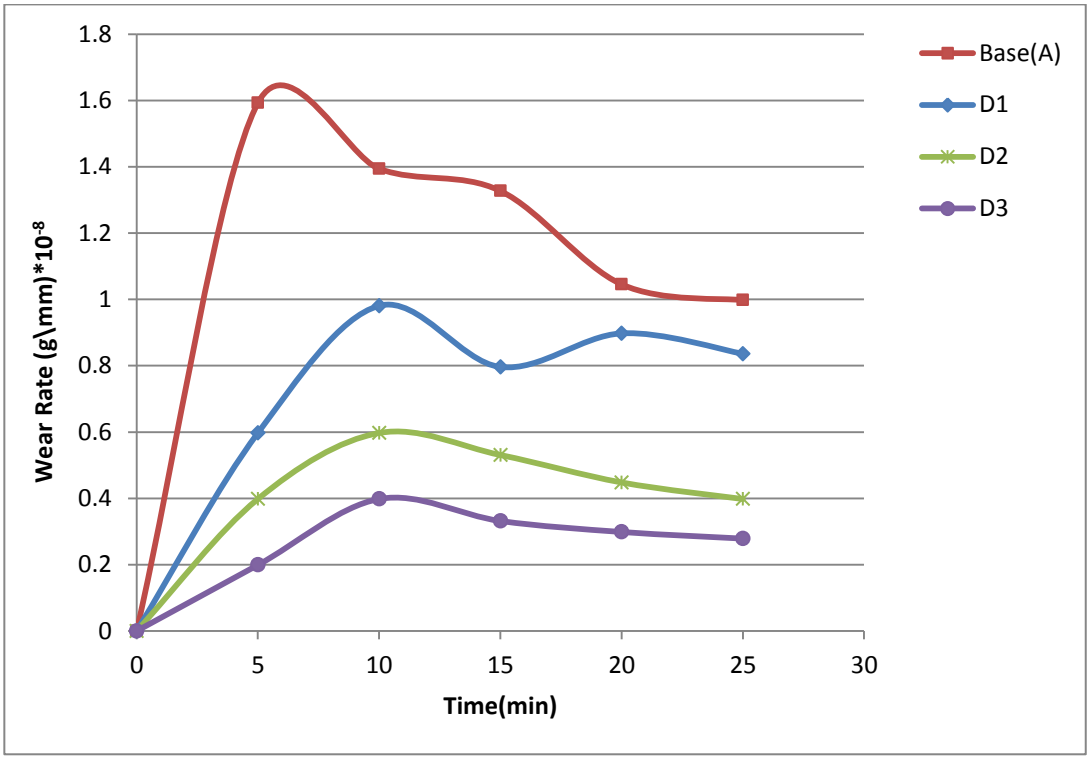

Figure (4.63): Wear rate vs time for A, D1, D2 and D3 alloy under 10N load

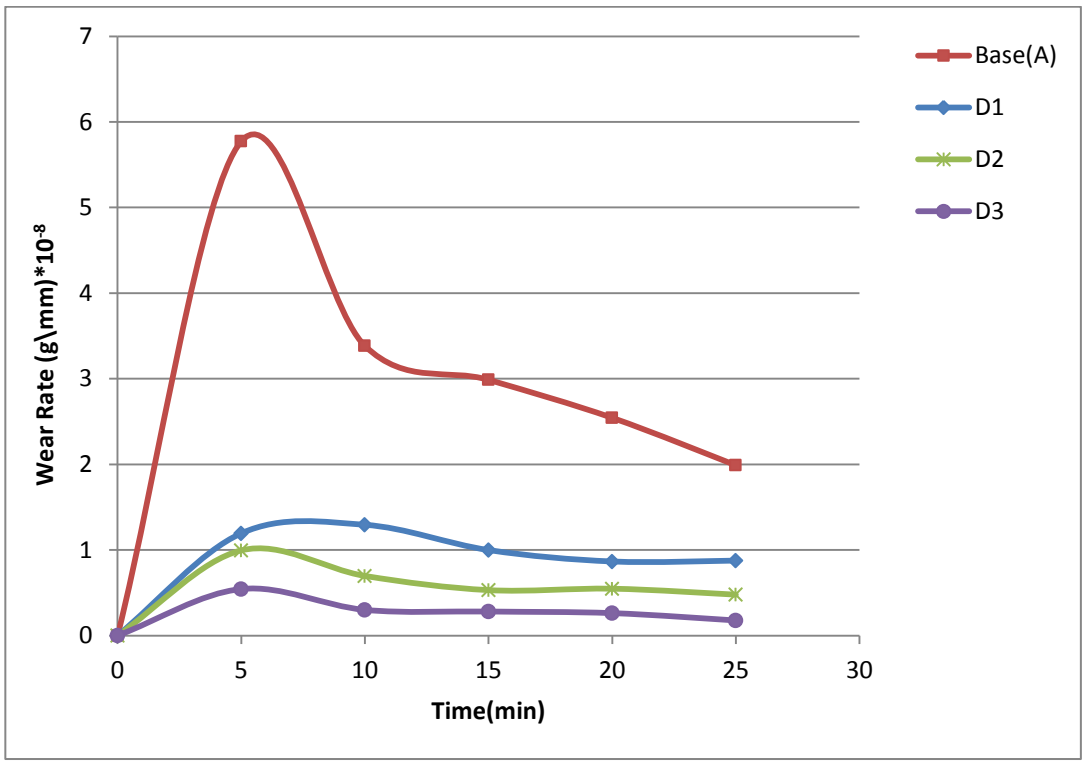

Figure (4.64): Wear rate vs time for A, D1, D2 and D3 alloy under 15N load

The figures ((4.59),(4.60),,(4.61),(4.62) and (4.63) and (4.64)) illustrate the wear rate vs time for all used alloys under various loads (10 and 15)N. From the

mentioned figures, it can be noted that the wear rate of all tested samples under 15N load is higher than that under10N.

The reason behind this variation is due to the increase in friction at the surface as the load on the material increases **[151].**

In addition, the wear rate increases as the time increases for all tested samples, this is certainly because more time of friction tends to remove more material from the surface, this increases in wear rate that has been attributed to increase the plastic deformation for the material on the surface , particles of the material pull out (debris) **[152]** .

From figures (4.59) to (4.62), it can be noted that the rate of wear decreased drastically with increasing the B and W percentage in the alloy, even it reaches the minimum value at the addition that contained 1.5%wt of B and W .This may due to the role of B and W addition in reducing porosity of the prepared alloys. In general the hardness of CoCrMo alloys with B and W additives increase as the element content increase, Therefore ,it can be noted from figure(4.59) to (4.62) which showed the effect of B and W on the wear rate of the CoCrMo alloys. Under constant load (10N),(15N) and constant time(25min) , the wear rate of CoCrMo decrease as the B and W increased.

The reason behind this reduction in wear rate is expected since the addition reduce the porosity and increase the friction coefficient , the pore play on important role medicating the potential sites of the micro-cracks forming and positively influencing the wear rate**[151].**

The addition of boron and tungsten increase the hardness as mention in section (4.8.1) then the wear resistance decrease .

For biomedical applications, a material's wear resistance is important not only for its mechanical stability but also for its biocompatibility because wear and the resultant creation of wear debris particles has been known to be a dominant factor limiting the implant material's long-term**[153]**

Figure (4.63) and figure (4.64) displays the wear rate for CoCrMo Alloy and CoCrMo with different addition of B_4C after the wear test under a load of 10 N , 15 N for 25 min respectively .

The addition of the ceramic material led to a clear reduction in wear volume loss and thus an increase in wear resistance , as shown in Figure (4.63) and (4.64) .The reason is due to the nature of the ceramic material, which is characterized by its high hardness , as shown in the previous paragraph results (4.8.1) .The effect of hardness on the wear resistance is often described using Archard's law (ASTM E8-03, 1994), which states that the wear volume loss tends to have an inverse relationship with hardness**[154]**.

Table(4.6):shows the wear rate under 10N load

Sample code	Wear rate(g/mm)*10^{-8}	Improving %
A	**0.997**	
B3	**0.254**	**25.476**
C3	**0.358**	**35.907**
D3	**0.278**	**27.883**

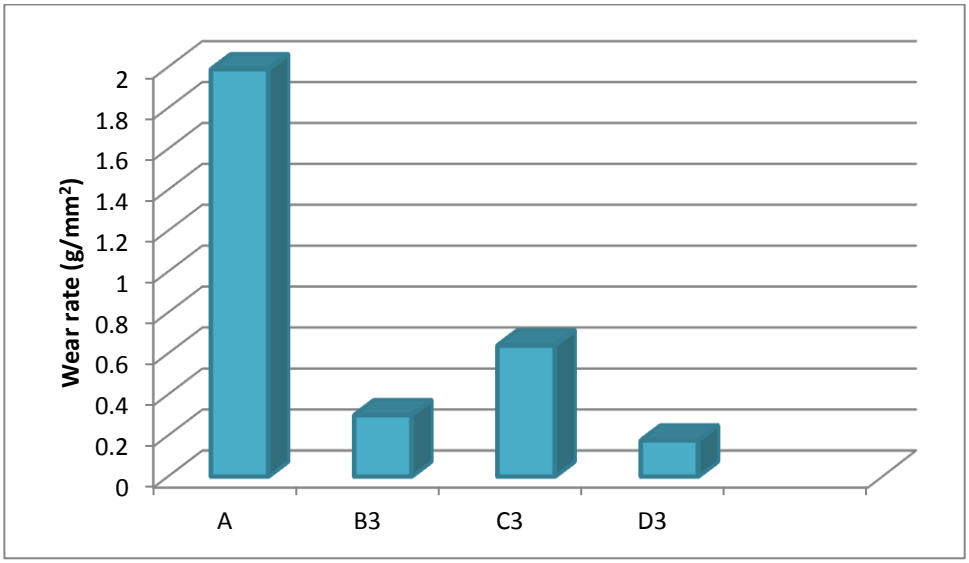

Figure(4.65): Comparison of wear rate of all alloys under 10N load

Table(4.7):shows the wear rate under 15N load

Sample code	Wear rate(g/mm)*10^{-8}	Improving %
A	**1.989**	
B3	**0.299**	**15.032**
C3	**0.639**	**32.126**
D3	**0.176**	**8.848**

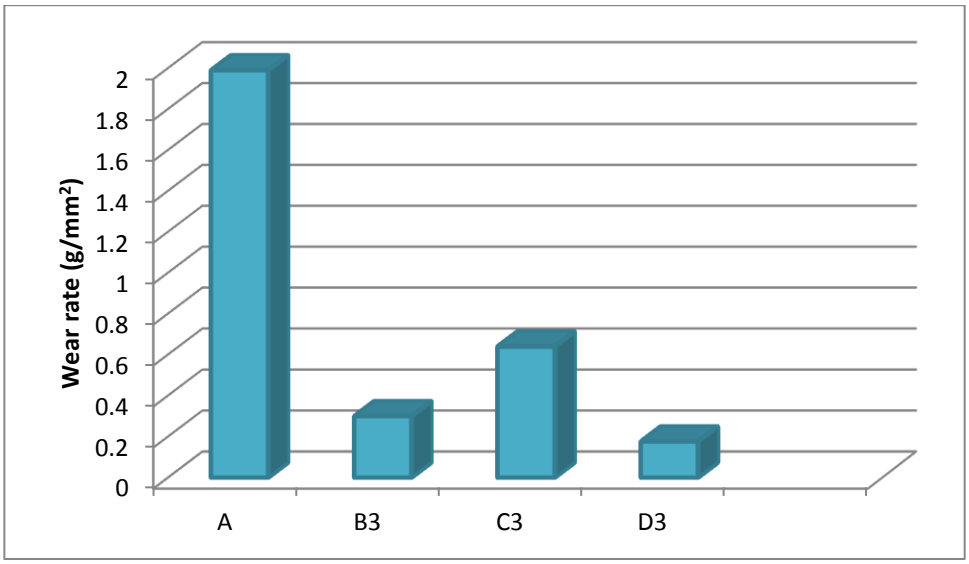

Figure(4.66): Comparison of wear rate of all alloys under 15N load

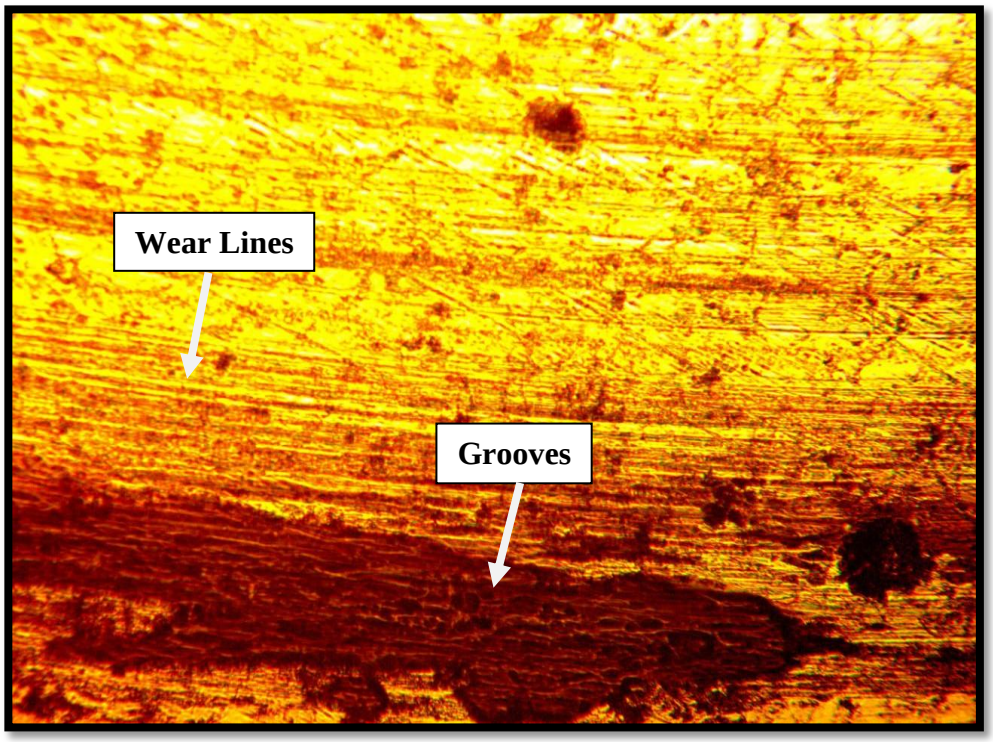

Figure(4.67):Topographic for (A)alloy by use light optical microscope with magnification 200X under(15N) load and (25min)time.

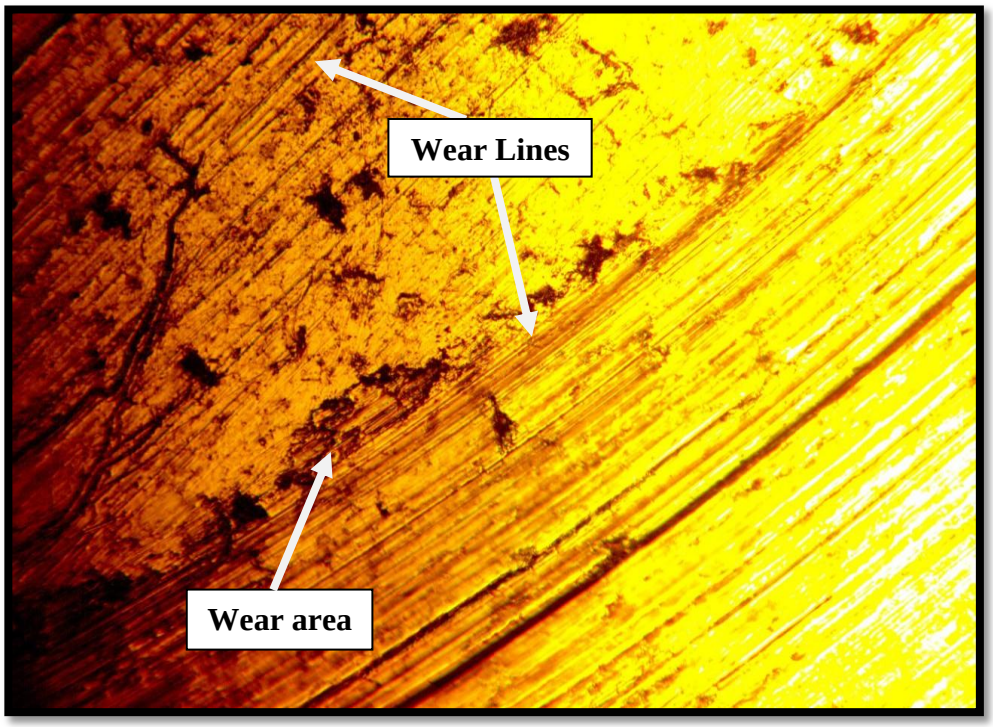

Figure(4.68): Topographic for (B3)alloy by use light optical microscope with magnification 200X under(15N) load and (25min)time.

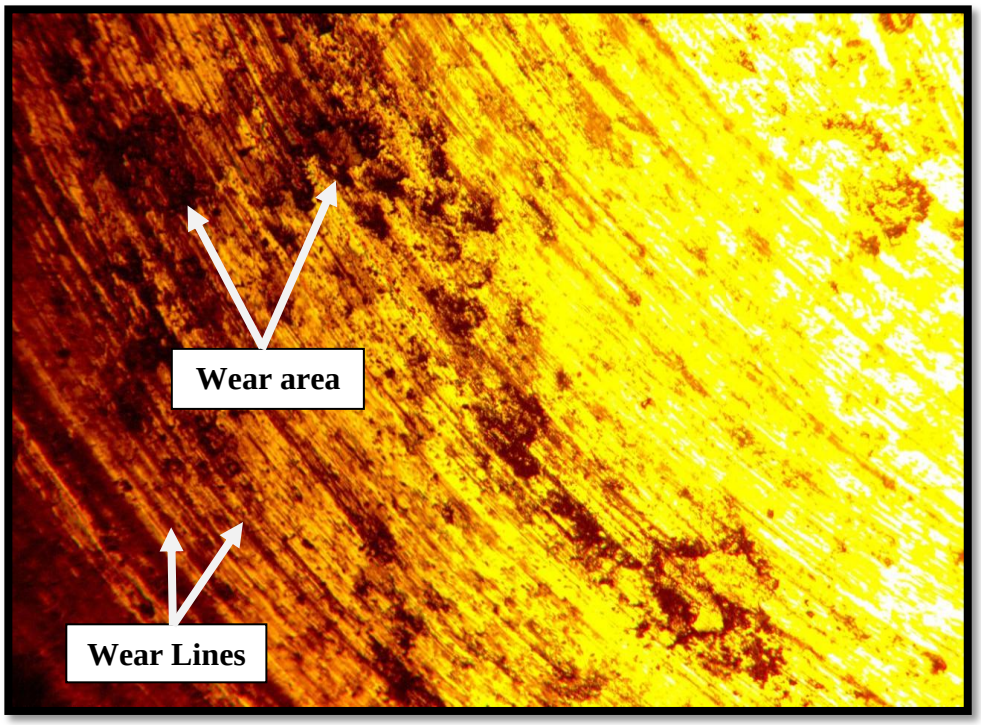

Figure(4.69): Topographic for (C3)alloy by use light optical microscope with magnification 200X under(15N) load and (25min)time.

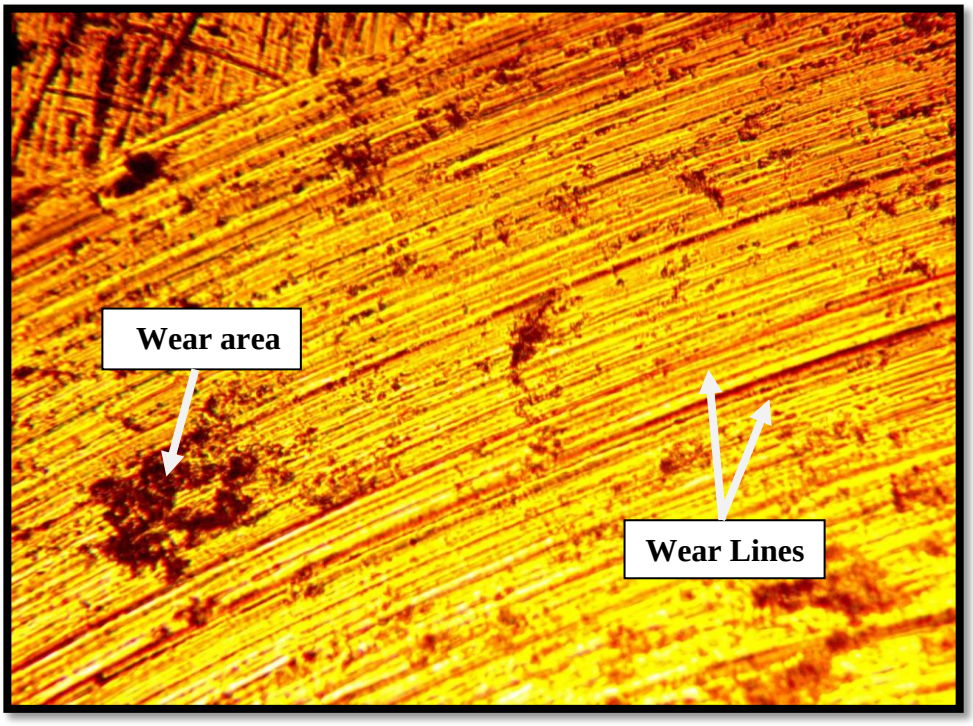

Figure (4.70): Topographic for (D3)alloy by use light optical microscope with magnification 200X under(15N) load and (25min)time.

Figures (4.67),(4.68),(4.69) and (4.70) show an optical microscopy image of the wear tracks of all samples after the wear test.

Compared with the base sample (A) an evident grooves was observed along the edges of the wear track on the surface of the base sample. The reason may be due to continuous plastic deformation **[155].**

From figures (4.68), (4.69) and (4.70) no clear grooves was formed and observed along the edges of the wear track on the surface of the sample with different additions.

This may be due to the increase in the hardness of the alloy after addition of B, W and added B_4C . This increase led to decrease weight lost with time and a decrease in the rate of wear. The reason may be due to further extrusion deformation becomes more difficult during the wear test **[155]**.So pile up was not observed in these images. Also from figure (4.70) we notice that the sample containing 5wt% of B_4C was the least damaged in the wear test and that the wear lines are very few and even almost non-existent. The reason may be due to some carbide can act as a protective barrier against the matrix grooves which is due to the good coherency with the surrounding matrix**[124]**.

4.10. Electrochemical Tests

4.10.1. Open circuit potential (OCP)-time measurement

The OCP-time was measured with respect to SCE in Ringer's solution and artificial saliva at 37±1 °C for all tested alloys. Figure (4.71) shows the evolution of corrosion potential of the alloys throughout time. The time period from (0 to 150) minutes and with interval of 5 minutes were potentially reported. The mean values of the OCP were recorded by using two samples for each alloy.

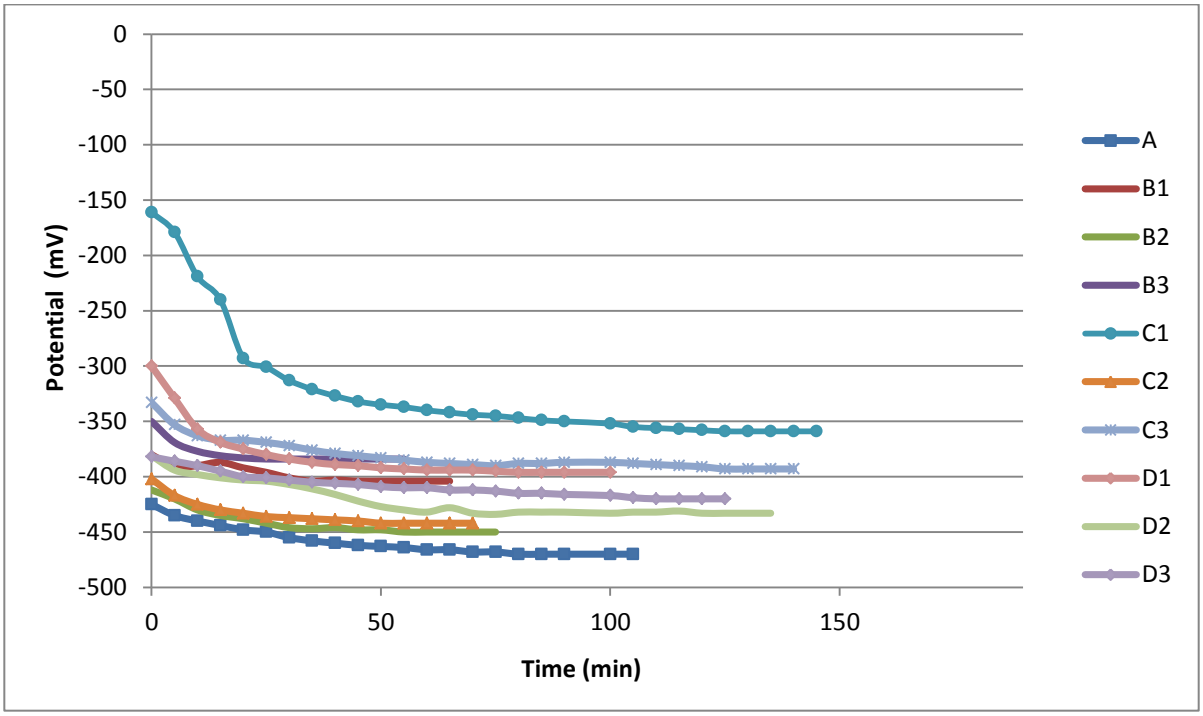

Figure (4.71) :The OCP-time in Ringer's solution at 37±1 C° for all tested alloys

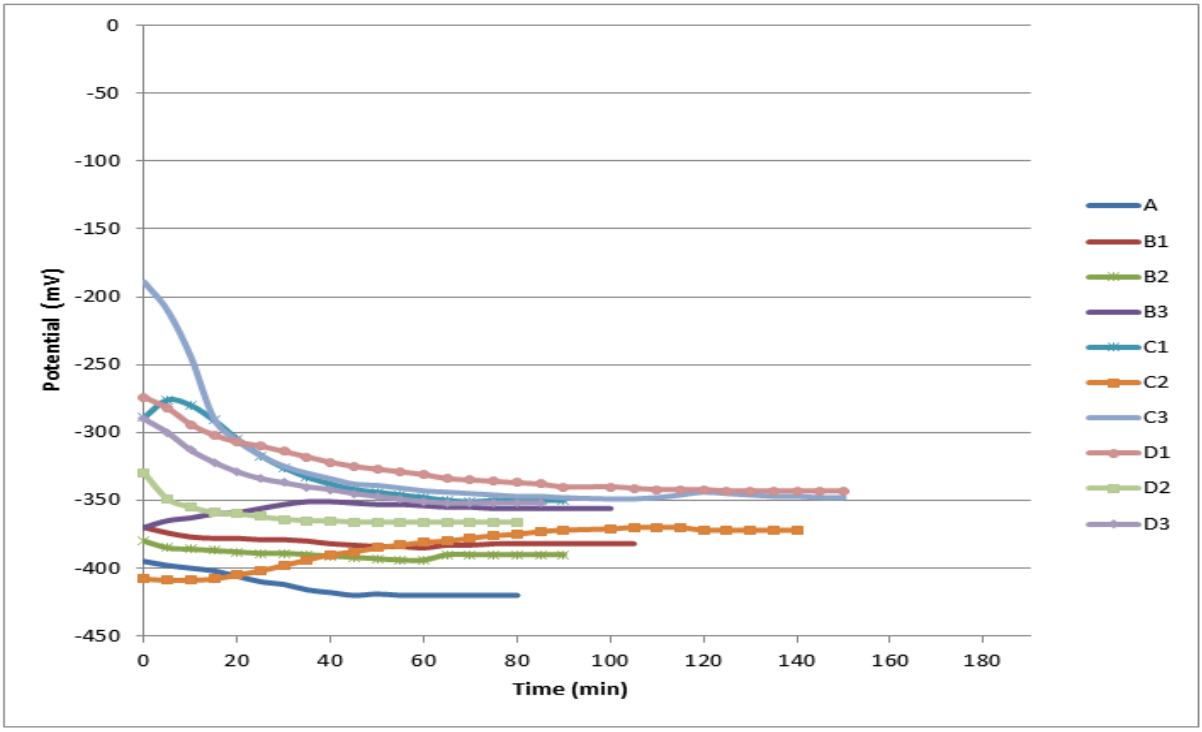

Figure (4.72): The OCP-time in artificial saliva at 37±1 C° for all tested alloys

The above figures shows the variation of open circuit potential (OCP) with time from which several deduction can be made. The first is that during the first 30 minutes were studied the corrosion potential increases at a greatest speed in this period in most case study. This initial increasing generally seems to be related to the formation and thickening of the oxide film on the metallic surface, improving its corrosion protection ability. Afterwards the OCP increases slowly because of the growth of the film onto the metallic surface. The second is that the corrosion potential reaches a level from which corrosion potential tends to stabilize. The constant OCP means that there is equilibrium between dissolution and deposition **[156].**

4.10.2. Potentiodynamic polarization

The corrosion behavior of all samples in Ringer's solution and artificial saliva has been studied. Corrosion parameters which extracted from potentiodynamic polarization test that are showing in figures (4.73) and (4.74), respectively.

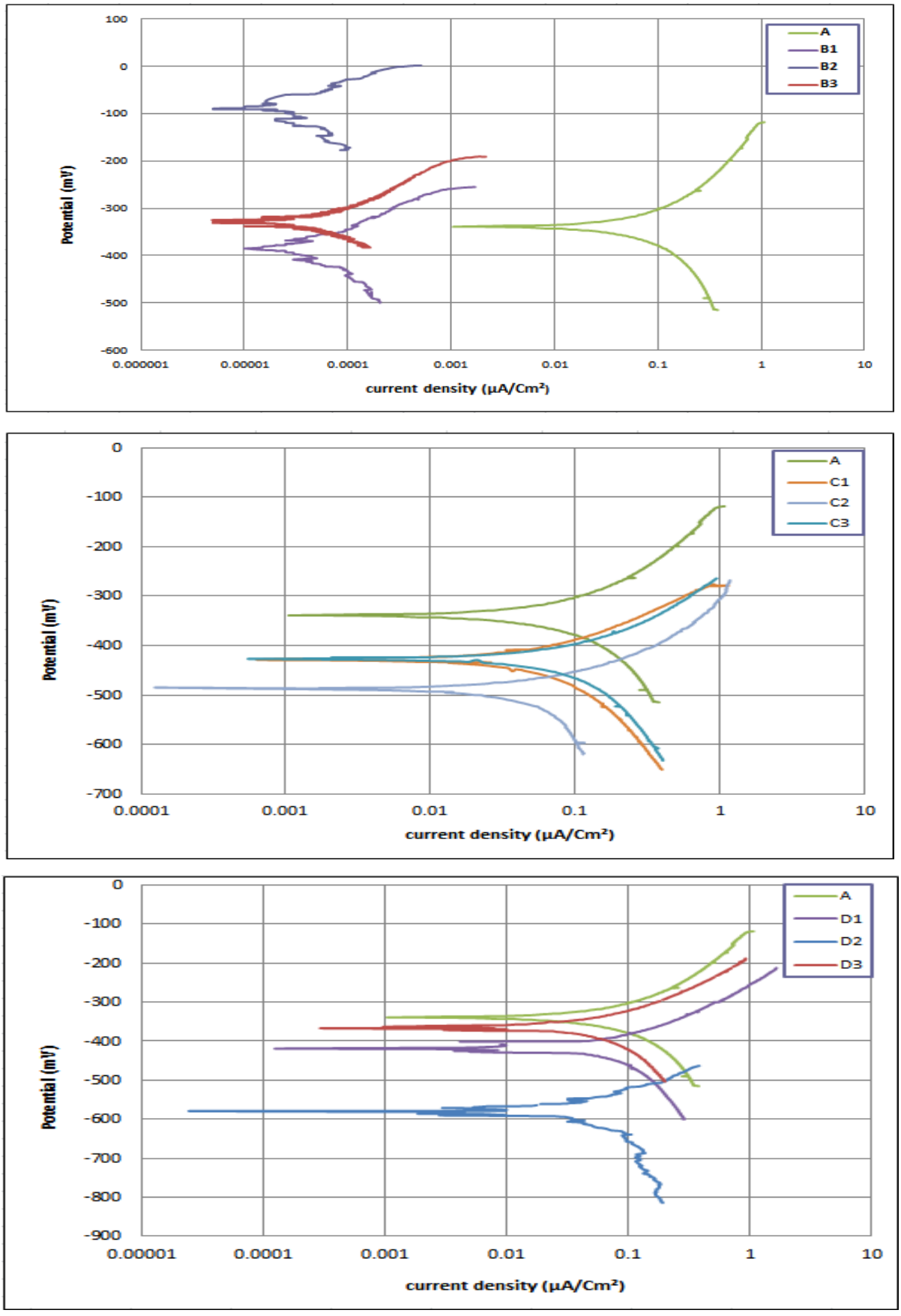

Figure (4.73): Potentiodynamic Polarization for all specimens in Ringer's Solution.

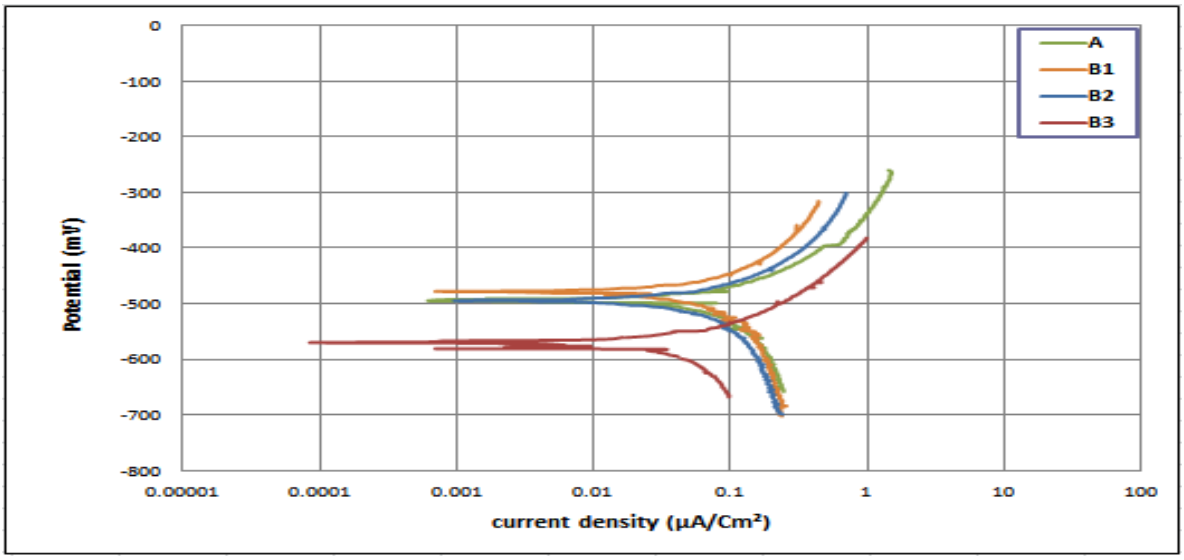

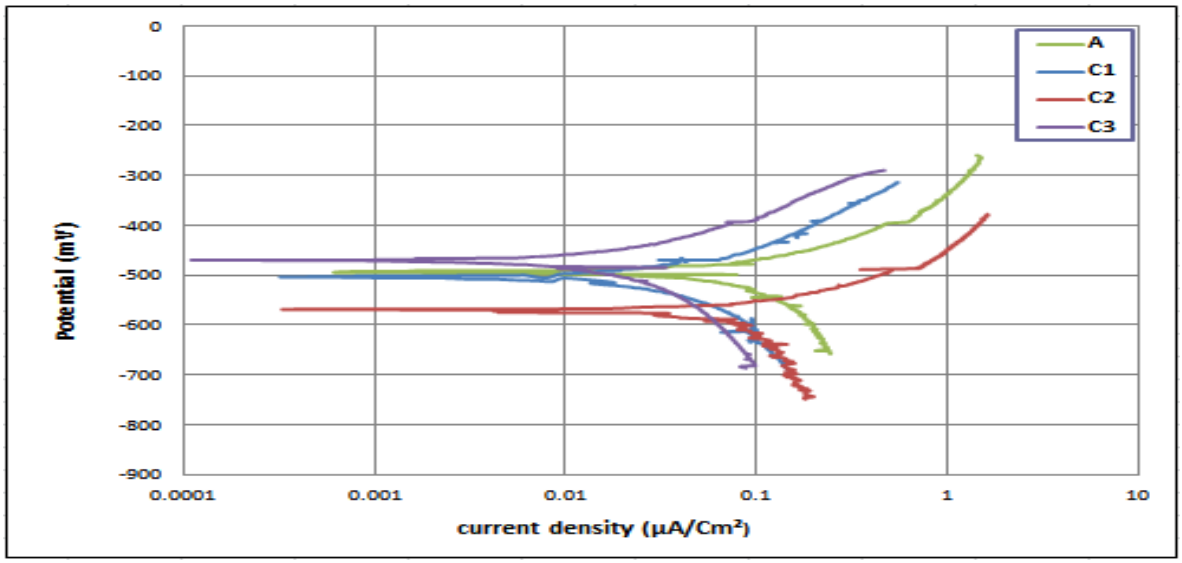

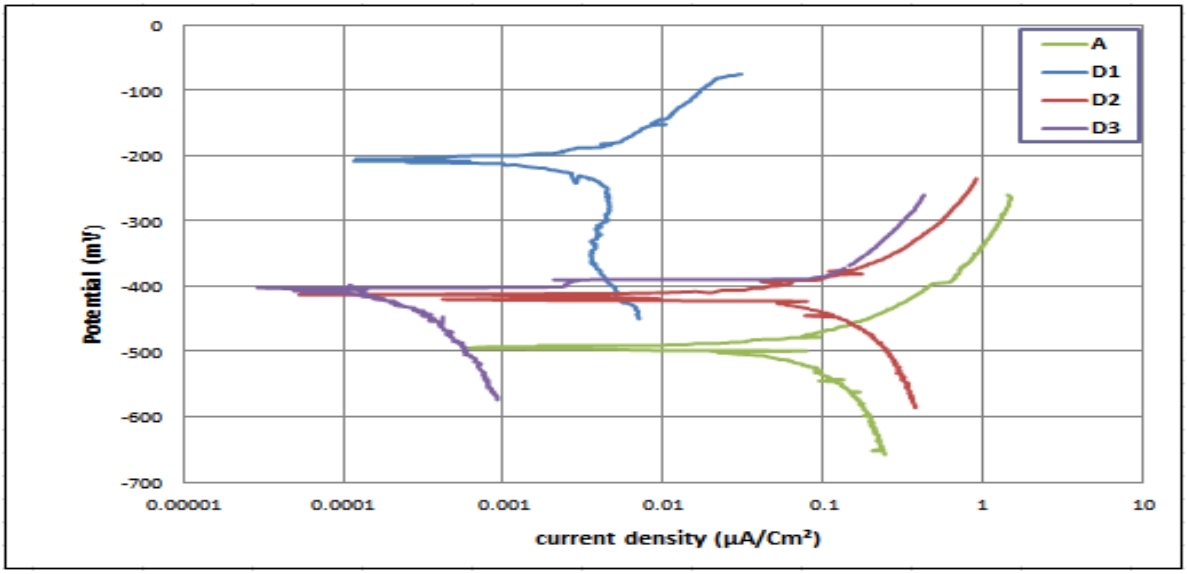

Figure (4.74): Potentiodynamic Polarization for all specimens in artificial saliva Solution.

Corrosion current (Icorr.), corrosion potential (Ecorr.) and corrosion rate (C.R.) for samples in Ringer's solution and artificial saliva at 37±1ºC were illustrated in table (4.8) and (4.9).

From Table (4.8), it can be noted that there is a significant improvements in corrosion resistance of the CoCrMo alloys with different additives of B (0.5 , 1and 1.5) wt%, Icorr. for samples is ranged from (0.0285 µA/cm2) for B1 alloy to (0.00167µA/cm2) for B3 alloy which are lower than Icorr. for A alloy which is (17.67µA/cm2)

Table(4.8): Shows The Corrosion Current (Icorr.), Corrosion Potential (Ecorr.) and Corrosion Rate (C.R.) for All Alloys in Ringer's Solution at 37±1ºC

Alloy	Sample Code	Icorr. $\mu A/cm^2$	Ecorr. mV	Corrosion Rate(C.R.)mpy	Rp	Improvement percentage%
F75	A	17.67	-341.8	13.49	0.68	
B	B1	0.0285	-385.5	0.0220	647.61	99.84
	B2	0.0047	-81.6	0.0037	346.17	99.97
	B3	0.00167	-327.3	0.00134	391.51	99.99
C	C1	10.48	-428.3	7.801	0.90	42.2
	C2	7.07	-489.4	5.458	0.96	59.5
	C3	5.84	-426	4.310	0.92	68.1
D	D1	13.77	-418.7	10.72	0.513	20.53
	D2	6.719	-597.5	5.5007	0.854	59.22
	D3	3.674	-366.1	3.1334	0.820	76.77

Also from Table (4.8), it can be noted that there is a significant improvement in corrosion resistance of the alloys with different addition of W(0.5 ,1 and 1.5)wt%,

Icorr. for samples is ranged from (10.48 μA/cm2) for C1 alloy to (5.84 μA/cm2) for C3 alloy which are lower than Icorr. for A alloy which is (17.67μA/cm2) and Ecorr. for C alloys are ranged from (-428.3 mV) for C1 alloy to (-426 mV) for C3 alloy which are higher than Ecorr. for A alloy which is (-341.8mV), which means improve of nobility of base alloy . which make C alloy more noble than A alloy.

The data listed in Table (4.8) showed an improvement in corrosion resistance of CoCrMo alloy with addition of B_4C (1,3 and 5)wt.%, Icorr. for D alloys is ranged from (13.77 μA/cm2) for C1 alloy to (3.674 $\mu A/cm^2$) for D3 alloy which are lower than Icorr. for A alloy which is (17.67 μA/cm2) and Ecorr. for D alloys is ranged from (-418.7 mV) for D1 alloy to (-366.1 mV) for D3 alloy which are lower than Ecorr. for A alloy which is (-341.8 mV).

From Table (4.9), it can be noted that there is an improvement in corrosion resistance of CoCrMo alloy with different additives of B (0.5, 1 and 1.5)wt% in artificial saliva , Icorr. for B alloys is graded from (12.629 μA/cm2) for B1 alloy to (6.219μA/cm2) for B3 alloy which are lower than Icorr. for A alloy which is (24.87 μA/cm2) and Ecorr. for B alloys is graded from (-480 mV) for B1 alloy to (493.8mV) for B3 alloy which are higher than Ecorr. for A alloy which is (-497.4).

Icorr. for C alloys is graded from (7.598 μA/cm2) for C1 alloy to (4.5 μA/cm2) for C3 alloy which are lower than Icorr. for A alloy which is (24.87 μA/cm2) and Ecorr. for C alloy is ranged from (-505.8 mV) for C1 alloy to (-472.4 mV) for C3 alloy which are higher than Ecorr. for A alloy which is (-497.4 mV).

Icorr. for D alloys is graded from (0.675μA/cm2) for D1 alloy to (0.0874μA/cm2) for D3 alloy which are lower than Icorr. for A alloy which is (24.87 μA/cm2) and Ecorr. for D alloy is ranged from (-205.1mV) for D1 alloy to (-407.4 mV) for D3 alloy which are lower than Ecorr. for A alloy which is (-497.4 mV).

Table(4.9): Shows The Corrosion Current (Icorr.), Corrosion Potential (Ecorr.) and Corrosion Rate (C.R.) for All Alloys in Artificial Saliva at 37±1°C

Alloy	Sample Code	Icorr. $\mu A/cm^2$	Ecorr. mV	Corrosion Rate(C.R.)mpy	Rp	Improvement percentage%
F75	A	24.87	-497.4	18.989	0.4014	
B	B1	12.629	-480	9.771	0.519	48.55
	B2	10.977	-571.7	8.4865	0.67655	55.31
	B3	6.219	-493.8	4.808	0.555	74.680
C	C1	7.598	-505.8	5.6535	1.1976	70.23
	C2	6.348	-570.8	4.7235	0.4011	75.13
	C3	4.5	-472.4	3.3209	1.9205	82.51
D	D1	0.675	-205.1	0.5261	8.93	97.23
	D2	0.2277	-419.5	0.186	2.1069	88.91
	D3	0.0874	-407.4	0.0745	20.794	99.61

From the two tables above it can be seen that there is a slightly increasing in corrosion current and corrosion rate for A, B and C samples in Ringer's solution as compared to samples in artificial saliva.

These results agree with the fact that the corrosion resistance of pure metal or an alloy strongly depends on the environment where it is exposed, the chemical composition, viscosity and so forth **[157].**

Table (4.8) and Table (4.9) show improvement in corrosion resistance of CoCrMo alloy with different additives of B in two corrode solutions as compared with CoCrMo alloy. So corrosion rate decreases with increasing B content as shown in figure (4.75).

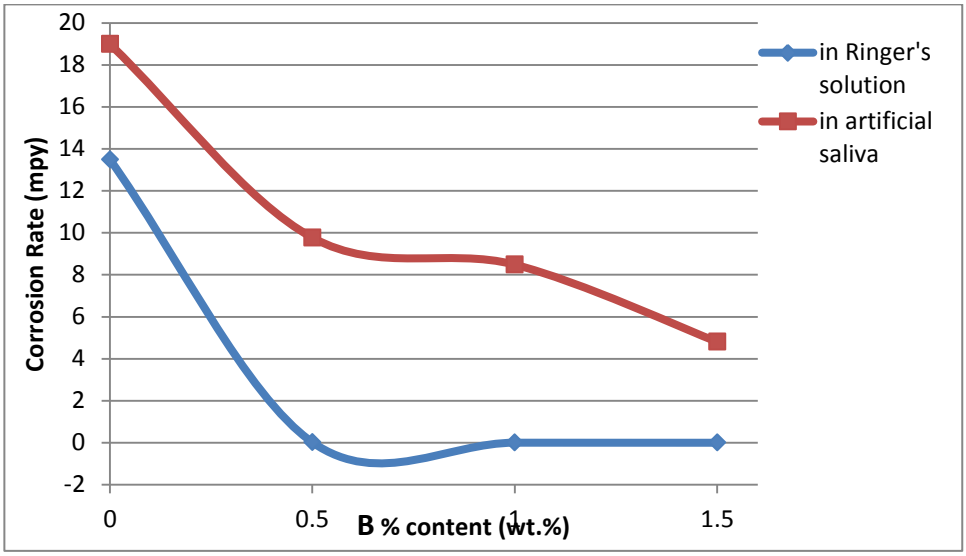

Figure (4.75) :The effect of **B** content on corrosion rate of A,B1,B2 and B3 alloys in artificial saliva and Ringer's solution at 37 °C.

From above Tables (4.8) and (4.9), it can be noted that there is an improvement in corrosion resistance with the additives of W element in two corrode solutions and corrosion resistance increases with increasing W content as shown in Figure (4.76) , this improvement return to that W element enhances corrosion resistance. This can be attributed to the behaviour of W element as a noble element, which enhances the corrosion resistance of CoCrMo alloy, these results are agree with**[136].** Therefore, the corrosion rate decreases when W content increases for all samples in two corroded solutions used as shown in figure (4.76).

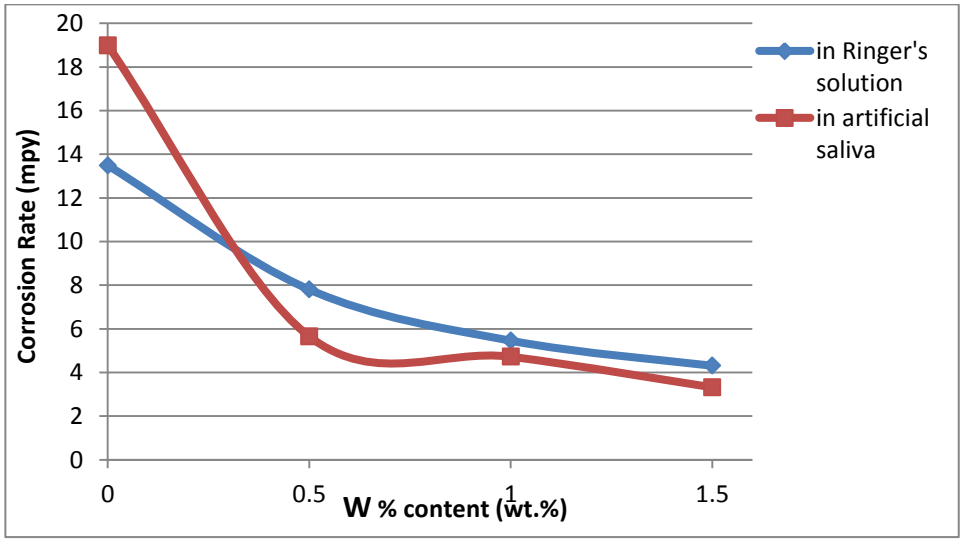

Figure (4.76) :The effect of **W** content on corrosion rate of A,C1,C2 and C3 alloys in artificial saliva and Ringer's solution at 37°C.

Tables ((4.8), (4.9)) shows improvement in corrosion resistance of CoCrMo alloys with different additives of B_4C in two corroded solutions as compared with CoCrMo alloy. the corrosion rate decreases as the B_4C content increases as shown in figure (4.77).

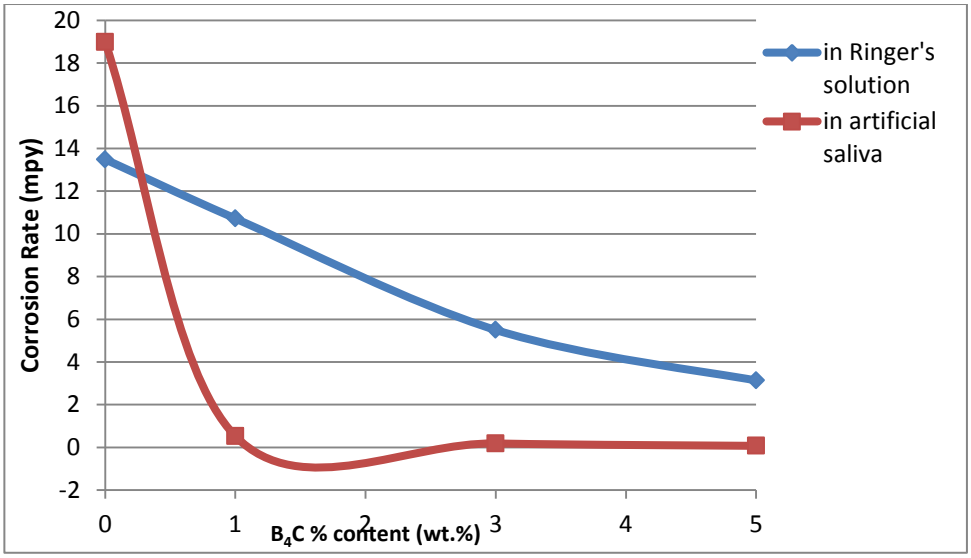

Figure (4.77): The effect of **B_4C** content on corrosion rate of A,D1,D2 and D3 alloys in artificial saliva and Ringer's solution at 37 °C.

4.10.3. Metals Ions Release Test

Metal ion release test is used to ensure the capability of alloys to be used in human bodies.

Released metals ions from the orthopedic implant within surrounding tissue by a variety of mechanisms, involve wear and corrosion such as corrosion fatigue, stress corrosion, fretting corrosion, etc..

Where the use of two solutions (Ringer's solution and artificial saliva) to be performed immersion tests with CoCrMo alloy to get quantitative data necessary for selection appropriated materials in accordance with a variety of medical usage condition.

Figures (4.78), (4.79), (4.80) and (4.81) show the amount of metals ions released after immersion in Ringer's solution and artificial saliva solution for 21 days at 37 C ±2.

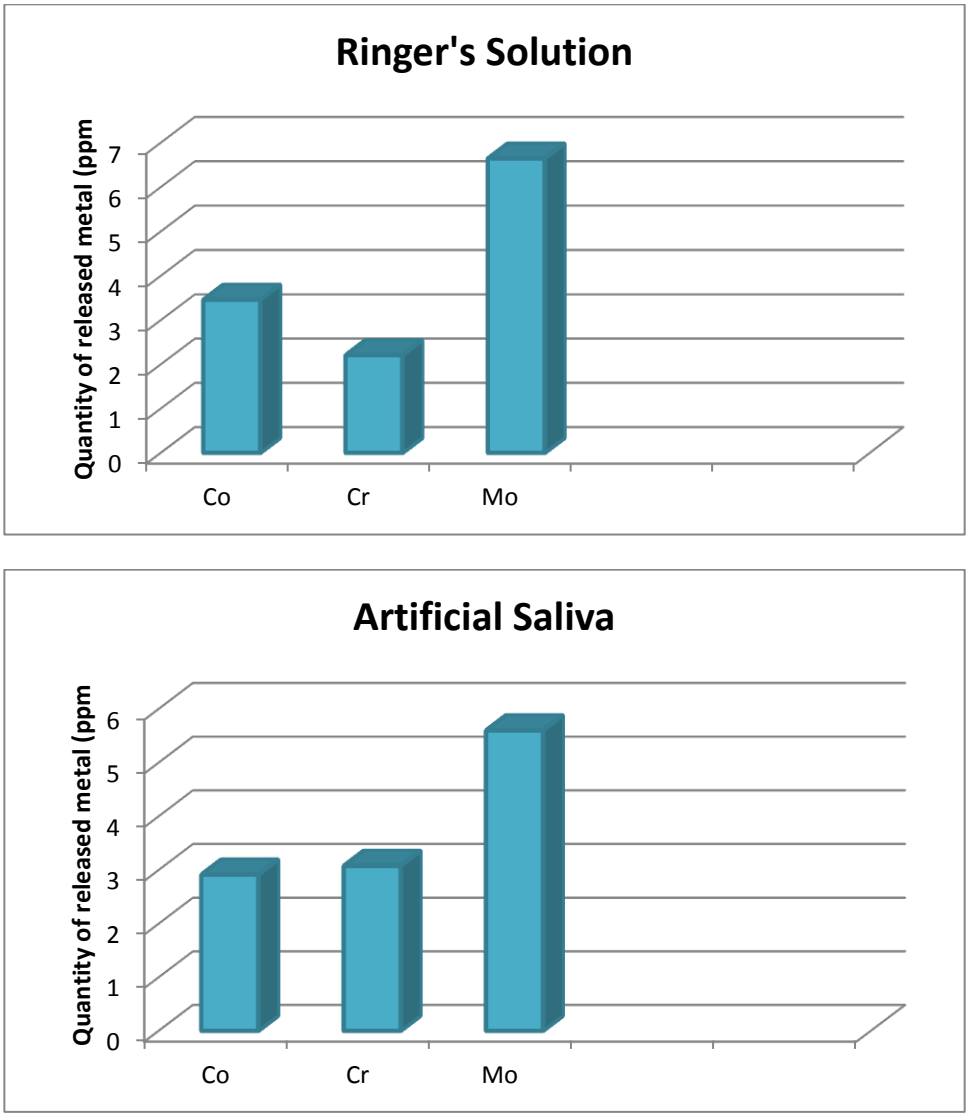

Figure(4.78): Metal ion release values for sample **A** in Ringer's solution and artificial saliva

From Figures (4.79), where can be observed base alloys with B additives, releases fewer ions of samples for all solutions as a compared with base alloy, base alloys with W additives which releases more percentage of ions.

The addition of 1.5% boron element to the alloy reduced the grain size and increased the number of grain boundaries, and thus the path of movement of the

ions became more difficult, and this reduced the percentage of release ions.In addition the role of boron, it was a noble element which enhancing the stability of the protective layer and thus, the entry of corrosive ions and attacking the surface of the metal is more difficult, and the exit of ions from the alloy is also more difficult**[158].**

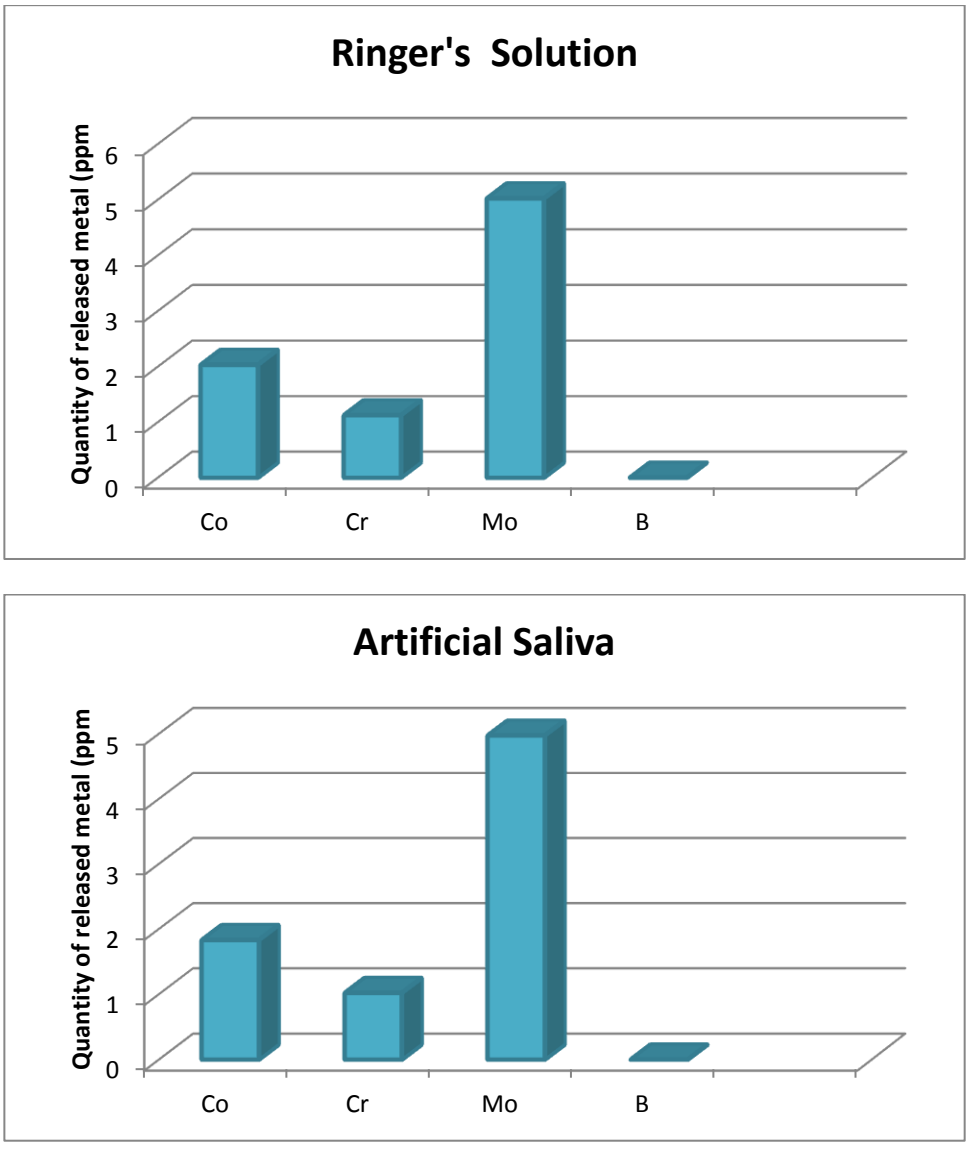

Figure(4.79): Metal ion release values for sample **B3** in Ringer's solution and artificial saliva

The addition of the tungsten element to the cobalt chromium alloy, reduce the ions release from the alloy, as shown in the figure and clarify in Table (4.10)and (4.11)

The reason is due to the role of tungsten in the formation of protective deposits on the crystal boundaries, which prevent the exit of metal ions and reduce the decomposition of the alloy**[136].**

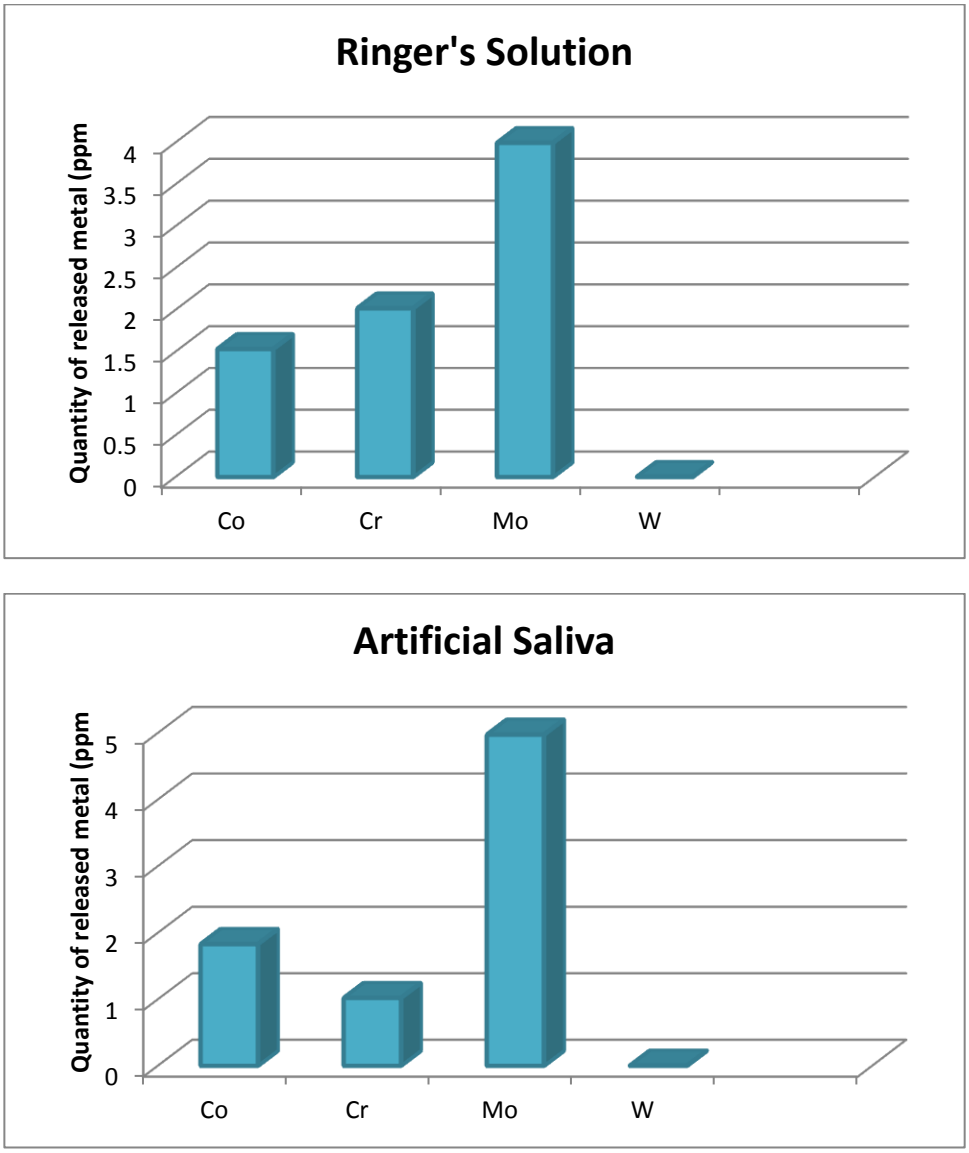

Figure(4.80): Metal ion release values for sample **C3** in Ringer's solution and artificial saliva

As for adding boron carbide, the additions reduces the ions release from alloy that descending to the solution compared to the base alloy. The reason is due to the role of boron carbide as an inert ceramic material that increases the area of the inert region on the surface of the alloy and thus reduces the descending ions.

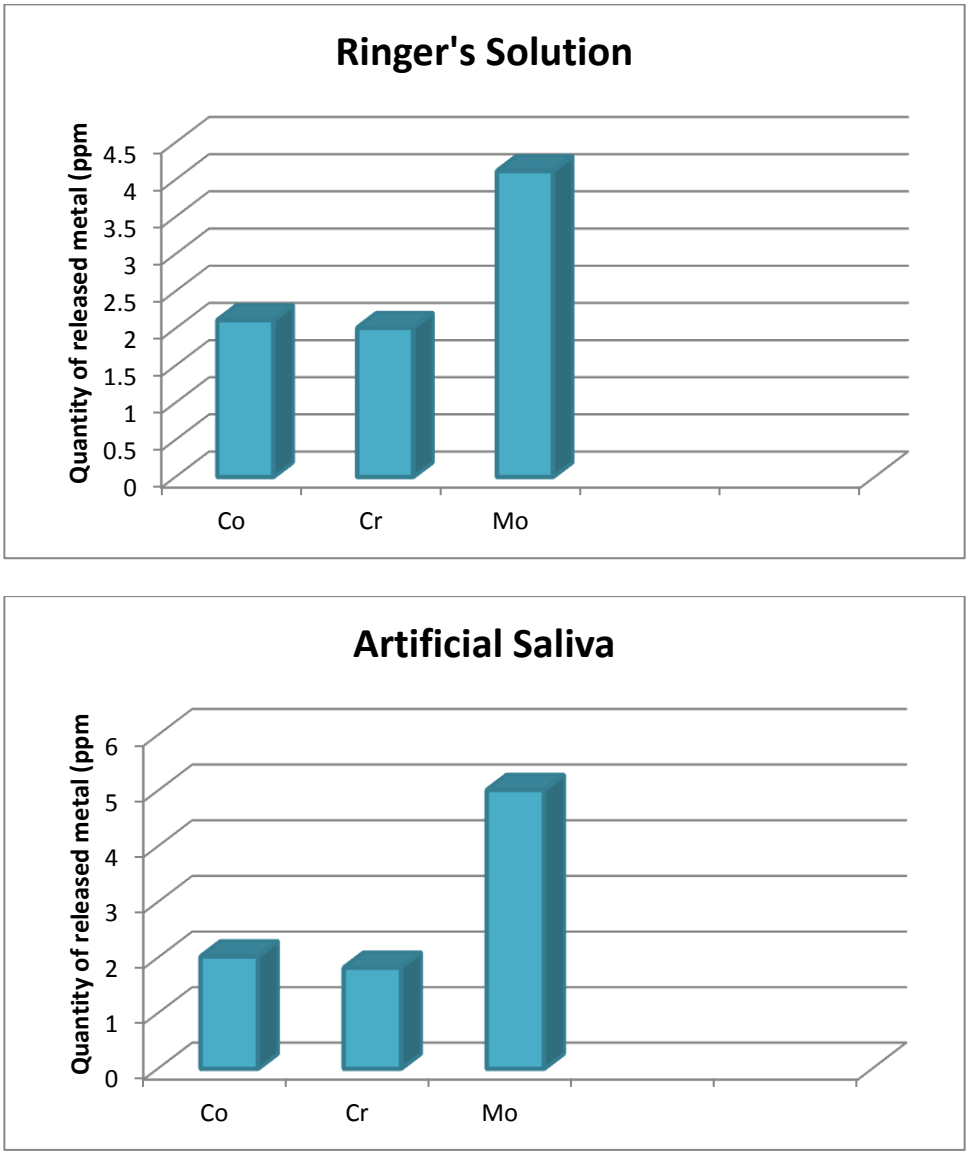

Figure(4.81): Metal ion release values for sample **D3** in Ringer's solution and in artificial saliva.

Table(4.10):Concentration of (Co, Cr, Mo, B, W) ions release from CoCrMo alloys in Ringer's solution after 21days of immersion at 37°C

Alloy Code	Co (ppm)	Cr (ppm)	Mo (ppm)	B (ppm)	W (ppm)
A	3.46	2.207	6.642	…….	…….
B3	2.032	1.123	5.021	Nill	…….
C3	1.531	2.017	3.994	…….	Nill
D3	2.112	2.009	4.117	…….	…….

Table(4.11):Concentration of (Co, Cr, Mo, B, W) ions release from CoCrMo alloys in artificial saliva solution after 21days of immersion at 37°C

Alloy Code	Co (ppm)	Cr (ppm)	Mo (ppm)	B (ppm)	W (ppm)
A	2.912	3.074	5.598	…….	…….
B3	1.829	1.019	4.973	Nill	…….
C3	2.07	1.921	3.217	…….	Nill
D3	2.021	1.819	5.012	…….	…….

5.1. Conclusion

According to the results of the present work, the following can be concluded:

1. sintering at 850° C for 6h of samples (with and without additives) is efficient to complete the transformation process of Co, Cr and Mo to alloy structure.

2. At room temperature, just three phases structure appear in all alloys (with and without additives), CoCrMo, CoCr and Co_2Mo_3.

3.The addition of B and W with (0.5 – 1.5) wt. % to F75 alloy resulted in decreasing the porosity compared to base alloy without B and W. While, the addition of B_4C with (1 ,3 and 5) wt.% causes increasing in of CoCrMo alloys porosity compared to base alloy without B4C.

4. The alloys with B and W additives (0.5 ,1 and 1.5) wt. % and B_4C with(1,3 and 5) wt.% have hardness values higher than that for CoCrMo alloy without B,W and B_4C additives.

5.The compression strength values with B,W and B_4C additives was higher than that for CoCrMo alloys without B, W and B4C additives.

6. The wear resistance increased with addition of B,W and B_4C to CoCrMo alloys , The sample of (5wt%)B_4C has lower weigh loss during wear test under different loads.

7. The corrosion resistance of CoCrMo alloys with B,W and B4C additives was higher than that for CoCrMo alloys without B, W and B4C additives in Ringer's solution and artificial saliva.

5.2. Recommendations

1.Study the effect of B and W additives together on mechanical and electrochemical properties properties of CoCrMo alloy.

2. Add other alloying elements and study the effect of these elements on the corrosion resistance of CoCrMo alloy in vitro and compared it effect with CoCrMo alloy with B,W and B_4C additives .

3. Study the effect of alloying elements on other mechanical properties

4. Study the effects of parameters such as shape and practical size of the used powders on the mechanical and electrochemical properties of prepared alloys.

5. Using another solutions such as plasma and hank's solution to study the effect of alloying elements on the properties of CoCrMo alloy.

References

[1] Park, J. B., & Lakes, R. S. (1992). "Introduction to biomaterials. In Biomaterials science and engineering" . Springer Science & Business Media, Boston, pp. 1-6.

[2] Moravej, M., and Mantovani, D. (2011) "Biodegradable metals for cardiovascular stent application": Interests and new opportunities'', International Journal of Molecular Sciences, Vol.12, No. 7, pp. 4250–4270.

[3] Holzapfel, B. M., Reichert, J. C., Schantz, J. T., Gbureck, U., Rackwitz, L., Nöth, U., ... & Hutmacher, D. W. (2013). "How smart do biomaterials need to be? " A translational science and clinical point of view. *Advanced drug delivery reviews*, Vol.*65*, No.4, pp.581-603.

[4] Callister, W. D., & Rethwisch, D. G. (2007). "Materials science and engineering" ,Vol. 7. New York: Wiley

[5] Teoh, S. H. (2004). "Introduction to biomaterials engineering and processing—an overview". In *Engineering materials for biomedical applications* , pp. 1-16.

[6] Niinomi, Mitsuo.(2008) "Metallic biomaterials." *Journal of Artificial Organs* Vol.11, No.3 , pp.105-110.

[7] Aherwar A, Singh AK, Patnaik A.(2016). "Cobalt based alloy: a better choice bio-material for hip implants". Trends Biomater Artif Organs. pp50–55.

[8] Ratner BD, Hoffman AS, Schoen FJ, Lemons JE, editors.(2013), "Biomaterials science": an introduction to materials in medicine. Burlington (VA): Academic Press;

[9] Zheng, Y., Liu, B. and Gu, X., (2009). "Research progress in biodegradable metallic materials for medical application". *Materials Review*, Vol.1, No.003, pp.1-10.

[10] Gu X, Zheng Y, Cheng Y, Zhong S, Xi T. (2009), "In vitro corrosion and biocompatibility of binary magnesium alloy". Biomaterials; Vol.30, No.4, pp.484–98.

[11] Hendra H., Dadan R., and Joy R. P. Djuansjah, (2011) , "Biomedical Engineering", Metals for Biomedical Applications, Faculty of Biomedical Engineering and Health Science, Universiti Teknologi Malaysia Malaysia, pp.411-430

[12] Moravej, M., and Mantovani, D. (2011) "Biodegradable metals for cardiovascular stent application: Interests and new opportunities", International Journal of Molecular Sciences, Vol. 12, No. 7, pp. 4250–4270.

[13] Sáenz V, Fuentes E., (2013), " Titanium and titanium alloys as biomaterials". In: Jürgen Gegner, editor. Tribology - fundamentals and advancements, Croatia: InTech; 2013

[14] Bai, L., Gong, C., Chen, X., Sun, Y., Zhang, J., Cai, L., Zhu, S. and Xie, S.Q., (2019). "Additive manufacturing of customized metallic orthopedic implants": Materials, structures, and surface modifications. *Metals*, Vol.*9*, No.9, pp.1004.

[15] Kuroda, D., Hiromoto, S., Hanawa, T. and Katada, Y., (2002). "Corrosion behavior of nickel-free high nitrogen austenitic stainless steel in simulated biological environments". *Materials Transactions*, Vol.*43*, No.12, pp.3100-3104.

[16] Hench, L.L.,(1991) "Bioceramics: from concept to clinic" , *Journal of the american ceramic society*, Vol. 74.7 , pp.1487-1510

[17] Liu, X., Chu, P.K. and Ding, C., (2004). "Surface modification of titanium, titanium alloys, and related materials for biomedical applications". *Materials Science and Engineering: R: Reports*, Vol.*47*, No.3-4, pp.49-121.

[18] Reclaru, L. and Ardelean, L.C., 2018. " Current Alternatives for Processing CoCr Dental Alloys Lucien".

[19] Messer R., and Wataha J.,(2002) , "ADVANCED MATERIALS", Dental Materials: Biocompatibility, pp.1-10.

[20] Kyomoto, M., Iwasaki, Y., Moro, T., Konno, T., Miyaji, F., Kawaguchi, H., Takatori, Y., Nakamura, K. and Ishihara, K., (2007). "High lubricious surface of cobalt–chromium–molybdenum alloy prepared by grafting poly (2-methacryloyloxyethyl phosphorylcholine) "*Biomaterials*, Vol.*28*, No.20, pp.3121-3130.

[21] Alvarado, J., Maldonado, R., Marxuach, J. and Otero, R., 2003. "Biomechanics of hip and knee prostheses". *Applications of Engineering Mechanics in Medicine*, pp.6-22.

[22] Kamardan, M. G., Zaidi, N. H. A., Dalimin, M. N., Zaidi, A. M. A., Jamaludin, S. B., & Jamil, M. M. A. (2010), " The sintering temperature effect on the shrinkage behavior of cobalt chromium alloy", American Journal of Applied Sciences, Vol.7, pp.1443-1448.

[23] S.V. Bhat,(2005), " Biomaterials", Alpha Science International Ltd., Harrow, UK, pp. 29.

[24] Dourandish, M., Godlinski, D., Simchi, A. and Firouzdor, V., 2008. "Sintering of biocompatible P/M Co–Cr–Mo alloy (F-75) for fabrication of porosity-graded composite structures". *Materials Science and Engineering: A*, Vol.*472*, No.1-2, pp.338-346.

[25] ALEXANDRU, I., POPOVICI, R., COJOCARU-FILIPIUC, V., BACIU, C., (1997), " Alegerea si utilizarea materialelor metalice", EDP, Bucuresti.

[26] BORTUN, C., GHIBAN, B., Aliaje de cobalt, Ed. Printech, Bucure'ti, 2009

[27] Hench, L.L., (1998) "Biomaterials: a forecast for the future". *Biomaterials*, Vol.*19*, No. 16 , pp.1419-1423.

[28] Huebsch, N. and Mooney, D.J., 2009. "Inspiration and application in the evolution of biomaterials". *Nature*, Vol.*462*,No.7272), pp.426-432.

[29] Ratner, B.D. and Bryant, S.J., (2004) "Biomaterials: where we have been and where we are going". *Annu. Rev. Biomed. Eng.*, No.*6*, pp.41-75.

[30] Lai, G. Y. (2007), "High-temperature corrosion and materials applications" ,ASM International, chapter 9.

[31] Shukla, K., Sugumaran, A.A., Khan, I., Ehiasarian, A.P. and Hovsepian, P.E., (2020) "Low pressure plasma nitrided CoCrMo alloy utilising HIPIMS discharge for biomedical applications", *Journal of the Mechanical Behavior of Biomedical Materials*, Vol.111, pp.104004.

[32] Hermawan, H., Ramdan, D., and Djuansjah, J. R.(2011) "Metals for biomedical applications", In Biomedical engineering-from theory to applications, Faculty of Biomedical Engineering and Health Science, University Teknologi Malaysia, Malaysia, Chapter 17

[33] Mattila, R.,(2012), "Hip and Knee Replacement Implants", Sirpa Nikunen and Tiina Pelander, nursing program, Turku University of Applied Sciences. dc.publisher Turun ammattikorkeakoulu.

[34] Knee Replacement & HipReplacement Patient Advocacy & Online Communit

[35] Lee, S.H., Takahashi, E., Nomura, N. and Chiba, A., (2006). " Effect of carbon addition on microstructure and mechanical properties of a wrought Co–Cr–Mo implant alloy". *Materials transactions*, Vol.*47*, No.2, pp.287-290.

[36] History and deveiopment of spinal implants/ spinal course. Academy leader in continuing dental education 2015

[37] Johnson, L.P. and Lane, J., (1895) *The Art of Thomas Hardy*. John Lane. 2nd ed, India University Library.

[38] LAMBOTTE, A., (1909). "Technique et indication des prothèses dans le traitement des fractures". *Presse med*, Vol.*17*, p.321.

[39] Sanli I, Arts JJC, Geurts J.,(2016), "Clinical and radiologic outcomes of a fully hydroxyapatite- coated femoral revision stem, excessive stress shielding incidence and its consequences". J Arthroplasty; Vol.3, No.1, pp.209-214

[40] Emerson, C. P.,(2015) , "The Microstructure and the Electrochemical Behavior of Cobalt Chromium Molybdenum Alloys from Retrieved Hip Implants", PhD thesis ,Florida International University, Miami, Florida.

[41] Hjalmarsson, L., (2009), "On Cobalt-Chrome Frameworks in Implant Dentistry, Department of Prosthetic Dentistry", Dental Materials Science Institute of Odontology.

[42] Niinomi, M., (2002), "Recent metallic materials for biomedical applications", Metallurgical and Materials Transactions, University of Gothenburg. Sahlgrenska Academy, Vol. 33, No. 3, pp.477–486.

[43] Dowson, D.,(2001), "New joints for the Millennium: wear control in total replacement hip joints". *Proceedings of the Institution of Mechanical Engineers, Part H: Journal of Engineering in Medicine*, Vol.*215*, No.4, pp.335-358.

[44] Wlodek ST, (1963) "Embrittlement of a Co-Cr-W (L-605) alloy". Trans ASM Vol.56, No.3, pp.287–303

[45] Chan, F.W., Bobyn, J.D., Medley, J.B., Krygier, J.J., Yue, S. and Tanzer, M., (1996), "Engineering issues and wear performance of metal on metal hip implants" *Clinical orthopaedics and related research*, Vol.333, pp.96-107.

[46] Yoda, K., Takaichi, A., Nomura, N., Tsutsumi, Y., Doi, H., Kurosu, S., Chiba, A., Igarashi, Y. and Hanawa, T., (2012) " Effects of chromium and nitrogen content on the microstructures and mechanical properties of as-cast Co-Cr-Mo alloys for dental applications " Acta Biomater., vol. 8, no. 7, pp. 2856–2862.

[47] Li, Y., Yamashita, Y., Tang, N., Liu, B., Kurosu, S., Matsumoto, H., Koizumi, Y. and Chiba, A., (2012) "Influence of carbon and nitrogen addition on microstructure and hot deformation behavior of biomedical Co–Cr–Mo alloy". *Materials Chemistry and Physics*, Vol.*135*, No.2-3, pp.849-854.

[48] Fujii, H., Asano, T., Matsuo, Y. and Sugie, Y., (2011). "Effect of Heat-Treatment on Localized Corrosion Behavior of Duplex Stainless

Steels in 3.5% NaCl Solution". *Journal of Materials Science and Engineering. A*, Vol.1, No.7A, p.899.

[49] Bauer, S., Schmuki, P., Von Der Mark, K. and Park, J., (2013). "Engineering biocompatible implant surfaces: Part I: Materials and surfaces". *Progress in Materials Science*, Vol.*58*, No.3, pp.261-326.

[50] Salinas-Rodrfguez, A.,(1999), "The Role of the FCC-HCP Phase Transformation During the Plastic Deformation of Co-Cr-Mo-C Alloys for Biomedical Applications,. in Cobalt-Base Alloys for Biomedical Applications", ASTM STP 1365. West Conshohocken, PA,: American Society for Testing and Materials, pp.108–121

[51] Nalbant, M., A. Altın, and H. Gökkaya,(2007), " The effect of cutting speed and cutting tool geometry on machinability properties of nickel-base Inconel 718 super alloys". Materials & Design, Vol.28, No.4, pp. 1334-1338.

[52] Bordin, A., Bruschi, S. and Ghiotti, A., (2014). " The effect of cutting speed and feed rate on the surface integrity in dry turning of CoCrMo alloy". *Procedia Cirp*,Vol. *13*, pp.219-224.

[53] Giacchi, J.V., Morando, C.N., Fornaro, O. and Palacio, H.A., (2011). "Microstructural characterization of as-cast biocompatible Co–Cr–Mo alloys". *Materials characterization*, Vol.*62*, No.1, pp.53-61.

[54] Vidal, C.V. and Muñoz, A.I., (2008) "Electrochemical characterisation of biomedical alloys for surgical implants in simulated body fluids". *Corrosion Science*, Vol.*50*, No.7, pp.1954-1961.

[55] Davis, J. R. (Editor.). (2000) "Nickel, Cobalt, and Their Alloys". ASM international, 1st ed.

[56] Ando, K., Omori, T., Sato, J., Sutou, Y., Oikawa, K., Kainuma, R., & Ishida, K. (2006) "Effect of alloying elements on fcc/hcp martensitic transformation and shape memory properties in Co-Al alloys", Materials Transactions. Vol.47, No.9, pp. 2381-2386.

[57] Cameron, C. B., & Ferriss, D. P. (1975) "Tribaloy intermetallic materials: New wear-and corrosion-resistant alloys", Anti-Corrosion Method. Material, Vol.22, No. 4, pp. 5-8

[58] Lenntech B.V.All right reserved.[online] https://www.lenntech.com/periodic/elements/b.htm/ (Accessed 1998 - 2021).

[59] Kauser, F., (2007) "Corrosion of Co-Cr-Mo alloys for biomedical applications". Department of Metallurgy and Materials, School of Engineering. University of Birmingham: Birmingham, pp.4-285.

[60] Daud, Z.C., Jamaludin, S.B., (2013) " The Effect of Sintering on the Properties of Powder Metallurgy PM F-75 Alloy", Advanced Material Research, Vol,795, pp. 573-577.

[61] Nordberg, Gunnar F., Bruce A. Fowler, and Monica Nordberg, eds. (2014)" *Handbook on the Toxicology of Metals*". chapter 58Tungsten, Academic press, pp.1297-1298, 2014.

[62] Leggett, R.W., 1997. "A model of the distribution and retention of tungsten in the human body". *Science of the total environment, 206*, no.2-3 , pp.147-165.

[63] Rieck, G. D.,(2013) *Tungsten and its Compounds*. Elsevier.

[64] Kalaiselvan, K., Dinaharan, I. and Murugan, N., (2014) " Characterization of friction stir welded boron carbide particulate reinforced AA6061 aluminum alloy stir cast composite". *Materials & Design*, Vol.*55*, pp.176-182.

[65] Dinaharan, I., (2016) "Influence of ceramic particulate type on microstructure and tensile strength of aluminum matrix composites produced using friction stir processing." *Journal of Asian Ceramic Societies*, Vol.4, No. 2 , pp.209-218.

[66] Morrell, R., (2016) "Refrence Module in Materials Science and Materials Engineering", National physical laboratory, Teddington, UK, pp.1-25,

[67] Suri, A.K., Subramanian, C., Sonber, J.K. and Murthy, T.C., (2010) "Synthesis and consolidation of boron carbide: a review". *International Materials Reviews*, Vol.*55*, No.1, pp.4-40.

[68]Santos, G., (2017) "The importance of metallic materials as biomaterials". Adv Tissue Eng Regen Med Open Access, Vol.3, No.1, p.00054.

[69] Narushima, T. and Ueda, K., (2015) "Co-Cr alloys as effective metallic biomaterials." In *Advances in Metallic Biomaterials*, Springer, Berlin, Heidelberg, pp. 157-178.

[70] Shih C. C., Lin S. J., and Chen Y. L., (2005) "The cytotoxicity of corrosion of NiTi shape memory alloys used for medical applications" , analytical and bioanalytical chemistry, Vol.381 , pp. 557-567.

[71] Trepanned C, Leung T. K., and Tabrizian M., (1999) "Preliminary investigated of the effect of surface treatments on biological response to

shape memory NiTi stent" ,Journal of biomedical materials research, Vol.48, pp.165-171

[72] Sathirachinda, N., Pettersson, R. and Pan, J., (2009). "Depletion effects at phase boundaries in 2205 duplex stainless steel characterized with SKPFM and TEM/EDS. *Corrosion Science*,Vol.51, No.8, pp.1850-1860.

[73] Ali, S., Rani, A.M.A., Baig, Z., Ahmed, S.W.,Hussain, G., Subramaniam, K., Hastuty, S. and Rao, T.V., (2020). "Biocompatibility and corrosion resistance of metallic biomaterials". *Corrosion Reviews*, Vol.*38*, No.5, pp.381-402.

[74] Williams, D.F., 2008. On the mechanisms of biocompatibility. *Biomaterials* ,Vol.*29* , No.20, pp.2941-2953.

[75] Hermawan, H., Ramdan, D. and Djuansjah, J.R., (2011). "Metals for biomedical applications". *Biomedical engineering-from theory to applications*, Vol.1, pp.411-430.

[76] Singh, R. and Dahotre, N.B., 2007. "Corrosion degradation and prevention by surface modification of biometallic materials". *Journal of Materials Science: Materials in Medicine*, Vol.18, No.5, pp.725-751.

[77] Mason S.E. and Rawlings R.D., (1985) " Fracture behavior of two Co-Mo-Cr-Si wear resistant alloys", Journal of Materials Science,Vol.20 , No.4 , pp.1248-1256.

[78] Süry, P., and Semlitsch, M. (1978) "Corrosion behavior of cast and forged cobalt-based alloys for double-alloy joint endoprostheses", Journal of Biomedical Materials Research Part A, Vol.12, No.5, pp.723-741.

[79] Hermawan, H., Ramdan, D., and Djuansjah, J. R.(2011) "Metals for biomedical applications" ,In Biomedical engineering-from theory to applications(Eds), Faculty of Biomedical Engineering and Health Science, University Teknologi Malaysia, Malaysia, Chapter 17, Vol.1, pp.411-430.

[80] Tommi K., David C. and Marja L., (2013) "Atomic Layer Deposition: *principles, characteristics, and nanotechnology applications*, 2nd edition, Scrivener Publishing-Wiley, Canada.

[81] Virtanen, S., Milošev, I., Gomez-Barrena, E., Trebše, R., Salo, J. and Konttinen, Y.T.,(2008). "Special modes of corrosion under physiological and simulated physiological conditions". *Acta biomaterialia*, Vol. *4*, No.3, pp.468-476.

[82] Khan, M., Kuiper, J. H., & Richardson, J. B., (2007) "Can cobalt levels estimate in-vivo wear of metal-on-metal bearings used in hip arthroplasty? ",Proceedings of the Institution of Mechanical Engineers, Part H: Journal of Engineering in Medicine, Vol.221, No. 8, pp. 929-942.

[83] Kauser, F.(2007) "Corrosion of CoCrMo alloys for biomedical applications", PhD Thesis. University of Birmingham.

[84] Geringer, J., Forest, B., & Combrade, P. (2005) "Fretting-corrosion of materials used as orthopaedic implants", Wear, Vol.259, No.7-12, pp.943-951.

[85] Manivasagam, G., Dhinasekaran, D. and Rajamanickam, A. (2010) "Biomedical implants: corrosion and its prevention-a review", Recent patents on corrosion science, 2, pp.40-54.

[86] Standard terminology relating to wear and erosion ,(2001) standard G-40-01, American Society for Testing and Materials.

[87] Bayer RG, Mechanical wear: fundamentals and testing, (2004) Marcel Dekker Inc.: New York, NY.

[88] Rony, L., Lancigu, R. and Hubert, L., 2018. Intraosseous metal implants in orthopedics: A review. *Morphologie*, *102*(339), pp.231-242.

[89] Mohammed, M.T., Khan, Z.A. and Siddiquee, A.N. (2013) "Influence of Microstructural Features on Wear Resistance of Biomedical Titanium Materials", . *International Journal of Biomedical and Biological Engineering*,Vol.7, No. 1, pp.49-53.

[90] Fellah, M., Labaïz, M., Assala, O. and Iost, A. (2014) "Comparative Tribologicalstudy of biomaterials AISI 316L and Ti-6Al-7Nb", TMS, Vol.237, pp.237-246.

[91] Bhushan, B. (2013) "Introduction to Tribology", 2nd ed., John Wiley & Sons, Ltd.: New York, NY, USA.

[92] Roylance, B.J., Williams, J.A. and Dwyer-Joyce, R., 2000. Wear debris and associated wear phenomena—fundamental research and practice. *Proceedings of the Institution of Mechanical Engineers, Part J: Journal of Engineering Tribology*, *214*(1), pp.79-105.

[93] Valefi, M. (2012). "Wear and Friction of Self-lubricating CuO-TZP Composites", PhD. Thesis, University of Twente, Enschede, the Netherlands.

[94] Aseel S. H. (2013) "Study of microstructure, corrosion and dry sliding wear of copper –aluminum-nickel shape memory alloys", MS.C thesis , materials engineering college , university of Babylon / Iraq.

[95] Bayer, R.G. (2002) "Fundamentals of wear failures", Materials Park, OH: ASM International, *Failure Analysis and Prevention*, Vol.11, pp.901-905.

[96] Callister Jr, W.D. and Rethwisch, D.G.,(2011) "Materials Science and Engineering An Introduction" . John Wiley & Sons, Inc, 10th edition,

[97] Vinarcik, E.J. (2002) "High integrity die casting processes", John Wiley & Sons, New York, Published simultaneously in Canada.

[98] Budinski, K.G. and Budinski, M.K. (2009) "Engineering materials", 9thed., Nature, Vol.25.

[99] Vasconcellos, L.M.R.D., Leite, D.D.O., Nascimento, F.O., Vasconcellos, L.G.O.D., Graca, M.L.D.A., Carvalho, Y.R. and Cairo, C.A.A., (2010) "Porous titanium for biomedical applications: an experimental study on rabbits". Medicina oral, patologia oral y cirugia bucal, 15, No.2, p.e407.

[100] Hammi, Y., Stone, T.W., Allison, P.G. and Horstemeyer, M.F. (2010) 'Fatigue Modeling of a Powder Metallurgy Main Bearing Cap', In SIMULIA Customer Conference.

[101] J.S. Colton, (2009) " metal powder processing ver. 1", Georgia institute of technology , manufacturing processes and equipment.

[102] Šalak, A. Selecká, M. and Danninger, H. (2005) "Machinability of Powder Metallurgy Steels", Cambridge International Science Publishing. Cambridge, UK.

[103] Kipouros, G.J., Caley, W.F. and Bishop, D.P. (2006) "On the advantages of using powder metallurgy in new light metal alloy design", Metallurgical and Materials Transactions A, Vol.37, No.12, pp.3429-3436.

[104] Groover, M.P. (2012) "Introduction to manufacturing processes", John Wiley & Sons, INC.

[105] Groover, M.P. (2002) *Solutions manual:* "Fundamentals of Modern Manufacturing"', 2nd ed., John Wiley & Sons, INC.

[106] Sharma, P.C. (2007) "Production Technology (Manufacturing Processes): Manufacturing Processes", S. Chand Publishing.

[107] Rajput, R.K. (2007) "A textbook of manufacturing technology (Manufacturing processes) ", Firewall Media.

[108] Rao, V. P. (2002) "Manufacturing Science and Technology: Manufacturing Processes and Machine Tools", New Age International, India.

[109] Thummler, F. and Oberacker, R. (1993) "An Introduction to Powder Metallurgy", The Institute of Materials, London, England.

[110] Sinka, C. (2007) "Modelling powder compaction", KONA Powder and Particle Journal, No.25, pp.4-22.

[111] Shatokha, V. (2012) "Sintering–Methods and Products",InTech, Rijeka, Croatia.

[112] Meluch, L. (2010) "Warm Compaction of Aluminum AlloyAlumix123", Doctor of Philosophy, The University of Birmingham,Birmingham, UK.

[113] Zak Fang, Z. (2010) "Sintering of advanced materials-fundamentalsand processes", Woodhead Publishing, USA.

[114] Al-Ethari, H.A. and Hamza, H., (2014) " Tool Life Modeling for Drilling NAB Alloy Reinforced by SIC and Graphite". International Journalof Engineering and Innovative Technology, Vol.3, No.7.

[115] Kadiman, N.N., Rashid, M.O.A., Muhamad, N. and Sulong, A.B., (2018) "Effects of Sintering Temperature on the Physical and Mechanical Properties of Injection-Molded Copper/Graphene Composite". Journal of Advanced Manufacturing Technology (JAMT), Vol.12, No.1, pp.49-60.

[116] Xu, Z., Hodgson, M.A., Chang, K., Chen, G., Yuan, X. and Cao, P., (2017) "Effect of sintering time on the densification, microstructure, weight loss and tensile properties of a powder metallurgical Fe-Mn-Si alloy". *Metals*, Vol.*7*, No.3, p.81.

[117] Robert W.W., Yang, C. C., Huang, C.A and Chen, Y.S., (2005) "Electrochemical corrosion studies on Co–Cr–Mo implant alloy in biological solutions', Materials chemistry and physics, Vol.93, No. 2-3, pp.531-538.

[118] Lee, S.H., Nomura, N. and Chiba, A., (2007) " Effect of Fe addition on microstructures and mechanical properties of Ni-and C-Free Co-Cr-Mo alloys". *Materials transactions*, Vol.*48*, No.8, pp.2207-2211.

[119] Dourandish, M., Godlinski, D., Simchi, A., & Firouzdor, V. (2008) "Sintering of biocompatible P/M Co–Cr–Mo alloy (F-75) for fabrication of porosity-graded composite structures", Materials Science and Engineering: A,Vol.472, No.1-2,pp338-346.

[120] Lee, S.H., Nomura, N. and Chiba, A., (2008) "Significant improvement in mechanical properties of biomedical Co, Cr and Mo alloys

with combination of N addition and Cr enrichment". The Japan institute of metals, Vol: 49, pp. 260-264.

[121] Songür, M., Çelikkan, H., Gökmeşe, F., Şimşek, S.A., Altun, N.Ş. and Aksu, M.L., (2009) "Electrochemical corrosion properties of metal alloys used in orthopaedic implants". *Journal of Applied Electrochemistry*, Vol.*39*, No.8, pp.1259-1265.

[122] Rodrigues, W.C., Broilo, L.R., Schaeffer, L., Knörnschild, G. and Espinoza, F.R.M., (2011) "Powder metallurgical processing of Co–28% Cr–6% Mo for dental implants: Physical, mechanical and electrochemical properties", *powder technology* Elsevier, Vol.*206*, No.3, pp.233-238.

[123] Milošev, I., (2012) "CoCrMo alloy for biomedical applications". In *Biomedical Applications*. Springer, Boston, MA.,Vol.55, pp. 1-72.

[124] Balagna, C., Spriano, S. and Faga, M.G., (2012) " Characterization of Co–Cr–Mo alloys after a thermal treatment for high wear resistance. *Materials Science and Engineering: C*, Vol. *32*, No.7, pp.1868-1877.

[125] Valero-Vidal, C., Casabán-Julián, L., Herraiz-Cardona, I. and Igual-Muñoz, A., (2013) " Influence of carbides and microstructure of CoCrMo alloys on their metallic dissolution resistance". *Materials Science and Engineering: C*, Vol.*33*, No.8, pp.4667-4676.

[126] Zangeneh, S., Ketabchi, M. and Lopez, H.F., (2014) " Nanoscale carbide precipitation in Co–28Cr–5Mo–0.3 C implant alloy during martensite transformation". *Materials Letters*, Vol.116, pp.188-190.

[127] Chen, Y., Li, Y., Kurosu, S., Yamanaka, K., Tang, N., Koizumi, Y. and Chiba, A., (2014) " Effects of sigma phase and carbide on the wear behavior of CoCrMo alloys in Hanks' solution. *Wear*, Vol.310, No.1-2, pp.51-62.

[128] Abbass, M. K., Ajeel, S. A., & Wadullah, H. M. (2014) "Study of Corrosion Resistance of Co-Cr-Mo Surgical Implants Alloy in Artificial Saliva", Engineering and Technology Journal, Part (A) Engineering, Vol.32, No.10, pp.2331-2339.

[129] Yamanaka, K., Mori, M. and Chiba, A., (2014) " Refinement of solidification microstructures by carbon addition in biomedical Co–28Cr–9W–1Si alloys". *Materials Letters*, Vol.116, pp.82-85.

[130] Alfirano ,2015." Effect of Alloying Elements on Microstructure of Biomedical Co-Cr-Mo F75 Alloy" , Advanced Materials Research, Vol.1112 , pp.421-424

[131] Khilfa, A. H. (2015) "Effect of Y and Ge addition on Mechanical properties and Corrosion behavior of Biomedical CoCrMo Alloy (F75) ", MSc thesis, University of Babylon, Iraq.

[132] Hassani, F.Z., Ketabchi, M., Bruschi, S. and Ghiotti, A., (2016) "Effects of carbide precipitation on the microstructural and tribological properties of Co–Cr–Mo–C medical implants after thermal treatment". *Journal of Materials Science*, Vol.*51*,No.9, pp.4495-4508.

[133] Abtan, E. A. (2018) "Effect of Indium and Tellurium on Behaviour of CoCrMo (F75) Biomedical Alloy", MSc thesis, University of Babylon, Iraq.

[134] Marco A.L. Hernandez-Rodriguez1, Dionisio A. Laverde-Cataño2, Diego Lozano3,Gabriela Martinez-Cazares3and Yaneth Bedolla-Gil,

(2019) " Influence of Boron Addition on the Microstructure and the Corrosion Resistance of CoCrMo Alloy".pp. 1-11

[135] M Omar M. A., Baharudin B.T., Sulaiman S., Ismail M.I., Omar M.A., 2020."Evaluation of chemical composition, heat treatment, mechanical properties and electrochemical polishing for additively manufactured stent using ASTM F75 cobalt based superalloy (CoCrMo) by selective laser melting (SLM)technology". pp.1-22

[136] Dong, X., Sun, Q., Zhou, Y., Qu, Y., Shi, H., Zhang, B., Xu, S., Liu, W., Li, N. and Yan, J., (2020). "Influence of microstructure on corrosion behavior of biomedical Co-Cr-Mo-W alloy fabricated by selective laser melting". *Corrosion Science*, Vol.170, pp.1-7

[137] ASTM B-328 (2003) Standard Test Method for Density, Oil Content, and Interconnected Porosity of Sintered Metal Structural Part and Oil –Impregnated Bearing, ASTM international

[138] Odahara, T., Matsumoto, H., & Chiba, A. (2008) "Mechanical Properties of Biomedical Co-33Cr-5Mo-0.3NAlloy at Elevated Temperatures", Materials transactions, Vol. 49, No. 9, pp.1963-1969.

[139] Jawad, M. S., (2015) "Effect of (Cu & Cr) Additives on Corrosion and Dry Sliding Wear of NiTi Shape Memory Alloy", MSc thesis, Submitted to the Council of the College of Materials engineering /University of Babylon.

[140] Annual Book of ASTM Standards, Wear and erosion; Metal Corrosion, volume 03.02, G5 – 87, 1988

[141] Chandra, A., Ryu, J.J., Karra, P., Shrotriya, P., Tvergaard, V., Gaisser, M. and Weik, T., (2011) "Life expectancy of modular Ti6Al4V hip implants: influence of stress and environment". *Journal of the*

mechanical behavior of biomedical materials, ELSEVER Vol.4, No.8, pp.1990-2001.

[142] Jaber, H.H. (2014) " The Effect of Addmixed Ti on Corrosion Resistant of High Copper Dental Amalgam" journal of Babylon University, Vol. 22, No.2, pp.413-421.

[143] Hanawa, T. (2004) 'Metal ion release from metal implants', Materials Science and Engineering: C, Vol. 24, No. 6-8, pp.745-752.

[144] Ali, A.K.A. and Dawood, N.M., 2020, November. "The Effect of Boron Addition on The Microstructure and Corrosion Resistance of Cu-Al-Ni Shape-Memory Alloys Prepared by Powder Technology". In *IOP Conference Series: Materials Science and Engineering* (Vol. 987, No. 1, p. 012028). IOP Publishing.

[145] Katsuyoshi K., (2012)," Powder Metallurgy" ,Published by InTech ,Janeza Trdine 9, 51000 Rijeka, Croatia. chapter2, Osaka University Japan, pp.31-46

[146] Ogden, H.R. and Holden, F.C. (1958) , " Metallography of titanium alloys" (No. TML-103), Battelle Memorial Inst, Titanium Metallurgical Lab., Columbus, Ohio.

[147] Nur Aidah Nabihahbinti Dandang,(2019) "Microstructures and Properties of CoCrMo alloy by Metal Injection Moulding Process", MSc thesis, Universiti Malaysia Pahang,

[148] Nawal M. D.,(2014) "Preparation And Characterization Of Bio Nitinol With Addition Of Copper" PhD. thesis, materials engineering department , university of technology/ Iraq.

[149] Aslan, N.S., Rajih, A.K. and Haleem, A.H.,,(2020) "Effect of Alloying Elements on the Erosion-Corrosion Behaviour of Cu-Based Alloys ",In: IOP Conference Series: Materials Science and Engineering. IOP Publishing, Vol. 987, No. 1, p. 012018.

[150] Wagner, W.R., Sakiyama-Elbert, S.E., Zhang, G. and Yaszemski, M.J. eds., 2020. "Biomaterials science: An introduction to materials in medicine". 4th ed, Academic Press ,Elsevier.

[151] Tripathy, I., (2011), "Effect of Microstructure on Sliding Wear Behaviour of Modified 9Cr-1Mo steel" , MS.C thesis , Metallurgical and Materials Engineering, National Institute of Technology, Rourkela.

[152] Sara. M.G, (2015) " Effect of (Cu & Cr) Additives on Corrosion and Dry Sliding Wear of NiTi Shape Memory Alloy" , MS.C thesis , materials engineering college , university of Babylon / Iraq , 2015.

[153] Wang, Q., Huang, C., & Zhang, L. (2012). "Microstructure and tribological properties of plasma nitriding cast CoCrMo alloy". Journal of Materials Science & Technology, Vol.28, No.1, pp.60-66.

[154] Abdalwahid K. R., (2016), "Metallurgical Engineering and Advanced Materials", part four, first edition.

[155] Li, L., Kim, M., Lee, S., Bae ,M.,& Lee, D.,(2016) "Influence of multiple ultrasonic impact treatments on surface roughness and wear performance of SUS301 steel", Surface and Coating Technology, Vol.307, pp.517-524.

[156] R. Singh And N. B. Pahotre ,(2007) " Corrosion Degradation And Prevention By Surface Modification Of Bio Metallic Materials" , J Mat. Sci: Mater, Vol. 18, , pp. 725 – 751.

[157] Sarkar, N.K. and Greener, E.H., (1974) "Corrosion behavior of the tin-containing silver-mercury phase of dental amalgam". *Journal of dental research*, Vol.*53*, No.4, pp.925-932.

[158] Hernandez-Rodriguez, M.A., Laverde-Cataño, D.A., Lozano, D., Martinez-Cazares, G. and Bedolla-Gil, Y., (2019) "Influence of boron addition on the microstructure and the corrosion resistance of CoCrMo alloy". *Metals* , Vol.9, No.3 , p.307.

Appendix(A)

SPECTRO X-LAB

Job Number: 0

Sample Name: **NUHA**
Description: N1

Date of Receipt: 02/06/2021
Date of Evaluation: 02/06/2021

Average Atomic Number: 0.00

Loss of Ignition: 1.0000 %

Z	Symbol	Element	Concentration		Abs. Error	
12	Mg	Magnesium	< 0.028	%	(0.0)	%
13	Al	Aluminum	< 0.0063	%	(0.0)	%
14	Si	Silicon	0.0460	%	0.0028	%
15	P	Phosphorus	< 0.0015	%	(0.0)	%
16	S	Sulfur	< 0.00069	%	(0.0)	%
22	Ti	Titanium	< 0.0018	%	(0.0)	%
23	V	Vanadium	0.0252	%	0.0019	%
24	Cr	Chromium	17.58	%	0.05	%
25	Mn	Manganese	1.919	%	0.021	%
26	Fe	Iron	2.419	%	0.025	%
27	Co	Cobalt	70.84	%	0.11	%
28	Ni	Nickel	2.563	%	0.026	%
29	Cu	Copper	0.0271	%	0.0056	%
30	Zn	Zinc	0.1004	%	0.0041	%
33	As	Arsenic	< 0.00019	%	(0.0)	%
40	Zr	Zirconium	< 0.050	%	(0.0)	%
41	Nb	Niobium	0.0082	%	0.0046	%
42	Mo	Molybdenum	3.248	%	0.049	%
47	Ag	Silver	0.0070	%	0.0022	%
48	Cd	Cadmium	0.00220	%	0.00082	%
50	Sn	Tin	< 0.0010	%	(0.0)	%
51	Sb	Antimony	0.00343	%	0.00093	%
74	W	Tungsten	0.209	%	0.019	%
82	Pb	Lead	< 0.0012	%	(0.0)	%

Sum of concentration 99.00 %

Date: 02/06/2021

A1/The Chemical Composition for Base(A) Alloy.

SPECTRO X-LAB

Job Number: 0

Sample Name: **NUHA**
Description: N4

Date of Receipt: 02/06/2021
Date of Evaluation: 02/06/2021

Average Atomic Number: 0.00

Loss of Ignition: 1.0051 %

Z	Symbol	Element	Concentration	Abs. Error
12	Mg	Magnesium	0.0537 %	0.0081 %
13	Al	Aluminum	0.0187 %	0.0024 %
14	Si	Silicon	0.0530 %	0.0030 %
15	P	Phosphorus	< 0.0015 %	(0.0) %
16	S	Sulfur	< 0.00067 %	(0.0) %
22	Ti	Titanium	0.00455 %	0.00030 %
23	V	Vanadium	0.0332 %	0.0023 %
24	Cr	Chromium	19.18 %	0.05 %
25	Mn	Manganese	1.212 %	0.020 %
26	Fe	Iron	3.590 %	0.028 %
27	Co	Cobalt	68.75 %	0.11 %
28	Ni	Nickel	2.632 %	0.027 %
29	Cu	Copper	0.0520 %	0.0064 %
30	Zn	Zinc	0.1181 %	0.0044 %
33	As	Arsenic	< 0.00021 %	(0.0) %
40	Zr	Zirconium	< 0.050 %	(0.0) %
41	Nb	Niobium	< 0.0038 %	(0.0013) %
42	Mo	Molybdenum	3.069 %	0.045 %
47	Ag	Silver	0.0050 %	0.0023 %
48	Cd	Cadmium	0.0016 %	0.0015 %
50	Sn	Tin	< 0.00051 %	(0.0) %
51	Sb	Antimony	0.0018 %	0.0018 %
74	W	Tungsten	0.210 %	0.019 %
82	Pb	Lead	< 0.0013 %	(0.0) %

Sum of concentration 98.99 %

Date: 02/06/2021

A2/The Chemical Composition for B3 Alloy(1.5%B).

SPECTRO X-LAB

Job Number: 0

Sample Name: **NUHA**
Description: N10

Date of Receipt: 02/06/2021
Date of Evaluation: 02/06/2021

Average Atomic Number: 0.00

Loss of Ignition: 1.0030 %

Z	Symbol	Element	Concentration		Abs. Error	
12	Mg	Magnesium	< 0.029	%	(0.0)	%
13	Al	Aluminum	< 0.0066	%	(0.0028)	%
14	Si	Silicon	< 0.0027	%	(0.0)	%
15	P	Phosphorus	< 0.0016	%	(0.0)	%
16	S	Sulfur	< 0.00074	%	(0.0)	%
22	Ti	Titanium	< 0.0020	%	(0.0)	%
23	V	Vanadium	0.0411	%	0.0027	%
24	Cr	Chromium	> 23.65	%	0.06	%
25	Mn	Manganese	1.041	%	0.021	%
26	Fe	Iron	1.827	%	0.022	%
27	Co	Cobalt	64.44	%	0.11	%
28	Ni	Nickel	2.868	%	0.024	%
29	Cu	Copper	0.0292	%	0.0056	%
30	Zn	Zinc	0.1002	%	0.0055	%
33	As	Arsenic	< 0.00026	%	(0.0)	%
40	Zr	Zirconium	< 0.050	%	(0.0)	%
41	Nb	Niobium	0.0055	%	0.0037	%
42	Mo	Molybdenum	3.171	%	0.044	%
47	Ag	Silver	0.0014	%	0.0014	%
48	Cd	Cadmium	< 0.00069	%	(0.00019)	%
50	Sn	Tin	< 0.0011	%	(0.0)	%
51	Sb	Antimony	< 0.0012	%	(0.0)	%
74	W	Tungsten	1.785	%	0.028	%
82	Pb	Lead	< 0.0013	%	(0.0)	%

Sum of concentration 99.00 %

Date: 02/06/2021

A3/The Chemical Composition for C3 Alloy(1.5%W).

SPECTRO X-LAB

Job Number: 0

Sample Name: **NUHA**
Description: N7

Date of Receipt: 02/06/2021
Date of Evaluation: 02/06/2021

Average Atomic Number: 0 00

Loss of Ignition: 1.0028 %

Z	Symbol	Element	Concentration		Abs. Error	
12	Mg	Magnesium	< 0.030	%	(0.0)	%
13	Al	Aluminum	< 0 0071	%	(0.0)	%
14	Si	Silicon	0.0347	%	0.0020	%
15	P	Phosphorus	< 0.0016	%	(0.0)	%
16	S	Sulfur	< 0.00069	%	(0.0)	%
22	Ti	Titanium	< 0.0020	%	(0.00042)	%
23	V	Vanadium	0.0281	%	0.0019	%
24	Cr	Chromium	20.59	%	0.05	%
25	Mn	Manganese	1.047	%	0.017	%
26	Fe	Iron	2.672	%	0.022	%
27	Co	Cobalt	68.89	%	0.10	%
28	Ni	Nickel	2.584	%	0.023	%
29	Cu	Copper	0.0189	%	0.0047	%
30	Zn	Zinc	0.0968	%	0.0036	%
33	As	Arsenic	< 0.00025	%	(0.0)	%
40	Zr	Zirconium	< 0.050	%	(0.0)	%
41	Nb	Niobium	< 0.0044	%	(0.0023)	%
42	Mo	Molybdenum	2.836	%	0.03?	%
47	Ag	Silver	0.0045	%	0.0021	%
48	Cd	Cadmium	0.0016	%	0.0011	%
50	Sn	Tin	< 0.0013	%	(0.0)	%
51	Sb	Antimony	< 0.0012	%	(0.0)	%
74	W	Tungsten	0.180	%	0.016	%
82	Pb	Lead	< 0.0015	%	(0.0)	%

Sum of concentration 99.00 %

Date: 02/06/2021

Page 1

A4/The Chemical Composition for D3(5%B4C) Alloy.

Appendix(B)

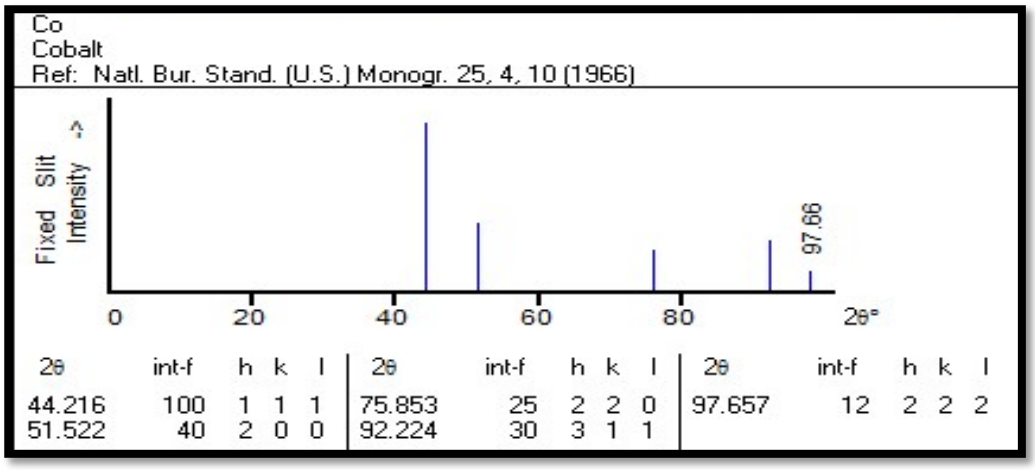

2θ	int-f	h	k	l	2θ	int-f	h	k	l	2θ	int-f	h	k	l
44.216	100	1	1	1	75.853	25	2	2	0	97.657	12	2	2	2
51.522	40	2	0	0	92.224	30	3	1	1					

B1/ XRD chart for pure Cobalt

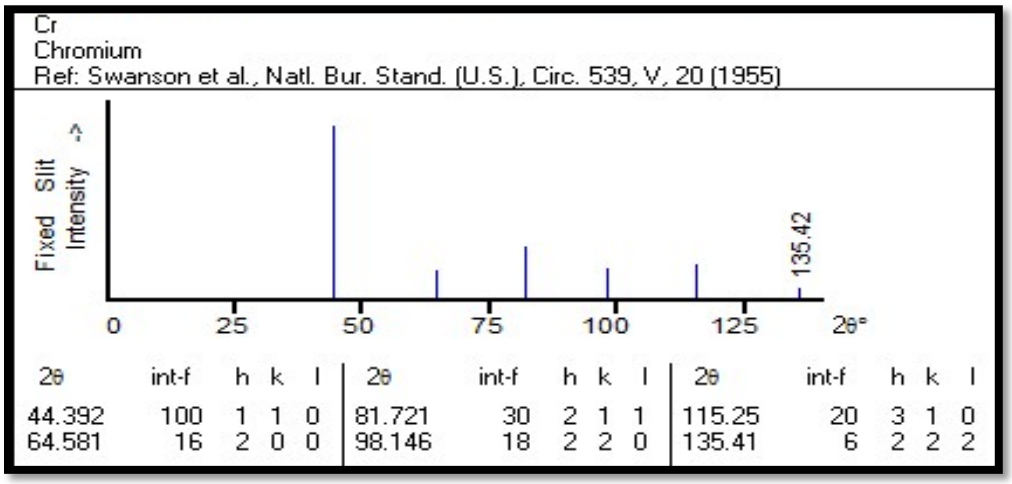

2θ	int-f	h	k	l	2θ	int-f	h	k	l	2θ	int-f	h	k	l
44.392	100	1	1	0	81.721	30	2	1	1	115.25	20	3	1	0
64.581	16	2	0	0	98.146	18	2	2	0	135.41	6	2	2	2

B2/ XRD chart for pure Chromium

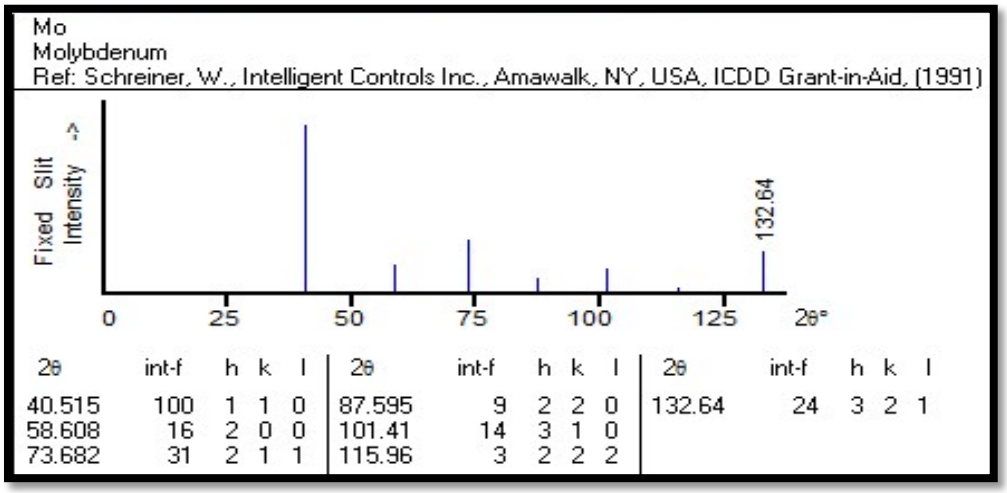

2θ	int-f	h	k	l	2θ	int-f	h	k	l	2θ	int-f	h	k	l
40.515	100	1	1	0	87.595	9	2	2	0	132.64	24	3	2	1
58.608	16	2	0	0	101.41	14	3	1	0					
73.682	31	2	1	1	115.96	3	2	2	2					

B3/ XRD chart for pure Molybdenum

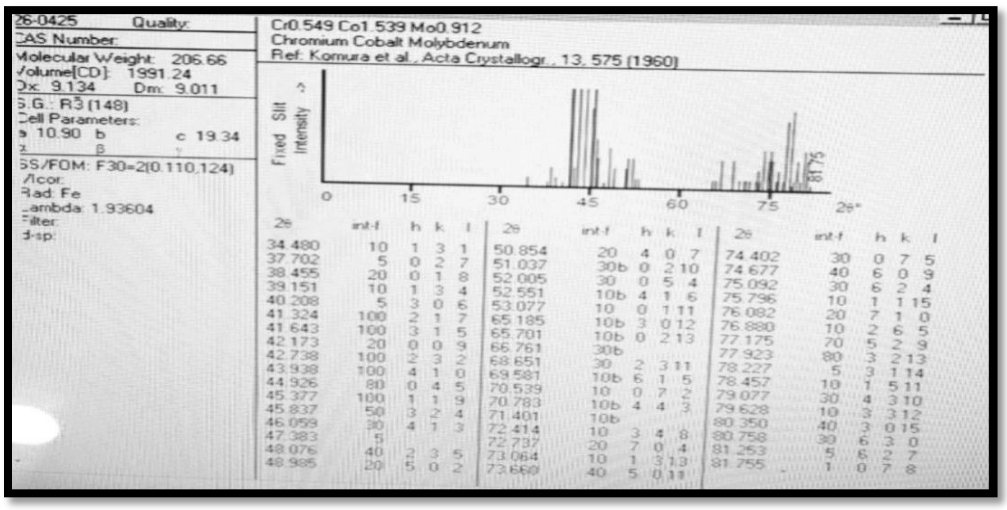

B4/XRD Chart for CoCrMo phase

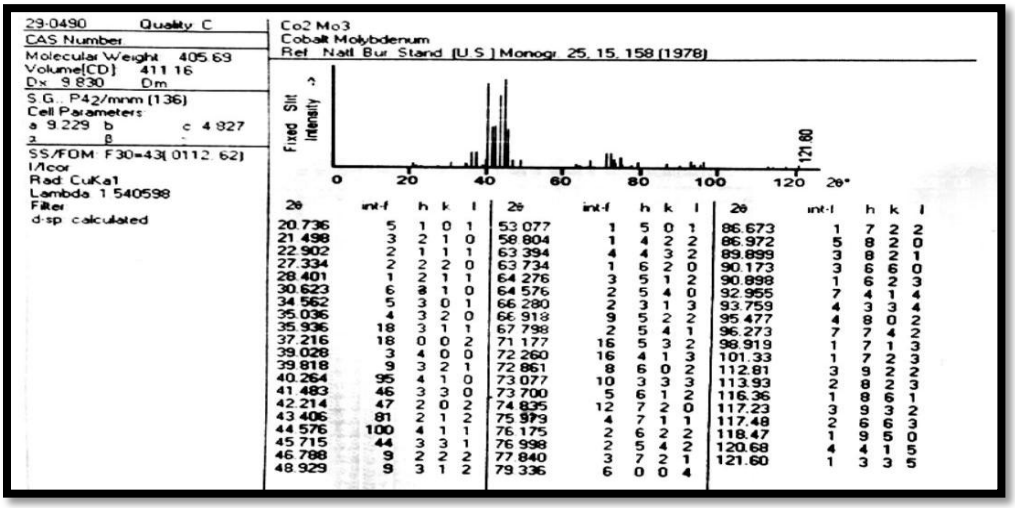

B5/XRD Chart for Co_2Mo_3 phase

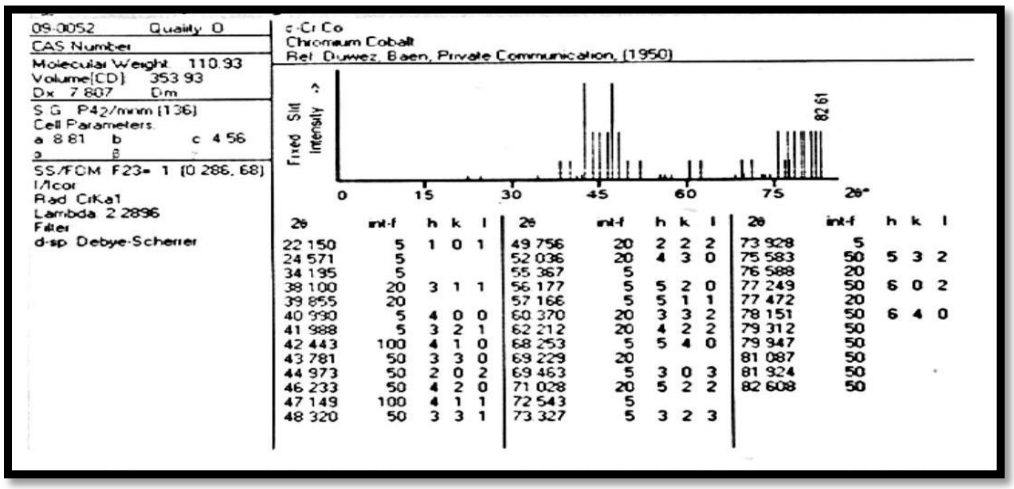

B6/XRD Chart for CrCo phase

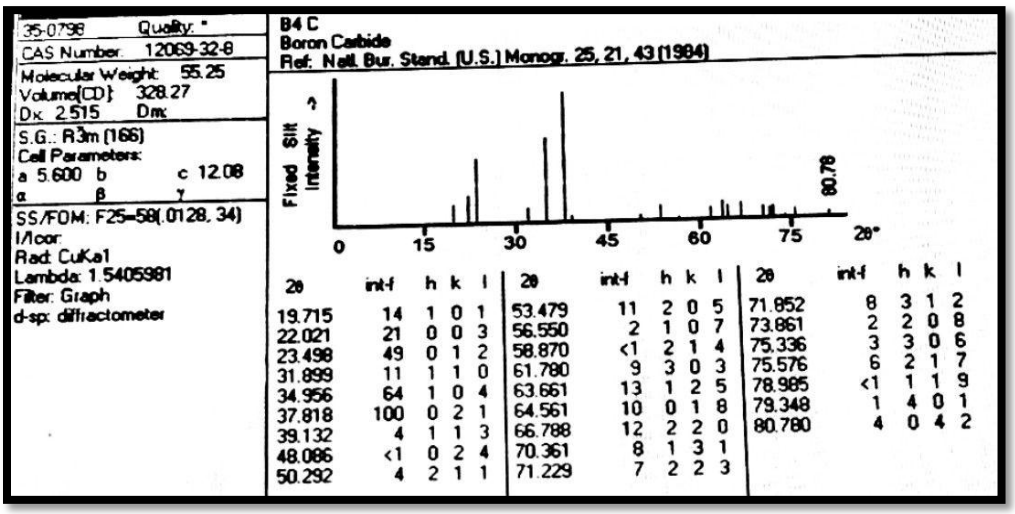

2θ	int-f	h	k	l
19.715	14	1	0	1
22.021	21	0	0	3
23.498	49	0	1	2
31.899	11	1	1	0
34.956	64	1	0	4
37.818	100	0	2	1
39.132	4	1	1	3
48.086	<1	0	2	4
50.292	4	2	1	1
53.479	11	2	0	5
56.550	2	1	0	7
58.870	<1	2	1	4
61.780	9	3	0	3
63.661	13	1	2	5
64.561	10	0	1	8
66.788	12	2	2	0
70.361	8	1	3	1
71.229	7	2	2	3
71.852	8	3	1	2
73.861	2	2	0	8
75.336	3	3	0	6
75.576	6	2	1	7
78.985	<1	1	1	9
79.348	1	4	0	1
80.780	4	0	4	2

B7/XRD Chart for B_4C phase

Appendix(C)

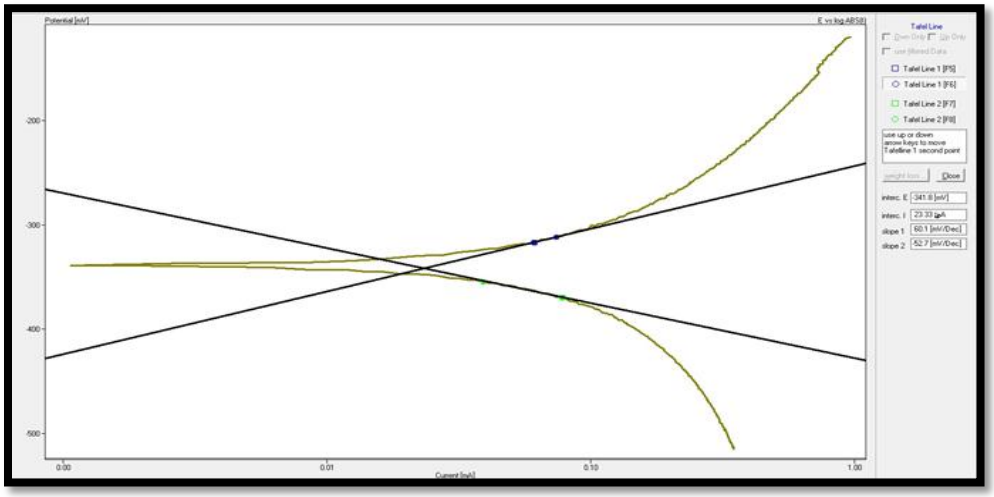

C1/ Potentiodynamic polarization for **A** alloy in Ringer's solution

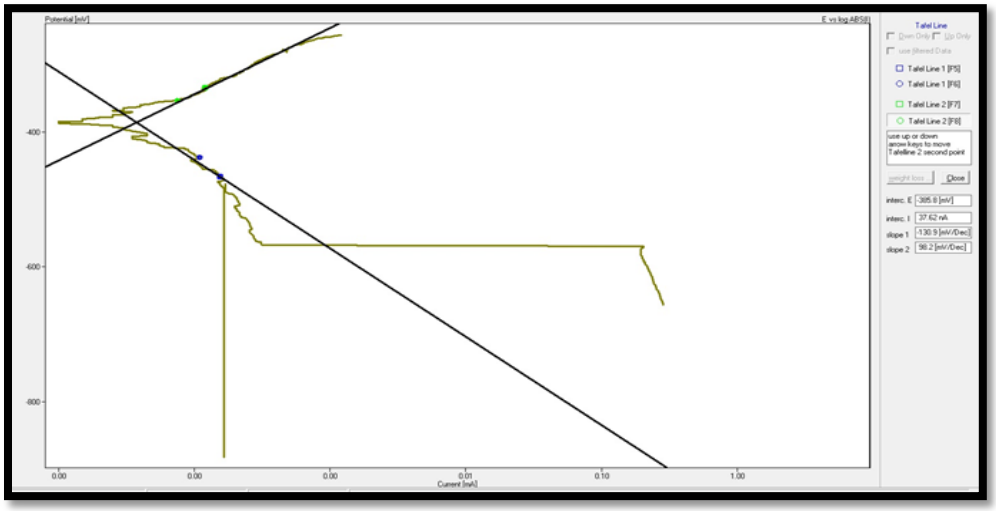

C2/ Potentiodynamic polarization for **B1** alloy in Ringer's solution

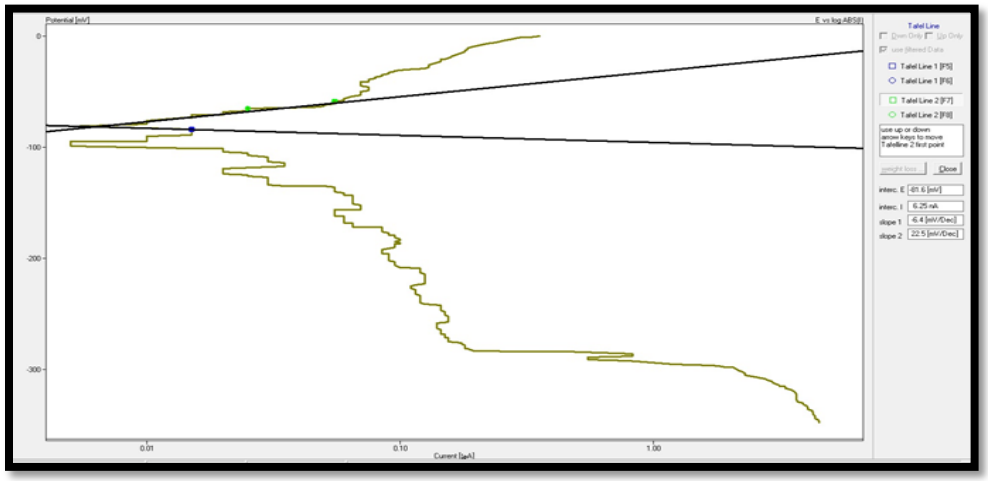

C3/ Potentiodynamic polarization for **B2** alloy in Ringer's solution

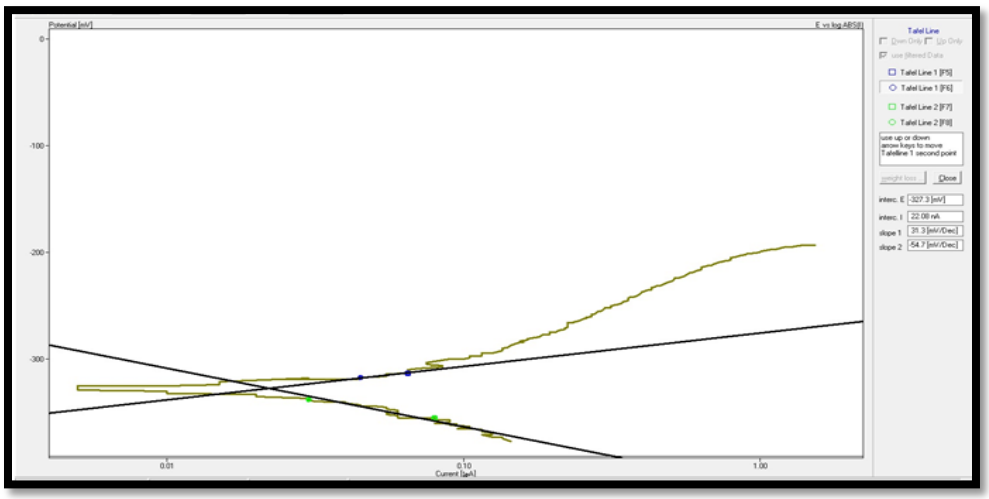

C4/Potentiodynamic polarization for **B3** alloy in Ringer's solution

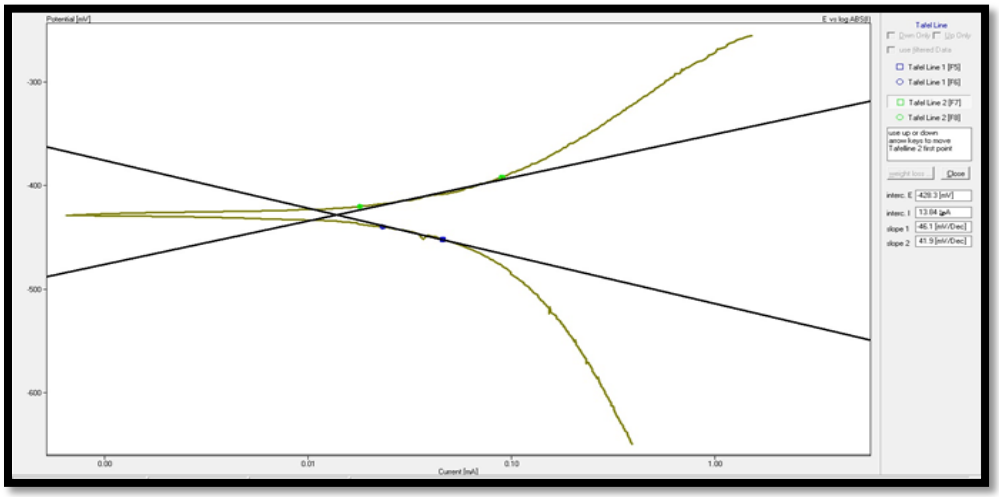

C5/Potentiodynamic polarization for **C1** alloy in Ringer's solution

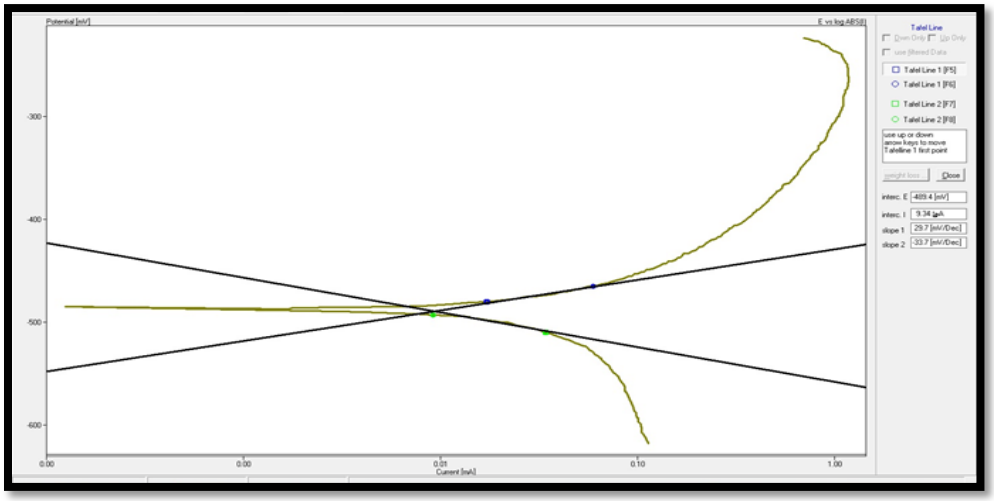

C6/Potentiodynamic polarization for **C2** alloy in Ringer's solution

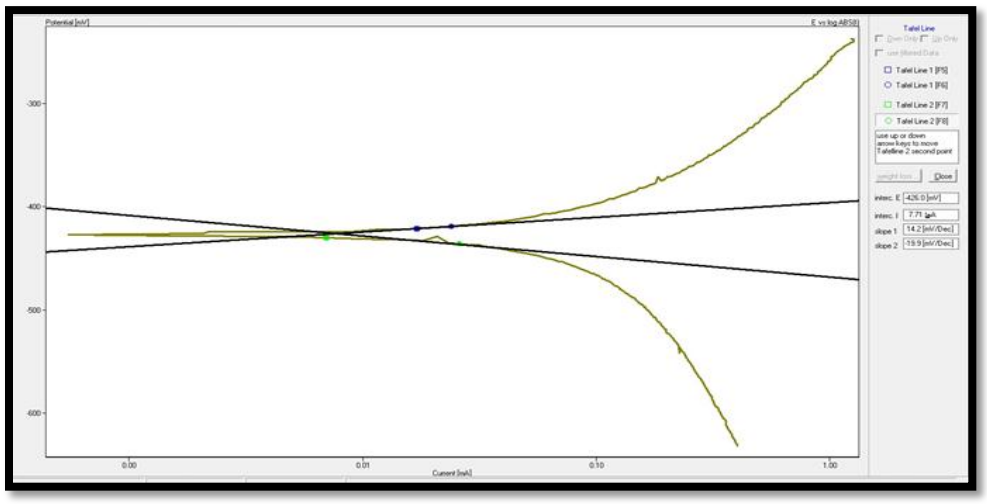

C7/ Potentiodynamic polarization for **C3** alloy in Ringer's solution

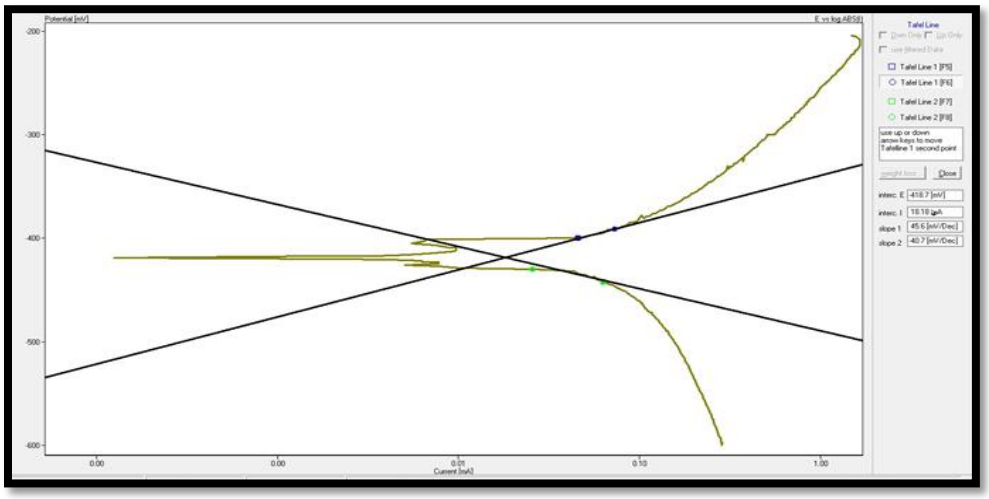

C8/Potentiodynamic polarization for **D1** alloy in Ringer's solution

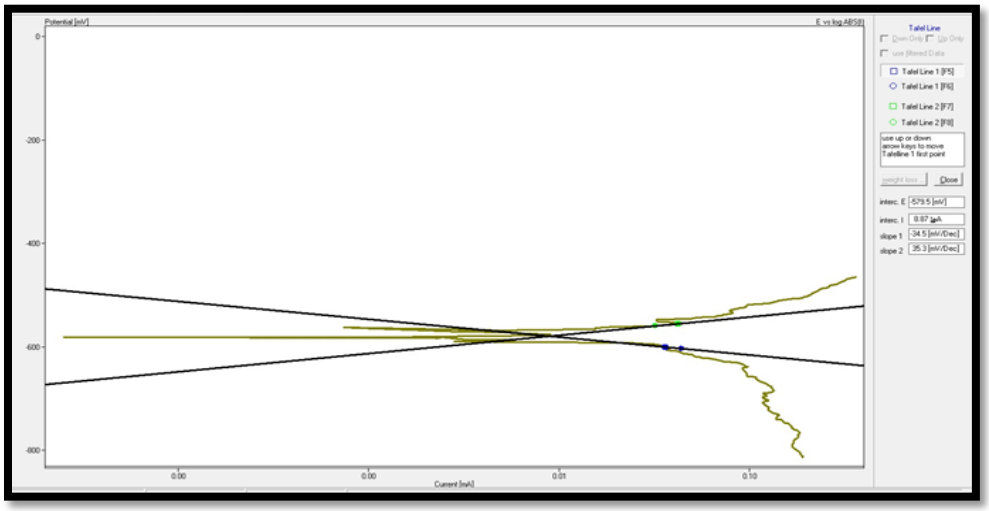

C9/Potentiodynamic polarization for **D2** alloy in Ringer's solution

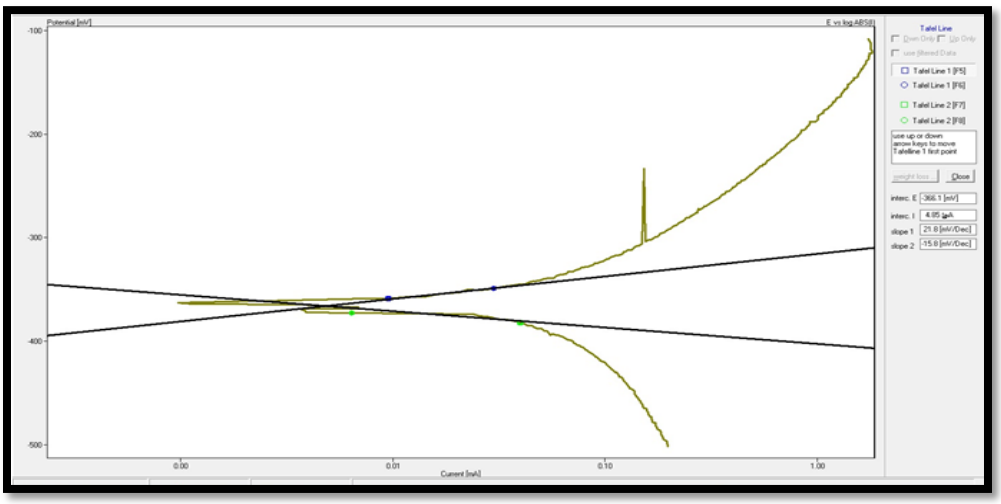

C10/Potentiodynamic polarization for **D3** alloy in Ringer's solution

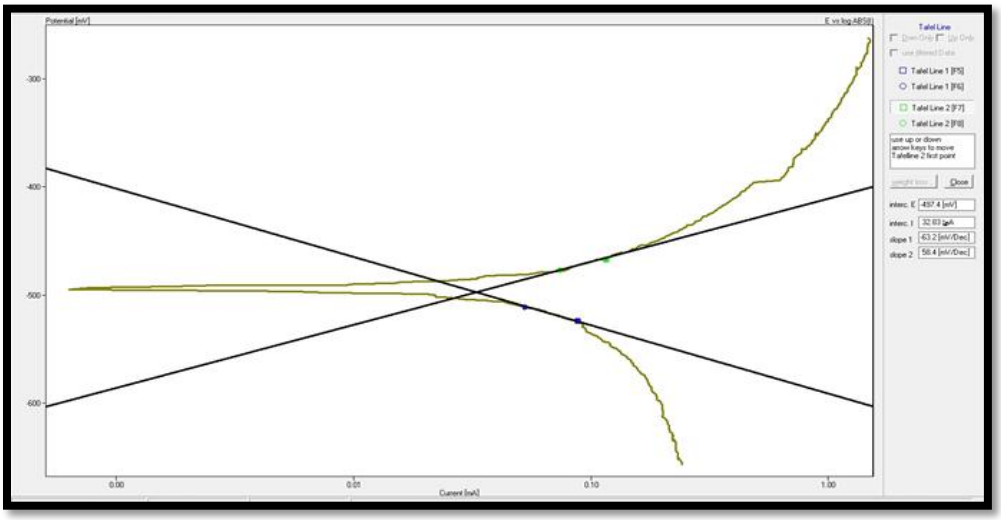

C11/Potentiodynamic polarization for **A** alloy in artificial saliva solution

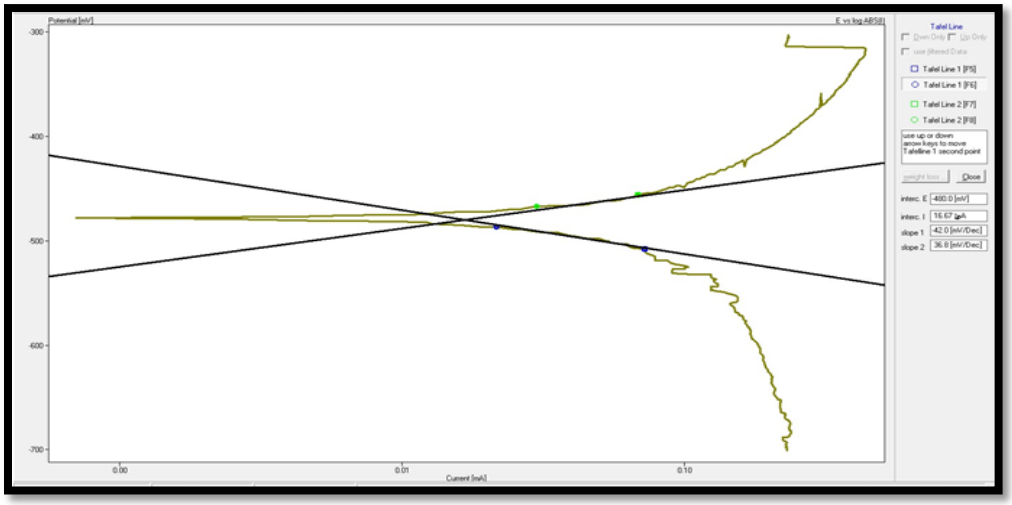

C12/ Potentiodynamic polarization for **B1** alloy in artificial saliva solution

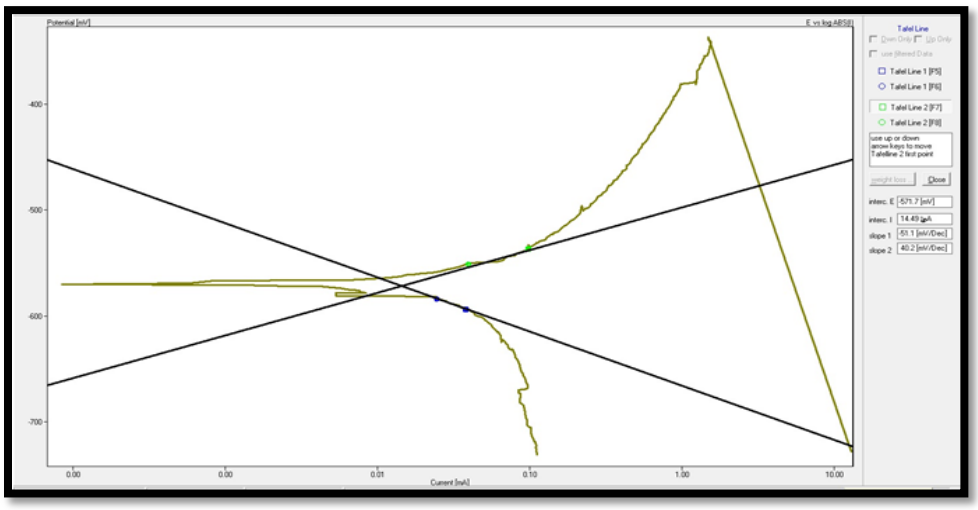

C13/Potentiodynamic polarization for **B2** alloy in artificial saliva solution

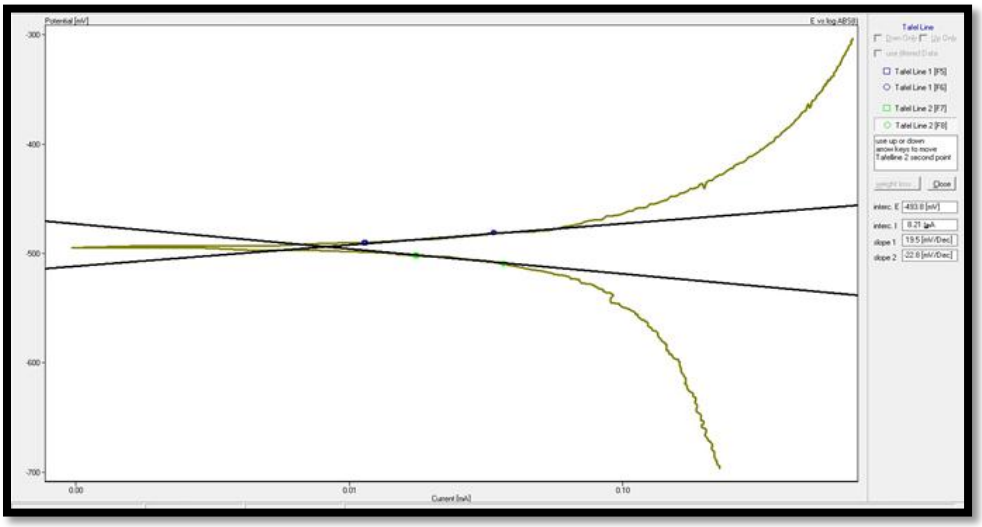

C14/Potentiodynamic polarization for **B3** alloy in artificial saliva solution

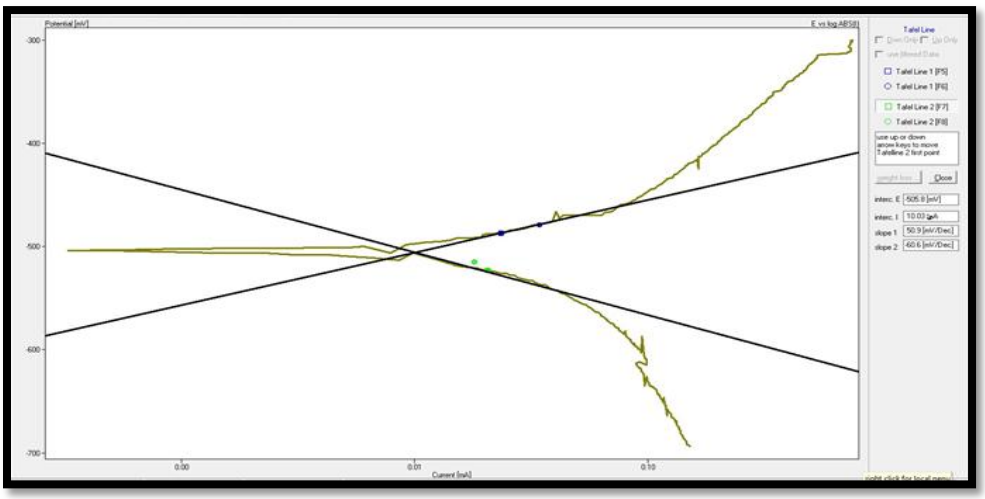

C15/Potentiodynamic polarization for **C1** alloy in artificial saliva solution

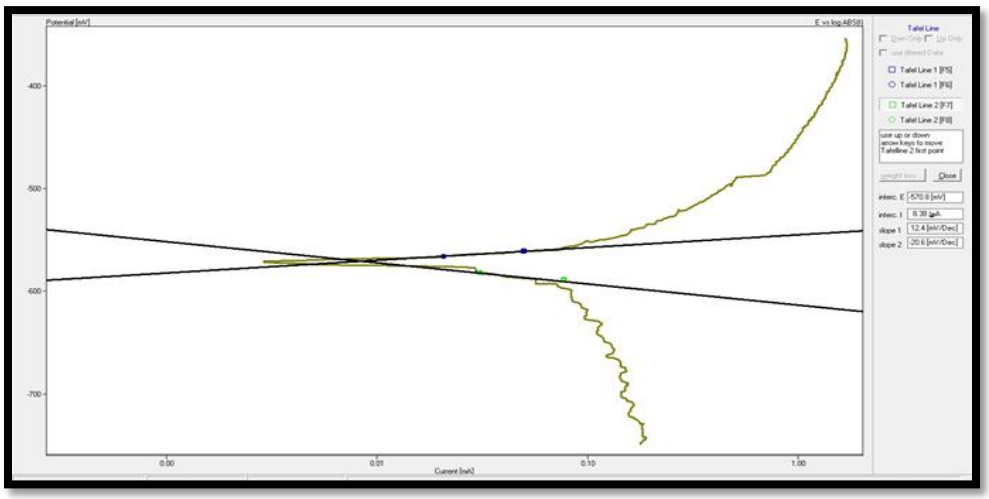

C16/Potentiodynamic polarization for **C2** alloy in artificial saliva solution

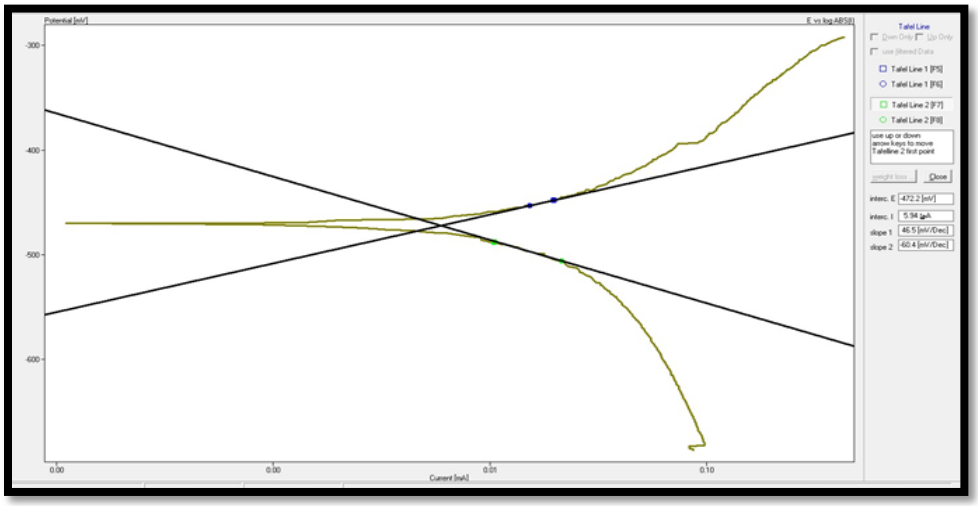

C17/ Potentiodynamic Polarization for **C3** alloy in artificial saliva solution

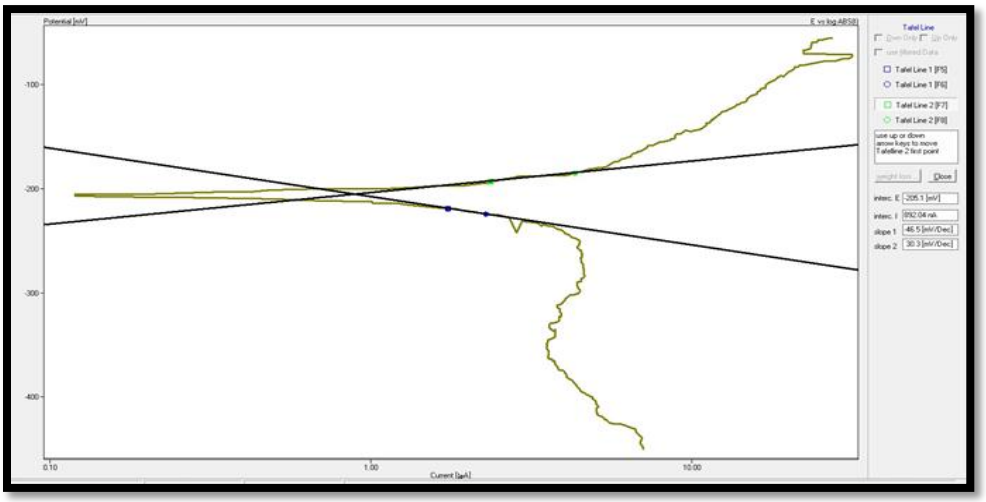

C18/ Potentiodynamic polarization for **D1** alloy in artificial saliva solution

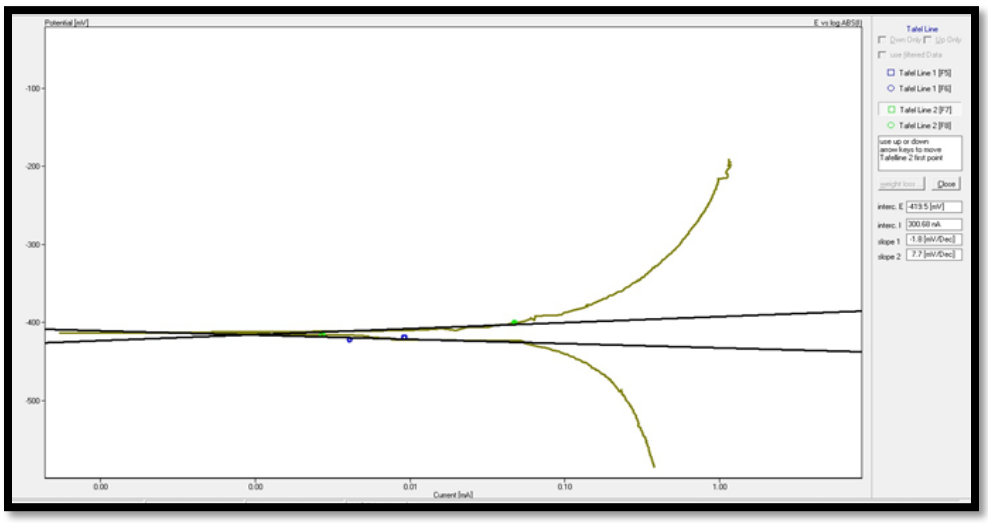

C19/ Potentiodynamic polarization for **D2** alloy in artificial saliva solution

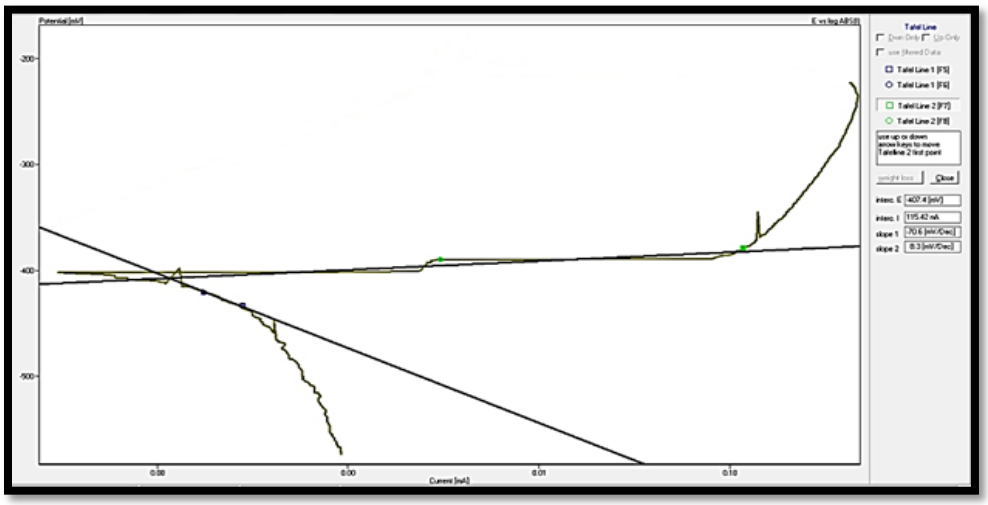

C20/Potentiodynamic polarization for **D3** alloy in artificial saliva solution

الخلاصة

تعتبر سبائك الكوبالت والكروم والموليبدينوم من السبائك المهمة التي تستخدم على نطاق واسع في تطبيقات تقويم العظام وزراعة الأسنان. الهدف من هذه الدراسة هو معرفة تأثير إضافة بعض العناصر مثل البورون والتنكستن وإضافة مادة سيراميكية كاربيد البورون على الخواص الفيزيائية والميكانيكية والكهروكيميائية لهذه السبيكة.

تم استخدام طريقة ميتالورجيا المساحيق لتحضير السبائك ، حيث تمت إضافة كل من التنكستن والبورون بنسب مختلفة (0.5 ، 1 ،1.5) نسبة وزنية بينما أضيف كاربيد البورون بنسب مختلفة (1،3 و 5)% بالوزن. تمت عملية الخلط لمدة ست ساعات ، ثم تم ضغطها بضغط ثابت 700 ميجا باسكال. كانت أبعاد العينات بعد عملية الضغط $d = 13mm$ و $t = 5\ mm$. إن عملية التلبيد التي تم إجراؤها عند درجة حرارة 850 درجة مئوية لمدة 6 ساعات لجميع العينات كانت كافية لتحويل جميع العناصر إلى تركيب سبيكة.

تشير النتائج إلى أن إضافة البورون يؤدي إلى انخفاض واضح في المسامية ، بينما إضافة التنكستن للسبيكة له فائدة منخفضة في تقليل نسب المسامية للسبائك المحضرة. أما بالنسبة لإضافة كاربيد البورون إلى سبيكة فقد أدى إلى زيادة ملحوظة في قيم مسامية السبيكة.

تظهر نتائج الكثافة بعد التلبيد زيادة في كثافة كل من العينات المحتوية على البورون وعينات التنكستن وانخفاض كبير في كثافة العينات المحتوية على كار بيد البورون.

أظهرت نتائج XRD أن جميع العينات (مع وبدون إضافات) التي تم ضغطها عند 700 ميجا باسكال وتلبيدها عند 850 درجة مئوية لمدة 6 ساعات تتكون من ثلاث اطوار رئيسية عند درجة حرارة الغرفة (CoCrMo و CoCr و Co_2Mo_3). ولكن في حالة إضافة كاربيد البورون إلى السبيكة ، فقد أظهرت نفس الاطوار مع وجود بيكات واضحة من كاربيد البورون في مخطط حيود الاشعة السينية.

ان صلادة السبيكة المحضرة ازدادت بشكل كبير مع إضافة القليل من البورون وكاربيد البورون في جميع النسب ، لكن أضافة التنكستن أظهر تأثير طفيف على قيمة الصلادة.العينة مع نسبة بورون (1.5%نسبة وزنية)كانت تمتلك اعلى صلادة بالنسبة لكل العناصر المضافة.

ازدادت مقاومة البلى مع اضافة (بورون , تنكستن وكاربيد البورون) لسبيكة CoCrMo. العينة مع نسبة (5%نسبة وزنية) من كاربيدالبورون كانت تملك اقل وزن مفقود خلال اختبار البلى تحت الاحمال المختلفة.

زادت مقاومة التآكل بشكل ملحوظ بعد إضافة البورون والتنكستن بنسب مختلفة(0.5 , 1 و1.5) نسبة وزنية ، حيث انخفض معدل التآكل للسبيكة الأساسية من (13.49 ميكرو أمبير / سم^2) و (18.989ميكرو أمبير / سم^2) في سائل الجسم. ومحلول اللعاب الصناعي على التوالي إلى (0.0013372 ميكرو أمبير / سم^2) و (4.808 ميكرو أمبير / سم^2) بعد إضافة 1.5% وزنا من البورون.

بينما انخفض معدل تآكل السبائك الأساسية من (13.49ميكرو أمبير / سم^2) و (18.989ميكرو أمبير / سم^2) في سائل الجسم واللعاب الصناعي على التوالي إلى (4.310 ميكرو أمبير / سم^2) و (3.3209 ميكرو أمبير / سم^2) بعد إضافة 1.5 %وزنا من التنكستن

أما بالنسبة لإضافة كاربيد البورون ، فقد زادت مقاومة التآكل لسبائك الكوبالت والكروم والموليبدينوم ، ولكن بنسبة (1 ,3 و5)% وزنا في كل المحاليل التأكلية.

نسبة التحسن عند اضافة البورون وصلت الى(99.99%) مع نسبة (1.5% نسبة وزنية)في سائل الجسم , بينما افضل نسبة تحسن عند اضافة التنكستن وصلت الى(82.51%) مع نسبة (1.5% نسبة وزنية) في محلول اللعاب الصناعي .اما نسبة التحسن عند اضافة كاربيد البورون وصلت الى (99.61%) مع نسبة (5% نسبة وزنية) في محلول اللعاب الصناعي.

أكد اختبار الأيونات الذائبة أن جميع أيونات Co و Cr و Mo الذائبة في سائل الجسم واللعاب قد انخفضت بشكل ملحوظ بعد إضافة نسبة 1.5 % بالوزن B و 1.5% بالوزن W

حيث لم يتم اكتشاف كل من أيونات البورون وأيونات التنكستن الذائبة بسبب الكمية الصغيرة من الأيونات الذائبة في المحاليل المسببة للتآكل.